

การประยุกต์เทคนิคทางธรณีฟิสิกส์และอุทกเคมีเพื่อการประเมินการแทรกซอนของน้ำทะเลในชั้น
หินอุ้มน้ำชายฝั่ง: กรณีศึกษาบริเวณอำเภอชะอำ จังหวัดเพชรบุรี



นางสาวจิราพร แซ่จู้

จุฬาลงกรณ์มหาวิทยาลัย
CHULALONGKORN UNIVERSITY

บทคัดย่อและแฟ้มข้อมูลฉบับเต็มของวิทยานิพนธ์ตั้งแต่ปีการศึกษา 2554 ที่ให้บริการในคลังปัญญาจุฬาฯ (CUIR)
เป็นแฟ้มข้อมูลของนิสิตเจ้าของวิทยานิพนธ์ ที่ส่งผ่านทางบัณฑิตวิทยาลัย

The abstract and full text of theses from the academic year 2011 in Chulalongkorn University Intellectual Repository (CUIR)
are the thesis authors' files submitted through the University Graduate School.

วิทยานิพนธ์นี้เป็นส่วนหนึ่งของการศึกษาตามหลักสูตรปริญญาวิทยาศาสตรมหาบัณฑิต

สาขาวิชาธรณีวิทยา ภาควิชาธรณีวิทยา

คณะวิทยาศาสตร์ จุฬาลงกรณ์มหาวิทยาลัย

ปีการศึกษา 2558

ลิขสิทธิ์ของจุฬาลงกรณ์มหาวิทยาลัย

APPLICATION OF GEOPHYSICAL AND HYDROCHEMICAL TECHNIQUES FOR
SEAWATER INTRUSION ASSESSMENT IN COASTAL AQUIFER: A CASE STUDY AT
AMPHOE CHA-AM, CHANGWAT PHETCHABURI



A Thesis Submitted in Partial Fulfillment of the Requirements
for the Degree of Master of Science Program in Geology
Department of Geology
Faculty of Science
Chulalongkorn University
Academic Year 2015
Copyright of Chulalongkorn University

Thesis Title	APPLICATION OF GEOPHYSICAL AND HYDROCHEMICAL TECHNIQUES FOR SEAWATER INTRUSION ASSESSMENT IN COASTAL AQUIFER: A CASE STUDY AT AMPHOE CHA-AM, CHANGWAT PHETCHABURI
By	Miss Jiraporn Sae-ju
Field of Study	Geology
Thesis Advisor	Assistant Professor Srilert Chotpantarat, Ph.D.
Thesis Co-Advisor	Assistant Professor Thanop Thitimakorn, Ph.D.

Accepted by the Faculty of Science, Chulalongkorn University in Partial Fulfillment of the Requirements for the Master's Degree

.....Dean of the Faculty of Science
(Associate Professor Polkit Sangvanich, Ph.D.)

THESIS COMMITTEE

.....Chairman
(Assistant Professor Pitsanupong Kanjanapayont, Dr.rer.nat.)

.....Thesis Advisor
(Assistant Professor Srilert Chotpantarat, Ph.D.)

.....Thesis Co-Advisor
(Assistant Professor Thanop Thitimakorn, Ph.D.)

.....Examiner
(Associate Professor Chakkaphan Sutthirat, Ph.D.)

.....External Examiner
(Assistant Professor Winit Youngme)

จิราพร แซ่จู่ : การประยุกต์เทคนิคทางธรณีฟิสิกส์และอุทกเคมีเพื่อการประเมินการแทรกซอนของน้ำทะเลในชั้นหินอุ้มน้ำชายฝั่ง: กรณีศึกษาบริเวณอำเภอชะอำ จังหวัดเพชรบุรี (APPLICATION OF GEOPHYSICAL AND HYDROCHEMICAL TECHNIQUES FOR SEAWATER INTRUSION ASSESSMENT IN COASTAL AQUIFER: A CASE STUDY AT AMPHOE CHA-AM, CHANGWAT PHETCHABURI) อ.ที่ปรึกษาวิทยานิพนธ์หลัก: ผศ. ดร. ศรีเลิศ โชติพันธรัตน์, อ.ที่ปรึกษาวิทยานิพนธ์ร่วม: ผศ. ดร.ฐานบ ธิติมากร, 173 หน้า.

การรุกคืบของน้ำทะเลในบริเวณพื้นที่ชายฝั่งเป็นหนึ่งในปัญหาสิ่งแวดล้อมที่สำคัญซึ่งจะส่งผลกระทบต่อทรัพยากรน้ำบาดาลในอนาคต ในงานวิจัยนี้มีพื้นที่ศึกษาตั้งอยู่บริเวณอำเภอชะอำ จังหวัดเพชรบุรี ประเทศไทย และดูเหมือนจะเป็นพื้นที่ที่ได้รับผลกระทบจากปัญหาดังกล่าว โดยวัตถุประสงค์ของงานวิจัยนี้คือเพื่อบูรณาการการสำรวจทางธรณีฟิสิกส์กับข้อมูลอุทกธรณีวิทยาและข้อมูลอุทกเคมีเพื่อสนับสนุนการประเมินการรุกคืบของน้ำทะเลเข้าสู่ชั้นน้ำบาดาลชายฝั่งในพื้นที่นี้ ศึกษาโดยใช้วิธีการสำรวจความต้านทานไฟฟ้าจำเพาะในแนวดิ่ง จำนวน 80 จุดสำรวจ จากนั้นเลือกใช้ 47 จุดสำรวจเพื่อสร้างเป็นภาคตัดขวางที่มีแนวการวางตัว ตะวันตก-ตะวันออก ทิศทางตั้งฉากกับแนวชายฝั่ง จำนวน 4 แนวโดยใช้โปรแกรม IPI2WIN ในการประมวลผลข้อมูล และอธิบายผลร่วมกับการวิเคราะห์เคมีของตัวอย่างน้ำบาดาล จำนวน 57 บ่อ ผลการศึกษาพบว่าการรุกคืบของน้ำทะเลจะเกิดขึ้นในชั้นตะกอนเศษหินเชิงเขาที่มีความลึกเฉลี่ยอยู่ในช่วง 50-60 เมตร และเห็นได้ชัดขึ้นเมื่อเข้าใกล้ชายฝั่ง โดยค่าความต้านทานไฟฟ้าจำเพาะที่น้อยกว่า 5 โอห์มเมตร จะแสดงถึงชั้นน้ำบาดาลมีการปนเปื้อนโดยน้ำทะเลรุกคืบสูง ตลอดจนช่วงระหว่าง 5-10 โอห์มเมตร แสดงให้เห็นว่าชั้นน้ำบาดาลได้รับการปนเปื้อนบางส่วนจากน้ำทะเลรุกคืบ ตามแผนภาพไพเพอร์ ตัวอย่างน้ำสามารถแบ่งได้เป็น 5 ประเภทและจัดกลุ่มได้ 3 กลุ่มคือ Ca-Na-HCO_3 และ $\text{Ca-HCO}_3\text{-Cl}$ (เฟชีย์ที่ได้รับอิทธิพลของน้ำทะเลเล็กน้อย), $\text{Ca-Na-HCO}_3\text{-Cl}$ (เฟชีย์ที่ได้รับอิทธิพลของน้ำทะเลปานกลาง) และ Ca-Na-Cl และ Na-Cl (เฟชีย์ที่ได้รับอิทธิพลของน้ำทะเลมาก) นอกจากนี้ พื้นที่ที่มีค่าความต้านทานไฟฟ้าจำเพาะต่ำจะสอดคล้องกับบริเวณที่มีค่าการนำไฟฟ้าของน้ำสูงและมักพบเป็น Na-Cl เฟชีย์ ในที่สุดของการศึกษาพบว่าตอนเหนือของพื้นที่ศึกษาพบการรุกคืบของน้ำทะเลมากกว่าบริเวณอื่นและรุกคืบเข้ามาในแผ่นดินประมาณ 8 กิโลเมตร

ภาควิชา	ธรณีวิทยา	ลายมือชื่อนิสิต
สาขาวิชา	ธรณีวิทยา	ลายมือชื่อ อ.ที่ปรึกษาหลัก
ปีการศึกษา	2558	ลายมือชื่อ อ.ที่ปรึกษาร่วม

5472230623 : MAJOR GEOLOGY

KEYWORDS: SEAWATER INTRUSION / VERTICAL ELECTRICAL SOUNDING / COASTAL AQUIFER / HYDROCHEMICAL

JIRAPORN SAE-JU: APPLICATION OF GEOPHYSICAL AND HYDROCHEMICAL TECHNIQUES FOR SEAWATER INTRUSION ASSESSMENT IN COASTAL AQUIFER: A CASE STUDY AT AMPHOE CHA-AM, CHANGWAT PHETCHABURI. ADVISOR: ASST. PROF. SRILERT CHOTPANTARAT, Ph.D., CO-ADVISOR: ASST. PROF. THANOP THITIMAKORN, Ph.D., 173 pp.

Seawater intrusion in coastal area is one of the important environmental problems that negatively affect on groundwater resources in the future. In this research, the study area is located in Amphoe Cha-Am, Changwat Phetchaburi, Thailand, and appears to be affected by this problem. The purposes of this research are to integrate the geophysical investigation with hydrogeological and hydrochemical data for further evaluating seawater intrusion into coastal aquifers in this area. The study conducted 80 of VES survey and then selected 47 VES to create 4 pseudo cross-section lines from West-East, running perpendicular to the coastal line, by using IPI2WIN software. The geophysical results were described together with hydrochemical analysis of 57 groundwater samples. The finding found that seawater intrusion occurs in Qcl aquifer with an average depth of 50-60 meters and presents more obviously near the coastal line. Resistivity value of less than 5 Ω m represents that the aquifer getting highly contaminated by seawater intrusion as well as of the range between 5-10 Ω m represents that the aquifer getting partially contaminated by seawater intrusion. According to the piper diagram, groundwater can be divided into 5 hydrochemical facies as follows: Ca-Na-HCO₃ and Ca-HCO₃-Cl (the facies getting low impact from seawater intrusion), Ca-Na-HCO₃-Cl (the facies getting moderate impact from seawater intrusion), Na-Cl (the facies getting a high impact from seawater intrusion). Furthermore, the area has low resistivity value, it corresponds to the high value of EC, and the facies is usually Na-Cl. Finally, the finding in this study found that the northern part of the study area has been faced seawater intrusion relative higher impact than other areas and seawater laterally intrude about of 8 kilometers inland.

Department: Geology

Student's Signature

Field of Study: Geology

Advisor's Signature

Academic Year: 2015

Co-Advisor's Signature

ACKNOWLEDGEMENTS

This thesis is successfully by getting help from many people. I appreciate with sincere thanks to my advisor, Assistant Professor Dr. Srilert Chotpantarat and my co-advisor, Assistant Professor Dr. Thanop Thitimakorn for good suggestion and advice as well as painstaking correction of the manuscript. Their guidance helped me all the time of research and writing of this thesis.

Besides my advisor and co-advisor, I express gratitude to my thesis committee: Assistant Professor Dr. Pitsanupong Kanjanapayont, Associate Professor Dr. Chakkaphan Sutthirat and Assistant Professor Winit Youngme for their guidance and recommendation.

I am very grateful to the Graduate School of Chulalongkorn University for funding support and Department of Groundwater Resources for supporting the data. I deeply acknowledge with sincere thanks to my supervisor and associate for their advice and assistance in these master classes.

I would like to thank Mr. Alongkot Fanka, Ms. Jensarin Vivatpinyo, Ms. Parisa Nimnate, Ms. Jirawan Thamrongrisakul, Mr. Tewanopparit Parkchai, Mr. Ronnakorn Jaimun, Ms. Wanlapa Wisittamasri, Mr. Stapana Kongseneucus and Mr. Attapon Sae-Ju for their field investigation supporters. Furthermore, I am grateful to Ms. Janleka Poothongkamand and Ms. Jiraprapa Niampan for their advice on laboratory experiment on Ion Chromatographic and Atomic Absorption Spectrometry. Also, special thanks to Ms. Sirintip Siripattaranukun for correction in this thesis.

Finally, I would like to acknowledge my lovely family, especially my parents for support everything in my life. Thanks to my sister, my brother for physical and mental supporting me. I would like to thank everyone who participated in the creation of this thesis was completed.

CONTENTS

	Page
THAI ABSTRACT	iv
ENGLISH ABSTRACT	v
ACKNOWLEDGEMENTS	vi
CONTENTS	vii
LIST OF TABLES	xii
LIST OF FIGURES	xiii
CHAPTER 1 INTRODUCTION.....	1
1.1 Background	1
1.2 Objectives	2
1.3 Scope of study	3
1.4 Location of the study area	3
1.5 Research methodology	3
1.6 Previous works	8
CHAPTER 2 THEORETICAL BACKGROUND	12
2.1 Groundwater system in coastal aquifers.....	12
2.1.1 The hydrologic cycle.....	12
2.1.2 Coastal aquifer.....	13
2.1.2.1 Badon Ghyben-Herzberg principle	13
2.1.2.2 Seawater Intrusion Problems.....	15
2.2 Hydrochemistry	16
2.2.1 Physical properties	18
2.2.2 Chemical properties.....	19

	Page
2.2.3 Hydrochemical Facies	21
2.2.3.1 Cation exchange of the salt / fresh water interface	21
2.2.3.2 Piper Diagram	22
2.2.3.3 Hydrochemical Facies Evolution (HFE) Diagram	24
2.3 Vertical Electrical Sounding	26
2.3.1 Theory of electrical resistivity survey	27
2.3.1.1 Basic Electricity	27
2.3.1.2 Current flow in homogeneous and inhomogeneous subsurface	30
2.3.2 Electrode configurations	35
2.3.2.1 Wenner configuration	35
2.3.2.2 Schlumberger configuration	36
2.3.2.3 Dipole-dipole configuration	37
2.3.3 Anomaly	38
2.3.3.1 Properties of electrical resistivity materials in crust	38
2.3.3.2 Factors affecting the change of electrical resistivity	38
CHAPTER 3 STUDY AREA	43
3.1 Location and topography	43
3.2 Meteorology	45
3.2.1 Seasons	45
3.2.2 Climate	46
3.2.3 Temperature	46
3.2.4 Relative Humidity	46

	Page
3.2.5 Rain	47
3.2.6 Cloud	47
3.2.7 Fog / Haze / Visibility.....	47
3.2.8 Wind	47
3.3 Land use	48
3.3.1 Agriculture area	48
3.3.2 Forest area.....	48
3.3.3 Facility area	48
3.3.4 Water body	48
3.4 Geology	51
3.4.1 Igneous Rock.....	51
3.4.1.1 Cretaceous Granite Rock (Kgr).....	54
3.4.2 Sedimentary Rock	54
3.4.2.1 Khao Chao Formation (CPk-2).....	54
3.4.2.2 Ratchaburi Group	55
3.4.3 Unconsolidated Sedimentary	55
3.4.3.1 Coastal tide-dominated deposits (Qms).....	55
3.4.3.2 Colluvial deposits (Qc).....	56
3.5 Hydrogeology	56
3.5.1 Unconsolidated aquifers	57
3.5.1.1 Quaternary Beach-Sand Deposits (Qbs).....	57
3.5.1.2 Quaternary Floodplain Deposits (Qfd).....	59

	Page
3.5.1.3 Quaternary Colluvial Deposits (Qcl)	59
3.5.2 Consolidated aquifers	59
3.5.2.1 Silurian Devonian Metamorphic aquifers (SDmm)	60
3.5.2.2 Permo-Carboniferous Metasediment aquifers (PCms).....	60
3.5.2.3 Permian Carbonate aquifers (Pc)	61
3.5.2.4 Cretaceous Granite aquifers (Gr)	61
CHAPTER 4 METHODOLOGY.....	62
4.1 Secondary data preparation and collection.....	62
4.2 Field work.....	64
4.2.1 Preliminary field survey	64
4.2.2 Field of geophysical survey.....	67
4.2.3 Groundwater sample collection	70
4.3 Laboratory work	73
4.3.1 Anion analysis.....	75
4.3.1.1 Ion Chromatography Method (IC).....	75
4.3.1.2 Titration Method	76
4.3.2 Cation analysis.....	79
4.3.2.1 Atomic Absorption Spectrometry Method (AAS).....	79
4.4 Data analysis and interpretation	81
4.4.1 Geophysical data.....	81
4.4.2 Groundwater chemistry analysis	83
4.4.3 Data interpretation	83

	Page
CHAPTER 5 RESULTS AND DISCUSSION	84
5.1 Regional groundwater flow direction	84
5.2 Geophysical data interpretation	88
5.2.1 Pseudo resistivity cross-section	89
5.2.2 Geoelectrical section	96
5.2.3 Apparent resistivity map	103
5.3 Hydrochemical results.....	106
5.3.1 Chemical characteristics of groundwater in the field.....	106
5.3.2 Hydrochemistry results	108
5.3.2 Piper diagram	109
5.3.3 Relationship between Na and Cl ions.....	116
5.3.4 Hydrochemical facies evolution diagram (HFED).....	117
5.4 Integrated interpretation of VES and EC results.....	120
CHAPTER 6 CONCLUSION AND RECOMMENDATIONS	122
6.1 Conclusions	122
6.2 Recommendation	123
REFERENCES	125
APPENDIX.....	129
VITA.....	173

LIST OF TABLES

Table 2.1 Dissolved constituents (Davis & DeWiest, 1967).....	17
Table 2.2 Resistivity of metal elements (Telford <i>et al.</i> , 1990).....	41
Table 2.3 Resistivity of minerals (Telford <i>et al.</i> , 1990).....	41
Table 2.4 Resistivity of rocks and sediments (Telford <i>et al.</i> , 1990) and (Satarugsa, 2007).....	42
Table 3.1 Coastal characteristic of the study area (Phetchaburi Rajabhat University, 2011).....	45
Table 3.2 The Geologic Time Scale (From: http://betterlesson.com/lesson/637787/geologic-timeline-discovery).....	52
Table 4.1 Sources of secondary data collection.....	63
Table 4.2 Formula for calculate alkalinity.....	78
Table 5.1 Hydrochemical analysis of groundwater samples.....	110
Table 5.2 Hydrochemical results and groundwater facies.....	114
Table 6.1 The levels of seawater intrusion with resistivity and EC values.....	122

LIST OF FIGURES

Figure 1.1 Topographic map of the study area (adapted from topographic maps edition No.1-RTSD L7018 series, sheet number 4934 I, 4934 II and 5034 IV).....	6
Figure 1.2 Flow chart of the research methodology.....	7
Figure 2.1 The Hydrologic Cycle. (National Aeronautics and Space Administration, 2010).....	13
Figure 2.2 Relationship of fresh water head and depth to seawater interface (Werner <i>et al.</i> , 2013).	14
Figure 2.3 Seawater Intrusion in coastal aquifer (Uzma, 2014).....	16
Figure 2.4 Piper diagram of water chemistry studies (Piper, 1944).....	23
Figure 2.5 Hydrochemical Facies classification of water (Galloway & Kaiser, 1980).....	24
Figure 2.6 Hydrochemical Facies Evolution (HFE) Diagram (Giménez-Forcada, 2010) .	26
Figure 2.7 Theory and primary concept about Resistivity Survey (Satarugsa, 2007).....	27
Figure 2.8 A simple electrical circuit.....	28
Figure 2.9 Single Point current source on the surface (incase homogeneous) (adapt from: Burger, 2006).....	31
Figure 2.10 Two current electrodes and two potential electrodes (incase homogeneous) (adapt from: Burger, 2006).....	33
Figure 2.11 Refraction of current flow lines at boundary of different resistivity layers. (a) Explain equation 2.18. (b) refraction($\rho_1 < \rho_2$). (c) refraction($\rho_1 > \rho_2$). (adapt from: Burger, 1992)	34
Figure 2.12 Electrode configurations (ASTM D6431 - 99, 2010)	37
Figure 3.1 Slope map of the study area (Land Development Department, 2011).....	44

Figure 3.2 Pie chart shows the percentage of land use in the study area (Land Development Department, 2011).....	49
Figure 3.3 Land use map of the study area (Land Development Department, 2011) ...	50
Figure 3.4 Geological Map in the study area. (adapted from the Department Mineral Resources, 2007)	53
Figure 3.5 Hydrological map in the study area. (adapted from the Department of Groundwater Resources, 2014)	58
Figure 4.1 Diagram shows data collection in office work study.....	64
Figure 4.2 Diagram of data collection in field work	65
Figure 4.3 Measurement of groundwater levels in the preliminary field survey	65
Figure 4.4 Map shows locations of field data collection.....	66
Figure 4.5 Equipment of the VES survey.....	68
Figure 4.6 Schlumberger configuration	69
Figure 4.7 Resistivity Meter showing channels connected to points A, B, M and N.	69
Figure 4.8 Resistivity survey showing connected the resistivity meter to 4 electrodes ..	69
Figure 4.9 Graph paper log-log scale for plot resistivity values in field	72
Figure 4.10 Groundwater level measurement and groundwater sampling collection	73
Figure 4.11 Showing filtered groundwater samples.	74
Figure 4.12 Diagram of laboratory work.....	74
Figure 4.13 Ion Chromatography.....	76
Figure 4.14 Titration Method with indicator.	77
Figure 4.15 Showing colors of Phenolphthalein alkalinity and MO alkalinity when dropped indicator.....	78
Figure 4.16 Atomic Absorption Spectrometry Method (AAS)	79

Figure 4.17 Diagram of data analysis and interpretation	81
Figure 4.18 IPI2WIN Software shows calculated and calibrated graph.....	82
Figure 4.19 IPI2WIN Software shows create pseudo cross-section	82
Figure 5.1 Groundwater flow map of rainy season.....	86
Figure 5.2 Groundwater flow map of dry season	87
Figure 5.3 Apparent resistivity type curve (type H) for three horizontal layers.	88
Figure 5.4 Example of field VES data plotted on a log-log scale graph at sounding number St-17	89
Figure 5.5 Map shows 4 cross-section lines (A-A', B-B', C-C' and D-D').....	90
Figure 5.6 IPI2WIN interpretation of VES St-25	91
Figure 5.7 Pseudo cross-section lines A-A'	94
Figure 5.8 Pseudo cross-section lines B-B'	94
Figure 5.9 Pseudo cross-section lines C-C'	95
Figure 5.10 Pseudo cross-section lines D-D'	95
Figure 5.11 Resistivity value versus lithologic-log from pseudo cross-section lines D- D' (well Q168 versus VES St 47 and well PW7962 versus VES St 34.....	97
Figure 5.12 Example for lithologic log data of well no. 5708C004.....	98
Figure 5.13 Geological cross-section lines A-A'	99
Figure 5.14 Geological cross-section lines B-B'	100
Figure 5.15 Geological cross-section lines C-C'	101
Figure 5.16 Geological cross-section lines D-D'	102
Figure 5.17 Apparent resistivity map for $AB/2=5, 10, 30, 50, 70, 100, 150$ and 200 meters	105
Figure 5.18 Showing pH of 58 groundwater samples.	106

Figure 5.19 Showing TDS of 58 groundwater samples.	107
Figure 5.20 Showing electrical conductivity of 58 groundwater samples.	107
Figure 5.21 Showing temperature of 58 groundwater samples.	107
Figure 5.22 Hydrochemical analysis of groundwater sample plotted in the piper diagram.....	114
Figure 5.23 Relationship plotting between Na and Cl concentration in groundwater ...	117
Figure 5.24 Hydrochemical Facies Evolution Diagram (HFED).....	119
Figure 5.25 Showing limit of seawater intrusion in Qcl aquifer based on EC contour map superimposed on resistivity map	121



CHAPTER 1

INTRODUCTION

1.1 Background

Many coastal areas in the world contain densely populated areas, as it is the area that has integrity of food and important economic activities such as urban development, trade and touristic activities. These are factors that attract people to settle up as a result, the water demand increases such as used for consumption, agriculture and industry. Groundwater resource is the alternative water source as compared with surface water, the groundwater is high quality, barely seasonal effects (i.e., constant temperature), the low storage cost (i.e., no spatial limitation) and huge available quantities. As mentioned reasons above, groundwater has long been pumped with a large quantity of water. As a result, the common phenomenon, so-called seawater intrusion, is occurred in many coastal areas in the world.

In the coastal aquifer, seawater is lied under fresh water since fresh water has less dense than seawater and, zone of contact between fresh water and seawater is brackish water (Bear, 1999). Fresh water is commonly over the top of heavier seawater and serves to push the seawater interface seaward. In contrary, when pumping the fresh groundwater from coastal aquifer with a large quantity, consequently, the pressure of fresh water is reduced, which in turn causes the seawater migrates further landward. Seawater intrusion problem is one of the most important environmental issues that negatively affect groundwater resources significantly since groundwater salinity can lead to reduction in fresh water availability and degradation of groundwater quality (Essink, 2001, Werner *et al.*, 2013). Therefore, the study of seawater intrusion into coastal aquifers is needed to identify the zones affected by seawater intrusion that should be able to prevent problems or remediate such problems efficiently.

The coastal study area is located at Amphoe Cha-am, Changwat Phetchaburi because it has been considered as densely populated area and one of the famous tourist areas in Thailand recently. So, the groundwater resource may be a primary water resource in the near future and is consequently drawn out over the yield in the aquifer. Under this situation, the natural equilibrium of seawater interface is directly changed and then the sea water will laterally move landward. Geophysical and hydrochemical techniques has been applied together to investigate areas disturbed by seawater intrusion (Song *et al.*, 2006, Cimino *et al.*, 2008, Kouzana *et al.*, 2010, Agoubi *et al.*, 2013, McInnis *et al.*, 2013). Geophysical techniques used the 1-D electrical resistivity surveys or vertical electrical sounding (VES). Since the electrical resistivity between fresh water saturated zones and seawater saturated zones is a large differences (Van Dam & Meulenkamp, 1967, Sabet, 1975) , it thus is capable of identifying the contrast in terms of resistivity values between seawater and freshwater in coastal aquifers. In addition, VES technique enable the large areas with less time-consuming and an economical cost, as compared with drilling exploration methods. However, geophysical survey data is not capable of identifying clearly lateral penetration of seawater in various lithologic units in a hydrogeological formation and groundwater facies or chemical constituents because the low resistivity is depended on various factors such as formation materials and groundwater chemistry (Zohdy *et al.*, 1974). As a result, in order to fulfill such limitations of geophysics for delineating seawater intrusion areas, the integration of hydrogeological investigation with a help of lithologic information (from drill wells) and chemical analysis of groundwater samples were carried out.

1.2 Objectives

The purposes of this study are listed as follows;

1. To investigate the geophysical and hydrochemical data in coastal aquifer in Amphoe Cha-am, Changwat Phetchaburi
2. To evaluate the seawater intrusion into coastal aquifers in Amphoe Cha-am, Changwat Phetchaburi

1.3 Scope of study

The study area is located on the coastline of the Gulf of Thailand at Amphoe Cha-am, Changwat Phetchaburi. There are two main parts that have been used in this study, which are geophysical investigation and hydrochemical analysis. The geophysical technique used the one-dimensional electrical resistivity surveys, well known as Vertical Electrical Sounding, VES. Groundwater samples were collected for hydrochemical analysis. Data from the analysis of two techniques were interpreted together for seawater intrusion assessment in coastal aquifer

1.4 Location of the study area

The study area is located in Amphoe Cha-am, Changwat Phetchaburi (Figure 1.1), which is the central part of Thailand, about 126 km south of Bangkok. The area is located in a topographic map of Royal Thai Survey Department, series L7018 scale 1:50,000, which is composed of three sheets: 4934I (Amphoe Tha-Yang), 4934II (Amphoe Hua-Hin) and 5034IV (Ban Tha-Node-Noi). The area lies between latitudes $12^{\circ}37.6' N$ and $12^{\circ}53.845' N$ and longitudes $99^{\circ}50.827' E$ and $99^{\circ}729' E$. The study area covers about 360 square kilometers and is bounded by the northern and western borders of Amphoe Tha-Yang, by the southern border of Changwat Prachuap-Khiri-Khan, and by the eastern border of the Gulf of Thailand.

1.5 Research methodology

The method of study showed in Figure 1.2. There are 6 steps listed below:

1. Literature reviews

This part was the literature review, including theory, investigation techniques and previous research of seawater intrusion in coastal aquifer of our country and foreign countries.

2. Collection of topographical data, geological data and hydrogeological data

After the study area was properly chosen, all data of this area, including topographic, geologic and hydrogeologic maps, was collected from several government agencies, such as Department of groundwater Resources (DGR), Department of Mineral Resources (DMR) and also previous studies in order to further apply in field investigation. The details of geology and hydrogeology of this area are described in Chapter 2.

3. Field investigation consisted of 1) electrical resistivity survey, 2) groundwater samples collection and 3) groundwater levels measurement. The details are shown below;

- Geophysics investigation was performed by VES method, using Schlumberger configuration.
- Groundwater levels measurement and groundwater sampling for hydrochemical analysis were carried out in all wells located in the study area.
- Analysis of hydrochemical properties of groundwater samples in the laboratory

4. Groundwater samples collected in the field were used for hydrochemical analysis to identify water types using the piper diagram. Cations analysis (Na^+ , K^+ , Ca^+ and Mg^+) were determined by Atomic Absorption Spectrometry (AAS) and anions analysis (SO_4^{2-} , NO_3^- and Cl^-) were analyzed by Ion Chromatographic (IC), and finally concentrations of HCO_3^- , CO_3^{2-} were determined using the titration method.

5. Interpretation of geophysical data, analysis and discussion of the results.

The geophysical data obtained from the field were interpreted and created the geological cross section. Then, the results of hydrochemical analysis of ground water

samples were integrated with geophysical data, to delineate the influence of seawater intrusion in this study area.

6. Conclusion and Discussions

All of the results were discussed and concluded in Chapter 5 and 6.



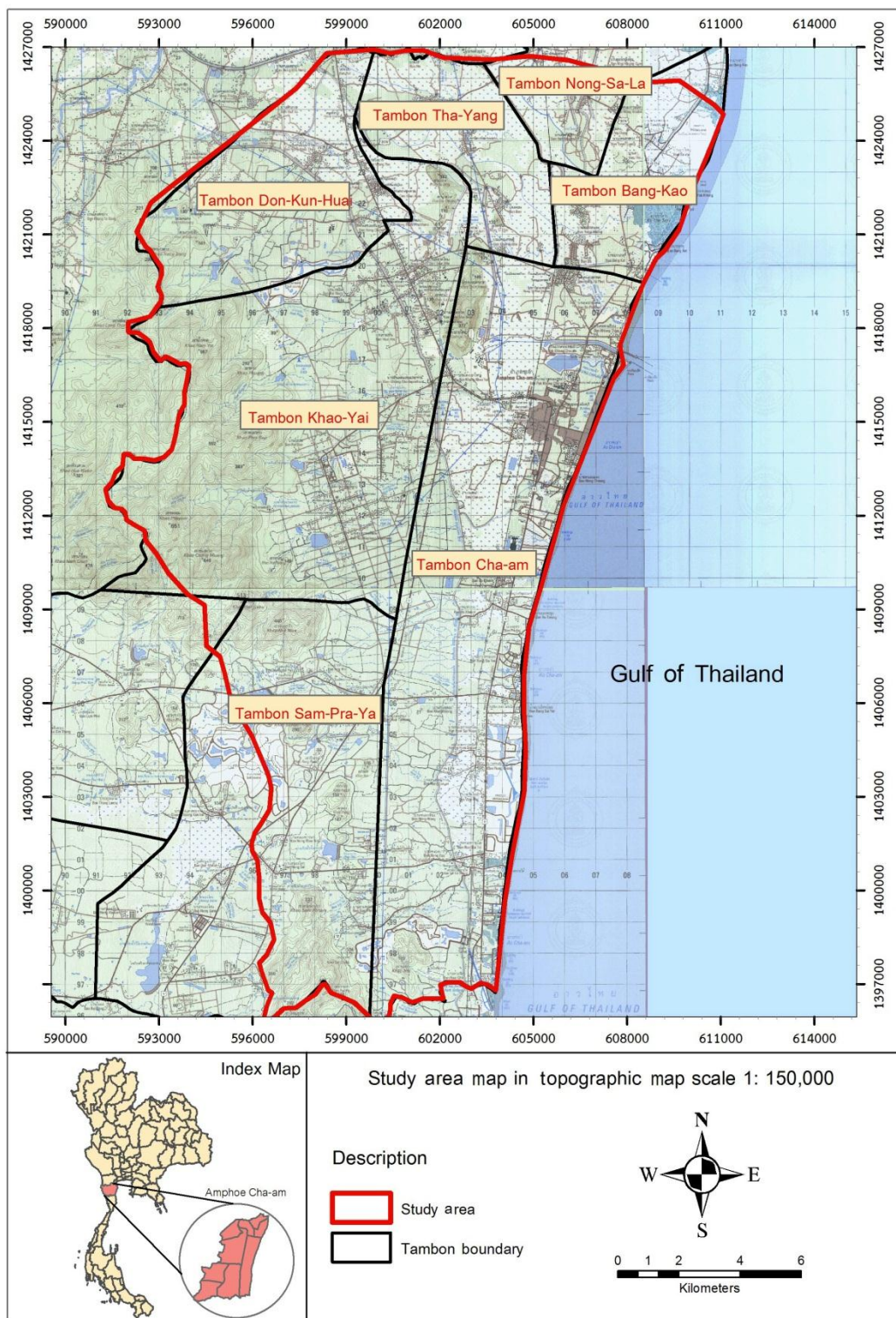


Figure 1.1 Topographic map of the study area (adapted from topographic maps edition No.1-RTSD L7018 series, sheet number 4934 I, 4934 II and 5034 IV).

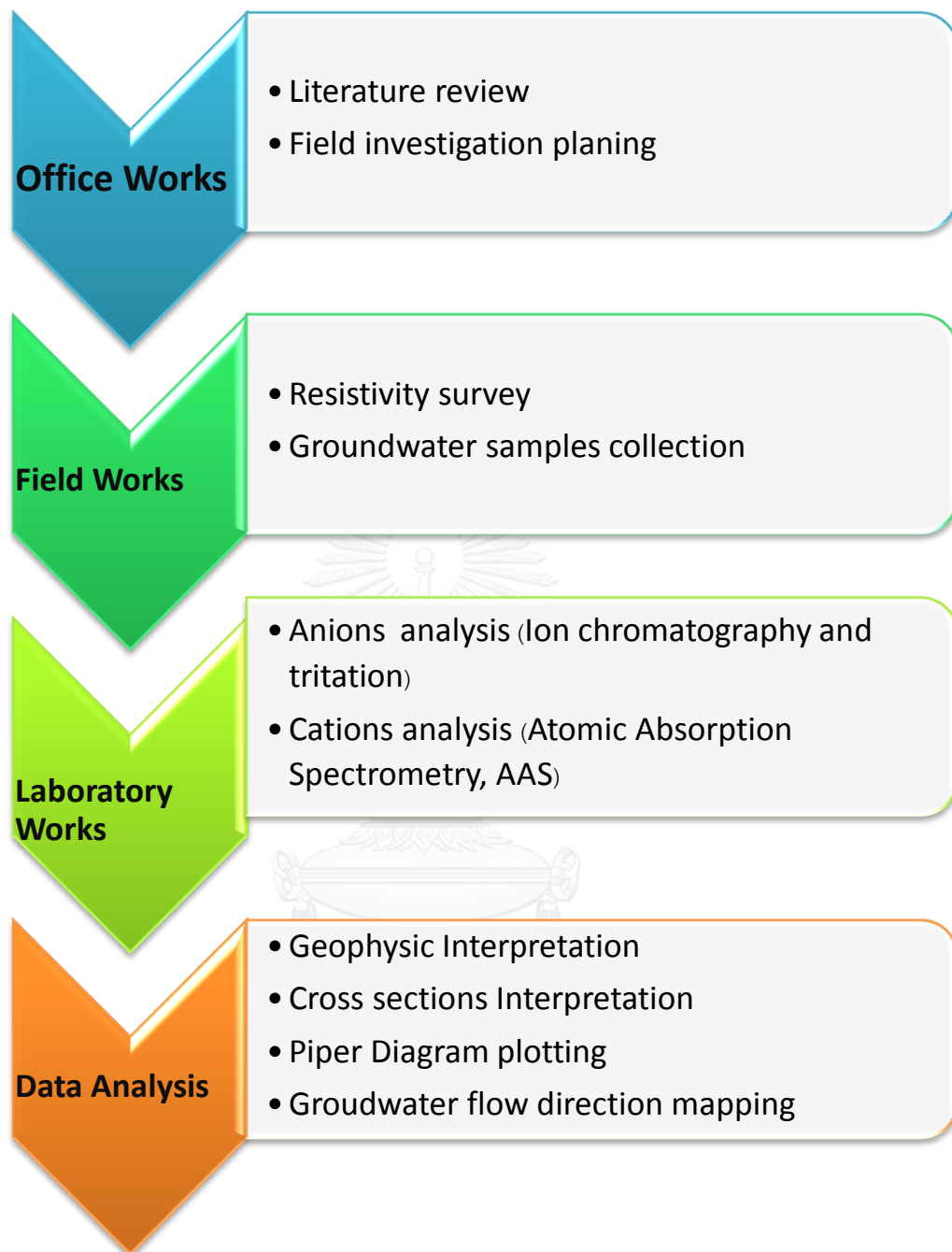


Figure 1.2 Flow chart of the research methodology.

1.6 Previous works

In Thailand, research of seawater intrusion is not widespread, especially the study by using geophysical and hydrochemical data together. The research that related to the study but using another method for examples, the mathematical model and physical modeling.

Bureau of Groundwater Potential Assessment, Department of Groundwater Resources (2011) compared the advantage and disadvantage of geophysical survey by 2 methods, 1 dimension resistivity; Vertical Electrical Sounding (VES) and 2 dimension resistivity survey for investigation fresh aquifer in the area that has a saline aquifer at Tumbon Namphong, Amphoe Namphong, Changwat Khon Kaen. The result of both methods can be classified resistivity and compared with borehole sampling data. Advantages and disadvantages can be summarized as follows; 1 Dimension method, the advantages are clearly separation between layers of sediment, rocks and saline water layers, explore the depths more than 200 meters and ease for moving exploration equipment. Disadvantages are unable to explore clay layers thickness, saline water layer cover on the top, takes a long time to interpret, apparent resistivity of soil and rocks is not obviously. 2 Dimension method advantages are display different of low-high resistivity clearly and avoid the expected area of saline water area, disadvantages are spent a lot of time, space, equipment and people to explore and expensive equipment.

Santijareankamon et al. (2011) studied groundwater flow pattern model of Songkhla Municipality by using a mathematical model, which is one of the purpose in the study to determine the extent of chloride in the present water pumping rate, by using estimated pumping safe yield model and prediction of seawater intrusion into aquifer in case of the increasing pumping rate. The seawater intrusion model of Samilar aquifer showed a standard of chloride. The higher standard of chloride have been found in the area near the Gulf of Thailand and Boyang aquifer, Songkhla lake such as, momument of Prince Chumphon, Laeam Son Aon, Samilar beach, Chalatat beach and Shrine of the city god. The extent of seawater intrusion from the coastal of Songkhla Lake to inland is about 300 meters. If used water increase by 10 % per year, the boundary of chloride

concentrations will be greater than 600 mg/l in Boyang aquifer and it will move to inland about 75 meters in 10 years.

Viengjunda (2010) studied seawater intrusion and the control method by using physical modeling created in the laboratory. The study consists of a line of groundwater well to compress fresh water, creating well pumping seawater out along the coastal and building an underground barrier. The result testing of natural condition and calculation from the relation of Ghyben-Herzberg condition were consistent, i.e., the effects of groundwater pumping will make the interface of the seawater and fresh water rise to the groundwater well, but it depends on the pumping rate, seawater level and the difference between seawater and fresh water. The compression fresh water 10 % of fresh water recharge rate would result in the interface between seawater and fresh water move to the coastline. The effectiveness of groundwater barrier depends on the depth of barrier that under the seawater level. The result showed that the depth of barrier is at the same level of seawater which is the most effective groundwater barrier.

Department of Groundwater Resources (2011) studied assessment of groundwater dewatering, seawater intrusion to prevent and correct the problem. Case study at Tumbon Tapra, Amphoe Mueang, Changwat Khon Kaen, because this area is supported by rock salt of Mahasarakham formation, so there is a high risk of being intrudes with saline water below. Many of the surveys were used in the project, one of them is the resistivity survey method at least 100 points, depth less than 200 meters/point. The results of interpretation, total of 112 points are the brackish-saline 26 points (23 %) and fresh water 86 points (77 %). Brackish aquifer located at Tumbon Mueang kao, Tumbon Phralub, Tumbon Donhun, Tumbon Thapra, Tumbon Buengnian, Amphoe Mueang, Changwat Khon Kaen and Tumbon Phonamg, Tumbon Nongbua, Tumbon pang, Amphoe Kosumpisai, Changwat Mahasarakham. The depth of brackish layer is in the range of 1 to 200 meters from the display imaging intrusion of saline water with geophysical techniques in less than 10 lines, 500 meters/line. The interpretation has been shown in cross section with the chemical analysis data of water samples.

Sakunrat et al. (2007) studied the severity of seawater intrusion into aquifer in case of groundwater quality changed in the Songkla Lake, Hatyai Basin. Groundwater quality had been analyzed alkaline-acid, turbidity, total dissolve solid, asperity, salt, chloride, sulphate, iron and manganese. The results showed that there was contamination of saline water in the study area but less quantities, which is not salty tastes as the problem continued to consumer.

For the international, there are widespread study for seawater intrusion problem in the coastal area, such as studied history and evaluation of seawater intrusion in the period; case study at Mersin-Kazanli, Turkey and studied by using geophysical survey method in conjunction with the analysis of the chemical composition of groundwater; for example 2 case studies with the same method but difference study area in Korea and Tunisia.

Demirel (2004) studied history and evaluation of seawater intrusion is time period at Mersin-Kazanli, Turkey, where contains densely industrialized area. Towns and factories in this area have extensive demand from groundwater, thus causing increase seawater intrusion. The studied by measuring electrical conductivity of groundwater and collect groundwater samples to analyze periodically of wells. In the years 1970-1980, this coastal aquifer has balance between fresh water and seawater. When factory has been drilling add 13 wells and pumping water in large quantities, thus resulting in the intrusion of seawater. The results of groundwater analyses and electrical conductivity use to explain development and history of seawater intrusion up to the year 2000. In 1999, the wells were closed completely because of groundwater in alluvial aquifer has a high Cl_2 concentration over 3000 mg/l. After that the analysis data of the concentration of chloride were used to create an expansion of seawater intrusion and found that seawater had been moved forward to inland about 500 meters in the Northern part of the area. In 2001, new wells were drilled in > 1 km far away from old wells and the sea. The composition of groundwater is Mg-Ca- HCO_3 type that is appropriate to using in agriculture and industry.

Song et al. (2006) studied seawater intrusion in the coastal area of Byunsan, Korea by using Vertical Electrical Sounding (VES) method interpreted with chemical analysis of groundwater and lithology log data. A total 30 VES curves is showed mostly H type that divided into three types: high, intermediate and low conductive. In accordance with the noticed resistivity values of the most conductive is in weathered layer. Furthermore, when based on TDS levels and HCO_3/Cl and Ca/Na molar ratios was found that 15 monitoring wells can separated into 2 groups: low HCO_3/Cl and Ca/Na ionic ratios corresponds highly conductive area and high ratios coincided with low conductive area, which low resistivity and low ionic ratios represented effects of seawater intrusion.

Kouzana et al. (2010) studied seawater intrusion at the coastal of Korba, Tunisia by using groundwater analysis and 38 Vertical Electrical Sounding (VES) points. Winsev software was carried out to interpret VES data with lithologic log data, and showed the results in iso-resistivity maps of seawater intrusion and geo-electric sections in the area. They were found that the boundary line in iso-resistivity maps showed different resistivity values that represented dry layer, fresh water saturated layer, brackish water and saline water saturated layer. Low resistivity of seawater is contrary to resistivity of fresh water thus VES can be used find the Interface zone of seawater and fresh water. The results of geo-electric sections founded that seawater move forward to inland approximately 3 kilometers. Diar El Hajjej, Garaet Sassi and Takelsa-Korba show high chloride concentrations in groundwater that represents these areas have influenced of seawater intrusion.

CHAPTER 2

THEORICAL BACKGROUND

2.1 Groundwater system in coastal aquifers

2.1.1 The hydrologic cycle

Groundwater is the water situated beneath surface in fractures of rocks pore spaces of sediments (The Royal Institute, 2011). Groundwater is hide natural water resource that carry larger quantity than surface water resources. More than 98% of the available fresh water is groundwater, which far exceeds the volume of surface water. Water in the world has different state and shape, continuous circulation circuit is called the hydrologic cycle or water cycle (Figure 2.1). Atmospheric or Meteoric water is in vapor state as cloud or haze and will be transformed into rain, precipitation, snow falling down to the earth when temperature is declined. Part of the liquid water call surface water, that will flow on surface to lower terrain such as swamp, stream, river, sea and ocean which eventually will be evaporated back to the atmosphere. The other part of the liquid water is called subsurface water, that infiltrate through the cavities of soils and rocks downward to lower layer or lower pressure area and eventually to river or sea. Subsurface water is divided into 2 parts; the first is situated between surface and water table. It is known as zone of Aeration or Unsaturated zone. This water type will infiltrate and situate in space of soil and rocks together with some air and it will be evaporated back to the atmosphere or consumed by plants and released to the atmosphere. The second is water that will infiltrate and store in pore spaces of soil and rock layers, the soil and rock layers saturated with water which is the zone of saturation. Water stored in the zone of saturation is known as groundwater. The top of this zone is called the water table. Then groundwater flow through the layers of rock and soil and discharges to a pond, lake, stream, river or ocean. Water flowing in a stream can be come from overland flow or seeped groundwater. The groundwater contribution to stream is base-flow, while the total flow in a stream is runoff. Furthermore, water stored in ponds, lakes, rivers and streams are surface water (Fetter, 2001).

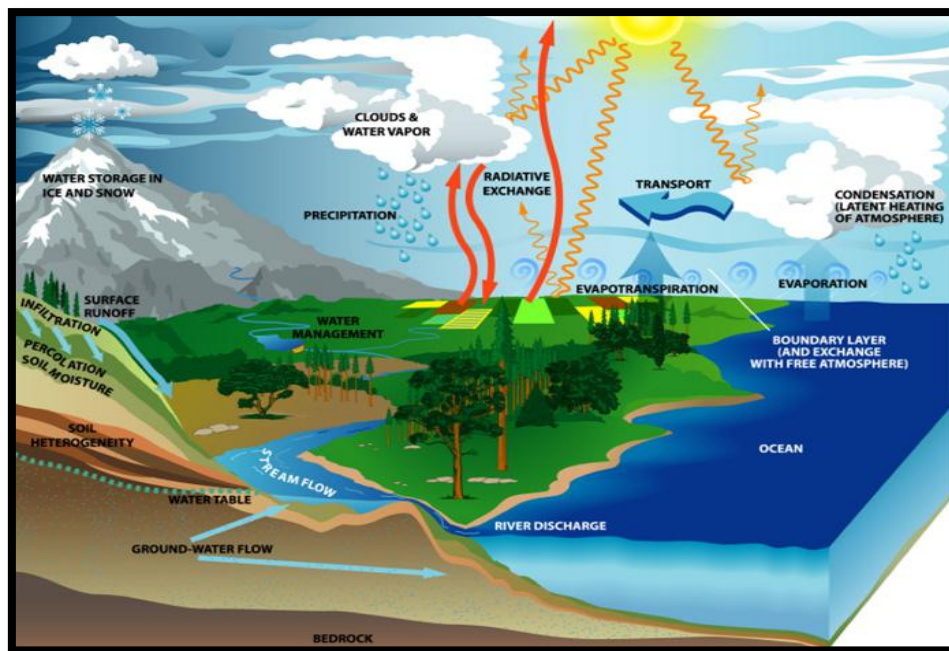


Figure 2.1 The Hydrologic Cycle. (National Aeronautics and Space Administration, 2010)

2.1.2 Coastal aquifer

An aquifer is defined as "a body of rock or regolith sufficiently permeable to conduct economically significant quantities of groundwater to springs or wells" (Skinner *et al.*, 1999). Importantly, the layer must be in the saturated zone, pore spaces and fractures in rocks of layers filled with water. Thus, aquifer in the coastal area that contacts with the sea is called Coastal Aquifer.

2.1.2.1 Badon Ghyben-Herzberg principle

In the early nineteenth century, 2 scientists are W. Baydon-Ghyben (1888-1889) and A. Herzberg (1901) studied a relation between fresh and saline groundwater in the coastal area, Europe. A study of both not involved, but the results of the study found a match, unconfined coastal aquifer will found saline water stay below the fresh water because density of saline water is greater than fresh water. The interface of fresh water and saline water is a transition zone, which is under the mean sea level about 40 times of the fresh water height (Figure 2.2). It is a hydraulic balance of fresh water and

saline water with different densities. The equation that describes is called the Ghyben-Herzberg relation (Fetter, 2001).

$$z = \frac{\rho_f}{\rho_s - \rho_f} h_f$$

Where (2.1)

Z is the depth to the saline water interface below sea level (L; ft or m)

h_f is the elevation of the water table above sea level (L; ft or m)

ρ_f is the density of fresh water (M/L³; g/cm³)

ρ_s is the density of saline water (M/L³; g/cm³)

For general seawater $\rho_s = 1.025 \text{ g/cm}^3$ and fresh water $\rho_f = 1.000 \text{ g/cm}^3$ will be the equation (2.2)

$$z = 40h_f$$

(2.2)

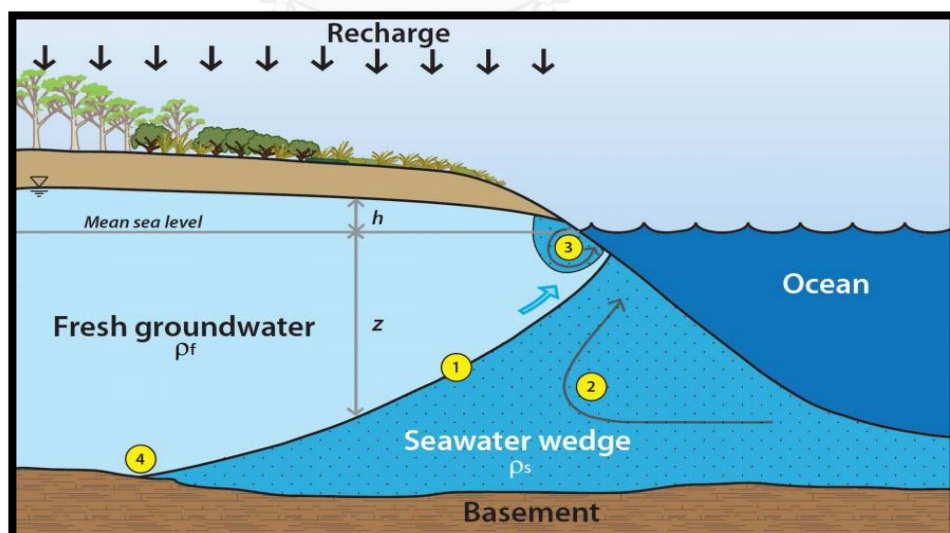


Figure 2.2 Relationship of fresh water head and depth to seawater interface (Werner *et al.*, 2013).

2.1.2.2 Seawater Intrusion Problems

Saline is a simple and common contaminants that found in groundwater. Seawater intrusion problem occurs when fresh water mixed or replaced by seawater in aquifer, It is happens in both deep and shallow aquifer. In the deep aquifer, the saline intrusion occurred before geological processes or saline water from rock salt layer below. For the shallow aquifer contamination may be come from waste water released from human activities. In coastal aquifer which is hydraulic continuity between groundwater and seawater, it might be seawater intrusion directly. Generally, saline water in aquifer may be derived from several sources such as,

- Seawater intrusion directly in the coastal area.
- Seawater intrusion into the coastline in the past and stored it in the rock layers.
- Salt from rock salt layers, salt dome or salt crystals are inserted in the rock.
- The increasing salt concentration in the water due to the evaporation in the lagoon, playa, etc.
- Excess water from irrigation and flow back into the aquifers.
- Wastewater from humans.

Seawater intrusion into coastal aquifers is a natural phenomenon. Groundwater flow direction into the sea, due to the density of seawater is greater than fresh water in the ground water. Therefore, groundwater is on top of the seawater and push seawater back out to the sea. If human still pumping a large quantity of ground water, the fresh water volume must be decreased. Finally, seawater can be replaced fresh water area (Figure 2.3) (Ramingwong, 2003).

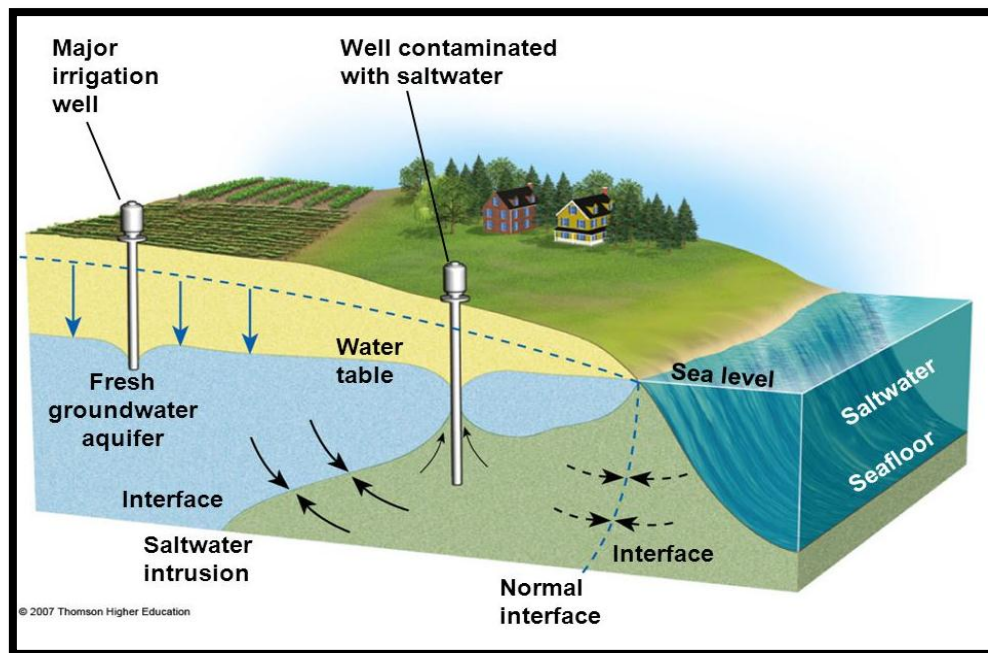


Figure 2.3 Seawater Intrusion in coastal aquifer (Uzma, 2014)

2.2 Hydrochemistry

Development of groundwater to utilize, the water quality and quantity are equal. Physical properties and Chemical properties of groundwater are indicator that the water is suitable for use in consumer, industrial and agricultural, much less how. In addition, the studied of ground water quality especially the dissolved elements that can be described a ground water occurrence and movement history. Normally, ground water is composed of a dissolved elements, the number of elements may in a range from 25 mg/l for spring water to 300,000 mg/l in brine water. The type and the number of elements depend on the environment, movement and the origin of groundwater. Typically, the quantity of elements in groundwater is more than surface water, because the groundwater can be contacted with minerals in the rock that is groundwater reservoirs. The dissolved elements in groundwater depend on mineral properties that is a component of the aquifer as mineral water soluble hard or easy. In addition, it also depends on the duration of groundwater storage or contact with these minerals. Therefore, if the ground water moves slowly, there will be a high quantity of elements.

That is why the quantity of elements in the groundwater increasing with depth. Generally, the groundwater near the surface or in shallow level are high quantity of bicarbonate, because of carbon dioxide that derived from decomposed of organic matter in the soil. The quantity of elements in groundwater will increase with depth, especially the quantity of chloride. General elements that found in the groundwater show in Table 2.1 (Ramingwong, 2003).

Table 2.1 Dissolved constituents (Davis & DeWiest, 1967)

Major Constituents (1.0 to 1000 ppm)	
Sodium	Bicarbonate
Calcium	Sulfate
Magnesium	Chloride
Silica	
Secondary Constituents (0.01 to 10.0 ppm)	
Iron	Carbonate
Strontium	Nitrate
Potassium	Fluoride
Boron	
Minor Constituents (0.0001 to 0.1 ppm)	
Antimony*	Lead
Aluminum	Lithium
Arsenic	Manganese
Barium	Molybdenum
Bromide	Nickel
Cadmium*	Phosphate
Chromium*	Rubidium*
Cobalt	Selenium
Copper	Titanium*
Germanium*	Uranium
Iodide	Vanadium
	Zinc
Trace Constituents (generally less than 0.001 ppm)	
Beryllium	Ruthenium*
Bismuth	Scandium*
Cerium*	Silver
Cesium	Thallium*
Gallium	Thorium*
Gold	Tin
Indium	Tungsten*
Lanthanum	Ytterbium
Niobium*	Yttrium*
Platinum	Zirconium*
Radium	

2.2.1 Physical properties (Promma, 2013)

- Acid / Base (pH):

The pH is an indicator of acid-base of water, varies between 0-14. The water has a pH value less than 7.0 is acidic, above 7.0 is base. Generally, pH of groundwater is 5.5 to 8.0.

- Temperature:

Temperature is an important factor in helping to accelerate the reactions that may occur in the water. But in general, the groundwater temperature is constant.

- Electrical Conductivity (EC)

The Electrical Conductivity of groundwater depends on the quantity of total dissolved solids (TDS). Therefore, electric conductivity measurement is quick and easy method to find the quantity of TDS that found in the groundwater. The unit of measure is Microsiemens per centimeter ($\mu\text{S}/\text{cm}$) or Micromhos per centimeter. Generally, groundwater has EC between 30 to 2,000 μS .

- Taste and Odor

Taste of groundwater is caused by different soluble substance. For example Sodium Chloride (NaCl), Sodium Sulfate (Na_2SO_4) and Calcium Sulfate (CaSO_4) etc. There are a variety of tastes such as salty, bitter etc. It depends on the quantity and type of soluble substance.

Odor is a result of the soluble organic compounds in groundwater such as Phenols, Hydrogen Sulfide etc.

- Color

Color in groundwater can be divided into 2 types: true color and appearance color. True color is caused by soluble elements in groundwater and the appearance color caused by various suspended in groundwater.

- Turbidity

Turbidity is caused by suspended solids in groundwater. Normally, groundwater is clear but the turbid water represents the contaminants.

2.2.2 Chemical properties

The dissolved elements in the groundwater may be invisible as physical characteristic. Nevertheless they may affect directly the quality of groundwater (Department of Groundwater Resources, 2001).

- Calcium (Ca^{2+})

Normally, Calcium is found in approximately 10 to 100 mg/l in groundwater. The important source of Calcium is Calcite, Aragonite, Dolomite, Anhydrite, Gypsum, Apatite, Fluorite, Feldspar, Amphibole and Pyroxene minerals.

- Magnesium (Mg^{2+})

Magnesium is usually found less than Calcium because important sources of Magnesium such as Dolomite mineral (CaMgCo_3) slowly dissolve. In addition, the crust has quantity of Calcite greater than Magnesium. Other source of Magnesium is Olivine, Biotite, Hornblende, Augite, Serpentine, talc and Diopside minerals. In groundwater, magnesium is found approximately 1 to 40 mg/l.

- Sodium (Na^+)

Normally, Sodium is found in approximately 1-20 mg/l. If the groundwater has Total dissolved solids up to 1,000 mg/l could be as high as Sodium 100 mg/l. The important source of Sodium is Plagioclase, Feldspar, Halite and some clay minerals.

- Potassium (K^+)

Potassium is found in a small amount in groundwater, approximately 10 mg/l. The area that found Potassium in high quantity is evaporation deposits area such as Silvite mineral (KCl) or the area that use of fertilizers in agriculture. Moreover, source of Potassium is Orthoclase, Microcline and Biotite minerals.

- Iron (Fe)

Iron is found in a small amount in groundwater when compare to other elements, approximately 1-20 mg/l. Iron cause enormous effect on water utilization. The water has a strong odor and rust stain on household utensils and

pipeline. There are 2 type of dissolved iron, Ferrous (Fe^{2+}) and Ferric (Fe^{3+}). Ferrous can dissolves in water and unstable, when contact to the air, it will be change to Ferric that can't dissolves in the water. Source of Iron is Pyroxene, Amphibole, Magnetite, Pyrite, Biotite, and Garnet minerals.

- Chloride (Cl^-)

The Chloride is found as Iron, 1 to many thousand mg/l in natural water. Many soluble Chlorides in the water cause briny or salty taste. Due to Chloride dissolved easily and it is an inert element for exchange or reaction. Thus, the Chloride in groundwater is stable and not crumbles in natural processes.

- Sulfate (SO_4^{2-})

Sulfate is found less than Chloride. The important source of Sulfate is Gypsum, Anhydrite or oxidation of Sulfide minerals. If high Sulfate contents, the water tastes bitter.

- Bicarbonate (HCO_3^-)

Bicarbonate is found in natural water particularly in groundwater, pH above 7. It has no effect on health, but as a result in agriculture and water treatment in term of hardness elimination process.

- Nitrate (NO_3^-)

The important source of Nitrate is organic decay such as trees, grass etc. Chemicals sources are waste water from factories and fertilizer. High nitrate in the water is dangerous to human especially for baby i.e. it can cause Blue baby disease. Generally, Nitrate is in groundwater approximately 0.1 to 10 mg/l. However, in the agricultural area may be found Nitrate up to 500 to 600 mg/l because of fertilizer.

- Total Dissolved Solid (TDS)

Total Dissolved Solid is a value of all elements and components in the water. It is an indicator of water quality. Normally, the water having total dissolved solid value less than 500 mg/l is good quality. World Health Organization classify the preferable level of TDS in water are as follow;

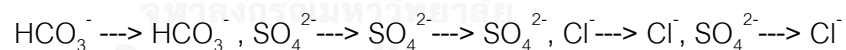
<300 mg/l rating is excellent.

300-600	mg/l	rating is good.
600-900	mg/l	rating is fair.
900-1,200	mg/l	rating is poor.
>1,200	mg/l	rating is unacceptable.

2.2.3 Hydrochemical Facies

The term "Hydrochemical Facies" was first used in the study geochemical of sediments in Union of Soviet Socialist Republics (Smor, 1967). Hydrochemical Facies are grouped, according to major ions in groundwater i.e. cation and anion. A group of cations is Na^+ , K^+ , Mg^{2+} and Ca^{2+} . A group of anions is Cl^- , SO_4^{2-} and HCO_3^- . Hydrochemical Facies are a classification of chemical characteristic of groundwater in hydrologic system. Types and concentration of ion dissolved in groundwater are the result of a chemical process that reflects the lithology and hydrologic flow patterns (Back, 1960).

Generally, the amount of major ions in groundwater has evolved with age and the flow distance of groundwater, due to the dissolution of minerals in the rocks where groundwater flowed through (Freeze & Cherry, 1979). The evolution of major ions in flow system as follows;

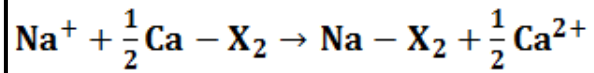


2.2.3.1 Cation exchange of the salt / fresh water interface

Ion exchange processes occurs when the concentration of either cation or anion in solution increased. It moves from the solution onto the surface of particles and separated the adsorbent ion to the solution to keep the balance of charge. Ion exchange processes are beneficial for study seawater intrusion into the coastal aquifer, as coastal aquifer has been changed recharge-discharge balance throughout. It is related with groundwater hydrochemistry and dynamic movement of the seawater interface (Ghiglieri *et al.*, 2012).

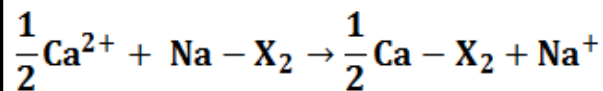
In the coastal areas, the ion composition of fresh water is regularly dominated by Ca^{2+} and HCO_3^- , cause of the calcite dissolution. The ions composition of

seawater is dominated by Na^+ and Cl^- . When seawater intrudes into fresh water aquifer, the cation exchange has occurs (Appelo & Postma, 2005):



(2.3)

It is reverse cation exchange reaction, i.e. release Ca^{2+} and adsorb Na^+ (variant "X" indicates soil exchanger). The reverse process of intrusion is freshening or re-freshing, direct cation exchange by releases Na^+ and adsorbs Ca^{2+} . Occurring when the fresh water that is calcium bicarbonate water type flushes a salinized aquifer (Appelo & Postma, 2005):



(2.4)

2.2.3.2 Piper Diagram

Piper diagram is a popular diagram that use for presentations of hydrochemical of water. Piper diagram shows concentration of ions from water samples analysis as milliequivalents per liter (meq/L) of the total anions and cations. The most of major ion in waters are Na^+ , K^+ , Ca^{2+} , Mg^{2+} , Cl^- , CO_3^{2-} , HCO_3^- and SO_4^{2-} . Diagram consist of three parts, the first is trilinear diagram below on the left shows the percentage of cation, consisting of Mg^{2+} , Ca^{2+} and group of $\text{Na}^+ + \text{K}^+$. The second trilinear diagram on the right shows the percentage of anion, consisting of Cl^- , SO_4^{2-} and group of $\text{CO}_3^{2-} + \text{HCO}_3^-$ and the last is rhombohedron shape diagram in the center for project point from both trilinear diagrams. Figure 2.4 shows the piper diagram that is used for water chemistry studies (Piper, 1944).

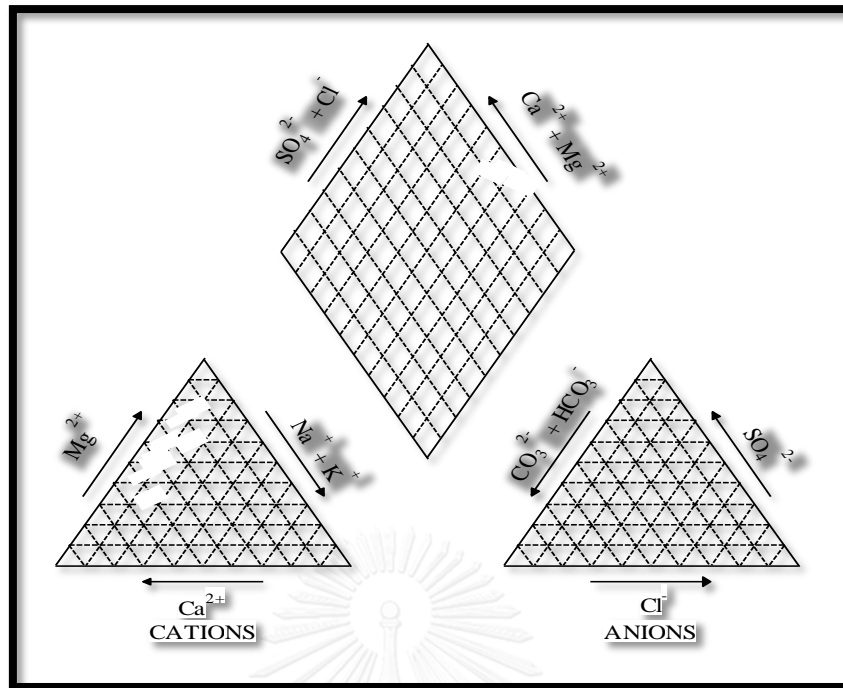


Figure 2.4 Piper diagram of water chemistry studies (Piper, 1944)

How to plot points by calculating the equivalents per million (epm) or milliequivalents per liter (meq/l) of cation and anion to the sum of epm of cation equal 100 %, the sum of epm of anion equal 100 % too. Calculated cation and anion into a percentage, then find the relationship of the two values. The percentage of total cation will be one point on the left trilinear diagram, anion on the right trilinear diagram. Projection the points of both cation and anion to rhombohedron shape diagram a point of the intersection lines is represent the chemical composition of water.

Furthermore, piper diagram can classify the chemical composition of water in the form of Hydrochemical facies which each have a composition of an important cations and anions differently. (Figure 2.5)

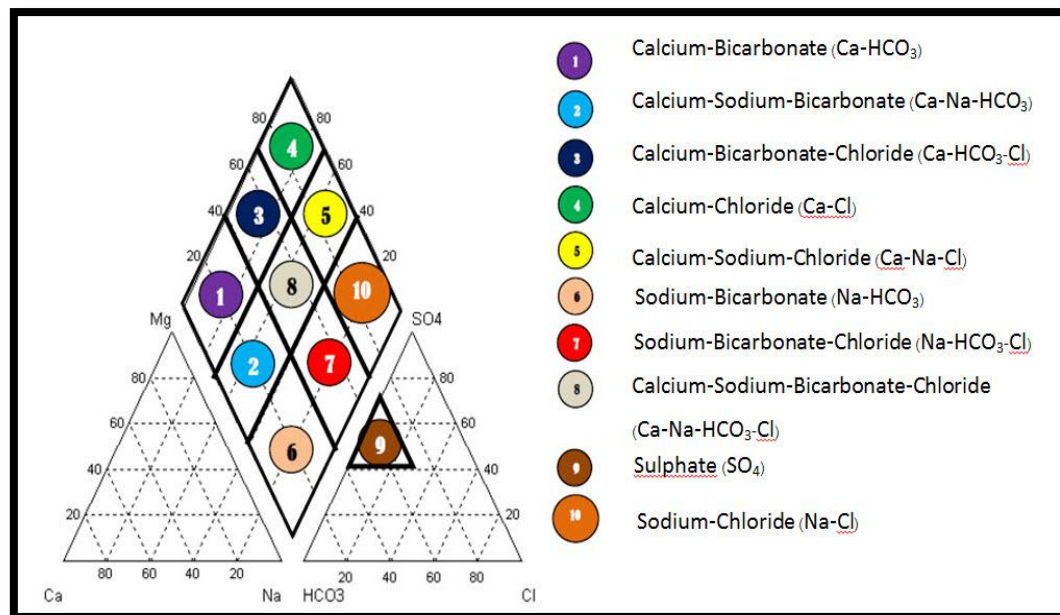


Figure 2.5 Hydrochemical Facies classification of water (Galloway & Kaiser, 1980)

2.2.3.3 Hydrochemical Facies Evolution (HFE) Diagram

HFE Diagram is a square diagram that describes seawater intrusion processes based on the evolution of hydrochemical facies of water, proposed by Gimenez Forcada (2010) and developed by Stuyfzand (1993). Basic criteria of HFE diagram is consider only the percentage of major ion in hydrochemical processes that related with dynamic of seawater intrusion interface, consist of Na^+ , Ca^{2+} , Cl^- , HCO_3^- and SO_4^{2-} . Ions are in the secondary position of end members (fresh water and seawater) when the discussion does not take into account, case of SO_4^{2-} , Mg^{2+} and K^+ . The percentage of SO_4^{2-} and HCO_3^- are considered using a dominant ion because both can represent major anion in the recharge water (fresh water). The percentage of Mg^{2+} in the exchange processes is not counted because it is an abnormal behavior in the ion exchange reactions. The percentage of K^+ is combined with Na^+ because the concentration of K^+ is very low when compared with Na^+ (Giménez-Forcada, 2010).

The diagram Figure 2.6, the x-axis represents percentage of $(\text{Na}^+ + \text{K}^+)$ and Ca^{2+} as meq/L that identify base-exchange reaction. The percentages are calculated from the total of cations (comprising Mg^{2+}). The representative point, selected from more than the concentration percentages, i.e. plot the percentage of Ca^{2+} from

$\%Ca^{2+} > \% (Na^+ + K^+)$ or plot the percentage of $(Na^+ + K^+)$ from $\% (Na^+ + K^+) > \%Ca^{2+}$. The y-axis represents of anions, percentage of Cl^- indicates seawater end member, as, percentage of HCO_3^- or SO_4^{2-} (depended on dominant anion in fresh water, by select show more percentage ion) represents the characteristic of recharge water. Diagram can be classified hydrochemical facies by considered the percentage of each ion, presenting 16 facies (32 facies if Mg^{2+} and SO_4^{2-} involve with HCO_3^- and Ca^{2+}) (Giménez-Forcada & Sánchez San Román, 2015). There are 4 heteropic facies (percentage of cation and anion $> 50\%$) consist of Na- HCO_3^- , Na-Cl, Ca- HCO_3^- and Ca-Cl. Furthermore, the characteristic in term "Mix", mix indicated either percentage of cation or anion $< 50\%$.

Diagram shows conservative mixing line (CML) between seawater and fresh water. The end point of seawater is a chemical composition analysis of seawater. The end point of fresh water composition selects from highest percentage of anions (HCO_3^- or SO_4^{2-}) and cations (Ca^{2+} or Mg^{2+}) recharge. The CML is divided seawater intrusion processes into 2 phases, i.e. intrusion phase (SwI) and freshening phase (FwI) (Giménez-Forcada, 2014). Intrusion phase is on the right of diagram, below the CML. When seawater intrusion, water will increase salinity (line I) and urge a reverse exchange reactions (line II). The evolution of water along the line III until near seawater, the sequence of facies is 13-14-15-16-12-8-4 respectively. On the other hand, freshening phase is on the left of diagram, above the CML. When the fresh water flushes saline water (line I') contribute to direct ion exchange reactions (line II'). The evolution of water along the line III' until near recharge fresh water, the sequence of facies is 4-3-2-1-5-9-13 respectively. The facies in the center is either the SwI or FwI phases, depending on the position of a point against the CML.

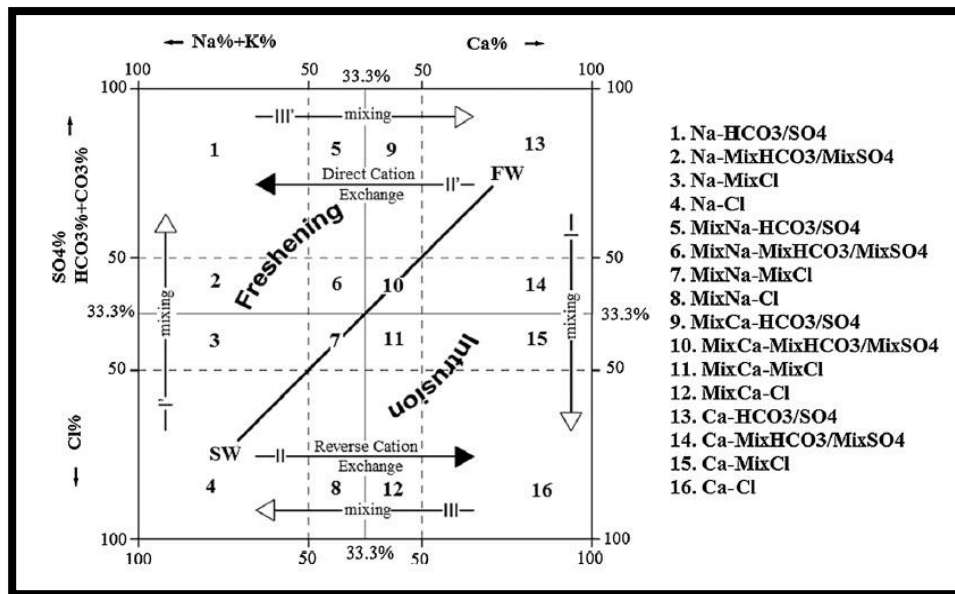


Figure 2.6 Hydrochemical Facies Evolution (HFE) Diagram (Giménez-Forcada, 2010)

2.3 Vertical Electrical Sounding

Geophysical surveys are the study to explore the subsurface of the Earth through the measurement of material physical properties. The survey is based on the principle, different materials different physical properties. In general, the survey will measure at the surface and interpreted to various depths below the surface. The importance of geophysical surveys is anomaly that causes by the different of material physical properties, then bring the anomaly values to interpret for geologic structure. In this study have been chosen the several geophysical survey methods which is the electrical resistivity survey (DC-resistivity survey).

Electrical resistivity survey is the electrical surveys that applied electrical theory to find subsurface geological structures. The present resistivity survey has 4 patterns of survey, i.e. 1 Dimension, 2 Dimension, 3 Dimension and 4 Dimension. 1 Dimension (1D) is a vertical sounding survey to get the data in the subsurface. 2 Dimension (2D) is a survey to create the profiling in vertical and horizontal. 3 Dimension (3D) is a survey to create the model in the subsurface. 4 Dimension (4D) is similar to 3D but increasing time axis to compare a model when times change. In this study uses 1dimension pattern, also known as Vertical Electrical Sounding method.

2.3.1 Theory of electrical resistivity survey

The electrical resistivity survey is a method of measuring the electrical potential at a point on the ground surface caused by the emission of direct current flow through the subsurface. Then the voltage is calculated, the resistance is determined, and materials interpretation is performed. The basic principle of the survey is the application of basic electricity (Figure 2.7).

2.3.1.1 Basic Electricity

An electrical circuit consists of a battery, a resistor, and connecting wires. Electric current flows from the anode of the battery through a connecting wire to the resistor, and then flows back to the cathode. An ammeter measures current flow out and a voltmeter measures the head and end of the resistor, which is a value of current and potential difference between the head and end of the resistor. This means that the potential at the point where current flows into the resistor is less than the potential at the point that flows out of the resistor, due to the electrical resistance occurring in the resistor (Figure 2.8).

The electric current flow occurs due to the driving force of electric charge, known as electromotive force (*emf*), the unit is *volt*. Moving of charge through the wire is called *current*. That is calculated from the equation:

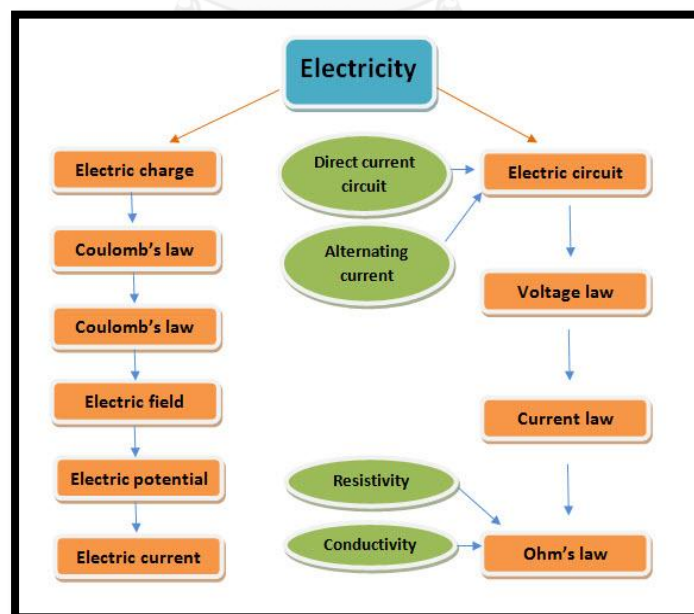


Figure 2.7 Theory and primary concept about Resistivity Survey (Satarugsa, 2007).

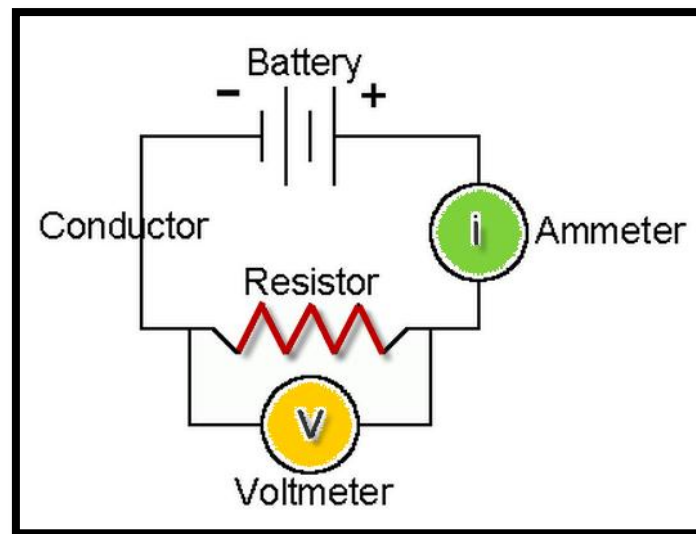


Figure 2.8 A simple electrical circuit

$$I = \frac{nq}{t}$$

(2.5)

When

I : Current (ampere; A)

n : Amount of charge

q : Charge (coulomb)

t : Time (second)

When considering the electric current flow through material in the subsurface, material cross-sectional area is A :

$$J = \frac{I}{A}$$

(2.6)

When

J : Current density (ampere/meter²; A/ m²)

A : Cross-sectional area (meter²; m²)

This means that the current value unchanged, if a larger cross-sectional area, the current density will be decrease. But if a smaller cross-sectional area, the current density will be increase. Because of the charges must be packed in smaller area to move the same amount.

Georg S. Ohm, 1787-1854 discovered that electric current direct proportional to voltage V , but reverse proportional to resistance R :

$$i \propto \frac{V}{R}$$

(2.7)

When changing proportional symbol to equal symbol, according to mathematical rules to enter the coefficient that represents the linear relationship. Ohm founded that the coefficient is 1. The relationship is known as Ohm's Law:

$$i = k \frac{V}{R} = (1) \frac{V}{R} = \frac{V}{R}$$

(2.8)

When considering the wire that shape is cylinder found the resistance (R) direct proportional to length (L), but reverse proportional to cross-sectional area A . That means if the length increases, the resistance will increases. When the current moves far up, it will cause more resistance. But if greater cross-sectional area, the resistance will decrease because of the current flows more convenient. Therefore, the relationship is:

$$R \propto \frac{L}{A}$$

(2.9)

When changing proportional symbol to equal symbol, according to mathematical rules to enter the coefficient that represents the linear relationship. In this equation defined as ρ and known as *resistivity*.

$$R = \rho \frac{L}{A}$$

(2.10)

$$\rho = R \frac{A}{L}$$

(2.11)

When

ρ : Resistivity (Ohm-meter; Ω -m)

R : Resistance (Volt; V)

A : Cross-sectional area (meter; m)

L : Length (meter; m)

2.3.1.2 Current flow in homogeneous and inhomogeneous subsurface

From basic electricity mentioned above can be applied to explore the subsurface. By releasing the electricity through current electrodes that stamps on the ground surface, if subsurface is conductors that allows current to flow through, the potential difference can be measured by the potential electrodes. When we know the value of electric current and voltage, it can calculate the electrical resistance. However, resistance depends on resistivity of rocks and soil layers and length of electric current flow per cross-sectional area that the current flow through. This section describes the current flowing through rock and soil layers both homogeneous subsurface and heterogeneous subsurface.

- Homogeneous subsurface

When stamped 2 electrodes (C_1 and P_1) on the surface that in the subsurface has uniform resistivity (ρ), release the current from battery through electrode

C_1 into the subsurface. Then measure the voltage from electrode P_1 . It was found that the current flowing spread outward through subsurface in all directions, similar to surface of sphere. At this surface has equal potential and distance r from C_1 , it is known as equipotential surface (Figure 2.9). When considering this surface is a very thin shell or dr very short distance, then using the equation 2.8 and 2.10 will be defined potential difference (ΔV , dV) between distance dr as follows;

$$dV = iR = i \left(\rho \frac{L}{A} \right) = i \left(\rho \frac{dr}{2\pi r^2} \right)$$

(2.12)

When determining the distance between C_1 and P_1 is D , the potential difference (V) at P_1 must be compare to the potential at point infinite far away, potential difference (V) must be measure between 2 points. Determine potential at point infinite is zero, because it is too far away to receive the current (Figure 2.9). From the equation 2.12, V calculated from (Van Nostrand & Cook, 1966);

$$V = \int_D^\infty dV = \frac{i\rho}{2\pi} \int_D^\infty \frac{dr}{r^2} = \frac{i\rho}{2\pi D}$$

(2.13)

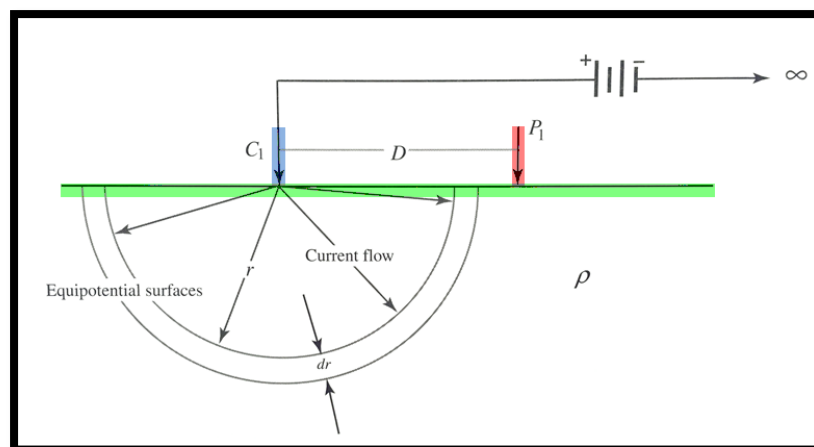


Figure 2.9 Single Point current source on the surface (incase homogeneous) (adapt from: Burger, 2006)

In case of the electricity current flows into subsurface by 2 current electrodes, C_1 and C_2 . When release the current from battery that is connected to both C_1 and C_2 , the current will flow from anode electrode (the source) to cathode electrode (the sink). Then use 2 electrodes (P_1 and P_2) stamped on the ground surface to measure the electrical potential difference between 2 electrodes (P_1 and P_2) (Figure 2.10). It will be able to calculate the electric potential of each electrode as follows;

$$V_{P_1} = \frac{i\rho}{2\pi r_1} - \frac{i\rho}{2\pi r_2}$$

(2.14)

$$V_{P_2} = \frac{i\rho}{2\pi r_3} - \frac{i\rho}{2\pi r_4}$$

(2.15)

Therefore, the potential difference between 2 electrodes (P_1 and P_2) is equal to;

$$\Delta V = V_{P_1} - V_{P_2} = \frac{i\rho}{2\pi r_1} - \frac{i\rho}{2\pi r_2} - \frac{i\rho}{2\pi r_3} + \frac{i\rho}{2\pi r_4}$$

$$\Delta V = \frac{i\rho}{2\pi} \left(\frac{1}{r_1} - \frac{1}{r_2} - \frac{1}{r_3} + \frac{1}{r_4} \right)$$

(2.16)

The equation for calculating the resistivity is;

$$\rho = \frac{2\pi\Delta V}{i} \left[\frac{1}{\frac{1}{r_1} - \frac{1}{r_2} - \frac{1}{r_3} + \frac{1}{r_4}} \right]$$

(2.17)

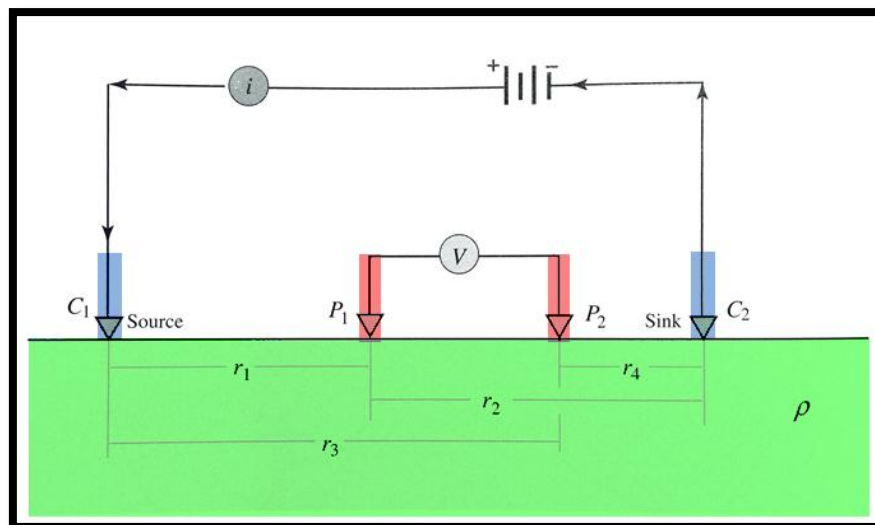


Figure 2.10 Two current electrodes and two potential electrodes (incase homogeneous)
(adapt from: Burger, 2006)

- Heterogeneous subsurface

In natural subsurface is not homogeneous throughout. It is a soil, sediments and rock layers that have different characteristics. When electric current flows through sediment or rock layer that has different resistivity, the current flow is distortedly orientation of flow lines (Figure 2.11). The equation of changing current flow line as follows (Hubbert, 1940);

$$\frac{\tan \theta_2}{\tan \theta_1} = \frac{\rho_1}{\rho_2}$$

(2.18)

The current flows from the first layer through the boundary of the second layer. If the first layer has resistivity value less than the second layer, orientation of currents flow line will bend into assume line that perpendicular to plain of boundary (Figure 2.11).

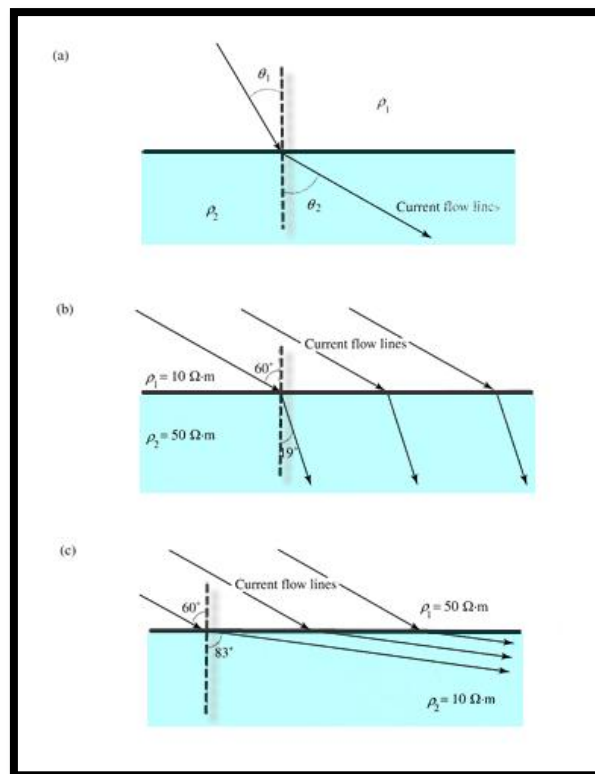


Figure 2.11 Refraction of current flow lines at boundary of different resistivity layers. (a) Explain equation 2.18. (b) refraction ($\rho_1 < \rho_2$). (c) refraction ($\rho_1 > \rho_2$). (adapt from: Burger, 1992)

From the equation 2.17 that assumed for determine resistivity of homogeneous subsurface. But in natural, the soil and rock layers is not homogeneous, thus definition new word that use for the resistivity survey in heterogeneous subsurface is apparent resistivity (ρ_a). The data from the survey is the apparent resistivity of many soil and rock types that the current flows through, is not the true resistivity of pure substance. The equation is the same as equation 2.17 changed only the variable on the left side shown as follow;

$$\rho_a = \frac{2\pi\Delta V}{i} \left[\frac{1}{\frac{1}{r_1} - \frac{1}{r_2} - \frac{1}{r_3} + \frac{1}{r_4}} \right]$$

(2.19)

2.3.2 Electrode configurations

Electrode configuration is stamping electrodes on the ground surface with different configurations. Each electrode configuration will be different in depth, including the formula for calculation apparent resistivity will be different. Generally, the electrodes of resistivity survey are consist of current electrode of 2 electrodes (C_1 and C_2 or A and B) and potential electrode of 2 electrodes (P_1 and P_2 or M and N). Electrode configurations have many pattern, there are both advantage and disadvantage. Electrode configurations are divided into 2 groups, linear configuration and non-linear configuration. However, the prevalence is linear configuration. From Standard of ASTM D6431-99 (2010) found the hydrogeology survey used 3 configurations, Wenner configuration, Schlumberger configuration and Dipole-dipole configuration (Figure 2.12). The determination apparent resistivity of 3 configurations will be used equation 2.19 in calculation. From equation 2.19, term in the bracket is term of constant K that is geometric factor. Represented K in equation will be:

$$\rho_a = \frac{2\pi\Delta V}{i} K$$

(2.20)

By each configuration will have a different K . The detail of each configuration and measuring apparent resistivity of each configuration as follows;

2.3.2.1 Wenner configuration

Wenner is the name of Frank Wenner, 1874-1915. Wenner configuration, 4 electrodes space is equal. By using the electrodes C_1 and C_2 that is outside release the current into the subsurface. Electrodes P_1 and P_2 is inside, it is measure different potential. Assuming the same space equal as a variable, it will have $3a$. The midpoint of the survey is between electrodes P_1 and P_2 (Figure 2.12).

Represent $r_1 = a$, $r_2 = 2a$, $r_3 = 2a$ and $r_4 = a$ into the equation 2.19, the apparent resistivity at the midpoint of the survey is

$$\rho_a = \frac{2\pi a \Delta V}{i}$$

(2.21)

Thus, the constant K of Wenner $K = 2\pi a$ configuration is;

Advantages of Wenner configuration are simple, the spacing a not too far for ability of tool to measure the voltage and easy to use formula calculation. Disadvantages are using long time in the field work because of have to move all 4 electrodes for 1 voltage value and sensitive to the lateral change of soil sediments and rocks in the shallow.

2.3.2.2 Schlumberger configuration

Schlumberger is the name of Conrad Schlumberger, 1874-1954. The configuration is similar to Wenner configuration. The spacing between electrodes C_1 and C_2 (space M to N) is less than space A to B division $2(AB/2)$. This configuration requires constant relationship $2(AB/2) > 5 MN$. Schlumberger configuration is moved P_1 and P_2 electrodes less than C_1 and C_2 electrodes (Figure 2.12).

Represent $r_1, r_4 = \frac{AB}{2} - \frac{MN}{2}$ and $r_2, r_3 = \frac{AB}{2} + \frac{MN}{2}$ into the equation 2.19, the apparent resistivity at the midpoint of the survey is

$$\rho_a = \frac{\pi}{MN} \frac{(AB)^2}{4} - \frac{(MN)^2}{4} \left(\frac{\Delta V}{I} \right)$$

(2.22)

Thus, the constant K of Schlumberge configuration is; $K = \frac{\pi}{MN} \frac{(AB)^2}{4} - \frac{(MN)^2}{4}$

Advantages of Schlumberge configuration are convenience used less time in field because do not moved electrodes frequently and decrease problem in lateral variation. Disadvantages of its is the long distance of current electrodes, have to walk too far to move. If the current electrodes are very far, the current may not reach to electrode as a result, the tool cannot measure the voltage.

2.3.2.3 Dipole-dipole configuration

The Dipole- Dipole configuration is not similar to another configuration. The spacing between electrodes C_1 and C_2 is equal to the spacing between P_1 and P_2 . But spacing between both current electrodes and both potential electrodes are very far away (Figure 2.12).

Represent $r_1, r_4 = a(n+1), r_2=na$ and $r_3 = a(n+2)$ into the equation 2.19, the apparent resistivity at the midpoint of the survey is

$$\rho_a = \pi a n (n+1)(n+2) \frac{\Delta V}{I}$$

(2.23)

Thus, the constant K of Dipole- Dipole configuration is; $K = \pi a n (n+1)(n+2)$

Advantages of Dipole- Dipole configuration are using wire less than another configuration and measuring lateral variation is well. Disadvantages are not suitable for survey horizontal plain and ratio of signal to noise is lower.

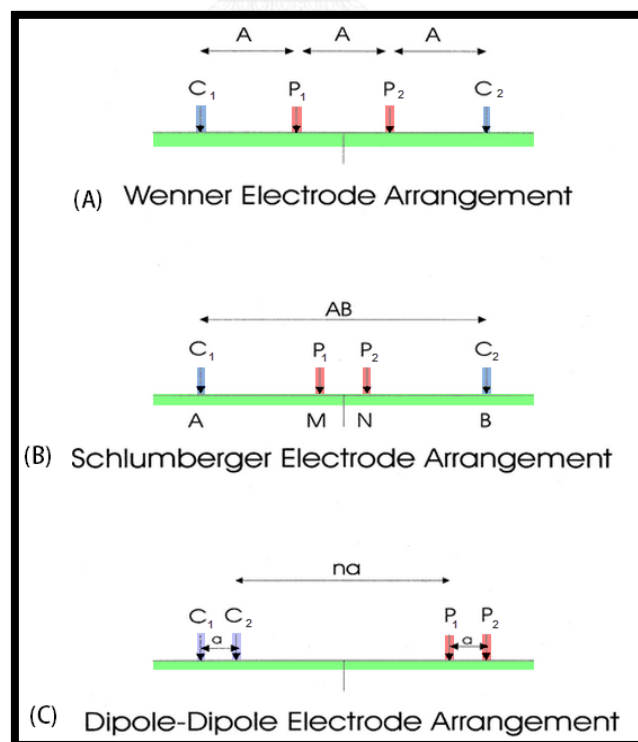


Figure 2.12 Electrode configurations (ASTM D6431 - 99, 2010)

2.3.3 Anomaly

2.3.3.1 Properties of electrical resistivity materials in crust

The ground surface consists of soil and rocks that mostly is insulator except the metals and graphite as conductor. Therefore, the resistivity survey was applied to measure the transfer or exchange of ions in pore spaces of soil and rocks that mainly fill with water. Naturally, the water in pore spaces must be a solution containing ion which result in soil layers and rock layers is a good conductor. Characteristic of fluid and porosity in pore spaces are main factors of the resistivity survey. Thus, it can be said that, composition of the crust is conductor arising from electrolytic conduction process and some minerals is matrix conduction included (Satarugsa, 2007).

Mineral conductor is mineral that allows electric current flowed through the body such as graphite, pyrholutite, pyrite, chalcopyrite, galena, magnetite and clay minerals. Generally, clay minerals found dispersed, thus soil and rocks that compose of clay minerals will be able to measure the resistivity (Telford *et al.*, 1990). The resistivity of elements, minerals and rocks are shown in Table 2.2, 2.3 and 2.4.

2.3.3.2 Factors affecting the change of electrical resistivity

Not only the types of rock control the electrical resistivity values of rocks but also many other factors, more important are those factors related. The significant factors that affect the change of electrical resistivity are follows as (Satarugsa, 2007):

- Ion quantity of electrolyte in porosity:

Archie (1942) found a relationship between porosity of sedimentary rocks that allowed water through in pore, the electrical resistivity values of sedimentary rocks and the electrical resistivity values of fluid in porosity, the rule known as Archie's law.

$$\frac{\rho_r}{\rho_e} = a\phi^{-m} = F$$

(2.24)

When

ρ_r : the resistivity of the rock

ρ_e : the resistivity of electrolyte in pores

ϕ : the porosity

a : saturation coefficient (0.6-1.0)

m : cementation factor

F : formation factor

- Clay type and Clay content

Clay minerals are capable of cation exchange, because most of the clay mineral results from the decomposition of other mineral such as group of feldspar and mica minerals. During the decomposition, both cations and anions are independently occurred. Most of cations are absorbed loosely at the surface of clay mineral that can be pulled to assemble with other compound. Thus, clay minerals affects to electrical resistivity (rocks must contain moisture).

- Texture

Texture is one of many factors affecting the electrical resistivity. In case of sedimentary rocks, the electrical resistivity depends on size, sphere and sorted of sediment grains, that imply the porosity of rock. If rock is well sorted, it will have high porosity and low resistivity. In case of igneous rocks, if many fractures in rocks, it is a low resistivity than rocks without fracture.

- Geological process

Geological process affects both increasing and decreasing resistivity depending on the process with rocks. The resistivity of rock will be decreased, if the rock was through geological process such as weathering, dissolution, faulting, etc. On the other hand, the resistivity will increase, when rocks are cementing and crystallization, etc.

- Saturation

Saturation affects the resistivity of rock as the following equation:

$$\frac{\rho_r}{\rho_e} = \frac{a\phi^{-m}}{S_w^n}$$

(2.25)

When

n : Constant value (~2)

S_w : Saturation of water filled in pore

- Permeability

Permeability affects the resistivity of rock as the following equation:

$$k = 0.136 \frac{\phi^{4.4}}{S_{wi}^2}$$

(2.26)

When

k : Permeability (mDarcy)

S_{wi} : irreducible water saturation

- Temperature

If the water temperature increases, it will have reduced viscosity. As a result, ions that contain in the liquid move faster. When ions moved faster, the flow of electric charge would move faster as well, because of the resistivity is low.

Table 2.2 Resistivity of metal elements (Telford *et al.*, 1990)

Element	Resistivity (Ωm)	Element	Resistivity (Ωm)
Copper	1.7×10^{-8}	Nickel	7.8×10^{-8}
Gold	2.4×10^{-8}	Platinum	1.1×10^{-7}
Aluminum	2.7×10^{-8}	Silver	1.6×10^{-8}
Iron	9.7×10^{-8}	Tungsten	5.7×10^{-8}
Lead	2.2×10^{-7}	Tin	1.1×10^{-7}
Mercury	9.6×10^{-7}	Uranium	3×10^{-7}
Antimony	4.5×10^{-7}	Zinc	5.8×10^{-8}
Arsenic	2.2×10^{-7}	Antimony	4.5×10^{-7}

Table 2.3 Resistivity of minerals (Telford *et al.*, 1990)

Mineral	Resistivity (Ωm)	Mineral	Resistivity (Ωm)
Quartz	$4 \times 10^{10} - 2 \times 10^{14}$	Hematite	$3.5 \times 10^3 - 10^7$
Anhydrite	10^9	Limonite	$10^{-3} - 5$
Rock salt	$30 - 10^{13}$	Ilmenite	$10^{-3} - 50$
Sylvite	$10^{11} - 10^{12}$	Diamond	$10 - 10^{14}$
Calcite	21×10^{12}	Stibnite	$10^5 - 10^{12}$
Fluorite	8×10^{13}	Galena	$3 \times 10^{-6} - 3 \times 10^2$
Serpentine	$2 \times 10^2 - 3 \times 10^3$	Bauxite	$2 \times 10^2 - 6 \times 10^3$
Hornblende	$2 \times 10^2 - 10^6$	Chromite	$1 - 10^6$
Mica	$9 \times 10^2 - 10^{14}$	Wolframite	$10 - 10^5$
Coal	$10 - 10^{11}$	Pyrolusite	$5 \times 10^{-3} - 10$
Lignite	$9 - 200$	Cobaltite	$3.5 \times 10^{-4} - 10^{-1}$
Pyrite	$2.9 \times 10^{-5} - 1.5$	Molybdenite	$10^{-3} - 10^6$
Sphalerite	$1.5 - 10^7$	Cinnabar	2×10^7
Rutile	$30 - 1000$	Covellite	$3 \times 10^{-7} - 8 \times 10^{-5}$

Table 2.4 Resistivity of rocks and sediments (Telford *et al.*, 1990) and (Satarugsa, 2007)

Rock	Resistivity (Ωm)
Granite	$3 \times 10^2 - 10^6$
Granite porphyry	4.5×10^3 (wet) – 1.3×10^6 (dry)
Albite	3×10^2 (wet) – 3.3×10^3 (dry)
Syenite	$10^2 - 10^6$
Diorite	$10^4 - 10^5$
Diorite porphyry	1.9×10^3 (wet) – 2.8×10^4 (dry)
Quartz Diorite	2×10^4 (wet) – 10.8×10^5 (dry)
Andesite	4.5×10^4 (wet) – 1.7×10^2 (dry)
Gabbro	$10^3 - 10^6$
Basalt	$10 - 1.3 \times 10^7$ (dry)
Peridotite	3×10^3 (wet) – 6.5×10^3 (dry)
Hornfels	8×10^3 (wet) – 6×10^7 (dry)
Schists	20×10^4
Slate	$6 \times 10^2 - 4 \times 10^7$
Gneiss	6.8×10^4 (wet) – 3×10^6 (dry)
Marble	$10^2 - 2.5 \times 10^8$ (dry)
Quartzite	$10 - 2 \times 10^8$
Shale	$20 - 2 \times 10^3$
Conglomerate	$10 - 8 \times 10^2$
Sandstone	$1 - 6.4 \times 10^8$
Limestone	$50 - 10^7$
Dolomite	$3.5 \times 10^2 - 5 \times 10^3$
Unconsolidated Sediment	20 – 200??
Clay	1 – 100
Alluvium Sand	10 - 800
Clayey Sand with salt water (Sakonnakorn basin)	1.3 – 7.8

CHAPTER 3

STUDY AREA

To assess seawater intrusion into coastal aquifers, researcher have to thoroughly understand the characteristics of the study area. The basic data should be collected, such as topography, meteorology, land use, geology and hydrogeology in order to plan for field study and then interpret the geophysical and hydrochemical results correctly.

3.1 Location and topography

The study area is located in Amphoe Cha-am, Changwat Phetchaburi, which is part of the central part of Thailand. The area is located in a topographic map of Royal Thai Survey Department, series L7018 with a scale of 1:50,000 composed of three sheets as follows: 4934I (Amphoe Tha-Yang), 4934II (Amphoe Hua-Hin) and 5034IV (Ban Tha-Node-Noi). The area lies between latitudes $12^{\circ}37.6'$ N and $12^{\circ}53.845'$ N and longitudes $99^{\circ}50.827'$ E and $99^{\circ}729'$ E. The area is bounded by the northern and western borders of Tha-Yang District, by the southern border of Prachuap-Khiri-Khan Province and by the eastern border of the Gulf of Thailand.

According to the topographic map (Figure 1.1) and the slope map of study area (Figure 3.1), it can be classified the topography into 2 major landforms. The first landform is a plain interleaved mountain that covers area 20 % of the area. The second landform is a low-plain or coastal plain that covers area 80 % of the area. Most of the plain interleaved mountain landform is located on the western of the area, which has a slope of more than 40 %. The mountain range run in the north-south direction along the costal line, dividing between Amphoe Cha-am and Amphoe Tha-Yang. The highest mountain of the area is the Pa-Yom Mountain (651 meters (msl)), the second and third highest mountain are the Yod-Num Mountain (557 meters (msl)) and the Pra-Rob Mountain (552 meters (msl)), respectively. We also found a high mountain ridge in the South of the area that is North-South trending to Prachuap Khiri Khan Province.

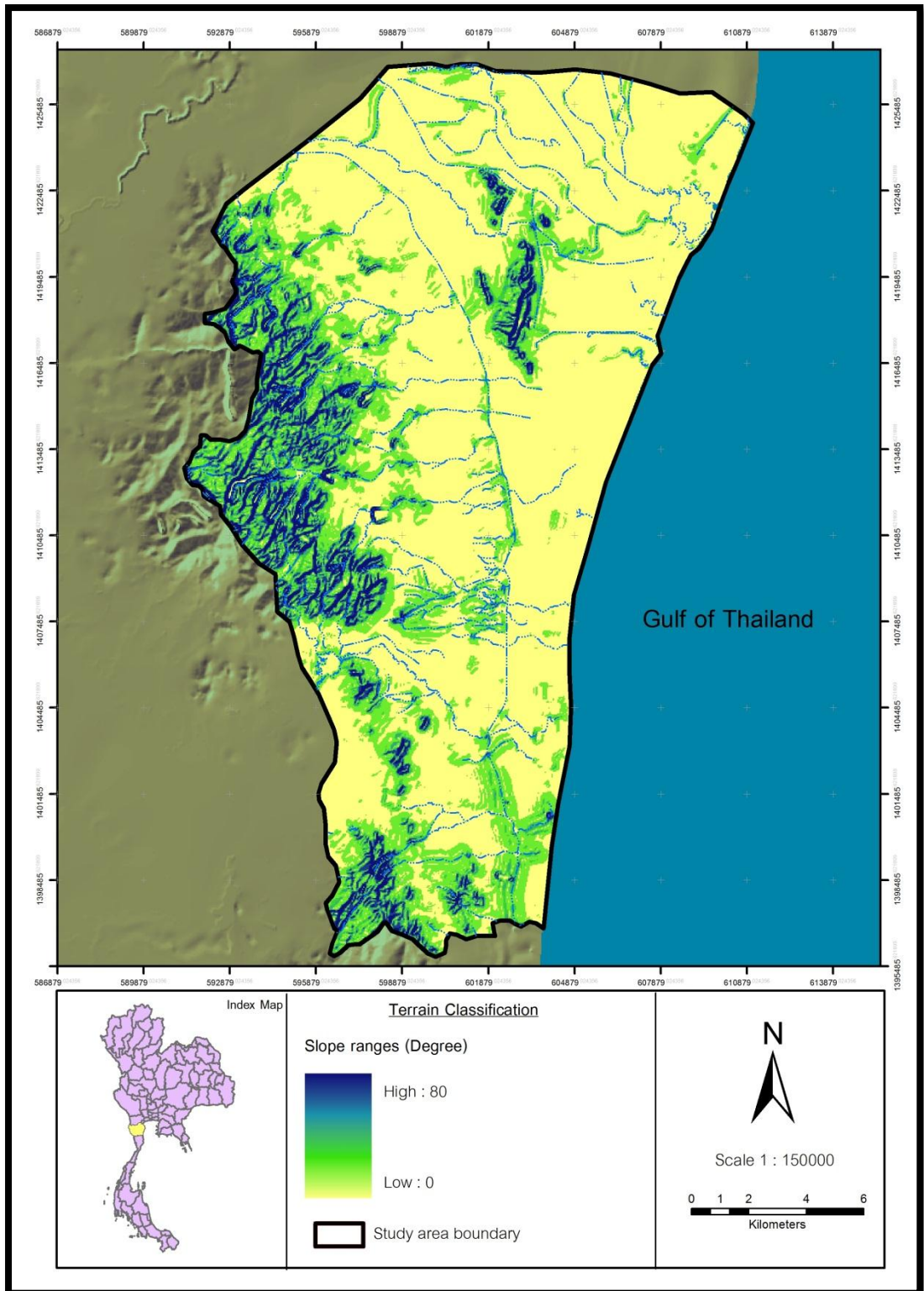


Figure 3.1 Slope map of the study area (Land Development Department, 2011)

Moreover, we found Limestone Mountain which resembles a bulb distribution in the North of the area. The Eastern side of the area is a low-plain or coastal plain to the Gulf of Thailand. The slope of the area is less than 2 % and an average height is 5 to 20 meters above mean sea level. The coastal characteristic is a beach sand and estuary that is caused by deposition of river sediments (Table 3.1). In the central of the area found alluvial plain at the narrow zone between mountains. The area average height is 30-60 meters above mean sea level.

Table 3.1 Coastal characteristic of the study area (Phetchaburi Rajabhat University, 2011)

Tambon	Beach Name	Characteristic			
		Sand beach (km)	Sandy Tidal flat (km)	Tidal flat (km)	Delta (km)
Nong-Sa-La	-	0.63	-	-	0.16
Bang-Kao	Bang-Khao Beach	8.45	-	-	0.23
Cha-Am	- Cha-Am Beach - Malektaiyawan Beach	23.50	-	-	0.28

3.2 Meteorology

Meteorological data of the Amphoe Cha-am consists of seasonal, climate, temperatures, relative humidity, precipitation, clouds, fog or haze and wind (Thai Marine Meteorological Center, 2006).

3.2.1 Seasons

Seasons of Amphoe Cha-am are considered from weather of Thailand that classify into three seasons.

- Summer: start from mid-February to mid-May. The weather is common hot and April is the hottest of the year.

- Rainy: start from mid-May to mid-October. It is a period of Southwest monsoon blows into Thailand. The weather is moist and rainy, the heaviest is in October.
- Winter: start from mid-October to mid-February. It is a period of Northeast monsoon blows covering Thailand, temperature drops and the weather is cold. In the coastal area may be rain, especially very heavy in November and will be decreased in December and January.

3.2.2 Climate

The climate of Amphoe Cha-am is under the influence of two the monsoons wind that circulation regularly as the season. The first is the Northeast monsoon that blows from Northeast in the winter. It resulted Amphoe Cha-am is less rain in the winter and some cold weather, but early in the season may have much rain. The second is Southwest monsoon. This wind blows regularly in the rainy season and blows across the Indian Ocean, so Thailand has a lot of rain. Nevertheless, Amphoe Cha-am is behind the Tanaosri Mountain ridge that is a rain shadow, so it is less rainfall during the rainy season. Mostly raining in winter is during October to November.

3.2.3 Temperature

Since Amphoe Cha-am is on the upper part of southern east of Thailand, the climate is similar to the Central part of Thailand. As a result of Cha-am is near the sea, steam and moisture will gain when the Northeast monsoon comes. An average temperature throughout the year is approx. 27.7 °C. The maximum temperature is 31.8 °C and the minimum is 23.8 °C.

3.2.4 Relative Humidity

It has high moisture almost all the year. During the winter, as the Northeast monsoon blows covering Thailand, the weather is generally dry and cold. Relative humidity is quite high in the morning, but it dropped quickly and low in the afternoon to

evening. The changing into summer, the weather is hot but humid due to the wind blows up from the sea. In the summer, relative humidity is higher in the winter and highest in the rainy season. Because of the Southwest monsoon blows covering Thailand that leads the steam and moisture from the sea to inland. Average relative humidity throughout the year is approx. 77 %, maximum 87 % and minimum 64 %.

3.2.5 Rain

Amphoe Cha-am is considered to be the area with the least quantity of rain because it is a rain shadow area. In the Northeast monsoon season, there will be less rain because of it blows through a narrow area. In the Southeast monsoon season, it is still light rain owing to Tanaosri Mountain as a wind barrier. Average rain by volume is approximately 853.3 millimeter per year. Rainfall averaged 104 days per year. The highest rainfall is in October, 174 millimeters per month or 15 days per month.

3.2.6 Cloud

It is a cloudy sky all over the year. In summer and winter season are partly cloudy sky but cloudy sky in rainy season.

3.2.7 Fog / Haze / Visibility

Amphoe Cha-am has rarely fog. Haze occurs mostly in December to April, about 28 - 30 days. The visible of eyes through haze is approx. 7 kilometers. The average visibility at 07.00 a.m. all year is about 11 kilometers, average all day is about 12 kilometers.

3.2.8 Wind

The circulation of wind in Amphoe Cha-am is rather steadily. During October to December is a Northeast wind, average speed of wind is 3 to 4 kilometers per hour. In January to May is Southeast wind, average speed of wind is 6 to 11 kilometers per hour. In June to August is South wind, average speed of wind is 12 to 13 kilometers per hour. In September is Southeast wind, average speed of wind is 13 kilometers per hour.

3.3 Land use

From the land use data of the Land Development Department and the data from field investigation found that in the study area could be classified the land use into 4 types, i.e. agriculture area, forest area, water body and facility area (Figure 3.2 and 3.3).

3.3.1 Agriculture area

Agriculture areas are the most common type of land use in the area. It covers 160.06 square kilometers or 44.47 % of the total area. The area was dispersed in the middle and the upper part of study area which is mostly the low land. These areas consist of various type of agriculture, i.e. paddy, mix orchard, banana, eucalyptus, lime, pineapple, mango, Para rubber, Casuarina, sugarcane, truck garden, mixed perennial, mixed field crops, cassava, tomato and coconut.

3.3.2 Forest area

Forest area is the second land used in this area, covers 118.08 square kilometers or 32.81 % of the total area. Forest areas are mostly located in the high plateau and mountain, in the western area and some scattered in the middle part. It consists of 3 forest types, dense deciduous forest, dense mangrove forest and teak forest.

3.3.3 Facility area

Most of the facility areas are scattered along the coastal line in central part and upper parts of the area. It covers 76.82 square kilometers or 21.34 percent of the total area. From the database and the investigation data found many facilities in the area that is institution land, factory, city, town, commercial, village, mine, poultry farm house, swine farm house, golf course, shrimp farm, airport and road.

3.3.4 Water body

The water body is a land use that is very small size compared to the whole area. It covers area only 4.95 square kilometers or just 1.38 % of the total area, because the

area does not have a large water source. The main source of water for agriculture is irrigation canal and water resource support is groundwater. Water body in the area consists of irrigation canal, lake, farm pond, river, canal and reservoir.

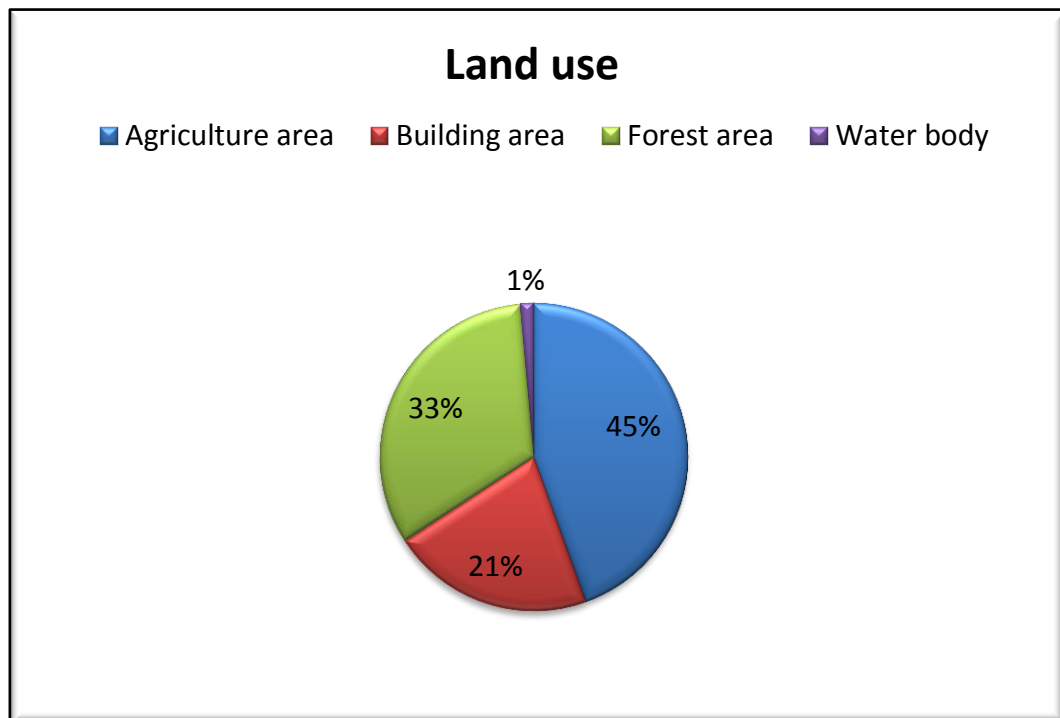


Figure 3.2 Pie chart shows the percentage of land use in the study area (Land Development Department, 2011).

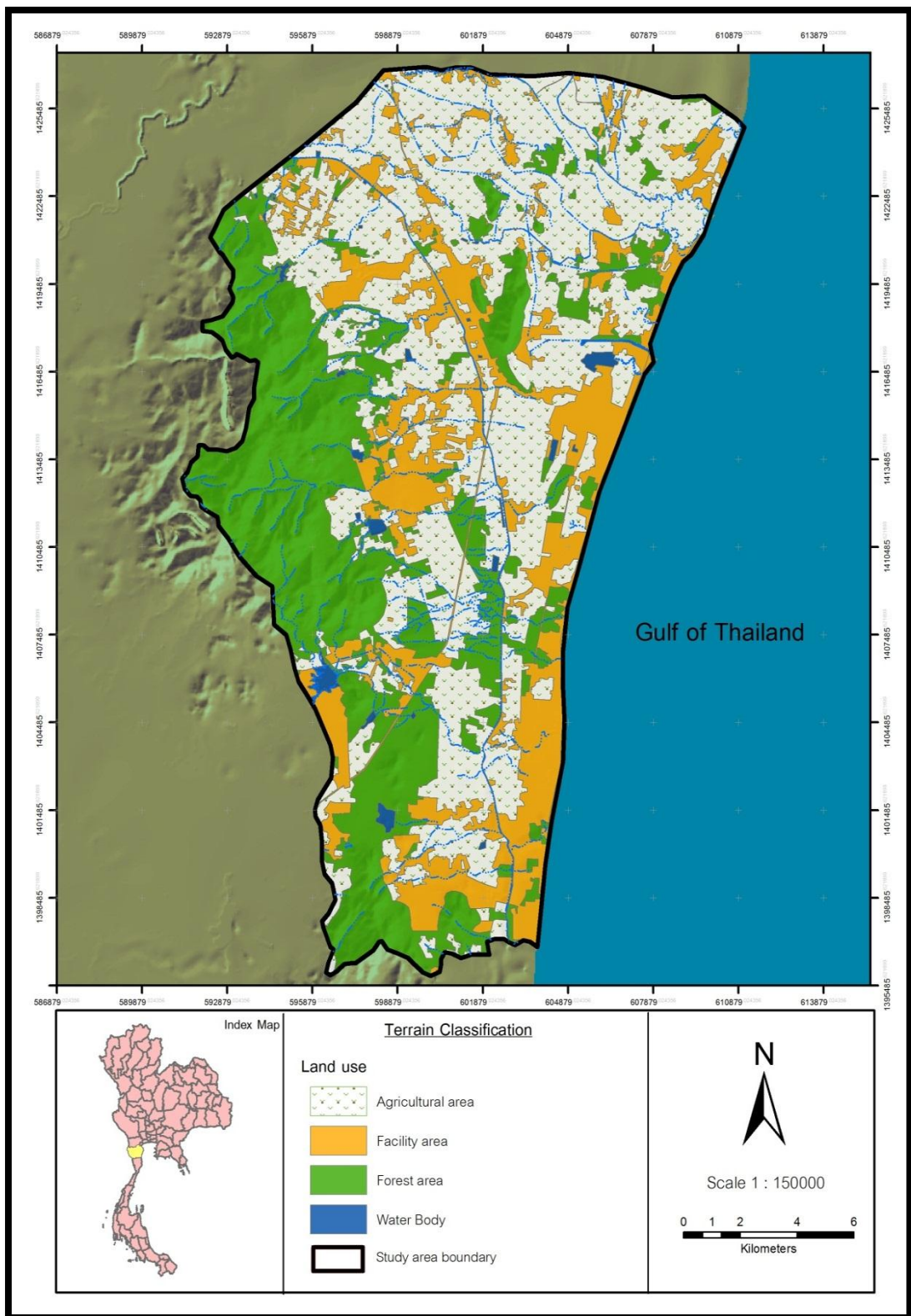


Figure 3.3 Land use map of the study area (Land Development Department, 2011)

3.4 Geology

Changwat Phetchaburi located on the Shan-Thai subcontinent, consisting of Permian rocks to Quaternary sediments (Table 3.2). The mountain ranges in Eastern of Changwat Phetchaburi area from the North to the South and isolate hills in Amphoe Cha-am, Tha-Yang and Ban-Laem mostly composed of Permian-Carboniferous sedimentary rocks, metasedimentary rocks and Permian dolomitic limestone distributed. These rocks are intruded by Cretaceous granite which appears as mountain range at the West of the Changwat Phetchaburi that is natural border between Thailand and Myanmar (Department of Mineral Resources, 2014).

Amphoe Cha-am is located on the East of Changwat Phetchaburi. Geological characteristics consist of igneous rock about 20 %, sedimentary rocks about 3 % and unconsolidated sedimentary about 77 %. It can be classified as 1 unit of igneous rock, 2 units of sedimentary rock and 2 units of unconsolidated sedimentary (Department of Mineral Resources, 2007) (Figure 3.4) as follows:

3.4.1 Igneous Rock

Igneous rock formed from cooling magma and lava that occurs from the melting of various rocks beneath the crust. Igneous rocks are divided according to characteristics of occurrence into 2 types, i.e. intrusive igneous rocks and extrusive igneous rocks. Intrusive igneous rocks occur by magma intruded up slowly then cooling before reaching the surface. Mineral compositions of rock crystallize and cool down slowly generating large and rough mineral crystals (mineral grain size bigger than 1 millimeter). Extrusive igneous rocks or volcanic rocks is occurred from the extruded lava that cool down quickly on the surface or near the surface, the crystal of mineral compositions is very small and invisible to eyes or no crystallization of minerals.

Igneous rock that founded in Amphoe Cha-am is intrusive igneous rock. There is one rock unit as follows:

Table 3.2 The Geologic Time Scale (From: <http://betterlesson.com/lesson/637787/geologic-timeline-discovery>).

Geological Time Scale					
ERA	PERIOD	EPOCH / AGE	Million Years Ago	EVENTS	
CENOZOIC <i>Age of Mammals</i> 65.5 mya – present day	<i>Quaternary</i>	<i>Holocene</i>	<i>Today</i>	Ice Age ends Humans are dominant	
		<i>Pleistocene</i>	– 0.01	Earliest Humans appear Ice Age begins	
	<i>Tertiary</i>	<i>Pliocene</i>	– 1.6		Hominids (human ancestors) appear
		<i>Miocene</i>	– 5.3		Grass becomes widespread
		<i>Oligocene</i>	– 23.7		Mammals are dominant
		<i>Eocene</i>	– 36.6		Eocene – Oligocene extinction event
		<i>Paleocene</i>	– 57.8		First large mammals appear
				– 65.5	
MESOZOIC <i>Age of Reptiles</i> 245 mya – 65.5 mya	<i>Cretaceous</i>	<i>Extinction of Dinosaurs</i>		K-T extinction event Earth looks closer to present-day Flowering plants appear	
	<i>Jurassic</i>		– 144	First Birds appear Pangaea splits into Laurasia, Gondwana Dinosaurs are dominant	
	<i>Triassic</i>	<i>First Dinosaurs</i>	– 208	Pangaea cracks First mammals appear Reptiles are dominant	
PALEOZOIC 570 mya – 245 mya	<i>Permian</i>	<i>Age of Amphibians</i>	– 245	Permian – Triassic extinction event Pangaea forms	
	<i>Carboniferous</i>		– 286	First reptiles appear First large cartilaginous fishes appear	
	<i>Devonian</i>	<i>Age of Fishes</i>	– 360	Late Devonian extinction event First land animals appear First amphibians appear	
	<i>Silurian</i>		– 408	First land plants appear First jawed fishes appear First insects appear	
	<i>Ordovician</i>	<i>Age of Invertebrates</i>	– 438	Ordovician – Silurian extinction event First vertebrates appear	
	<i>Cambrian</i>		– 505	End Botomian extinction event First fungi appear Trilobites are dominant	
PRECAMBRIAN 4600 mya – 570 mya	<i>Proterozoic Eon</i>		– 570	First soft-bodied animals appear First multicellular life appear	
	<i>Achean Eon</i>		– 2500	Photosynthesizing cyanobacteria appear First unicellular life appear	
	<i>Hadean Eon</i>	<i>Priscoan Period</i>	– 3800	Atmosphere and oceans form Oldest rocks form as Earth cools	
			4600		
Formation of Earth					

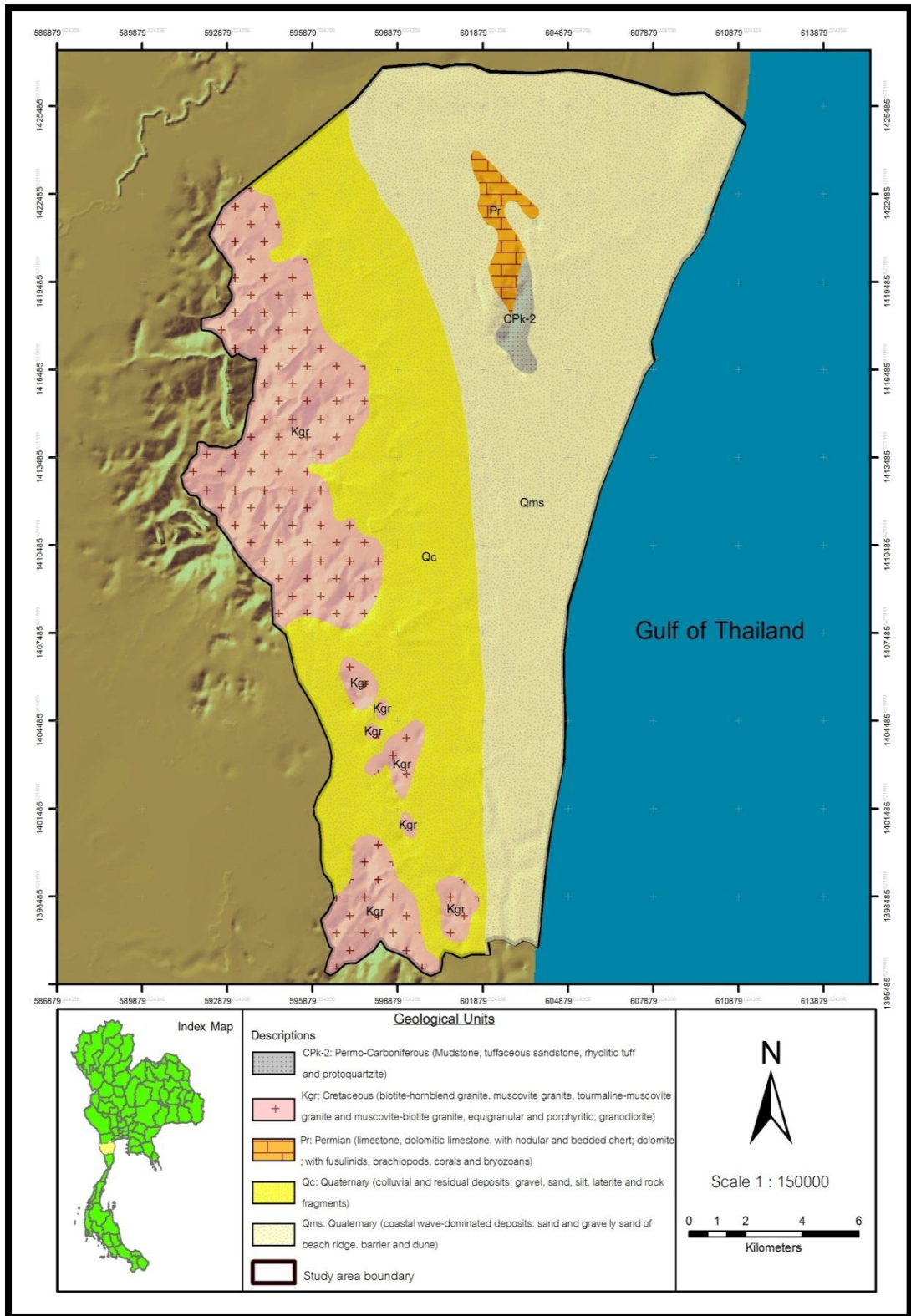


Figure 3.4 Geological Map in the study area. (adapted from the Department Mineral Resources, 2007)

3.4.1.1 Cretaceous Granite Rock (Kgr)

Age of granite rock in Amphoe Cha-am is 210 ± 4 million years (Beckinsale *et al.*, 1979). The rock is a consecutive batholith, North-South trending in the West of Cha-am a long to Changwat Prachuap-Khiri-Khan. Some of granite has mineral crystals arranged in strips, straight line and curve like Gneiss that is often called gneissic granite. General characteristic of cretaceous granite rocks are granite pale color, equigranular and porphyritic texture, large feldspar minerals, mineral crystals arranged in strips from normal to multi-layers of white and black. Cretaceous granite rocks can be classified by the mineral compositions of the rock such as biotite-hornblende granite, muscovite-granite, tourmaline-muscovite granite and muscovite-biotite granite (Department of Mineral Resources, 2014).

3.4.2 Sedimentary Rock

Sedimentary rock caused by the accumulation and sedimentation of debris that come from a crash or leaching soluble of source rocks. The naturally such as water, wind, glaciers seawater will lead to sediment accumulation in the basin. When the sediment accumulation in the basin is more, it will be compressed and cemented to form rock. Some types of sedimentary rock formed from the precipitation by chemical reaction, such as limestone, dolomite, etc.

Sedimentary rock that founded in Amphoe Cha-am can be divided according to the age. There are two rock units as follows:

3.4.2.1 Khao Chao Formation (CPk-2)

Khao Chao Formation is Permian – Carboniferous sedimentary rock, classified in the Kaeng Krachan Group (Piyasin, 1975). Name of formation comes from the name of mountain in the North of Kaeng Krachan dam. This formation is in the north of Cha-am. The thickness of formation is about 760 meters. The formation is composed of quartzitic sandstone, gray to light gray colors, fine to medium grained, well sorted, sub-angular to sub-rounded. Texture size of the middle part is fine more than the upper part. The middle part comprises thin beds of shale, siltstone, sandstone and light gray to

dark gray mudstone. The top of the formation consists of inter-bedded of mudstone and white to reddish brown, sub-rounded, fine to medium grained sandstone and accumulation of crinoid stem and thin shell beds (Department of Mineral Resources, 2014).

3.4.2.2 Ratchaburi Group

Ratchaburi Group is group of Permian sedimentary rock that mostly consists of limestone and some sandstone, siltstone, shale, dolomite and chert (J.C. Javanaphet, 1969). The trend line is North-South as can be seen from Amphoe Sangkhlaburi Changwat Kanchanaburi to Changwat Yala. The characteristic of Ratchaburi Group is pale gray to dark gray limestone that shows lamination to not lamination and some chert nodule. Fossils are found in rocks as fusulinid, brachiopod, coral, ammonoid and crinoid. Ratchaburi Group in Amphoe Cha-am is a monadnock that is distributed in the North of the area (Department of Mineral Resources, 2014).

3.4.3 Unconsolidated Sedimentary

Unconsolidated Sedimentary is a small organic or inorganic material such as rock, sand, gravel, soil that is caused by the natural decomposition process. The sediment will be transported by current flow to deposit in the basin.

Unconsolidated Sedimentary found in Amphoe Cha-am is Quaternary sediment age about 1.8 million years before the present. It can be classified by type of sediment and environment of sedimentation into two units as follows:

3.4.3.1 Coastal tide-dominated deposits (Qms)

The sedimentary sequence is soft marine clay and clay with silt alternations. Humus and shells are generally present. This deposition occurs in tidal flat area and delta area. Sediment deposition caused by influence of tides, during the seawater intrusion to inland in the early Holocene and regression in the middle Holocene to present (Sinsakul, 1992). This sedimentary sequence is on top of the Pleistocene terrestrial sediments. In Amphoe Cha-am founds distribution in the Eastern that border

with the gulf of Thailand, covering Amphoe Na-Yang, Nong-Sa-La, Bang-Kao and Cha-am (Department of Mineral Resources, 2014).

3.4.3.2 Colluvial deposits (Qc)

Colluvial deposits (Qc) is caused by decomposition in situ of hard rocks and sediment accumulation along the foothill, so often these sediments are found near the mountain. The sedimentary sequence is sand layers with some clay, sub-angular fragments and poorly sorted or silt layers and fine sand with clay. Rock fragments are varied depending on the source rock such as quartzite, sandstone, siltstone, granite, laterite and terra rossa (red sediments). In Amphoe Cha-am founds distribution in the Western, Amphoe Don-Kun-Huai, Huai-Sai-Naeu, Kao-Yai, Sam-Pra-Ya, Rai-Mai-Pattana and Cha-am (Department of Mineral Resources, 2014).

3.5 Hydrogeology

Hydrogeological characteristics means geological features associated with the occurrence, distribution, flow and quality of groundwater including rock composition, geological structures and geological environment effect, etc. These geological conditions are the criteria to determine properties of rock that is a groundwater reservoir, also known as hydrogeological properties. The significant properties are storage and discharge properties. Due to the natural unconsolidated and consolidated rocks are different geological feature resulting in different properties. Therefore, in hydrogeology is classified in to two main types, unconsolidated rocks and consolidated rocks. Then classify into sub hydrogeologic units again that is similar to the classification of geologic units. The classification of hydrogeologic units may be consistent or inconsistent with classification of geological units, it depends on the hydrogeological properties.

Amphoe Cha-am underlain with unconsolidated aquifer and consolidated aquifer. More than 60% of Amphoe Cha-am underlain with unconsolidated aquifer, that is consists of beach sand aquifer, flood plain deposit aquifer and colluvial sediments aquifer. Consolidated aquifers are composed of 40 %, Silurian-Devonian metamorphic

aquifer, Permian-Carboniferous metasedimentary aquifer, Permian limestone aquifer and Cretaceous granite aquifer (Department of Groundwater Resources, 2001)(Figure 3.5).

3.5.1 Unconsolidated aquifers

Unconsolidated deposits comprise of sand, gravel, silt, rock fragments and clay which does not cemented. The sedimentary deposition occurs in many environments such as river, delta and sea. The appearance of sedimentary deposition will separately as layers that each layer has its own properties, quantity and quality of groundwater are either same or different depending on the geological and hydrogeological of the area. Generally unconsolidated deposits, groundwater will be accumulated in pore spaces between grains. However, the unconsolidated deposits which are sand or gravel layers can be stored groundwater to be more or less depending on various properties as follows; thickness of sedimentary deposits, sorting grains of sediment, grain shape of sediment.

Unconsolidated deposits in Amphoe Cha-am are quaternary sediments that can be classified by the depositional environment into 3 aquifers. There are Quaternary Beach-Sand Deposits (Qbs), Quaternary Floodplain Deposits (Qfd) and Quaternary Colluvial Deposits (Qcl). The details are as follows:

3.5.1.1 Quaternary Beach-Sand Deposits (Qbs)

Quaternary Beach Sand Deposits is the common sediments in the coastal plains area. In Amphoe Cha-am, beach sand deposits aquifer is distributed along the East Coast from North to South. The beach sand aquifer is formed from the accumulation of sand being swept by the wind wave from the sea. The sediments are well sorted and rounded. Groundwater will be accumulated in the pore space between the sand grains deposited in the old sand ridge. The average depth of aquifer is 5 to 8 meters, water level height 1 to 2 meters. Well yield is less than 2 m³/ hour. The quality of groundwater is good with total dissolve solid content, less than 500 mg / l.

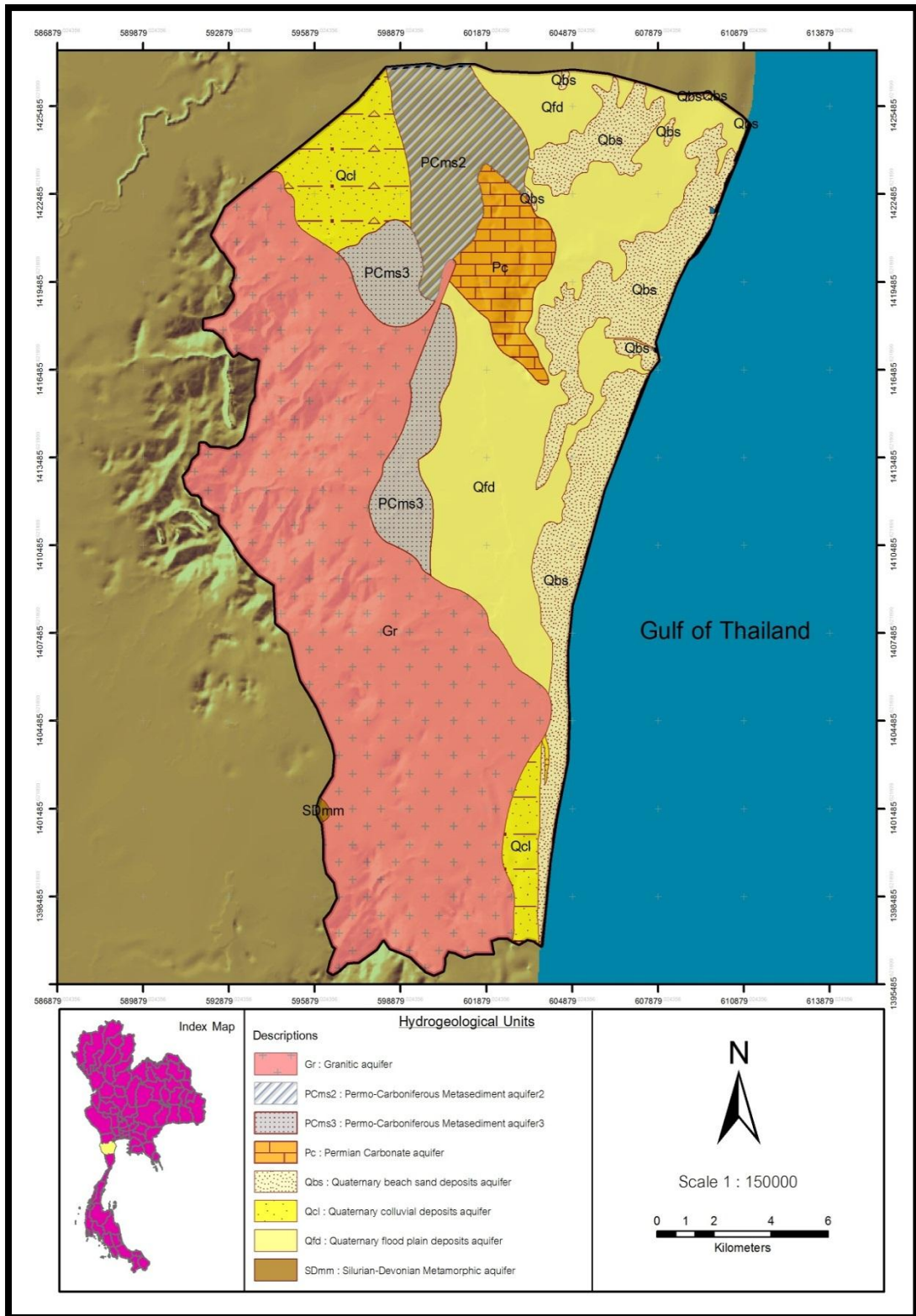


Figure 3.5 Hydrological map in the study area. (adapted from the Department of Groundwater Resources, 2014)

3.5.1.2 Quaternary Floodplain Deposits (Qfd)

Quaternary Floodplain Deposits is sediments deposited along meandering belts and floodplains area. In Amphoe Cha-am, floodplain deposits aquifer mostly were dispersed over a wide area in the upper part between beach sand aquifer in the East and granitic aquifer in the West and covers the most area in the lower area. Aquifer consists of sand, silt and clay of channel, river and flood basin deposits. The sediments are well sorted and rounded. Groundwater will be accumulated in the pore space between the gravel and sand grains. The average depth of aquifer is 25 to 45 meters and water level height 3 to 8 meters. Well yield is between 2 to 10 m³ / hour. The quality of groundwater is medium with total dissolve solid content about 500 to 1500 mg / l.

3.5.1.3 Quaternary Colluvial Deposits (Qcl)

Quaternary Colluvial Deposits is sediments deposited near the mountain or along the foothills caused by decomposition of source rocks in the area. In Amphoe Cha-am, colluvial deposits aquifer is found near the foothill of the granite mountain in the North and the South of area. Aquifer consists of gravel, sand, quartzite fragments, granite fragments and clay. The sediments are poorly sorted, angular to sub-angular because of weathering of source rock and rapidly deposition. Groundwater will be accumulated in the pore space between the gravel grains. The average depth of aquifer is 30 to 50 meters. Well yield is less than 2 m³ / hour. The quality of groundwater is good with total dissolve solid content of less than 500 mg / l.

3.5.2 Consolidated aquifers

Groundwater in consolidated rocks are contained in the space of various geological structures such as fractures, cracks, faults, bedding plain, cavity or cave in the rock layer and gap in weathering rocks. The quantity of groundwater depends on size and continuity of these structures, i.e. the structure with large cavity and good continuity will be store a lot of groundwater.

Consolidated rocks in Amphoe Cha-am can be classified into 4 hydrogeologic units or 5 aquifers. There are Silurian Devonian Metamorphic aquifers (SDmm), Permian Carboniferous Metasediment aquifers2 (PCms2), Permian Carboniferous Metasediment aquifers3 (PCms3), Permian Carbonate aquifers (Pc) and Cretaceous Granite aquifers (Gr). The details are as follows:

3.5.2.1 Silurian Devonian Metamorphic aquifers (SDmm)

Silurian Devonian Metamorphic aquifers consist of quartzite, phyllite and pale gray quartz vein. In Amphoe Cha-am, SDmm aquifer has been found in a small area in the lower West. Groundwater will be accumulated in the fracture, joint zone, fault and bedding plain. The average depth of aquifer is 30 to 35 meters, water level height 3 to 5 meters. Well yield ranged is less than 2 m³ / hour. The quality of groundwater is good with total dissolve solid content of less than 500 ml / l.

3.5.2.2 Permo-Carboniferous Metasediment aquifers (PCms)

Permian Carboniferous Metasediment aquifer is a Low-grade metamorphic rock of Keang Krachan Group. PCms founded in the study area can be separated by characteristic of rock group into 2 units, PCms2 and PCms3.

- *Permian Carboniferous Metasediment aquifers 2 (PCms2)* mostly consists of mudstone and shale inter bedded with sandstone (greenish gray), folding. In Amphoe Cha-am, PCms2 aquifer has been found in the Northern part. Groundwater will be accumulated in the fracture, joint zone, fault, folding and bedding plain. The average depth of aquifer is 50 to 200 meters. Well yield ranged is less than 2 cubic meters per hour but some part can developed groundwater more than 10 cubic meters per hour in fracture zone.

- *Permian Carboniferous Metasediment aquifers 3 (PCms3)* mostly consists of quartz rich sandstone inter bedded with thin shale (greenish gray and dark brown), folding. In Amphoe Cha-am, PCms3 aquifer has been found at the border of granite aquifer in the upper East of the area. Groundwater will be accumulated in the

fracture, joint zone and folding. The average depth of aquifer is 50 to 100 meters. Well yield ranged is more than 20 cubic meters per hour.

3.5.2.3 Permian Carbonate aquifers (Pc)

Permian Carbonate aquifers consist of gray to dark gray massive limestone, dolomitic limestone with shale and sandstone interbedded, some part of chert nodule. In Amphoe Cha-am, Pc aquifer has been found dispersing a small monadnock in the North of the area. Groundwater will be accumulated in the fracture, joint zone, fault, weathered zone and cavity or cave in the rock layers. The average depth of aquifer is 10 to 50 meters, water level height 3 to 5 meters. Well yield is ranged between 10 to 20 m³ / hour. The quality of groundwater is good with total dissolve solid content of less than 500 milligram per liter.

3.5.2.4 Cretaceous Granite aquifers (Gr)

Cretaceous Granite aquifer is granite rock that is consists of many type of mineral such as biotite, hornblende, muscovite and tourmaline. The rock is pale gray color, equigranular and porphyritic texture. In Amphoe Cha-am, Gr aquifer has been found dispersing along the large mountain ranges of the North to South on the West of the area. The most area is in Amphoe Kao-Yai and some area is in the south of Amphoe Don-Kun-Huai. Groundwater will be accumulated in the fracture, joint zone, fault and weathered zone. The average depth of aquifer is 50 to 150 meters, water level height 6 to 9 meters. Well yield is less than 2 cubic meters per hour but some area can developed groundwater more than 20 cubic meters per hour (fault zone). The quality of groundwater is good with total dissolve solid content of less than 500 milligram per liter.

CHAPTER 4

METHODOLOGY

This chapter describes all methods used for this research mainly consisting of 4 sections. Firstly, literatures review and secondary data of this study were conducted this study area. Secondly field collection data was carried out and can be divided into 3 parts, as follows: 1) a preliminary field survey, 2) 1 dimensional resistivity survey and 3) groundwater level measurement and groundwater sampling. Thirdly chemical analysis of groundwater samples in field and laboratory was analyzed. In the last section, geophysical data and chemical results of groundwater were analyzed and integrated together for delineating the area, impacting by seawater intrusion. The details are described as follows:

4.1 Secondary data preparation and collection

The first section is secondary data preparation and collection from previous researches and the government agency (see Table 4.1). Moreover, literatures review of associated research done in the national and international publication. By reviewing as mentioned, this research topic was formulated based on previous research suggestions.

After selecting the area, gathers data about the study area in detail and form several sources shown in Table 4.1 and Figure 4.1, such as geological data, geographical data, meteorological data, land use data, hydrogeological data, well data (i.e., position, well depth, cutting analysis and bore hole logging) and results of previous 1-D resistivity survey data in the area. Then, after gathering secondary data, all collection data was used to further plan for 1-D resistivity survey and groundwater level measurement and groundwater sampling.

Table 4.1 Sources of secondary data collection

No.	Data	Source	Year
1	General Data		
	- Amphoe Boundary	Department of Provincial Administration (DPA)	1998
	- Village location	Department of Provincial Administration (DPA)	2000
2	Topographical Data		
	- Topographic Map	Royal Thai Survey Department (RTSD)	2009
	- DEM Map	Department of Groundwater Resources (DGR)	2014
	- Stream line Data	Department of Groundwater Resources (DGR)	2014
3	Land use Data		
	- Land use Map	Land Development Department (LDD)	2010
4	Meteorological Data		
	- Meteorological Data	Thai Meteorological Department (TMD)	2011
5	Geological Data		
	- Geological Map	Department of Mineral Resources (DMR)	2007
	- Geologic Units	Department of Mineral Resources (DMR)	2007
6	Hydrogeological Data		
	- Hydrogeological Map	Department of Groundwater Resources (DGR)	2014
	- Aquifer Unit	Department of Groundwater Resources (DGR)	2014
	- Groundwater well Data	Department of Groundwater Resources (DGR)	2011-2014
	- Resistivity Data	Department of Groundwater Resources (DGR)	2014

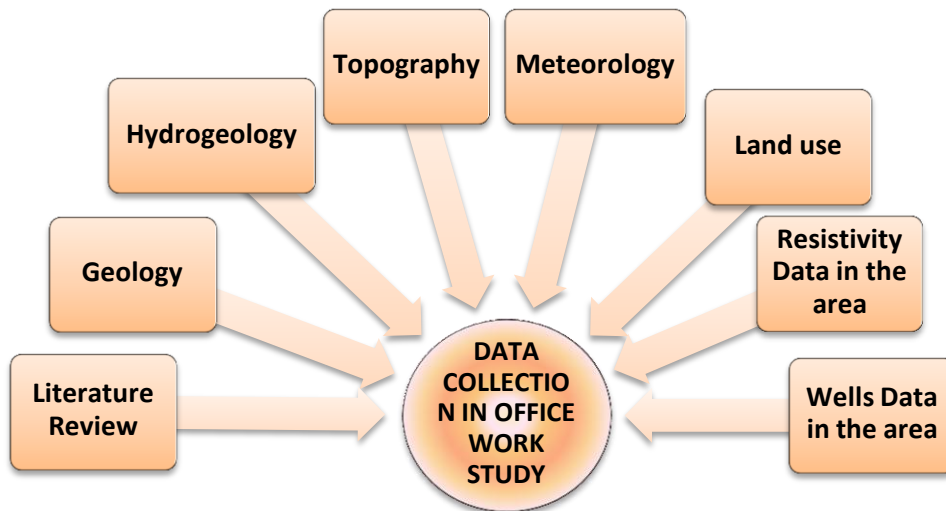


Figure 4.1 Diagram shows data collection in office work study

4.2 Field work

The field work was carried out after completing data collection. This field work section was divided into 3 parts. The first part was preliminary field survey. The second part was field of geophysical survey. The last part was field of groundwater sampling collection (see Figure 4.2).

4.2.1 Preliminary field survey

Preliminary field survey is carried out to check the reliability of all data, for examples, to assess the suitability of area for geophysical survey, to investigate the general geology and locations of groundwater wells and randomly measure groundwater levels (see Figure 4.3). Location of groundwater level measurement was showed in Figure 4.4 and Table B1 in appendix B1.

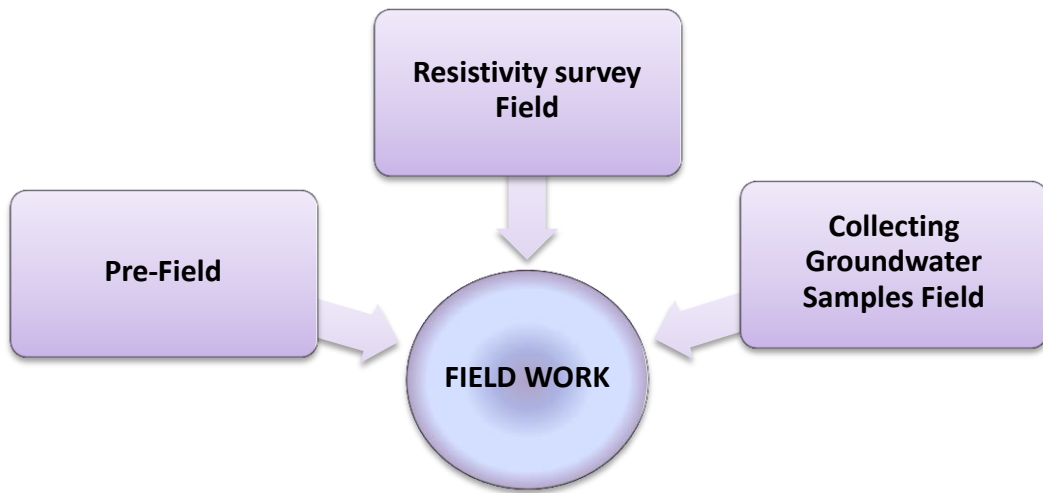


Figure 4.2 Diagram of data collection in field work



Figure 4.3 Measurement of groundwater levels in the preliminary field survey

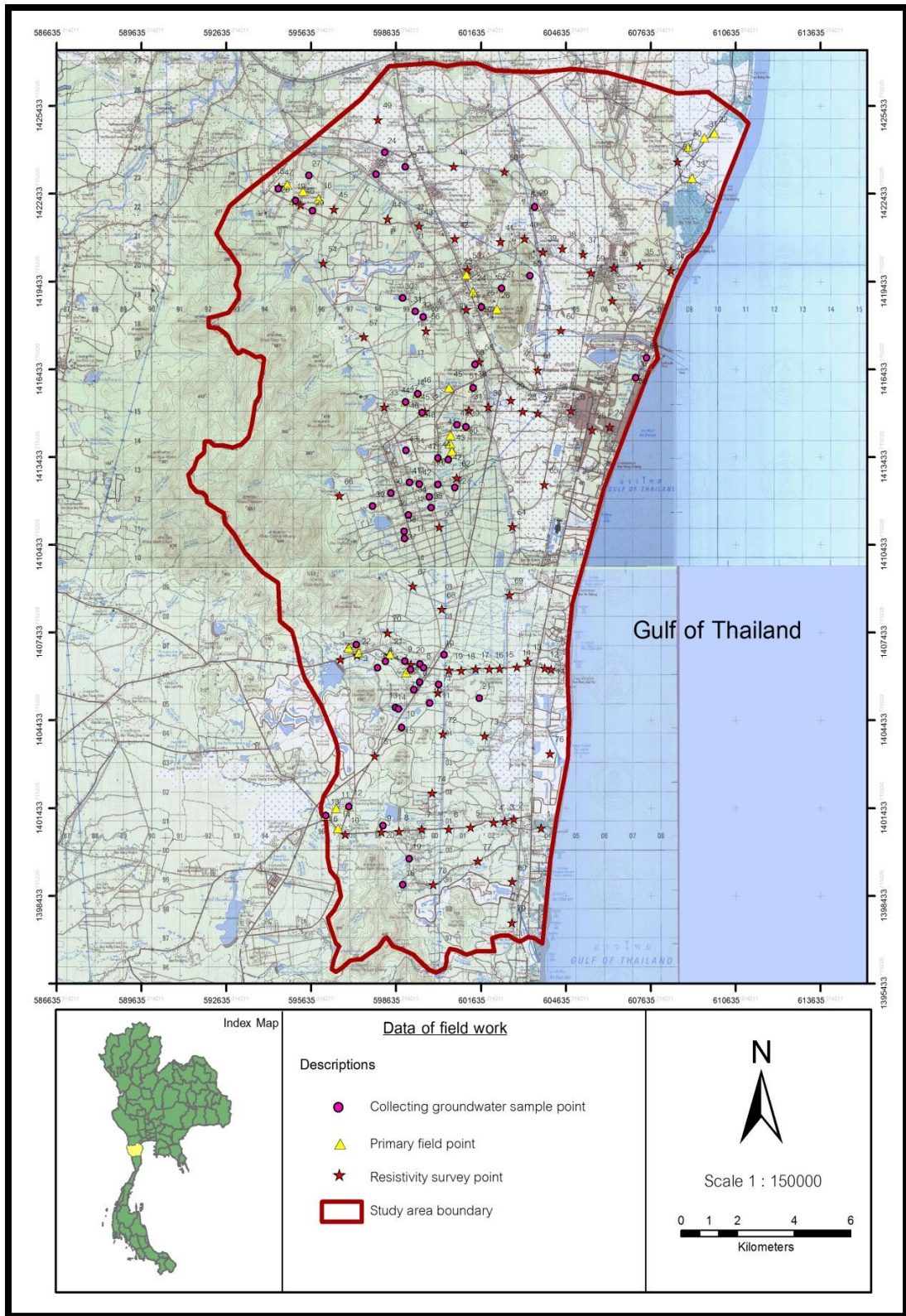


Figure 4.4 Map shows locations of field data collection

4.2.2 Field of geophysical survey

One-dimensional resistivity survey, known as Vertical Electrical Sounding (VES) was applied in this research. The results of VES survey method is the resistivity of soil and rocks layers in vertical. Therefore, the correct interpretation of VES is necessary to use the information of local geology and drilling information of groundwater wells. In this research, 80 points of VES survey have been collected by using Schlumberger configuration because it can remove the lateral variation problems and takes less time-consuming in the survey (Figure 4.4 and Table A1 in Appendix A1). Steps of the 1-dimensional resistivity survey are described as follows:

1. Prepared equipment used in the survey (see Figure 4.5);
 - Resistivity Meter (Syscal R1 Plus model, Iris)
 - 200 meters Roll wires 2 rolls and 50 meters roll wires 2 rolls
 - Hammer 4 units
 - Electrode 4 units (2 current electrodes and 2 potential electrodes)
 - GPS (Global Positioning System) 1 unit
 - Tape or rope for distance measurement
 - Walky-talky 3 units
 - Battery 12 Volt 1 unit
 - Field chair 2 units
 - Graph papers to record data in field
 - Map of survey point
2. Chose positions of resistivity survey from the topographic map based on site accessibility and information needed. The resistivity survey was undertaken by placing resistivity meter at the proper location, which should be dry and not direct sunlight, and then write down the coordinates of the survey point, elevation and line bearing.

3. Stamped four electrodes on the ground surface in the same straight line according to the Schlumberger configuration. The spacing between 2 outside electrodes (potential) is AB, and between 2 inside electrodes (current) is MN, that is installed in the center of the spacing AB. This configuration spacing AB must be 5 times greater than the spacing MN ($AB > 5MN$) (see Figure 4.6).
4. Connected Resistivity meter to A and B with current electrodes and M and N with potential electrodes (Figures 4.7 and 4.8)
5. Turned on switch of resistivity Meter and setting the parameters (mode, pattern array and spacing). After setting up successfully, press the start button to release the electrical current to subsurface. After completely finishing, the result would be automatically shown the values of resistivity and can be further used for interpretation.



Figure 4.5 Equipment of the VES survey.

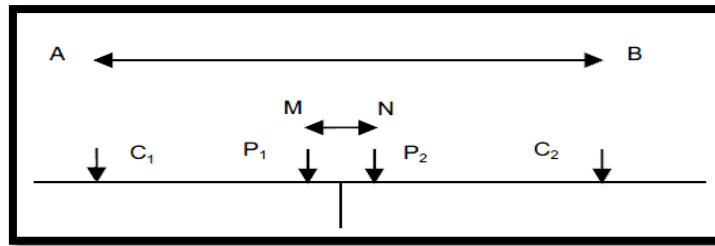


Figure 4.6 Schlumberger configuration



Figure 4.7 Resistivity Meter showing channels connected to points A, B, M and N.



Figure 4.8 Resistivity survey showing connected the resistivity meter to 4 electrodes

6. Collected resistivity value and plotted resistivity graph to check data error (see Figure 4.9). If found data error on the graph, we have to survey that error depth again.
7. Surveyed in the next depth by moving out 4 electrodes and installing in the new location, according to the relationship of $2(AB/2) > 5 MN$ at all depths. (see Figure 4.9).
8. When finished, then turn off Resistivity Meter and move the instruments to install in the same manner next station. When the survey is completed, all data was then gathered to further interpret with hydrochemical results, described in the following section.

4.2.3 Groundwater sample collection

57 groundwater samples were collected in the study area. In each well, the groundwater sample were collected in 2 bottles of 500 mL Poly-Ethylene (PE) (1 bottle with adding nitric acid (HNO_3) to maintain the acidity of water and the other with no adding nitric acid, used for anion analysis) . Groundwater samples were kept at $4^\circ C$ to reduce process of microorganisms and reduced the speed of physical and chemical processes. Locations of groundwater samples are shown in Figure 4.4 and TableB2 in Appendix A2. The method of groundwater sampling is as follows (Figure 4.10):

1. Preparation equipment
 - Poly-Ethylene (PE) bottle size 500 milliliters, 200 bottles
 - Nitric acid (concentration 1:1) 25 milliliters, 1 bottle
 - Parafilm-M, 1 roll
 - Water quality probes (pH, temperature, conductivity and salinity)
 - Water-level meter
 - Bailer (Teflon, PVC) size 1.8 inch
 - Deionized water 5 liters
 - Foam box

2. In the field survey, the static head was measured in each well with groundwater level meter and then was recorded such data together with its location.
3. All groundwater sampling equipment were cleansed before using to collect groundwater samples with deionized water
4. If the well installed pump, water must be pumped out 5 to 10 minutes before collecting groundwater sample from the tap In case of open wells, groundwater were collected by bailer by slackingdown in the well until bailer contact water surface and then letting it sank slowly to prevent the ripple in the well and while pulling it up . Before collecting groundwater sample, the stand water would be drawn it out 2 to 3 bailers.
5. Groundwater samples were measured pH, temperature and conductivity by Water Quality Checker that had already been calibrated.
6. 2 groundwater sampling bottles (with nitric acid and without nitric acid) was rinsed by groundwater sample at each well about 2 to 3 times before collecting groundwater sample. Then groundwater samples were kept at 4 °C.
7. Write all details of groundwater wells to side of groundwater bottle carefully and keep them at 4 °C prior to analyzing in the laboratory.

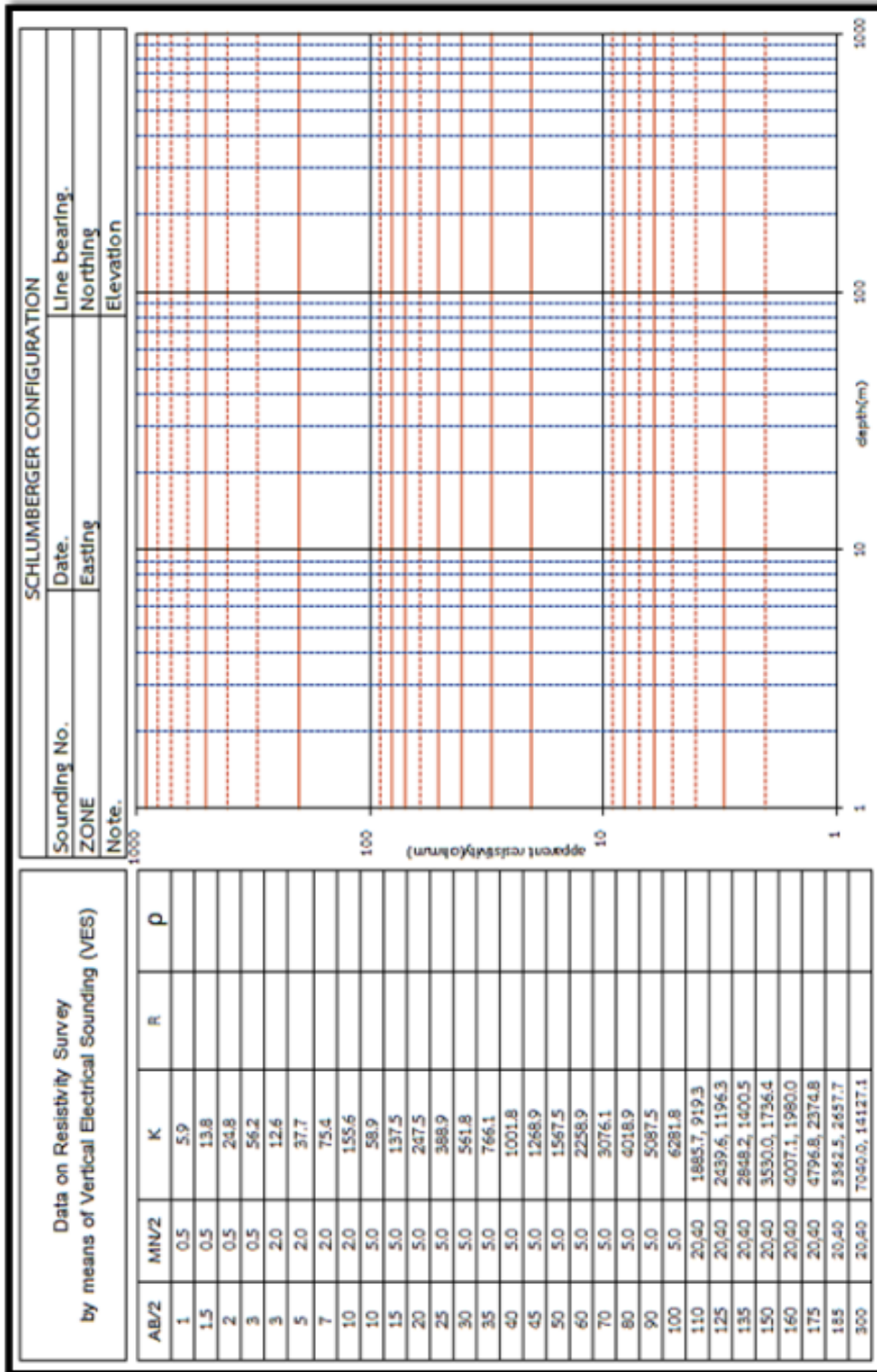


Figure 4.9 Graph paper log-log scale for plot resistivity values in field



Figure 4.10 Groundwater level measurement and groundwater sampling collection

4.3 Laboratory work

Before water chemical analysis, groundwater samples were filtered through GF/C filter paper (Figure 4.11), then took water samples to be analyzed further. Chemical compositions in groundwater samples collected (57 samples), split into 2 parts as anion analysis and cation analysis were analyzed. The chemical analysis was carried out for group of cations (Ca^{2+} , Mg^{2+} , Na^+ , K^+ and Fe^{2+}) analyzed by Absorption Spectrometry Method (AAS) whereas group of anion (Cl^- , Br^- , NO_3^{2-} and SO_4^{2-}) were analyzed by Ion Chromatographic Method (IC) and CO_3^{2-} , HCO_3^- were analyzed by volumetric titration method (Figure 4.12). The details are as follows:



Figure 4.11 Showing filtered groundwater samples.

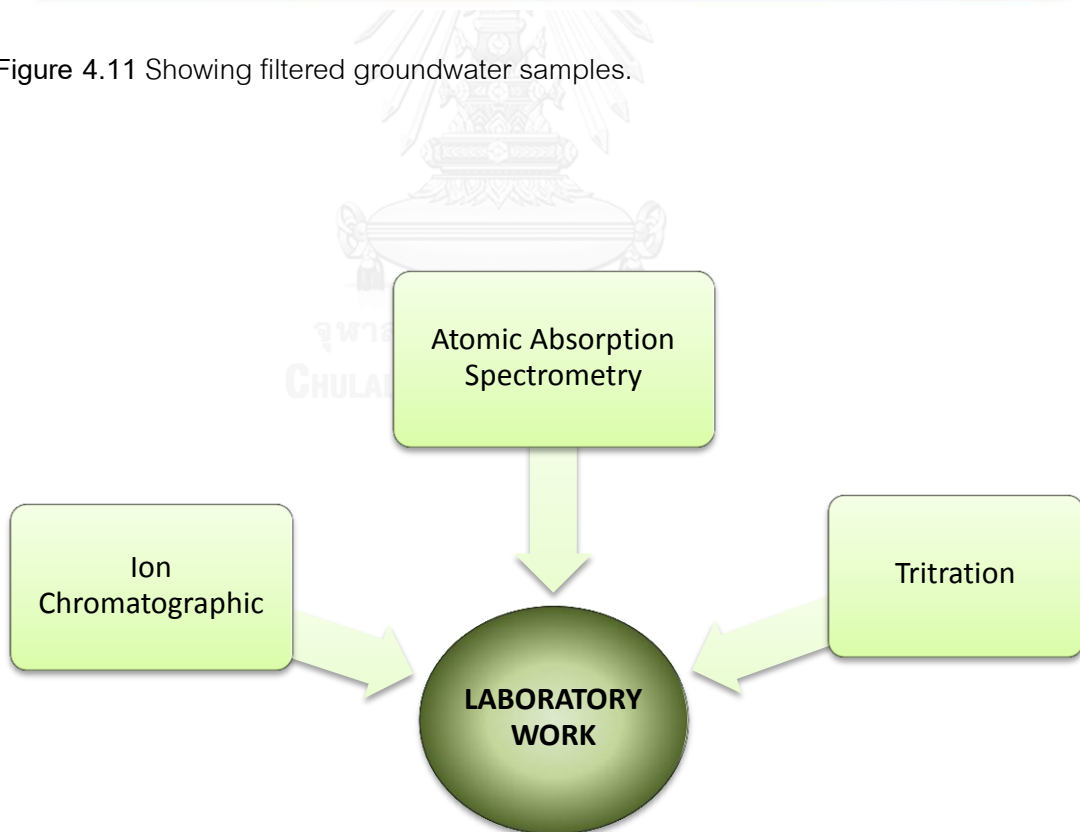


Figure 4.12 Diagram of laboratory work

4.3.1 Anion analysis

4.3.1.1 Ion Chromatography Method (IC)

Group of anions (F^- , Cl^- , Br^- , NO_3^{2-} and SO_4^{2-}) were analyzed by Ion Chromatography Method (IC). IC is a tool that used chromatograph techniques to separate the mixture substances in ionized state, based on the principle ion exchange in the column. The system consists of a carrier, which is a mobile phase called "Eluent" by most of the buffer solution. Eluent takes a sample to the column, which is stationary phase. Ion in mobile phase and ion in the sample will be completely exchanged with charge on the skin of stationary phases. Generally, the smaller ions are separated before (Figure 4.13).

The methods were as follows:

1. Prepared a standard solution to create the calibration curve with concentrations of 0.5, 5 and 10 ppm. (detection limit of standard is 10 ppm).
2. Prepared the Eluent (mobile phase), in this case we used 0.08423 g of $NaHCO_3$ (1mM) combined with 0.33915 g of Na_2CO_3 (3.2 mM) and filled distilled water (DI) to make a volume to 1 liter.
3. Injected 3 concentrated standard samples into the IC to create a calibration curve that is the result of plotted graph between standard concentration and the area under peak.
4. After created a calibration curve, water samples were injected into the IC took about 10 minutes per 1 sample. In between the water sample injection, the distilled water was injected into the IC to clean the column before the next water sample.
5. The concentrations would automatically be shown as comparing with the calibration curve. Then concentrations of each ion were recorded for further analysis and interpretation.



Figure 4.13 Ion Chromatography

4.3.1.2 Titration Method

This research use titration method for analyzing anions such as CO_3^{2-} and HCO_3^- . This method based on the alkalinity of the water that could be obtained by titrating water with strong acid (i.e., hydrochloric acid and sulfuric acid), which is splitted into concentration H^+ until it reaches to the equivalence point. To indicate the equivalence point, there are 2 ways, by using indicator and pH. By using indicators, it can be chosen either Phenolphthalein and Methyl Orange or mixture of Bromcresol Green and Methyl Red. Phenolphthalein was used for Alkalinity measurement, called Phenolphthalein alkalinity (P-Alkalinity), while mixture of Bromcresol Green and Methyl Red are used for Alkalinity measurement called M.O alkalinity (T-Alkalinity) (Figure 4.14).

The methods are as follows:

1. Prepared standard solution sulfuric acid 0.02 N by diluting 1N sulfuric acid 20 ml. with distilled water and then adjusting the volume to 1 liter.
2. Pipetted water sample to Erlenmeyer flask 50 ml.
3. Dropped 2 drops Phenolphthalein indicator into water sample. If water sample has Phenolphthalein alkalinity, it will be turned to be pink color,

and then titrated with standard solution sulfuric acid until pink color will be disappeared (Figure 4.15), volume of usage acid were recorded. On the contrary, if the water is not presented pink color, when added Phenolphthalein indicator, indicating that water sample has no Phenolphthalein alkalinity.

4. Dropped 3 drops of mixed of Bromcresol Green and Methyl indicator into water sample from (3.) to find M.O alkalinity, which is indicated by appearing to sky blue color. Then standard solution sulfuric acid was titrated until the sky blue color was changed to pinkish orange color (Figure 4.15). Finally, volume of acid used was recorded.

5. Calculate alkalinity by using formula in Table 4.2.

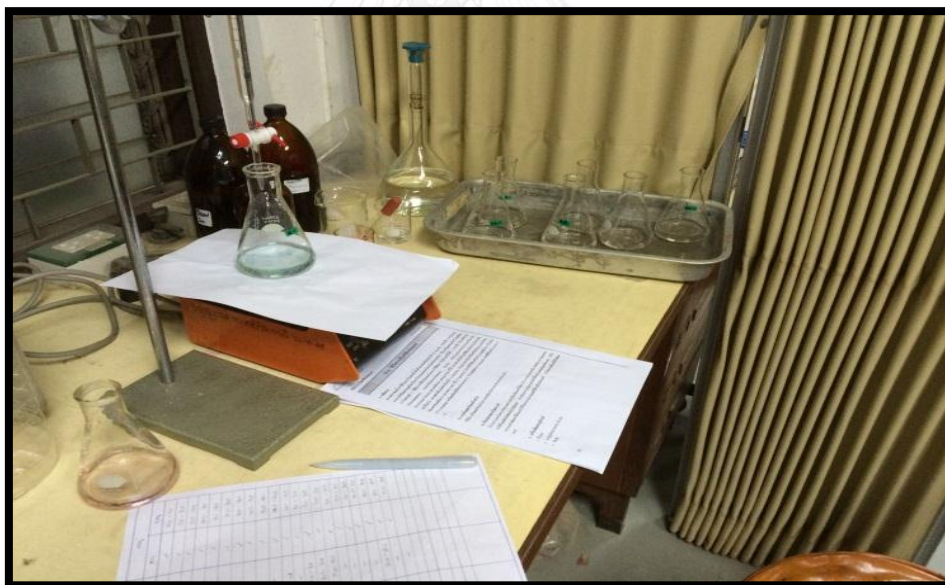


Figure 4.14 Titration Method with indicator.

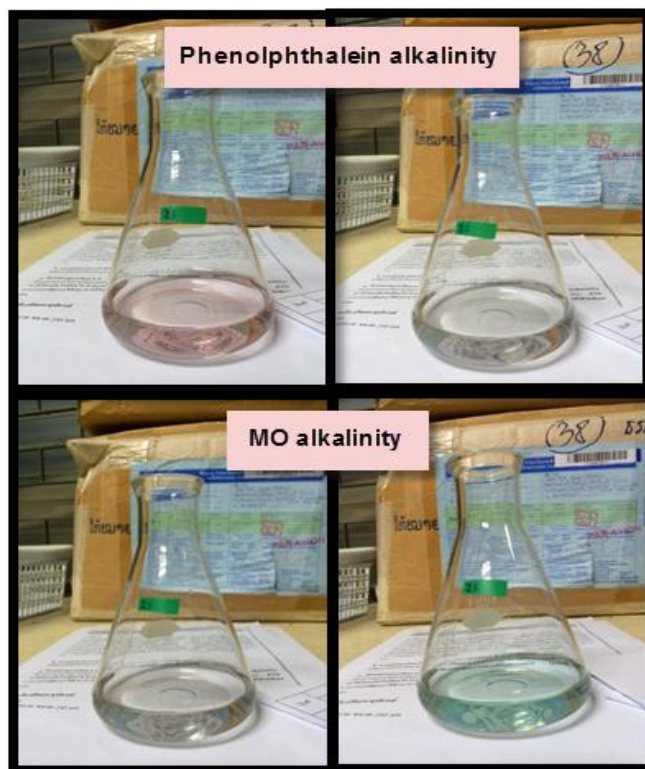


Figure 4.15 Showing colors of Phenolphthalein alkalinity and MO alkalinity when dropped indicator.

Table 4.2 Formula for calculate alkalinity.

Alkalinity	Formula	Parameter
Phenolphthalein alkalinity (P-Alkalinity)	$\frac{AXNX50,000}{\text{Volume of sample (ml.)}}$	A = volume (ml.) of standard solution sulfuric acid until equivalence point of Phenolphthalein N = Normality (N.) of standard solution sulfuric
M.O alkalinity	$\frac{BXNX50,000}{\text{Volume of sample (ml.)}}$	B = volume (ml.) of standard solution sulfuric acid until equivalence point of mixture of Bromcresol Green and Methyl.
Total alkalinity	$M.O\ alkalinity + P - Alkalinity$	

4.3.2 Cation analysis

4.3.2.1 Atomic Absorption Spectrometry Method (AAS)

Flam Atomic Absorption Spectrometry (FAAS) (Figure 4.16) Method was applied to analyze cations Ca^{2+} , Mg^{2+} , Na^+ , K^+ and Fe^{2+} . FAAS is a measurement of light absorption at wavelength-specific elements that needs to analyst. The principle of FAAS is that the fire with a certain wavelength is absorbed when passing through small droplets of a sample and can then be determined the amount of analyst concentration by the relationship between the measured absorbance and the analyst concentration. The nebulizer sprays the liquid sample into the chamber into small drops as an aerosol. The light from the light source get into the sample and pass through the monochromater which serves to spread out, according to the various wavelengths of light falling on the detector. The data will be forwarded to processing unit to evaluate results. The analysis is fast about 20 seconds to 1 minute per sample and uses medium quantities of sample approximately 3 to 7 ml. per sample. However, there are limitations in the ability to analyze in ppm level (detection limit not less).



Figure 4.16 Atomic Absorption Spectrometry Method (AAS)

The methods are as follows:

1. Prepared a standard solution to create the calibration curve for 5 elements (Ca^{2+} , Mg^{2+} , Na^+ , K^+ and Fe^{2+}).
 - Standard solution of Ca^{2+} with concentration 1, 2, 3, 4 and 5 ppm (detection limit of standard is 5 ppm).
 - Standard solution of Mg^{2+} with concentration 0.05, 0.1, 0.15, 0.2 and 0.25 ppm (detection limit of standard is 0.25 ppm).
 - Standard solution of Na^+ with concentration 0.1, 0.2, 0.3, 0.4 and 0.5 ppm (detection limit of standard is 0.5 ppm).
 - Standard solution of K^+ with concentration 0.2, 0.4, 0.6, 0.8 and 1 ppm (detection limit of standard is 1 ppm).
 - Standard solution of Fe^{2+} with concentration 0.6, 1.2, 1.8, 2.4 and 3 ppm (detection limit of standard is 1 ppm).
 - Blank solution (distilled water)
2. Injected a blank solution into AAS to adjust absorbance value as 0.00 before analyst. Then, all various concentration of standard solution injected into AAS to create a standard curve.
3. After the standard curve created, water samples had been analyzed by injecting into the AAS and wait for 20 seconds per sample and recorded the result. Between injecting each water sample, the blank water was injected to clean up the tube.
4. The result is so called “the standard curve”, constructed from the relationship between absorbance values with the analyst concentration, can be used for further groundwater concentration analysis.

4.4 Data analysis and interpretation

In the last section (Figure 4.17), all hydrochemical data were analyzed and interpreted together with geophysical data. The first part, geophysical data was interpreted using IPI2WIN software version 3.1.2c that developed by Moscow State University (Bobachav, 2003) and the results of inverse modeling were shown as a geological section. The second part, result of chemical analysis of groundwater samples can be analyzed by the piper and hydrochemical facies evolution (HFE) diagrams. The last part is integration of all results and present as cross-section and an assessment map of areas influenced by seawater intrusion. The details are as follows:

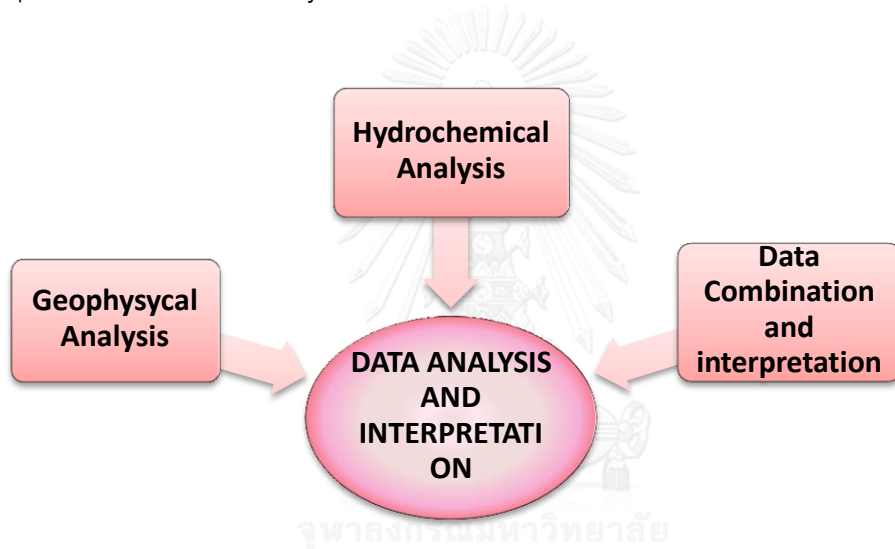


Figure 4.17 Diagram of data analysis and interpretation

4.4.1 Geophysical data

Resistivity data derived from field was interpreted by using IPI2WIN software. By adding the data, then the software was calculated and calibrated graph with the most possibility (Figure 4.18). The interpretation from the program displays as a layer according to the resistance values and the one can adjust their value accordingly. After processing all geophysical survey points completely, the hydrogeological cross-section was constructed with the help of lithologic data (Figure 4.19).

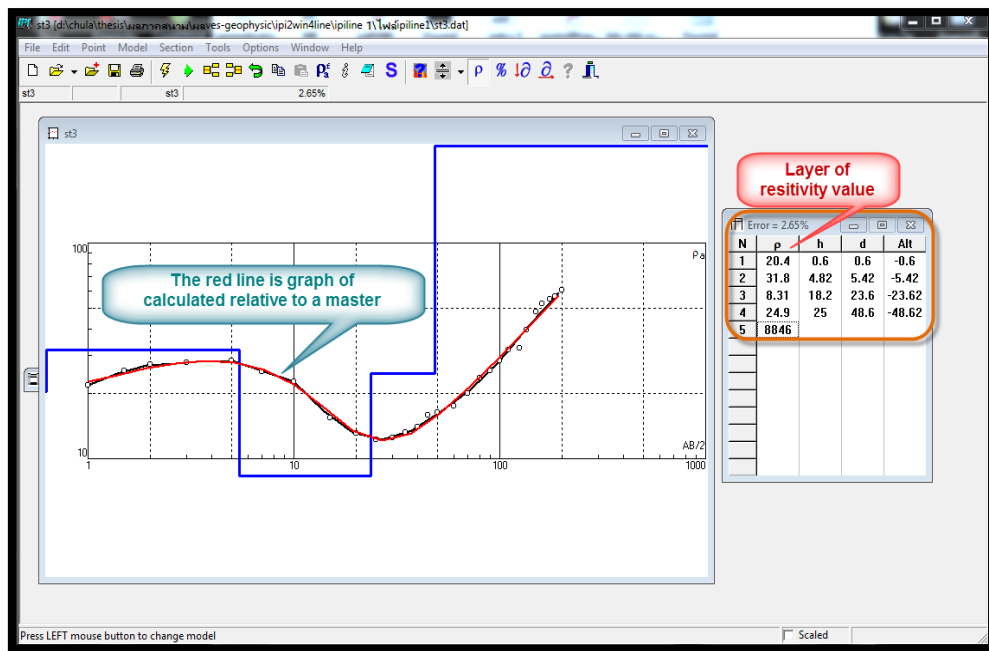


Figure 4.18 IPI2WIN Software shows calculated and calibrated graph

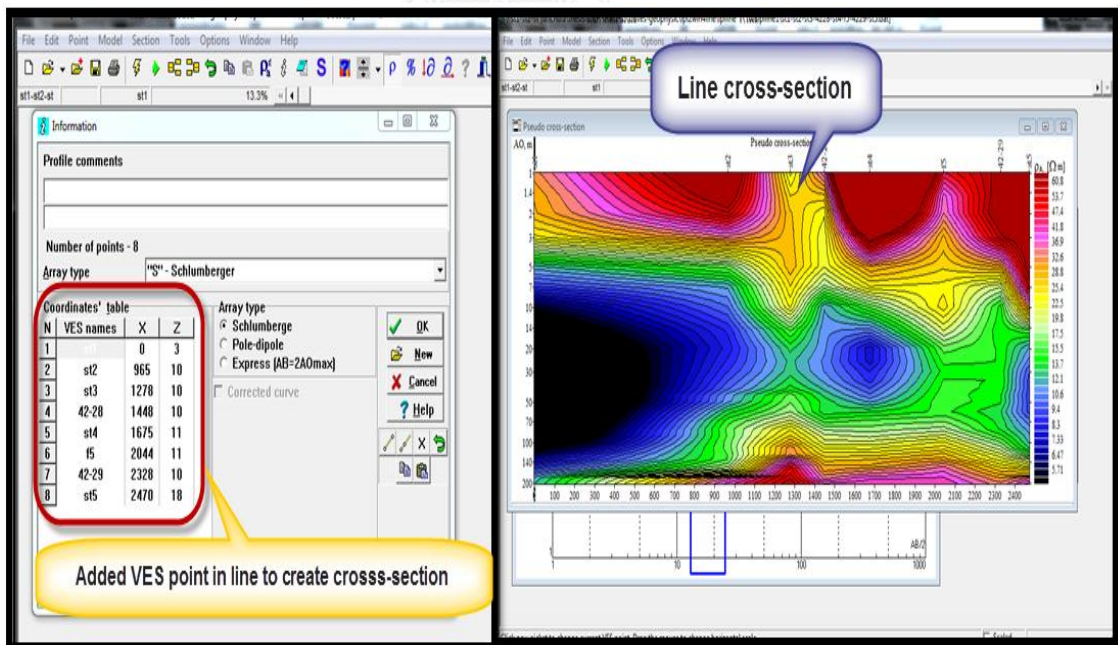


Figure 4.19 IPI2WIN Software shows create pseudo cross-section

4.4.2 Groundwater chemistry analysis

The chemical analysis results of groundwater samples were and plotted in piper and HFE diagram to classify type of water and explain the evolution of water, accounting for groundwater flow direction (the details of each diagram in Chapter 2).

4.4.3 Data interpretation

The data integration of all results both geophysical and hydrochemical results can delineate the area influenced by seawater intrusion, finally shown as the seawater intrusion map.



CHAPTER 5

RESULTS AND DISCUSSION

In this chapter the results of the field study and laboratory are presented, interpreted and discussed using the theory and findings from literature. The results are divided into 3 parts: 1) Regional flow direction of groundwater 2) Geophysical interpretation 3) Hydrochemical interpretation. The last section of this chapter is the integration of geophysical and hydrochemical results.

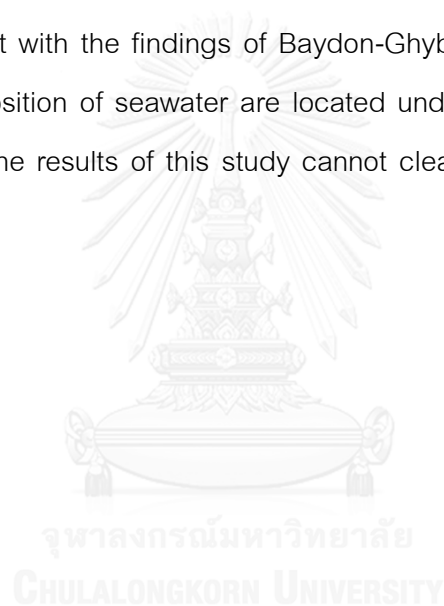
5.1 Regional groundwater flow direction

The basic data in the study area, such as geologic map, topographic map and hydrogeologic map including lithologic log and electric log, can be used to classify into 5 aquifers as follows: Quaternary flood plain deposits aquifer (Qfd), Quaternary colluvial deposits aquifer (Qcl), Granitic aquifer (Gr), Permian aquifer (Pr) and Permian-Carboniferous aquifer (PCms). The regional groundwater flows from recharge area, where is high mountain located on the western part of the area to the coastal discharge areas on the eastern part of the area (see Figures 5.1 and 5.2).

In this research, groundwater level measurement was collected two periods (in July, 2013 and February, 2014) to determine regional groundwater flow direction. In the first period in July, 2013 (Rainy season), groundwater levels were collected in 51 wells where their locations were given in the Appendix B1. In the second period in February (Dry season), groundwater levels were collected in 73 wells, where their location were given in the Appendix B2. ArcGIS 9.3 was used in order to create a groundwater flow map, which arrows represented direction of groundwater flow (Figures 5.1 and 5.2). Groundwater level in rainy season showed a slightly larger difference than that in dry season. As comparing the groundwater levels shown in Figures 5.1 and 5.2, it found that the groundwater level in dry season slightly shifted inland. The flow direction mainly flows from a mountainous recharge area in the western part to the low-lying discharge areas in the eastern part of the study area, which agrees with the theory of groundwater flow of the coastal area.

According to observation of groundwater levels in both season, we found that the quantity of freshwater supplied in coastal aquifer was reduced, suggesting that the geophysical survey in dry season can be clearly identified seawater intrusion into aquifer better than that in rainy season. These supported by the research of De Franco et al (2009) they monitored seawater intrusion into aquifer about 9 months in Italy and found that during the autumn-winter season seawater intruded into aquifer as much as possible and regression in spring-summer season due to the support of fresh water the mainland.

In addition, this research found that the position of fresh groundwater and seawater is consistent with the findings of Baydon-Ghyben (1888-1889) and Herzberg (1901), who found position of seawater are located underneath fresh water due to a greater density, but the results of this study cannot clearly indicate the seawater and fresh water interface.



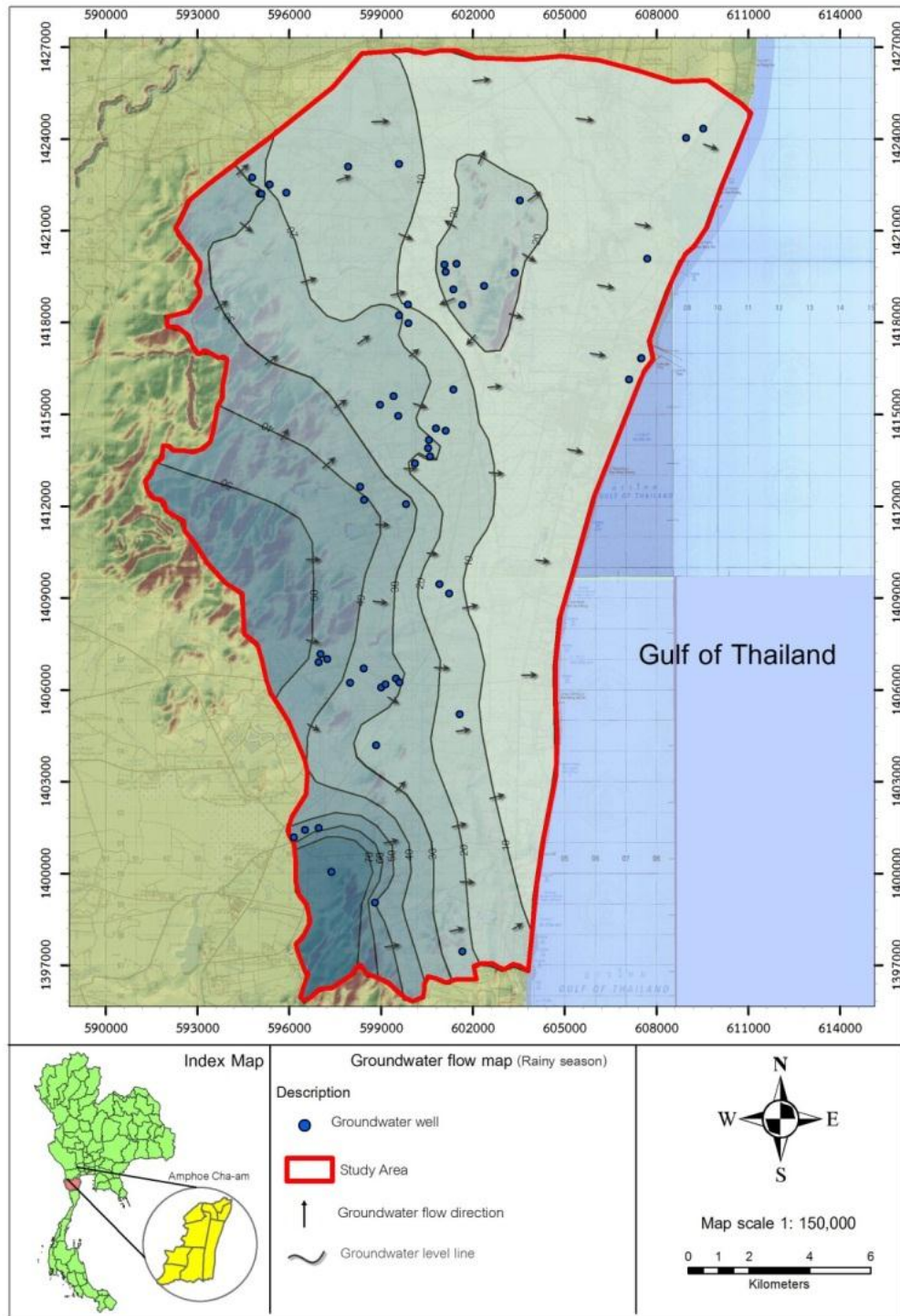


Figure 5.1 Groundwater flow map of rainy season

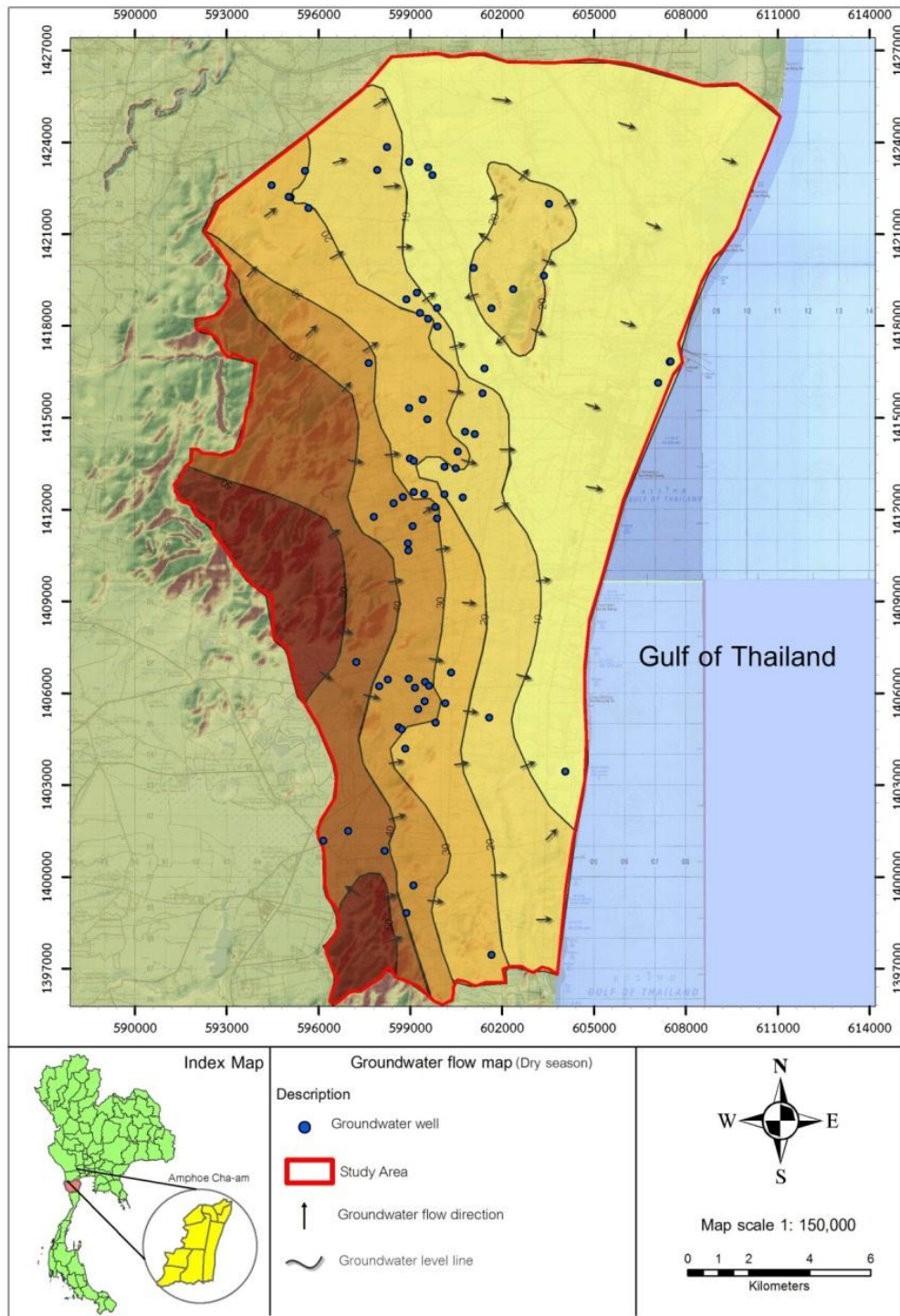


Figure 5.2 Groundwater flow map of dry season

5.2 Geophysical data interpretation

The 80 VES data were collected by using Schlumberger electrodes configuration with maximum electrode spacing $AB/2$ 200 meters. The locations of VES surveys were shown in Table A1 of appendix A1. Results of the VES survey were displayed on the log-log graph between electrode spacing and apparent resistivity value that can be used to identify soil and rock layers. Shape and slope of VES data on graph represents changes of the layer that has different resistivity (Telford et al. 1990). All 80 of VES data showed the H type curve (Figure 5.3) (Telford et al. 1990). This implied that there were 3 layers in the subsurface that consist of resistivity with $\rho_1 > \rho_2 < \rho_3$ (ρ_1 = resistivity of upper layer, ρ_2 = resistivity intermediate layer and ρ_3 = resistivity bottom layer) and consistent with characteristics of geology and hydrogeology of study area. The top layers represent the unsaturated sediments and the middle layer was saturated sediments. The bottom layer interpreted as bed rock. For example, to plot apparent resistivity on the graph shown in Figure 5.4 showed the example of type H resistivity profile and all VES graphs were shown in Table A2 of appendix A.

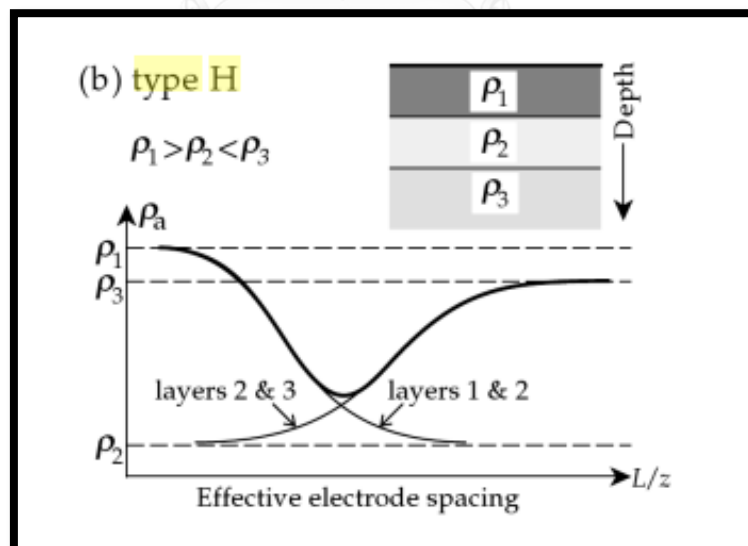


Figure 5.3 Apparent resistivity type curve (type H) for three horizontal layers.

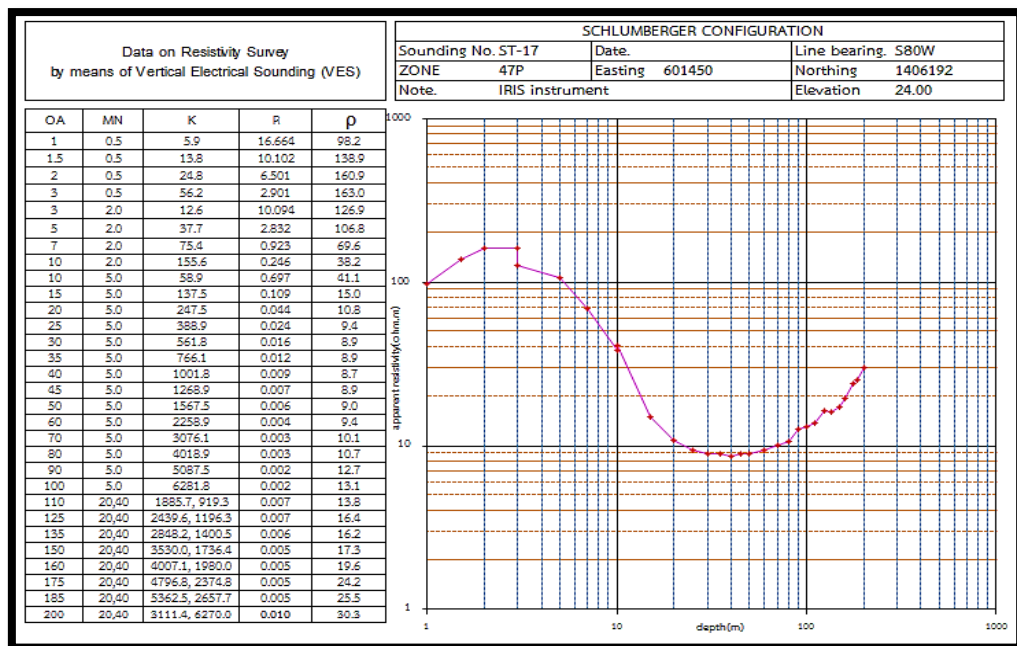


Figure 5.4 Example of field VES data plotted on a log-log scale graph at sounding number St-17

5.2.1 Pseudo resistivity cross-section

Pseudo cross-sections were generated from several 1D VES data along the purposed by using IPI2WIN software version 3.1.2c that developed by Moscow State University (Bobachev, 2003). There were 47 VES from this study and 9 VES from database of DGR were used to create 4 pseudo cross-sections, namely A-A', B-B' C-C' and D-D'. All of cross-section lines were created from West to East that was perpendicular to the coastal line (Figure 5.5). For example, curve matching of VES by IPI2WIN shown in Figure 5.6 and all of curves shown in appendix A2.

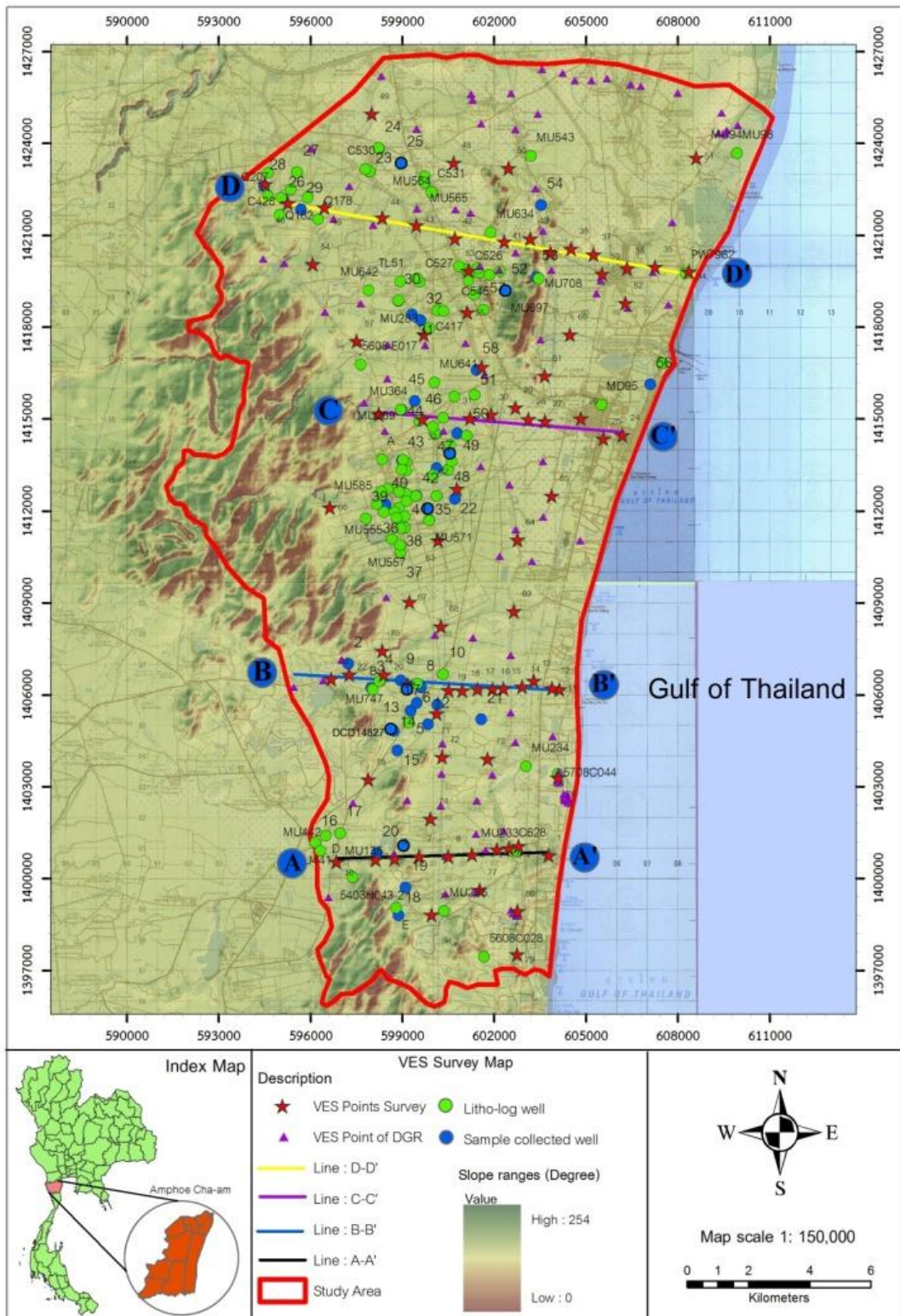


Figure 5.5 Map shows 4 cross-section lines (A-A', B-B', C-C' and D-D')

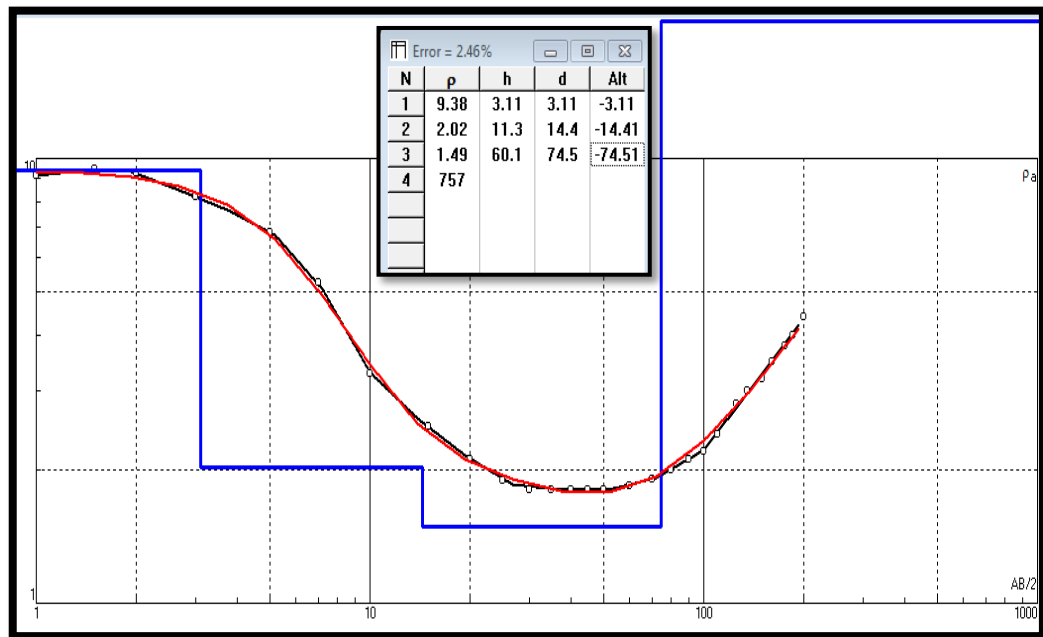


Figure 5.6 IPI2WIN interpretation of VES St-25

Figure 5.6 shows results of interpretation of VES St25 that apparent resistivity is black line and master curve is red line. It was found that at St 25 location it can be divided into 4 layers (blue line). The top layer has resistivity of $9.38 \Omega\text{m}$ with thickness of 3.11 meters and depth of 3.11 meters. Second layer has resistivity of $2.02 \Omega\text{m}$, thickness of 11.3 meters and depth of 14.4 meters. Third layer has resistivity of $1.49 \Omega\text{m}$, thickness of 60.1 meters and 74.5 meter depth. The bottom layer is bedrock layer that has resistivity $757 \Omega\text{m}$. The RMS error is 2.46 %.

After layers were interpreted of all points and then pseudo cross- section for 4 lines were generated.

Pseudo cross-section A-A' (Figure 5.7) has 14 VES that consist of St1, St2, St3, 42-28, St4, F5, 42-29, St5, St6, F6, St7, St8, St9 and St10. This line is located at the lower part of the study area and the total length is approximately 6,750 meters. It was found that the surface layer (0-10 meters) has resistivity range from 10 to 1,000 Ωm . It was interpreted as unsaturated zone of Qfd aquifer. At the western side of the profile, the very high resistivity (400 – 1,000 Ωm .) is observed. It is granite batholith that intrudes in base rock, because granite outcrop is found near the St8. In the eastern side, at depth

of 130-200 meters, the layer that has resistivity of 50-100 Ωm which is the bedrock layer. The top of this side shows resistivity values between 3- 40 Ωm . It represents sediment that saturated with water. Especially near the coastal line there is very low resistivity zone (<5 Ωm .) It may be represents the influences of seawater intrusion that intrude to inland about 1 kilometer from the coast line.

Pseudo cross-section B-B' consist of 16 VES points that are St11, St12, St13, St14, St15, St16, St17, St18, St19, St20, St21, St22, St23, 42-126 and 42-125 and start from East to West. This line is close to A-A' profile and total distance approximately 8,450 meters. From Figure 5.7 it was found that the surface layer (0-10 meters) has resistivity anomalies between 50 and 400 Ωm . It represents unsaturated zone of Qfd aquifer. The next layer shows resistivity values range from 2 to 20 Ωm . It is interpreted as sediment layer that is saturated with water. Near the coastal line there is low resistivity zone (<5 Ωm .) that is extend inland approximately 2 kilometers. It may be represent the influences of seawater intrusion. In the west side of profile at depth 20-200 meters it shows zone of resistivity range from 60 to 250 Ωm . that represent bedrock layer.

Pseudo cross-section C-C' consist of 12 VES that consist of St24, St25, St26, St27, St28, St29, St30, St31, 41-205, St32, 41-191 and St33 and start from East to West. This profile is between B-B' and D-D' profile. Total distance of this line is approximately 7,975 meters. From Figure 5.8, the surface (0-10 meters) layer has resistivity range from 6 to 700 Ωm . It represents unsaturated zone of Qfd aquifer. The next layer shows resistivity values between 2 – 20 Ωm . It represents sediment layer that is saturated with water. Near the coastal line there is low resistivity zone (<5 Ωm .) that is extended inland approximately 3.2 kilometers. It may be represent the influences of seawater intrusion. In the western side of profile at depth 40-200 meters shows resistivity values between 60-200 Ωm . that represent bedrock layer.

Pseudo cross-section D-D' consist of 14 VES that consist of St34, St35, St36, St37, St39, St41, St42, St43, St44, 41-174, 41-173, St45, St46 and St47 and start from East to West. This profile is on the northern part of the study area and the total length is approximately 14,300 meters. From Figure 5.9 it was found that the surface (0-10

meters) layer has resistivity range from 1.5 to 400 Ωm . It represents unsaturated zone of Qfd aquifer. In this profile there is low resistivity anomalies ($<5 \Omega\text{m}$.) near the surface (St7). It may be caused by the waste water from community area. The next layer shows resistivity values range from 1.5 to 20 Ωm . It represents sediment layer that is saturated with water. Near the coastal line, the low resistivity zone ($<5 \Omega\text{m}$.) is extended far from the coastal to inland approximately 4 kilometers. It may be represent the influences of seawater intrusion. In the west side of profile (90-200 meters) the bedrock is found with resistivity values of 40-100 Ωm .

Soil or rock layer with low resistivity may be caused by many reasons, such as the clay content or salt water in the porosity. This research used the litho-log data compared with VES data survey and found that the low resistivity at the area near coastal may be caused by the seawater. Figure 5.11 shows resistivity value compared with litho-log of lines D-D'. Left side shows litho-log of Q168 well versus VES of St47 that represents position far from coastal and right side shows litho-log of PW7962 well versus VES of St34 that represents position near coastal. It was found that the low resistivity ($<5 \Omega\text{m}$.) at VES St34 corresponds to gravelly clay layer but VES St47 the layer that component of clay or clayey gravel shows the resistivity 10-20 Ωm only. From the comparison it can be concluded that although layer has clay component but resistivity value is not very low ($<5 \Omega\text{m}$.). So, the area that shows very low resistivity may be influenced by seawater intrusion. This is consistent with a study of Ravindran (2013), Kaya et al. (2015) and Gopinath and Srinivasamoorthy (2015). They found that the area where low resistivity ($<5 \Omega\text{m}$.) is influenced by seawater intrusion

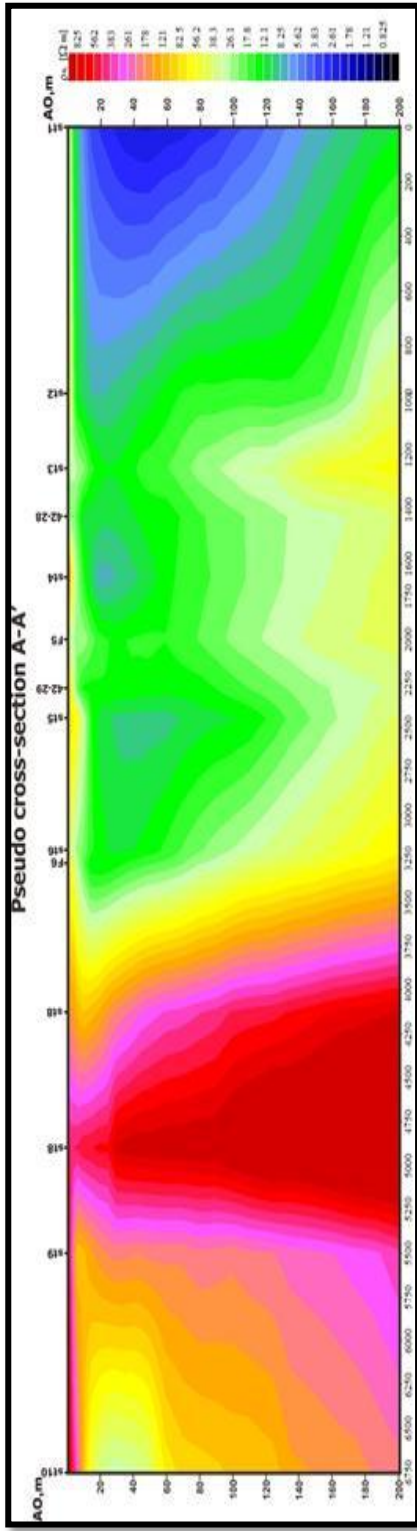


Figure 5.7 Pseudo cross-section lines A-A'

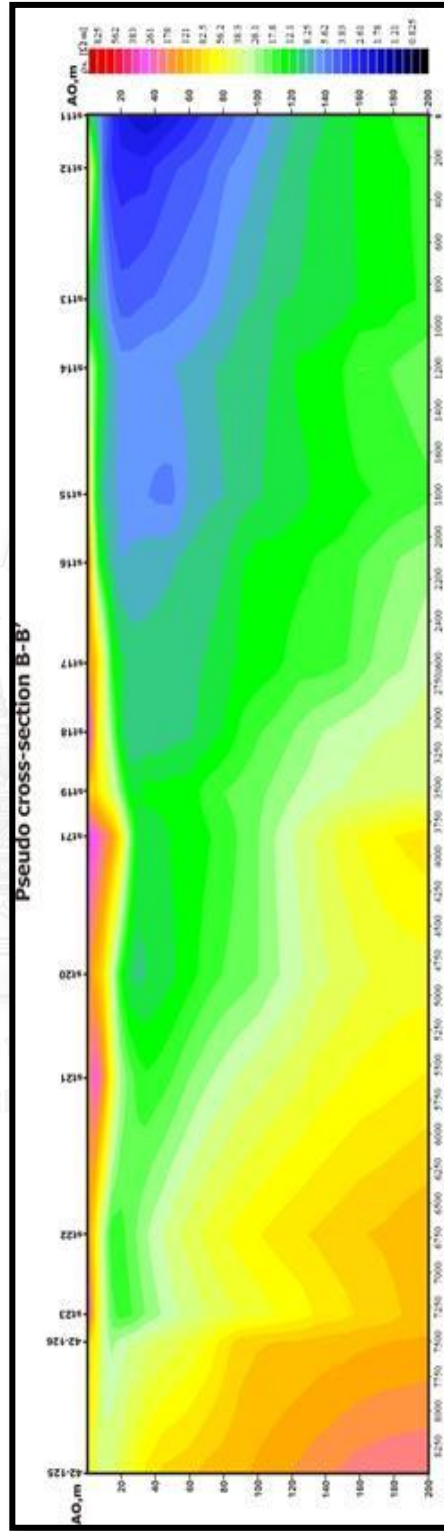


Figure 5.8 Pseudo cross-section lines B-B'

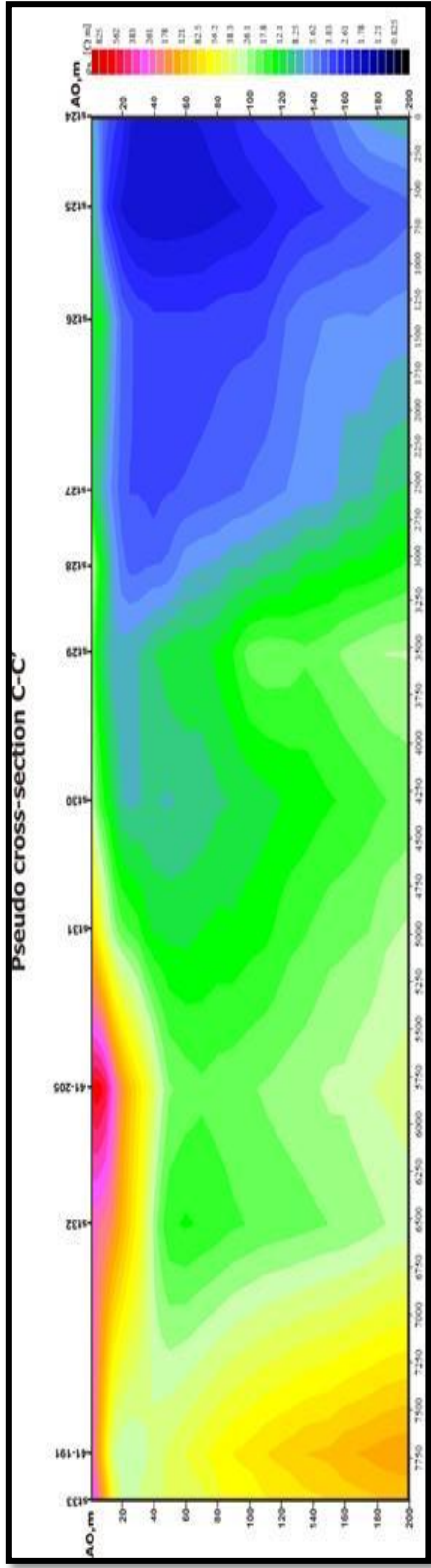


Figure 5.9 Pseudo cross-section lines C-C'

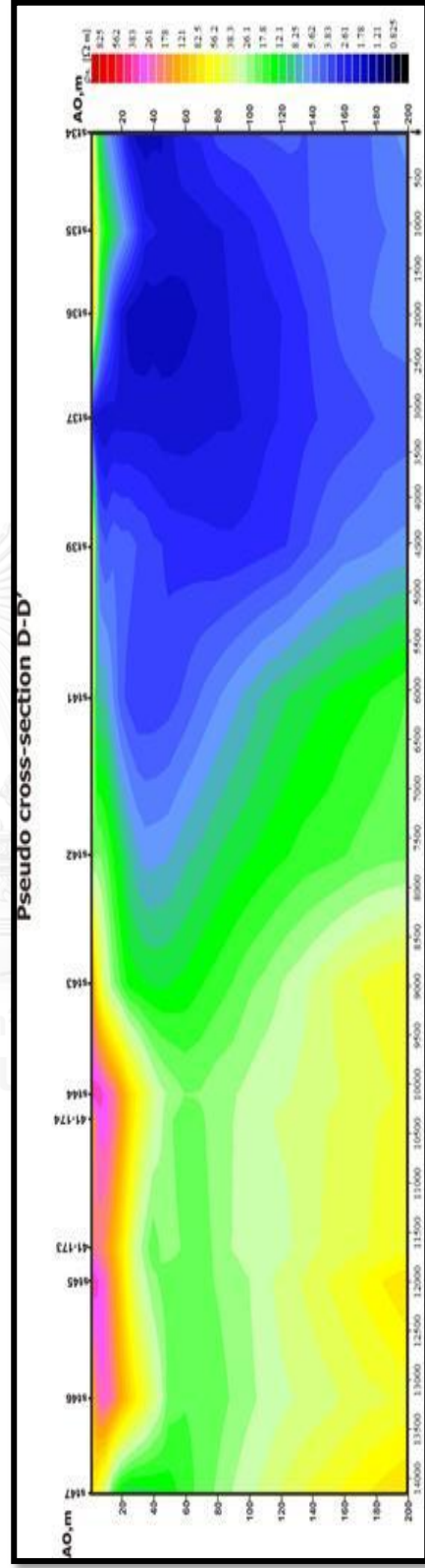


Figure 5.10 Pseudo cross-section lines D-D'

5.2.2 Geoelectrical section

When pseudo cross-section of 4 profiles was analyzed with borehole log and electric log data (example of lithologic log data shows in Figure 5.12 and appendix C1), the comparison of these two data can be established that shows in Figure 5.13, 5.14, 5.15 and 5.16.

The 4 Geo-electrical cross-sections clearly show the boundaries of each aquifer. The top layer is Qfd aquifer which consists of sand (well sorted and high sphere), approximate 0-20 meter thick. The next layer is Qcl aquifer which consists of clayey gravel (poorly sorted and angular to sub-angular) and interbedded with sand in some area. The average thickness is about 50-60 meters, but it may be up to 100 meters in the area near the coastal line. The next layer in Qcl aquifer is PCms aquifer which consists of sandstone (greenish gray) and shale. The average depth is about 50-200 meters. In the A-A' and B-B' profiles which is located in the lower part of the study area, the PCms aquifer were not found. Granite (Gr) aquifer can be found in all profile. In the D-D' profile, Pr aquifer is found and it is located in the central part of profile. It overlies on the top of PCms aquifer at approximate depth of 50-60 meters. Because this area has limitation amount of borehole log data, therefore interpretation to create a cross-section in some area require some interpolation (dash line in cross-section).

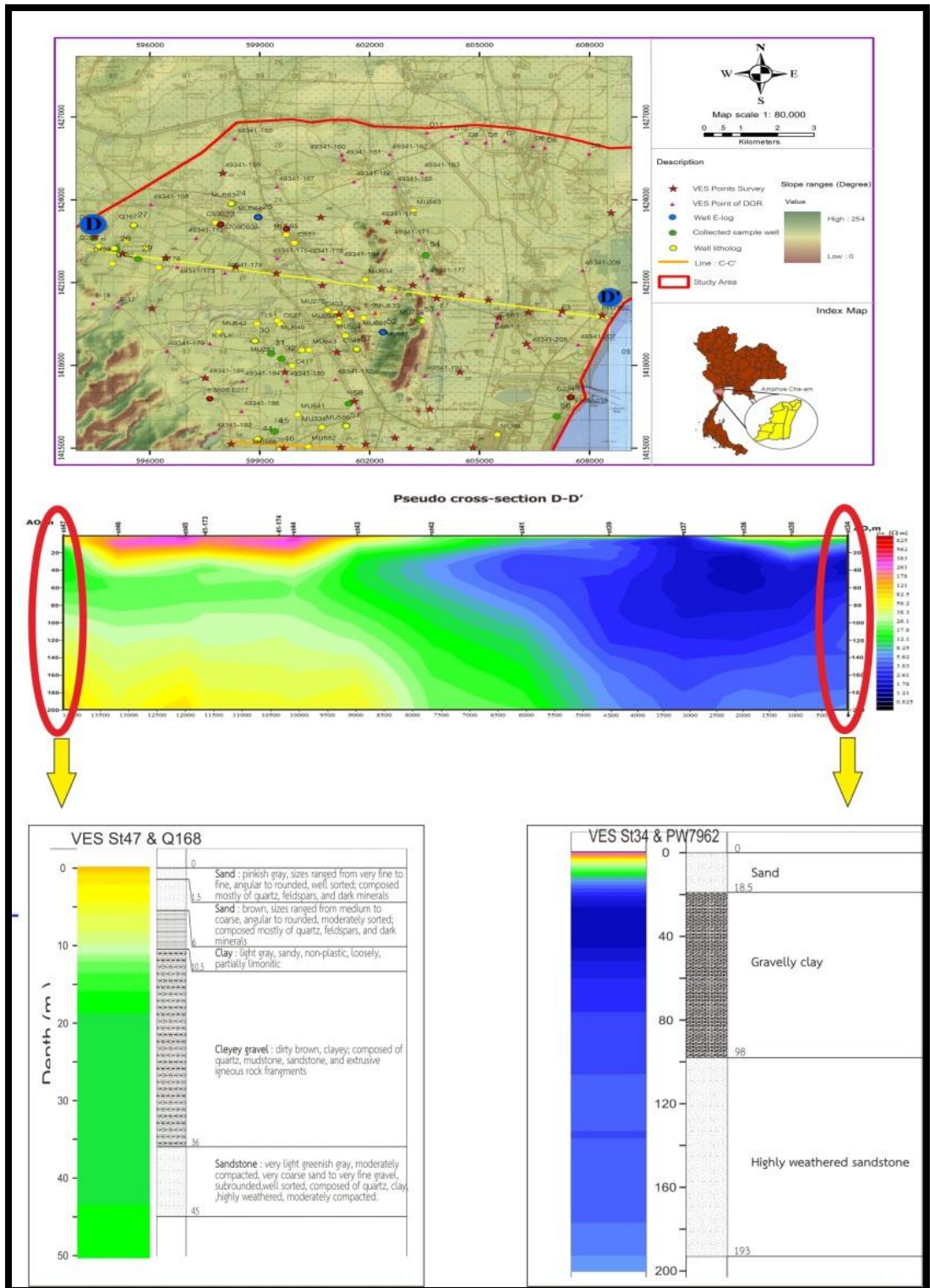


Figure 5.11 Resistivity value versus lithologic-log from pseudo cross-section lines D-D' (well Q168 versus VES St 47 and well PW7962 versus VES St 34)

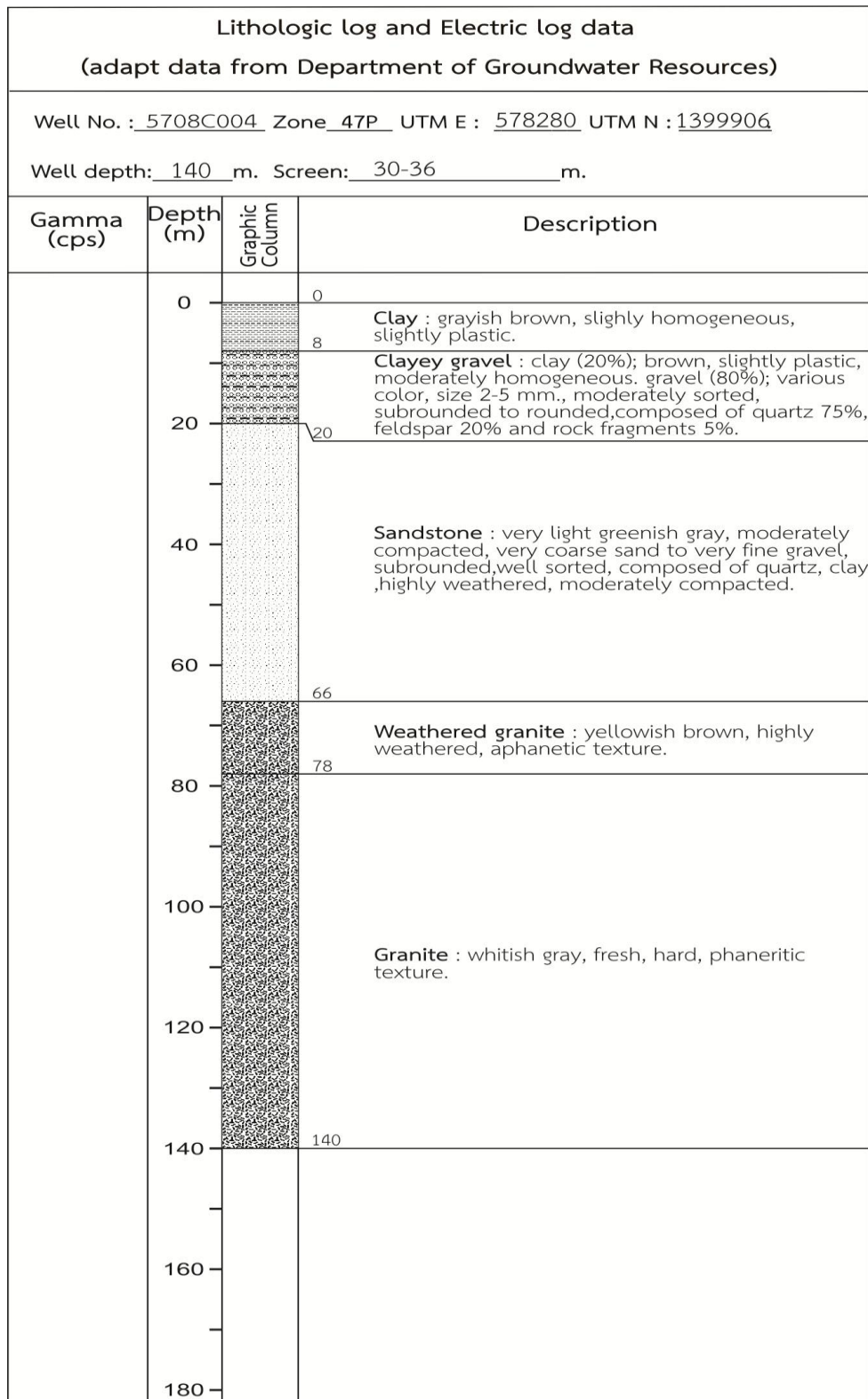


Figure 5.12 Example for lithologic log data of well no. 5708C004

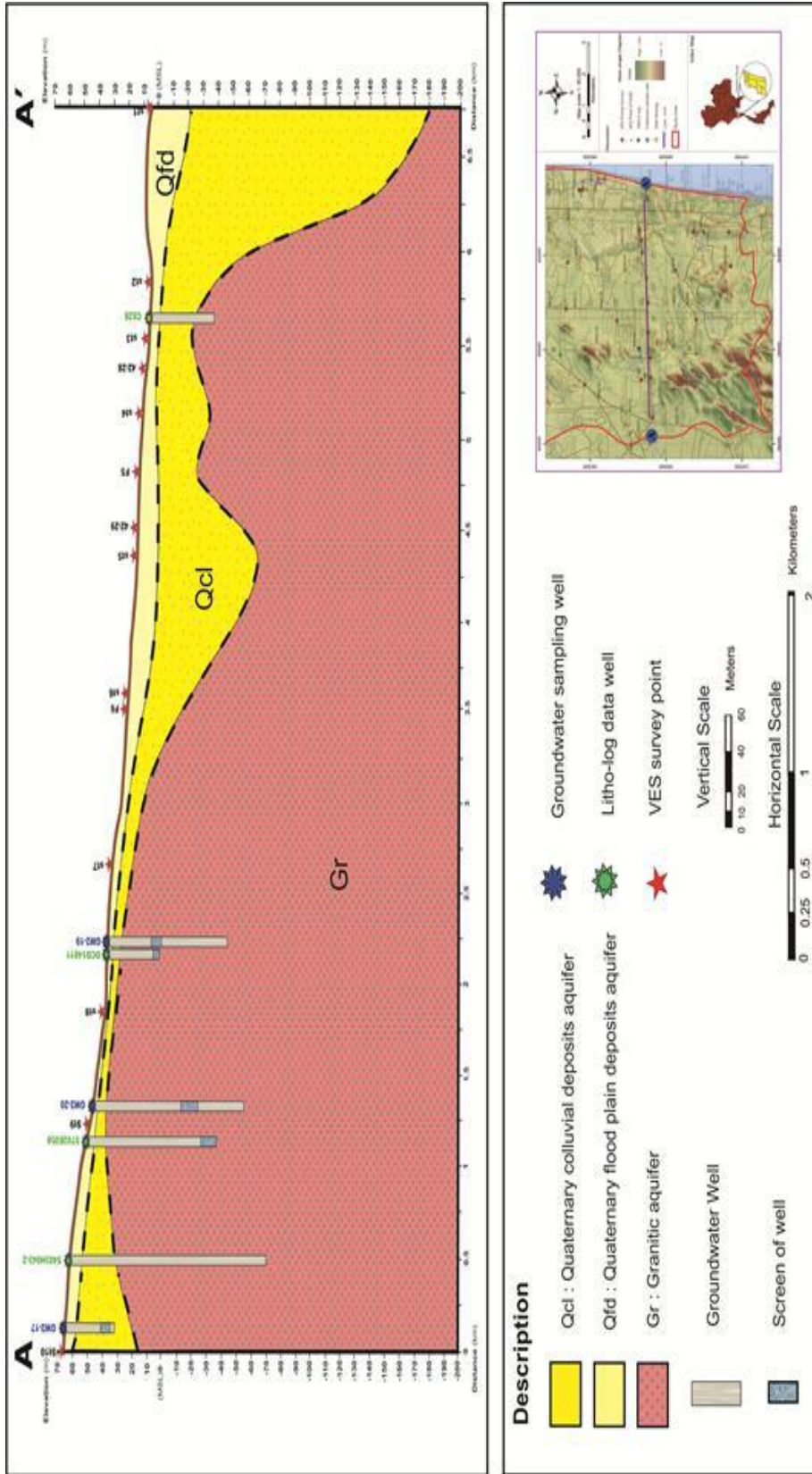


Figure 5.13 Geological cross-section lines A-A'

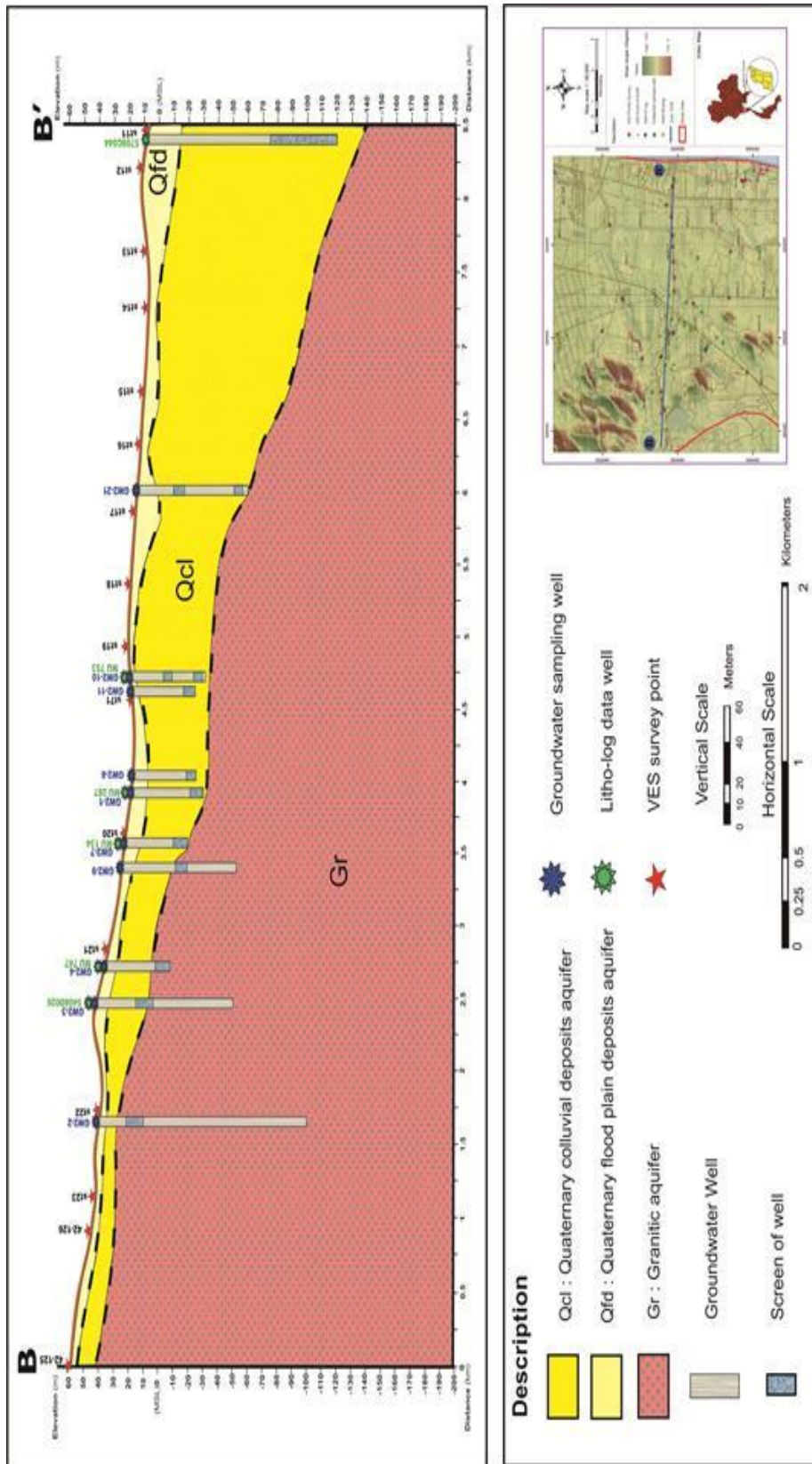


Figure 5.14 Geological cross-section lines B-B'

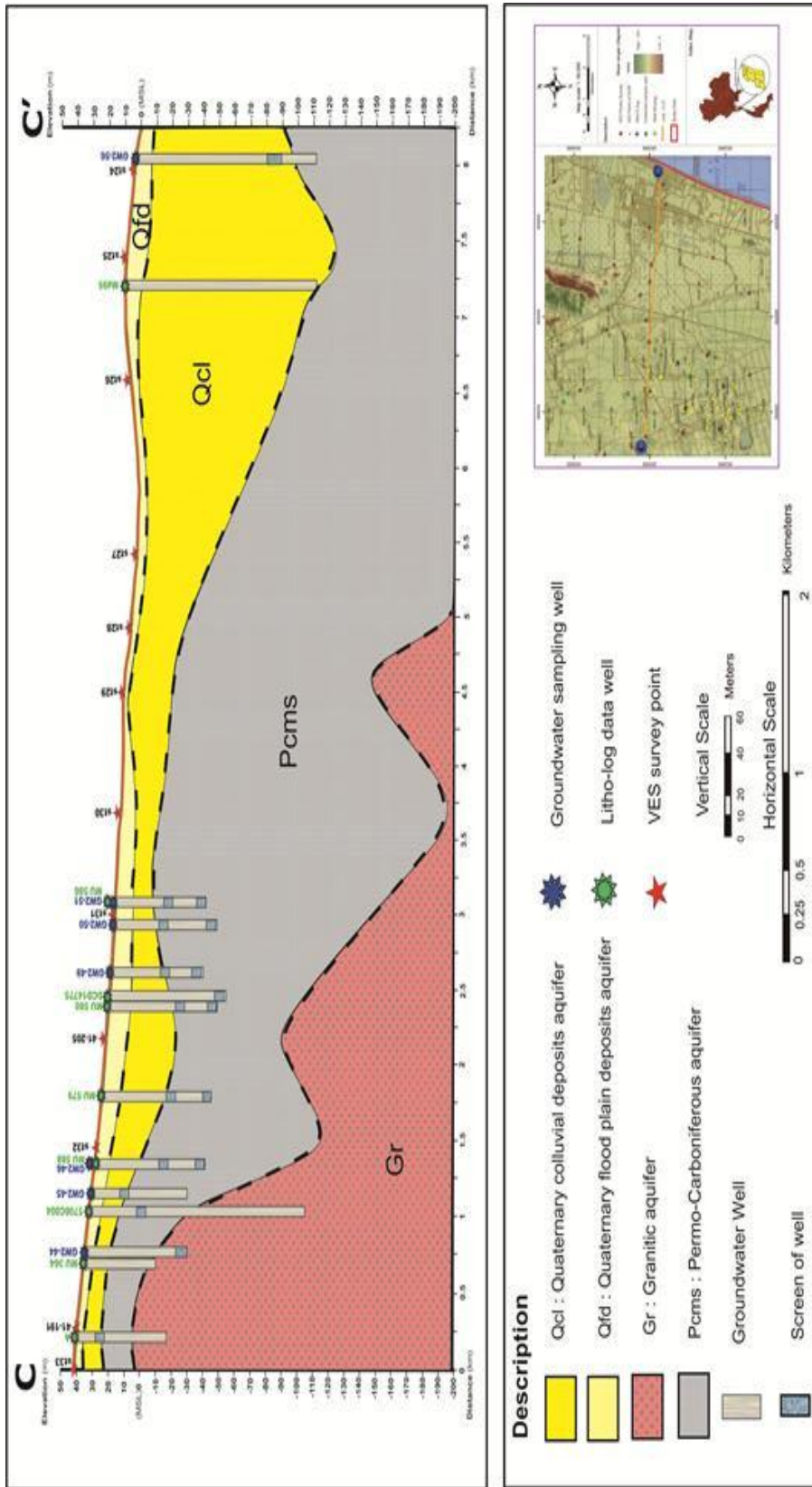


Figure 5.15 Geological cross-section lines C-C'

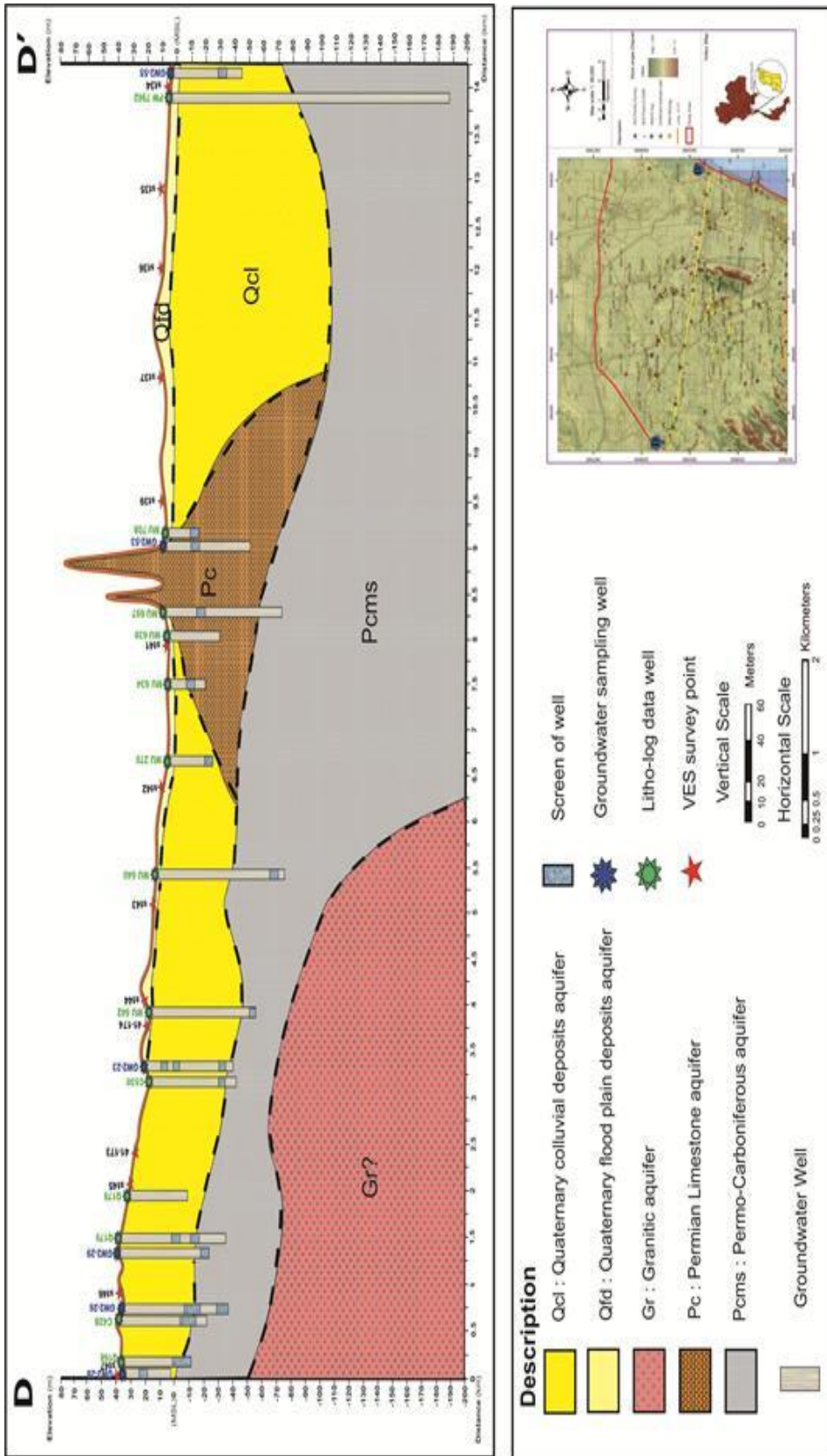


Figure 5.16 Geological cross-section lines D-D'

5.2.3 Apparent resistivity map

Apparent resistivity map is map that established from apparent resistivity of VES to be able to compare the resistivity of various depths. In this study, the apparent resistivity map for $AB/2=5$, 10, 30, 50, 70, 100, 150 and 200 meters were selected to create the map. Using ArcGIS9.3 the maps generate as Figure 5.17 that shows all different depth maps. Dark blue color on the map represents low resistivity and red color represents high resistivity respectively. Map for $AB/2=5$ meters represents the apparent resistivity at depth approximately 3.5 meters. It shows the apparent resistivity values ranging from 0.5 to 1800 Ωm . The map for $AB/2=10$ meters represents the apparent resistivity at depth approximately 7 meters. It shows the apparent resistivity values range from 0.7 to 970 Ωm . The map for $AB/2=30$ meters represents the apparent resistivity at depth approximately 21 meters. It shows the apparent resistivity values ranging from 0.6 to 870 Ωm . The map for $AB/2=50$ meters represents the apparent resistivity at depth approximately 35 meters. It shows the apparent resistivity values ranging from 1.1 to 950 Ωm . The map for $AB/2=70$ meters represents the apparent resistivity at depth approximately 49 meters. It shows the apparent resistivity values ranging from 1.3 to 1000 Ωm . The map for $AB/2=100$ meters represents the apparent resistivity at depth approximately 70 meters. It shows the apparent resistivity values ranging from 1.4 to 1200 Ωm . The map for $AB/2=150$ meters represents the apparent resistivity at depth approximately 105 meters. It shows the apparent resistivity values ranging from 1.5 to 1500 Ωm . The map for $AB/2=200$ meters represents the apparent resistivity at depth approximately 140 meters. It shows the apparent resistivity values ranging from 1.9 to 1900 Ωm .

From the Figure 5.17 it is found that all depth shows the location of low apparent resistivity ($<5 \Omega\text{m}$) in the same place. It is located on the east side of the study area that covers Tumbon Tha-Yang, Nong-Sa-La, Bang-Kao and some area of Tambon Cha-Am. Map of $AB/2=5$ and 10 meters show low apparent resistivity distributed in sporadic pattern. It is found in a wide area in map of $AB/2=30$, 50 and 70 meters and decreased in map of $AB/2=100$, 150 and 200 meters. The area that shows the high apparent

resistivity ($>1,000 \Omega\text{m}$) is located on the western side of the study area. It covers the most area of Tumbon Khao-Yai and Sam-Pra-Ya that corresponds to bedrock in the area.

From Figure 5.17 it was found that the map of $AB/2=70$ meters has the most wide dark blue ($<5 \Omega\text{m}$.) area which corresponds depth about 50 meters from the surface. When compared to cross-section, it was found that this depth is in Qcl aquifer. It can be concluded that the coastal aquifer (Qcl) has high influence of seawater intrusion.



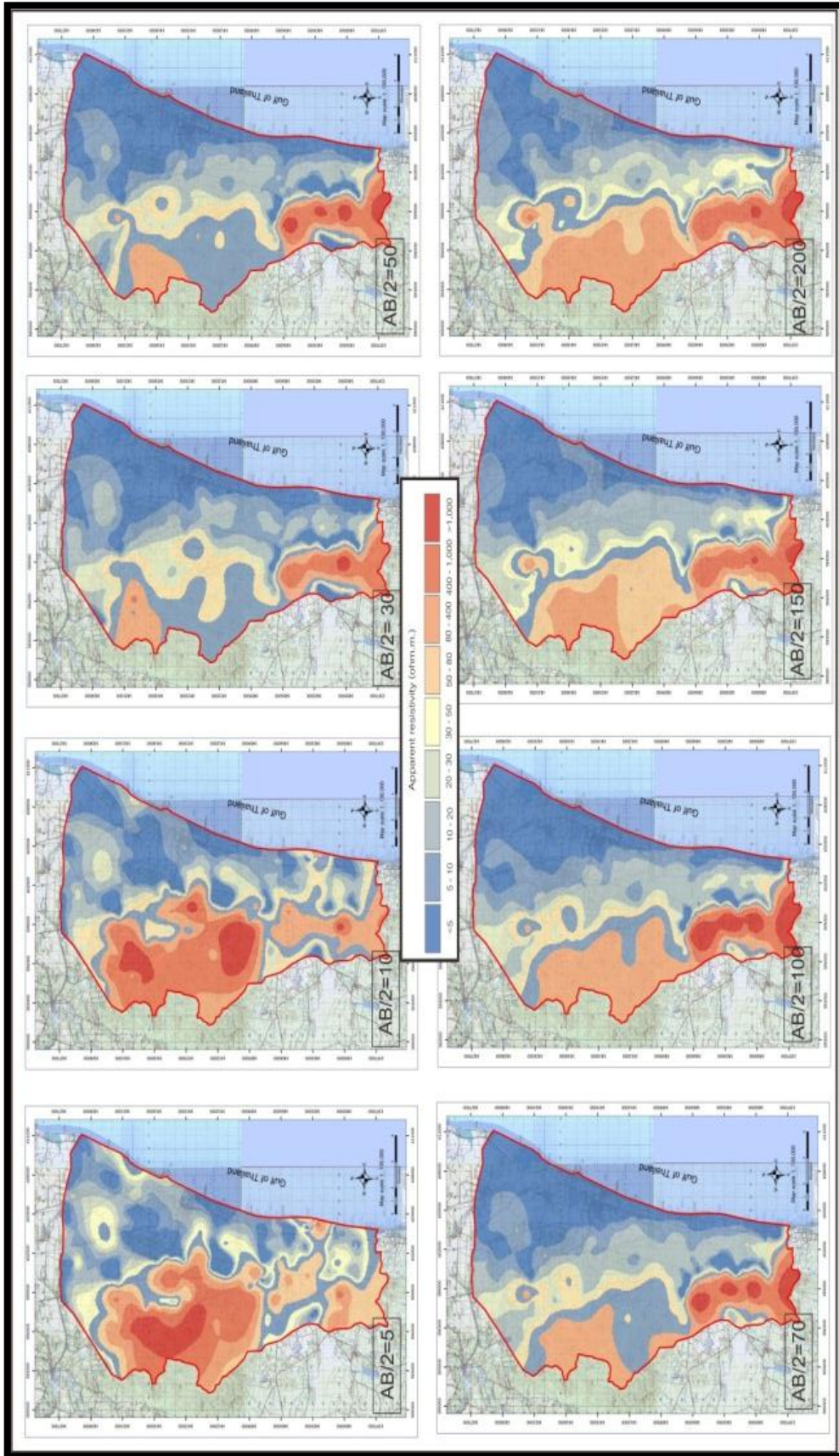


Figure 5.17 Apparent resistivity map for AB/2=5, 10, 30, 50, 70, 100, 150 and 200 meters

5.3 Hydrochemical results

5.3.1 Chemical characteristics of groundwater in the field

By in situ measurement, chemical characteristics of groundwater samples were shown in Table B2 of Appendix B2 found that pH values were in the range of 6.6-11.2 as shown in Figure 5.18. There were 35 samples (see Table B2 of appendix B2) exceeding over the groundwater standard for human consumption (MNRE, 2012), that pH values are in the range of 6.5-9.2.

Total dissolved solids (TDS) of groundwater samples were in the range of 195-3580 mg/l (see Figure 5.19). There were 33 samples (see Table B2 of appendix B2) exceeding the TDS standard of groundwater for human consumption (MNRE, 2012) that is lower than 600 mg/l.

Electrical Conductivity (EC) of groundwater samples were in the range of 292-5360 mS/cm (see Figure 5.20). There were 6 samples (W16, W18, W53, W54, W55, W56) exceeding over 2000 mS/cm while EC in groundwater is generally between 30-2000 mS/cm.

Temperature, of groundwater samples (see Figure 5.21) was found relatively constant in the range of 25.1-32.2 °C.

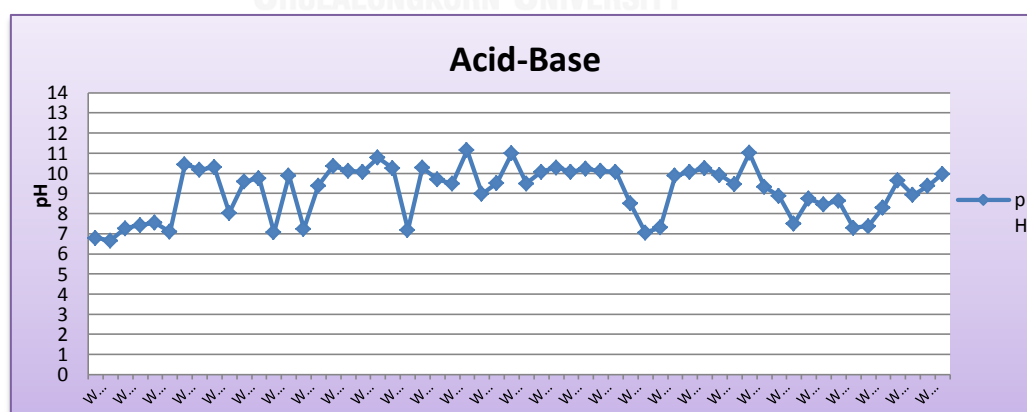


Figure 5.18 Showing pH of 58 groundwater samples.

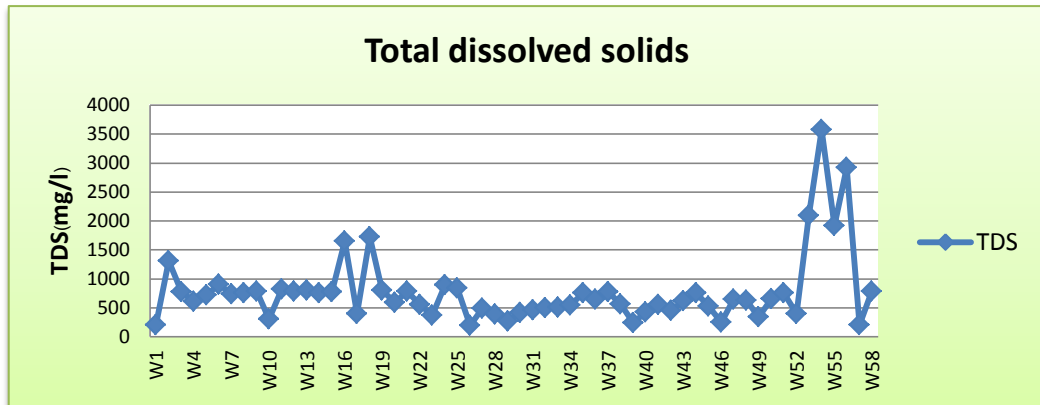


Figure 5.19 Showing TDS of 58 groundwater samples.

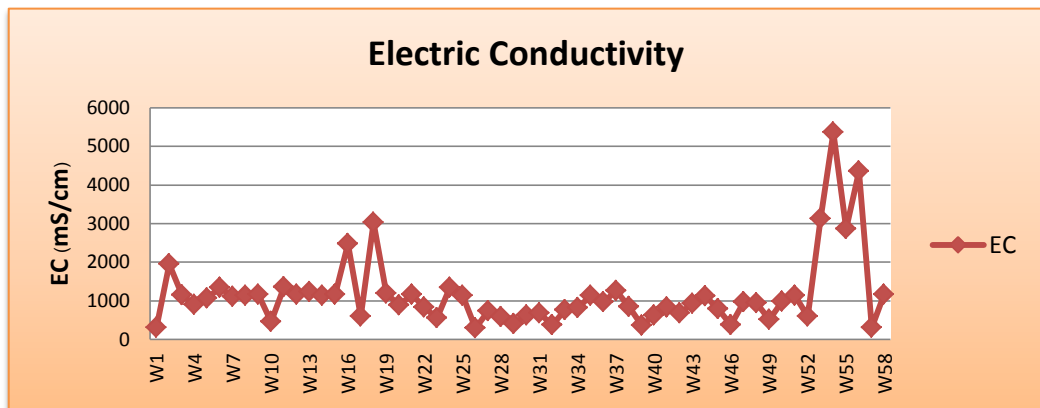


Figure 5.20 Showing electrical conductivity of 58 groundwater samples.

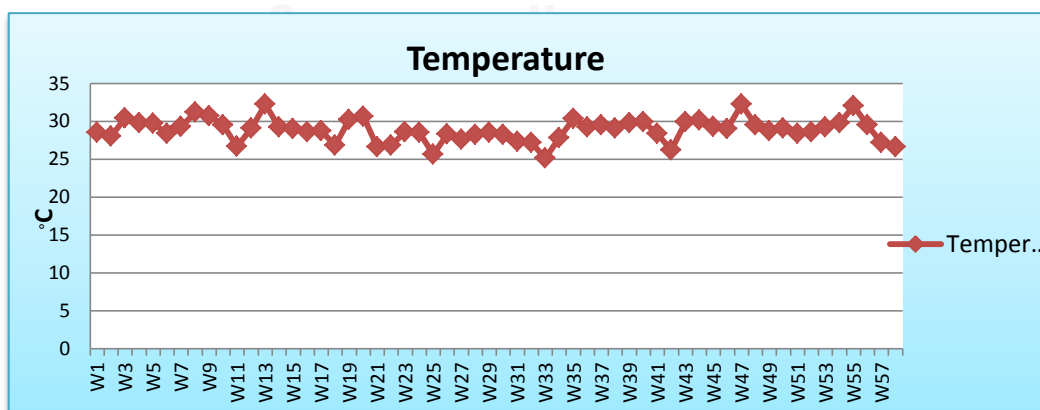


Figure 5.21 Showing temperature of 58 groundwater samples.

5.3.2 Hydrochemistry results

Hydrochemical analysis of 58 groundwater samples showed in Table 5.1. When comparing with groundwater standard for human consumption (MNRE, 2012), the details were depicted as follows;

Concentrations of sodium (Na^+) in 58 groundwater samples were in the range of 15.2-665 mg/l. There were only 6 samples (W16, W38, W53, W54, W55, W56) exceeding over the groundwater standard (< 200 mg/l).

Concentrations of potassium (K^+) in 58 groundwater samples were in the range of 3.25-58.3 mg/l. There were only 7 samples (W16, W17, W29, W36, W37, W49, W50) exceeding over the groundwater standard (<20 mg/l).

Concentrations of calcium (Ca^{2+}) in 58 groundwater samples were in the range of 14.95-214.95 mg/l. There were only 1 samples (W53) exceeding over the groundwater standard (<200 mg/l).

Concentrations of magnesium (Mg^{2+}) in 58 groundwater samples were in the range of 3.4-47.2 mg/l. Mg concentrations in all samples do not exceed the groundwater standard (<125 mg/l).

Concentrations of carbonate (CO_3^{2-}) in 58 groundwater samples were in the range of 0.00-67.2 mg/l. Carbonate concentration in all samples do not exceed the groundwater standard (<500 mg/l).

Concentration of bicarbonate (HCO_3^-) in 58 groundwater samples were in the range of 19.52-189.5 mg/l. Bicarbonate concentration in all samples do not exceed the groundwater standard (<500 mg/l).

Concentrations of chloride (Cl^-) in 58 groundwater samples were in the range of 15.48-1,489.2 mg/l. There were 12 samples (see Table 5.1) exceeding over the groundwater standard (<250 mg/l).

Concentrations of fluoride (F^-) in 58 groundwater samples were in the range of 0.09-4.32 mg/l. There were 42 samples (see Table 5.1) exceeding over the groundwater standard (<0.7 mg/l).

Concentrations of sulphate (SO_4^{2-}) in 58 groundwater samples were in the range of 0.03-167.4 mg/l. Sulphate concentration in all samples do not exceed the groundwater standard (<200 mg/l).

Concentrations of total iron in 58 groundwater samples were in the range of 0.00-2.73 mg/l. There were 7 samples (W15, W28, W29, W32, W37, W38, W45) exceeding over the groundwater standard (< 0.5 mg/l).

Concentrations of nitrate (NO_3^-) in 58 groundwater samples were in the range of 0.00-28.88 mg/l. Nitrate concentration in all samples do not exceed the groundwater standard (<45 mg/l).

The reliability of the results of hydrochemical analysis determines the charge balance of cation and anion (% Δ), that calculation detail of charge balance was shown in Appendix B3 and Table B3. Charge balances (% Δ) of 58 groundwater samples were shown in Table 5.1. According to charge balance calculation, 42 samples were acceptable (% Δ <10) (ALS Environmental) and can be further used for discussion and interpretation in the following sections. The unreliable results (16 samples) may be resulted from a process of groundwater collection and preservation, as well as dilution of concentration of samples.

5.3.2 Piper diagram

Hydrochemical facies classification of groundwater samples can be plotted on a piper diagram (Galloway and Kaiser, 1980) as shown in Figure 2.5. This research used the Groundwater Chart Program from USGS for plotting the piper diagram. Results from the piper diagram showed that 40 groundwater samples (% Δ <10) can be divided into 5 facies, consisting of Calcium-Sodium-Bicarbonate (Ca-Na-HCO₃), Calcium-Bicarbonate-Chloride (Ca-HCO₃-Cl), Calcium-Sodium-Bicarbonate-Chloride (Ca-Na-HCO₃-Cl), Calcium-Sodium-Chloride (Ca-Na-Cl) and Sodium-Chloride (Na-Cl) (see Figure 5.22 and Table 5.2).

Table 5.1 Hydrochemical analysis of groundwater samples

Sample No.	Well No.	TDS (mg/l)	EC (μ S/cm)	K (mg/L)	Fe (mg/L)	Ca (mg/L)	Mg (mg/L)	Na (mg/L)	F (mg/L)	Cl (mg/L)	Br (mg/L)	NO ₃ (mg/L)	SO ₄ (mg/L)	CO ₃ (mg/L)	HCO ₃ (mg/L)	% Δ
W1	MU287	205	1000	12.25	N/D	35.4	5.6	95.8	0.347	82.12	0.839	0.64	7.16	25.2	51.24	23.105
W2	5608G006	1307	1951	4.5	0.008	100.6	18.9	159	2.033	215.075	1.671	3.857	24.2	67.2	136.64	9.162
W3	5408D026	773	1155	5.7	N/D	98.95	17.7	109.75	2.901	89.2	1.678	1.501	12.16	64.8	131.76	22.247
W4	MU747	607	905	8.4	N/D	48.4	13.3	82	1.184	128.92	1.368	0.353	0.708	39.6	80.52	7.185
W5	PCR9	718	1071	13.45	N/D	49.65	17.4	64.2	1.254	79.53	1.84	N/D	0.223	63.6	129.32	4.130
W6	C629	905	1348	16.05	N/D	48.01	18.2	129.6	1.195	219.525	1.535	7.9	13.2	22.4	72.3	5.202
W7	MU134	739	1105	14.75	N/D	41.9	9	115.5	0.823	229.5	1.475	0.308	0.054	18	36.6	3.402
W8	Private	761	1137	11	N/D	45.3	12	137.75	1.806	215.4	2.098	N/D	1.763	18	118.6	4.783
W9	Private	781	1170	7.7	N/D	58.95	12.9	40.2	3.180	84.84	1.94	2.889	4.928	N/D	132.6	9.927
W10	MU753	602	1123	9.15	0.147	17.6	8.7	54.6	0.134	119.88	1.065	0.033	9.939	N/D	48.8	-2.149
W11	Private	825	1360	17.45	N/D	46.9	18.5	127.25	1.239	216.475	1.919	10.52	9.615	N/D	141.52	2.452
W12	¶1642	781	1166	13.35	N/D	69.4	20.5	115	1.265	167.6	2.566	7.367	5.736	N/D	119.56	17.754
W13	DCD14827	805	1230	6.55	N/D	70.6	34	103.2	1.462	169.975	2.008	1.449	16.3	N/D	112.24	21.629
W14	5508C019	757	1130	4.75	N/D	58.95	34	92.2	1.192	164.94	2.791	N/D	2.402	52.8	107.36	9.137
W15	DCD14809	779	1162	6.8	0.548	68.75	19.7	90.6	0.833	180.95	2.228	0.149	0.046	N/D	145.9	9.978
W16	Private	1650	879	43	N/D	86.15	24.6	241	0.513	336.28	3.654	28.88	44	N/D	158.6	8.641
W17	MU135	397	594	20.8	N/D	45.35	11.7	32	0.134	56.14	1.583	0.183	12.83	N/D	158.6	7.142
W18	Private	1720	3024	4.75	N/D	168.4	27.8	199.6	3.115	400.88	3.589	10.64	84.96	60	122	4.461
W19	Private	801	1196	14.55	N/D	70.3	18.2	40.5	1.25	72.8	2.996	9.478	12.32	N/D	182.7	8.826
W20	ND	591	883	4.65	N/D	81.2	12.1	32.4	0.969	69.4	2.758	1.245	12.27	N/D	189.5	9.745
W21	5408D022	782	1168	16.3	0.009	45.65	18.4	133	1.156	252	2.984	3.334	10.24	N/D	122	2.255

Table 5.1 Hydrochemical analysis of groundwater samples (continue)

Sample No.	Well No.	TDS (mg/l)	EC (μ S/cm)	K (mg/L)	Fe (mg/L)	Ca (mg/L)	Mg (mg/L)	Na (mg/L)	F (mg/L)	Cl (mg/L)	Br (mg/L)	No3 (mg/L)	SO ₄ (mg/L)	CO ₃ (mg/L)	HCO ₃ (mg/L)	% Δ
W22	DCD14772	556	830	8.95	0.103	50	13.8	107.6	2.728	204.78	2.198	0.034	4.215	N/D	102.48	6.208
W23	5608C045	375	562	10.05	N/D	61.15	9.6	44.4	0.269	135.2	1.684	0.074	26.3	N/D	70.4	4.433
W24	MU563	900	1347	6.55	0.056	71.05	32.6	122.5	1.588	279.5	3.156	3.561	65.3	N/D	68.32	4.982
W25	MU564	843	1130	6.05	N/D	93.9	47.2	198.8	1.234	477.8	4.536	1.061	71.75	N/D	68.32	3.630
W26	5408D011	195	292	14.1	N/D	15.65	4	33	1.944	34.6	0.836	12.02	1.287	N/D	21.96	13.368
W27	Q167	494	739	19.55	0.048	57.3	8.7	68	1.955	129.8	1.578	2.093	0.921	N/D	84.8	14.824
W28	Q1607	391	584	12.7	0.879	45.95	9.8	62	1.934	125.6	1.664	0.183	0.031	N/D	94.6	9.056
W29	Private	267	400	23.65	0.925	18.9	3.4	24.8	2.219	50.4	0.754	0.973	0.185	28.8	58.56	-8.031
W30	MU283	420	627	16.35	0.209	45.4	7.1	42.9	2.154	87.6	1.541	0.567	6.204	N/D	124.6	4.608
W31	PCR10	460	687	9.05	N/D	45.15	11.7	87.6	2.492	100.5	1.68	0.072	8.604	N/D	70.76	26.942
W32	DCD14768	503	375	18.4	2.73	44.6	12.3	40.1	1.551	64.3	2.021	0.086	0.061	20.1	122	9.680
W33	MU348	507	757	10.05	N/D	56.3	13.1	70.2	1.308	130.15	1.946	5.401	3.659	N/D	132.5	6.632
W34	MU363	548	1015	8.65	N/D	51.4	13.1	118.2	1.199	259.6	0.953	1	8.577	N/D	62.3	2.377
W35	MU571	762	1138	15.65	0.069	45.6	17.2	134.6	1.001	289.8	2.659	1.949	9.96	N/D	82.6	3.334
W36	MU332	649	1002	57.3	N/D	59.35	21.8	82	0.288	178.6	2.225	N/D	24.2	N/D	112.24	14.043
W37	MU359	780	1267	58.3	1.104	58.75	17.8	123.4	0.199	247.95	3.282	0.316	29.25	N/D	97.6	9.942
W38	MU557	565	848	43.1	1.721	125.55	36.6	215.5	0.307	380.24	3.959	0.129	131.56	N/D	122	12.171
W39	MU458	239	357	15.1	0.387	15.5	5.9	33	0.170	64.3	0.812	1.052	2.281	N/D	34.6	10.366
W40	5608C007	426	631	12.2	N/D	41.8	11.4	80	1.059	100.6	1.608	0.058	1.647	N/D	31.72	33.522
W41	MU361	559	834	11.2	N/D	49	13.6	87.6	4.325	97.3	1.711	4.303	24.43	51.6	104.92	4.512
W42	MU335	454	677	15.8	N/D	44.85	11.1	75.8	1.342	86.7	1.778	1.63	3.014	N/D	75.64	27.902
W43	MU549	621	929	14.15	N/D	76.1	18.9	93.8	1.975	154.3	2.084	8.536	5.307	51.6	104.92	7.020
W44	DCD14766	753	1124	12	0.007	58.35	16.4	82.4	2.310	170.425	1.806	0	2.524	52.8	107.36	-1.354

Table 5.1 Hydrochemical analysis of groundwater samples (continue)

Sample No.	Well No.	TDS (mg/l)	EC (μ S/cm)	K (mg/L)	Fe (mg/L)	Ca (mg/L)	Mg (mg/L)	Na (mg/L)	F (mg/L)	Cl (mg/L)	Br (mg/L)	NO ₃ (mg/L)	SO ₄ (mg/L)	CO ₃ (mg/L)	HCO ₃ (mg/L)	% Δ
W45	AFD8794	531	793	12.25	1.665	36.2	3.6	60.9	1.984	62.26	0.64	6.487	10.9	40.8	82.96	-0.991
W46	MU588	254	379	8.25	0.019	24.75	7.8	32.4	0.743	15.486	1.05	0.042	5.706	16	54.2	27.687
W47	DCD14773	649	970	12.95	N/D	61.3	16.8	89.6	1.705	134.6	1.933	14.78	8.539	N/D	136.64	8.798
W48	MU578	629	939	17.05	N/D	70.9	18.3	85.2	1.564	53.18	2.169	16.88	10.12	N/D	87.84	35.666
W49	DOH11441	340	514	29.35	0.062	24.6	12	42.1	0.665	60.72	1.104	0.467	8.423	36	72.4	5.378
W50	MU331	660	986	20.95	0.066	66.25	22	92.4	0.771	184.2	2.135	0.356	3.86	39.6	80.52	9.848
W51	MU586	762	1138	13.3	N/D	72.9	12.9	84.3	1.960	171.1	2.244	2.601	4.256	14	122	7.023
W52	MU697	397	598	3.25	N/D	65.2	10.2	64.2	0.099	100.4	1.085	1.06	11.8	40	89.4	7.876
W53	¶1605	2090	3120	4.85	N/D	214.55	30.5	288.4	N/D	920.9	4.776	9.142	74.8	36	73.2	-8.290
W54	PCR16	3580	5360	14	N/D	38.05	37.8	665	0.247	1489.2	6.372	3.524	167.4	50.4	102.48	-17.723
W55	¶86	1920	2860	9.35	N/D	73.5	31.4	284.6	0.408	662.2	4.611	N/D	24.2	40.1	117.12	-8.603
W56	¶88	2920	4360	15.15	N/D	82.2	41.8	541	0.294	935.6	6.101	N/D	160.6	64.8	131.76	-3.928
W57	C545	207	310	10.5	N/D	60.35	12.5	56.4	1.206	92.16	2.565	1.012	12.34	62.4	126.88	-2.354
W58	Private	784	1169	7.15	N/D	14.95	3.8	15.2	0.193	43.46	0.638	0.122	0.119	N/D	19.52	10.028
Seawater		37675.2	53821.7	396.931	0.488	841.1	1083.43	11106.3	9.7944	21192.1	37.7172	N/D	2793.78	70.3998	143.142	-2.780

* Detection limit of IC standard (anion) = 10 ppm, AAS standard for Ca²⁺ = 5 ppm, Mg²⁺ = 0.25 ppm, Na⁺ = 0.5 ppm, K⁺ = 1 ppm and Fe = 3 ppm

** Acceptable % error balance is less than ± 10 % (ALS Environmental)

***N/D = Not detected

Calcium-Sodium-Bicarbonate facies (Ca-Na-HCO_3) is fresh water and is found in W5 which was opened a well screen to Gr aquifer. This groundwater facie is younger and weak acid, which is generally found in high terrain or recharge area (Appelo & Postma, 2005).

Calcium-Bicarbonate-Chloride facies ($\text{Ca-HCO}_3\text{-Cl}$) was found in W19 and W20 that was opened a well screen to Gr aquifer. This groundwater facies is in water-bearing permeable rocks because when groundwater moves through the rock formation, ion exchange process happens (Appelo & Postma, 2005). The quality water of this facies is fresh water.

Calcium-Sodium-Bicarbonate-Chloride facies ($\text{Ca-Na-HCO}_3\text{-Cl}$) was found in 8 wells (W2, W4, W9, W14, W15, W43, W44, and W20), which were opened a well screen to Gr aquifer while 9 wells (W29, W30, W32, W33, W41, W47, W50, W51 and W20) that were opened a well screen to PCms aquifer. Moreover, only 1 well (W 52) and 3 wells were opened a well screen in Pr aquifer and Qcl aquifer, respectively. This facies present a complex chemical pattern since the water is influenced by many factors. It may result from mixing of fresh water with seawater (Appelo & Postma, 2005).

Calcium-Sodium-Chloride facies (Ca-Na-Cl) was found in W53 that was opened a well screen to Pr aquifer while 3 wells (W24, W25 and W34) were opened a well screen to Qcl aquifer and 2 wells (W22 and W23) were opened a well screen to both Qcl and PCms aquifers . Groundwater facies may have been changed due to the influence of seawater intrusion by ion exchange process (Appelo & Postma, 2005).

Sodium-Chloride facies (Na-Cl) was found in 10 wells (W6, W7, W8, W10, W11, W21, W35, W37, W55 and W56) that was opened a well screen to Qcl aquifer. Groundwater facies indicates that these wells have been influenced by seawater intrusion, and the quality water is saline water.

According to the piper diagram followed Galloway and Kaiser (1980), groundwater facies can be classified into 5 facies, which corresponds to the influence of seawater intrusion, not only depending on the distance from the coastal, but also on depth of well or screen level of well. Most groundwater samples in Qcl aquifer has been

relatively influenced by seawater intrusion. In general, an average depth of QCl aquifer ranges from 20 to 50 meters and the thickness is typically higher than 100 meters as approaching the coastal line. Na-Cl facies and Ca-Na-Cl facies mainly found in QCl aquifer. Groundwater facies of groundwater collected from PCMs and Gr aquifers, which have been opened a well screen in the high weathering zone (underneath QCl aquifer) at a depth of 40-60 meters is Ca-Na-HCO₃-Cl facies, suggesting that groundwater is moderately affected by seawater intrusion. Moreover, groundwater facies in PCMs and Gr aquifers in which a well screen opened to, at a depth of 60-80 meters, are Ca-HCO₃-Cl and Ca-Na-HCO₃ facies, suggesting that groundwater is slightly affected by seawater intrusion.

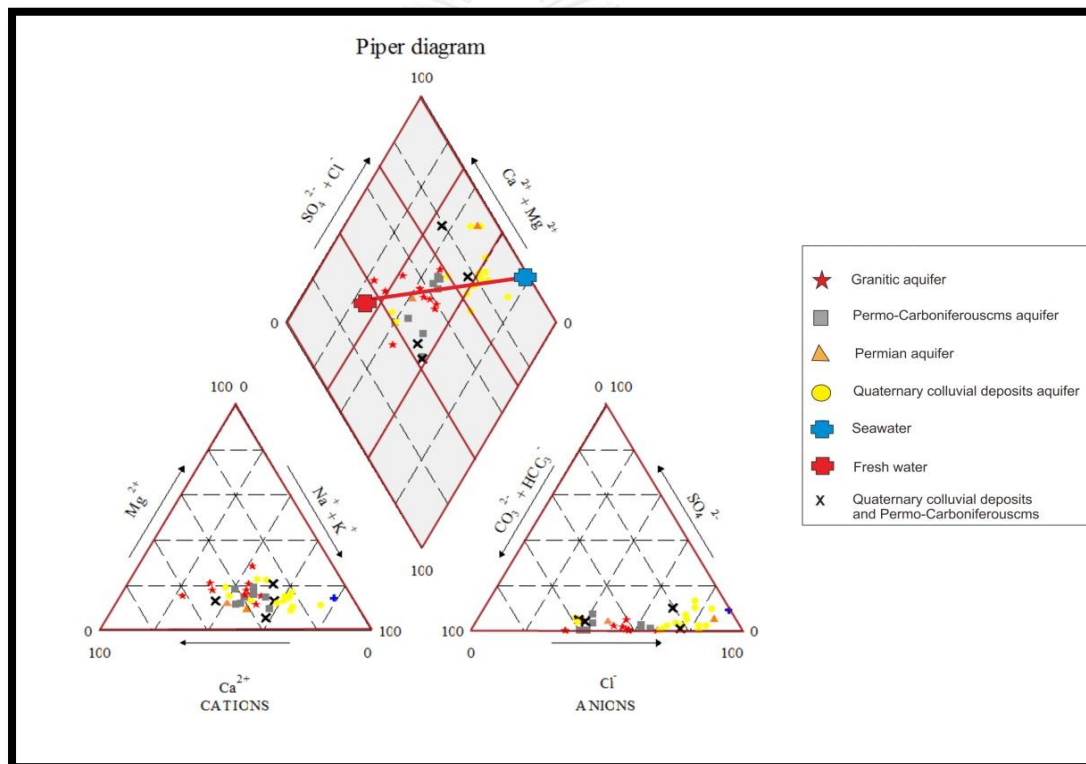


Figure 5.22 Hydrochemical analysis of groundwater sample plotted in the piper diagram

Table 5.2 Hydrochemical results and groundwater facies

Sample No.	Well No.	% Δ	Aquifer	Water type
W2	5608G006	9.162	Gr	Ca-Na-HCO ₃ -Cl
W4	MU747	7.185	Gr	Ca-Na-HCO ₃ -Cl
W5	PCR9	4.130	Gr	Ca-Na-HCO ₃
W6	C629	5.202	QCl	Na-Cl

Sample No.	Well No.	% Δ	Aquifer	Water type
W7	MU134	3.402	Qcl	Na-Cl
W8	Private	4.783	Qcl	Na-Cl
W9	Private	9.927	Gr	Ca-Na-HCO ₃ -Cl
W10	MU753	-2.149	Qcl	Na-Cl
W11	Private	2.452	Qcl	Na-Cl
W14	5508C019	9.137	Gr	Ca-Na-HCO ₃ -Cl
W15	DCD14809	9.978	Gr	Ca-Na-HCO ₃ -Cl
W17	MU135	7.142	Qcl	Ca-Na-HCO ₃ -Cl
W19	Private	8.826	Gr	Ca-HCO ₃ -Cl
W20	ND	9.745	Gr	Ca-HCO ₃ -Cl
W21	5408D022	2.255	Qcl	Na-Cl
W22	DCD14772	6.208	Qcl+PCms	Ca-Na-Cl
W23	5608C045	4.433	Qcl+PCms	Ca-Na-Cl
W24	MU563	4.982	Qcl	Ca-Na-Cl
W25	MU564	3.630	Qcl	Ca-Na-Cl
W28	၁1607	9.056	Qcl	Ca-Na-Hco ₃ -Cl
W29	Private	-8.031	PCms	Ca-Na-HCO ₃ -Cl
W30	MU283	4.608	PCms	Ca-Na-HCO ₃ -Cl
W32	DCD14768	9.680	PCms	Ca-Na-HCO ₃ -Cl
W33	MU348	6.632	PCms	Ca-Na-HCO ₃ -Cl
W34	MU363	2.377	Qcl	Ca-Na-Cl
W35	MU571	3.334	Qcl	Na-Cl
W37	MU359	9.942	Qcl	Na-Cl
W41	MU361	4.512	PCms	Ca-Na-HCO ₃ -Cl
W43	MU549	7.020	Gr	Ca-Na-HCO ₃ -Cl
W44	DCD14766	-1.354	Gr	Ca-Na-HCO ₃ -Cl
W45	AFD8794	-0.991	Qcl+PCms	Ca-Na-HCO ₃ -Cl
W47	DCD14773	8.798	PCms	Ca-Na-HCO ₃ -Cl
W49	DOH11441	5.378	Qcl+PCms	Ca-Na-HCO ₃ -Cl
W50	MU331	9.848	PCms	Ca-Na-HCO ₃ -Cl
W51	MU586	7.023	PCms	Ca-Na-HCO ₃ -Cl
W52	MU697	7.876	Pr	Ca-Na-HCO ₃ -Cl
W53	၁1605	-8.290	Pr	Ca-Na-Cl
W55	၁86	-8.603	Qcl	Na-Cl
W56	၁88	-3.928	Qcl	Na-Cl
W57	C545	-2.354	Qcl	Ca-Na-HCO ₃ -Cl
Seawater		-2.780	-	Na-Cl

The red line on the piper diagram (Figure 5.22) is the line that shows hydrochemical evolution of groundwater facies by the cation exchange reaction (Appelo and Postma, 2005). This line is resulting from 2 points that plotted between the composition of seawater (blue point) and fresh water (red point) on the piper diagram. By using this line, hydrochemical results of groundwater samples are fallen in the zone between blue and red points, representing mixed water between fresh water and seawater occurs. Groundwater facies closely to the blue point are Na-Cl facies and Ca-Na-Cl facies, while groundwater facies closely to the red point are Ca-HCO₃-Cl and Ca-Na-HCO₃. Groundwater facies found between blue and red points are Ca-Na-HCO₃-Cl facies. As mentioned earlier, these are similar to the study of Zghibi et al (2014) who study about contamination in Korba unconfined aquifer, which is influenced by seawater intrusion. They showed a chemical analysis of water on the piper diagram and then interpret results by creating Theoretical Mixing Line (TML) of seawater and fresh water. They found that groundwater showed paths of hydrochemical evolution along TML line. The groundwater facies can be changed from Ca-SO₄ type to Ca-Cl type to Na-Cl type, and vice versa, from Ca-SO₄ type directly to Na-Cl type, indicating that the chemical composition of groundwater is changed by cation exchange reaction.

5.3.3 Relationship between Na and Cl ions

Dominant ions in seawater are Na and Cl while dominant ions in fresh water are Ca and HCO₃ (Appelo & Postma, 2005). Therefore, the study of seawater intrusion have to focus on dominant ion of seawater which is Na and Cl. Plotted graph comparing between Na and Cl found that it exhibits strong correlation in which samples, falling on a 1:1 line with R² of 0.941. This relationship suggests that both ions have the same origin from seawater. The concentrations of Na and Cl depend on the degree of seawater intrusion into the aquifer.

From Figure 5.23, groundwater can be divided into 3 groups. The first group located in red circle, mainly consists of samples in Qcl aquifer that get severely influenced by seawater intrusion. Groundwater types in this group showed Na-Cl and Ca-Na-Cl. The second group appeared in green circle, consists of sample from PCms

and Gr aquifers, which get moderately influenced by seawater intrusion. Groundwater types in this group showed Ca-Na-HCO₃-Cl facies. The last group appeared in blue circle, consists of samples from the deeper zone (as compared to the second group) of PCms and Gr aquifers, which get slightly influenced by seawater intrusion. Groundwater types in this group showed Ca-HCO₃-Cl facies and Ca-Na-HCO₃ facies. These are consistent with the study of Agoubi et al. (2013) and Zghibi et al. (2014) that study about characteristics of the groundwater chemistry influenced by seawater intrusion. They found that groundwater influenced by seawater intrusion has dominant ions of Na and Cl. Therefore, when plotting Na and Cl, both ions are well defined correlation, in which groundwater sample fall on 1:1 line, indicating that both ions come from the same source (seawater).

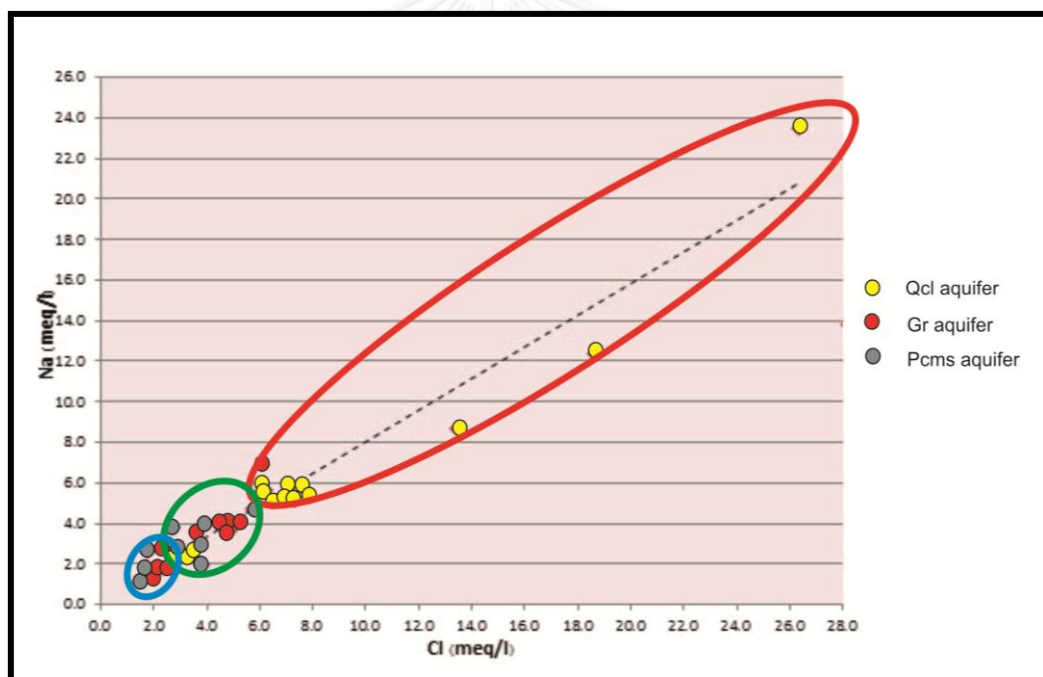


Figure 5.23 Relationship plotting between Na and Cl concentration in groundwater

5.3.4 Hydrochemical facies evolution diagram (HFED)

The study of Al-Agha and Nakhal (2004) found that plotting the results of groundwater samples on the piper diagram can be interpreted about phases of freshening and intrusion, but it is difficult to recognize the sequence of facies in detail.

Therefore, this research used Hydrochemical Facies Evolution diagram (HFED) developed by Forcada (2010) to describe the dynamic of seawater intrusion. Percentage of major ions in hydrochemical process associated with dynamic of seawater intrusion interface, consisting of Ca^{2+} , Na^+ , HCO_3^- , SO_4^{2-} , Cl^- , has been considered in HFED. The results are shown in Figure 5.24

From Figure 5.24, red block (no. 4) is Na-Cl facies (seawater) and blue block (no. 13) is Ca- HCO_3 facies (fresh water). After plotting percentage of ions on the diagram, it will generate a mixing line between fresh water and seawater to divide phases of seawater intrusion. When the groundwater samples appear above the mixing line, it represents freshening phase, and if it is below mixing line, indicating that it is during intrusion phase. The results found that most of samples fall close to the mixing line (facies path 4-7-10-13) demonstrating mixing between seawater and fresh water. Some samples fell in the intrusion phase (below the mixing line). In this initial phase, water gradually increase the salinity along path 13-14-15-16 facies cause a reverse exchange, water show Ca-Cl facies (no. 16), which is not found sample in these facies. Finally in this phase, water evolves toward facies that are close to seawater (Na-Cl facies) along path 16-12-8-4 facies, which most of samples are found in these groundwater facies. But, in this research, groundwater sample falling in Na-mixCl (no. 3), Na-mix HCO_3 (no. 2), Na- HCO_3 (no. 1) and MixNa- HCO_3 (no. 5), which are characteristic of the freshening process, was not found in all groundwater samples.

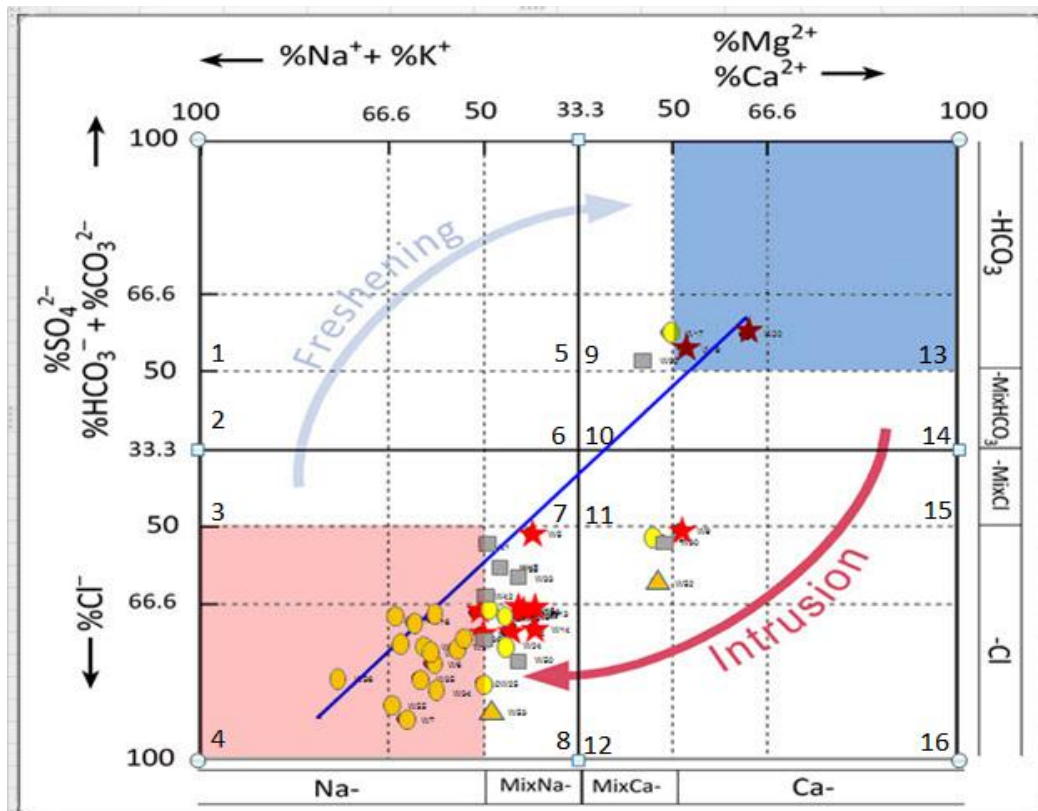


Figure 5.24 Hydrochemical Facies Evolution Diagram (HFED)

The most samples that fall in Na-Cl (no. 4) facies are sample from Qcl aquifer which corresponds to Na-Cl facies appeared in piper diagram, indicating groundwater samples in Qcl severely influenced by seawater intrusion. Samples from weathering PCms and Gr aquifer are fallen in MixNa-Cl facie (no. 8) and MixCa-Cl (no. 12) which corresponds to Ca-Na-HCO₃-Cl facies of piper diagram indicate moderate influence of seawater intrusion. Samples from PCms and Gr aquifer in deeper level show Ca- HCO₃-Cl facies of piper diagram and in HFED fall in MixNa-Cl facie (no. 8) and MixCa-Cl (no. 12). Even in HFED it falls in facies of fresh water but close to the mixing line, therefore, it slightly influenced by seawater. These were consistent with the study of Ghiglieri et al. (2012) which used HFED for depicting salinization processes in the coastal aquifers in Italy. They found that the sample were plotted on HFED, followed the succession of facies along the mixing line, indicating that seawater and fresh water are slightly mixed or ionic exchange process occurs. They used the HFED results compared with EC contour lines, showing that seawater has intruded quite far inland.

5.4 Integrated interpretation of VES and EC results

VES data has a limit for interpretation because there are many factors that show resistivity values $<5 \Omega\text{m}$ in coastal aquifers. Therefore, it needed to use results of hydrochemical analysis and EC value to explain the results together. The VES sections were overlaid on the EC map of Qcl aquifer and then can draw the extent of intrusion as shown in Figure 5.25. The zone that has resistivity values $<5 \Omega\text{m}$ in the VES sections are considered to be seawater intrusion. Furthermore, EC map showed the location of high EC ($>1500\mu\text{s/cm}$) corresponding to where the location of low resistivity values ($<5 \Omega\text{m}$). From this relationship, it can be concluded that Qcl aquifer is highly influenced by seawater intrusion with resistivity values in the range of 0 to $10 \Omega\text{m}$, especially in upper part of the area. The boundary line is shown in Figure 5.19. Section A-A' has been influenced by seawater intrusion about 3 kilometers inland, where first kilometer from the coastal line was highly influenced with the resistivity values $<5 \Omega\text{m}$ while the last 2 kilometers was moderately influenced and represent brackish water with the resistivity values ranging 5 to $10 \Omega\text{m}$. Section B-B' has been influenced by seawater intrusion about 5 kilometers inland, where 2 kilometers from coastal line was highly influenced with the resistivity values $<5 \Omega\text{m}$ while the last 3 kilometers was moderately influenced with the resistivity values ranging from 5 to $10 \Omega\text{m}$. Section C-C' has been influenced by seawater intrusion about 4.7 kilometers inland where 3.2 kilometers from the coastal line was high influenced with resistivity values $<5 \Omega\text{m}$ while the next 1.5 kilometers was moderately influenced with the resistivity values 5 to $10 \Omega\text{m}$. Section D-D' has been influenced by seawater intrusion about 8 kilometers inland where 4 kilometers from the coastal line was highly influenced with resistivity values $<5 \Omega\text{m}$ while the next 4 kilometers was moderately influenced with the resistivity values 5 to $10 \Omega\text{m}$.

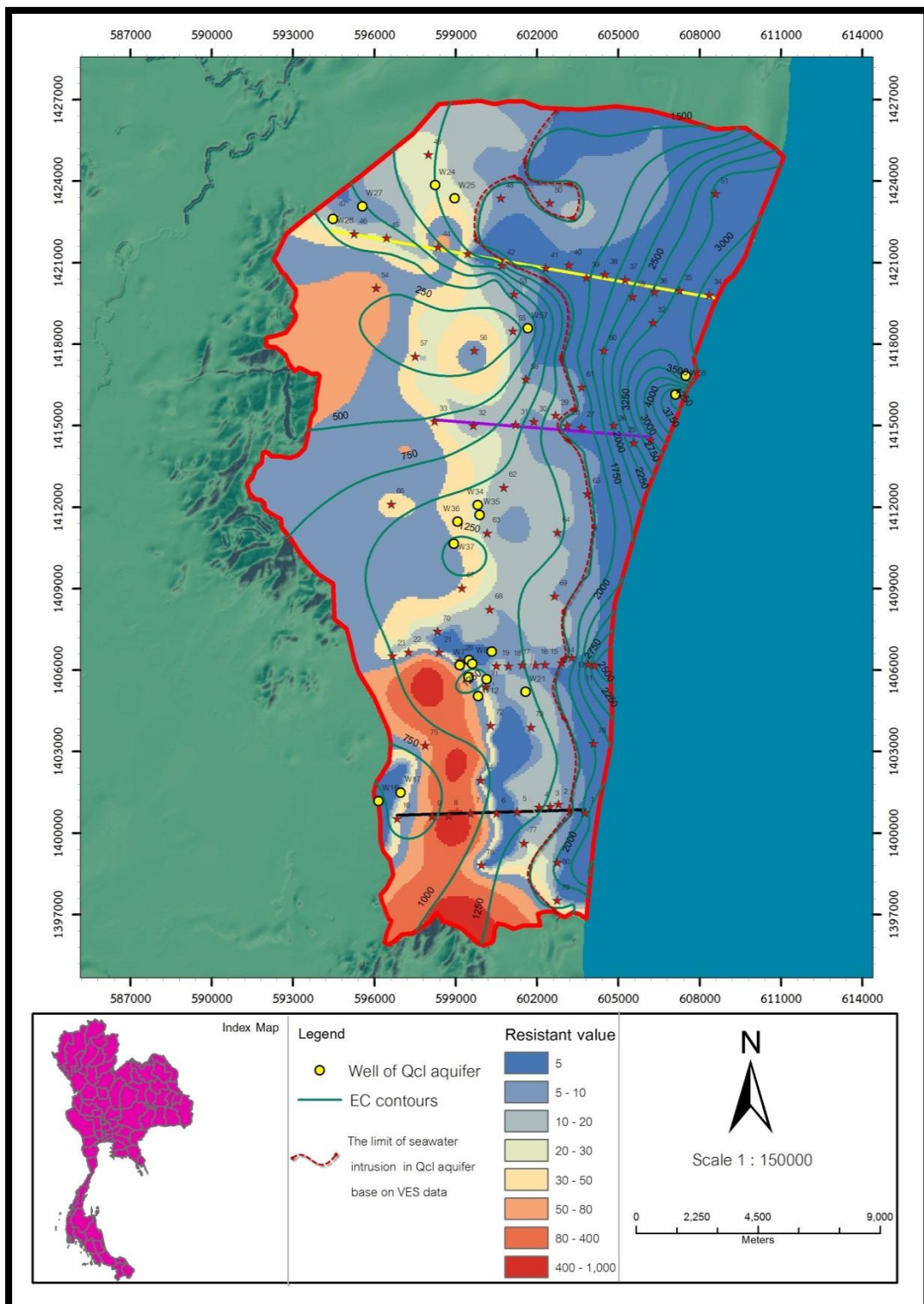


Figure 5.25 Showing limit of seawater intrusion in Qcl aquifer based on EC contour map superimposed on resistivity map

CHAPTER 6

CONCLUSION AND RECOMMENDATIONS

6.1 Conclusions

In this research, 80 VES survey was conducted using a Schlumberger configuration integrated with hydrochemical analysis of 58 groundwater samples to indicate seawater intrusion into coastal aquifers. Four pseudo cross-sections were generated from 80 VES data. There were in good agreement with those obtained from hydrogeological data and lithologic log in the study area. The resistivity map at different depths, which were generated from VES data, successfully revealed the interaction of seawater and freshwater along the coastal line. The geophysical results found that seawater mainly intrudes in Qcl aquifer. The resistivity values of $<5 \Omega\text{m}$ found at the depth approx. 50 meters. However, the VES has a limitation for evaluating the seawater intrusion in highly contaminated aquifer located closely to coastal line. Therefore, evaluation of seawater intrusion in coastal area with VES data needs a help of hydrochemical and hydrogeological data to describe seawater intrusion more accurately. According to hydrochemical analysis of 58 groundwater samples, five types of groundwater facies (Ca-Na-HCO₃, Ca-HCO₃-Cl, Ca-Na-HCO₃-Cl, Ca-Na-Cl and Na-Cl) are noticed and depended upon aquifer types and depths. Na-Cl facies is typically found in Qcl aquifer that correspond to the resistivity values of $< 5 \Omega\text{m}$. As geophysical and hydrochemical results, the levels of seawater intrusion can be classified into three zones by using these following criteria as shown in Table 6.1.

Table 6.1 The levels of seawater intrusion with resistivity and EC values

Level of seawater intrusion	Resistivity (Ωm)	EC ($\mu\text{s/cm}$)	Groundater Facies
Extremely	< 5	>1500	Na-Cl
Moderately	5-10	1000-1500	Na-Cl, Ca-Na-Cl, Ca-Na-HCO ₃ -Cl, Ca-Na-HCO ₃ , Ca-HCO ₃ -Cl
Slightly	>10	<1000	Ca-Na-Cl, Ca-Na-HCO ₃ , Ca-Na-HCO ₃ -Cl, Ca-HCO ₃ -Cl

6.2 Recommendation

1. Evaluation of seawater intrusion in coastal area with VES needs a help of the lithologic data to interpret more accurately, especially in the aquifer having a lot of clay components.

2. VES investigation should consider on the distance between each VES survey point. Especially, VES points selected to show a pseudo cross-section should be equally investigated in term of space to get the good interpretation. Furthermore, VES investigation should be carefully interpreted at the VES point near the coastal line because the depth of survey cannot penetrate through the highly seawater contaminated groundwater than those points, that is far away from the coastal line, even though the space of current electrodes is equally. Groundwater samples should be a good representative of the aquifer. So the information of wells have to be reliable, for example, level of well screen and depth.

4. The hydrochemical analysis should concern about checking ion balance error before plotting on the piper diagram and/or other interpretation.

5. In order to study of the dynamic and evolution of seawater intrusion, groundwater samples should be periodically collected at least 2 periods.

6. In the future, if this area needs to use the groundwater resources, people should use groundwater in the rock aquifers (PCms and Gr aquifers) at depth of higher than 70 meters.

7. In the future, the proper criteria for selecting the study area of seawater intrusion should consider these followings:

- Groundwater demand in the area: The area has been potentially contaminated by seawater when pumping a large amount of groundwater.

- Geological and hydrogeological characteristics: the unconsolidated aquifer with high thickness layer should be potentially contaminated by seawater than the consolidated aquifer.

- Amount of groundwater recharge: the area with low groundwater recharge rate has been potentially contaminated by seawater than that of high groundwater recharge rate.



REFERENCES

- Agoubi, B., Kharroubi, A., Abichou, T. & Abida, H. (2013). *Applied Water Science* **3**, 415-429.
- Al-Agha, M. R. & El-Nakhal, H. A. (2004). *Hydrological sciences journal* **49**.
- Appelo, C. A. J. & Postma, D. (2005). *Geochemistry, groundwater and pollution*. CRC press.
- Archie, G. E. (1942). **146**, 54 - 62.
- ASTM D6431 - 99 (2010). *Standard Guide for Using the Direct Current Resistivity Method for Subsurface Investigation*. West Conshohocken, PA: ASTM International.
- Back, W. (1960). *Internat. Geol. Cong* **21**, 87-95.
- Bear, J. (1999). *Seawater intrusion in coastal aquifers*. Springer Science & Business Media.
- Beckinsale, R. D., Suensilpong, S., Nakapadungrat, S. & Walsh, J. N. (1979). *Journal of the Geological Society* **136:529-537**.
- Bobachev, A. A. (2003). *IPI2Win software*, <http://geophys.geol.msu.ru/ipi2win.htm>.
- Burger, H. R., Anne F. Sheehan., Craig H Jones (2006). *Introduction to Applied Geophysics: Exploring the Shallow Subsurface*. W. W. Norton & Company.
- Cimino, A., Cosentino, C., Oieni, A. & Tranchina, L. (2008). *Environmental Geology* **55**, 1473-1482.
- Davis, S. N. & DeWiest, R. J. M. (1967). *Hydrogeology*. New York: John Wiley & Sons, Inc.
- De Franco, R., Biella, G., Tosi, L., Teatini, P., Lozej, A., Chiozzotto, B., Giada, M., Rizzetto, F., Claude, C., Mayer, A., Bassan, V. & Gasparetto-Stori, G. (2009). *Journal of Applied Geophysics* **69**, 117-130.
- Demirel, Z. (2004). *Journal of Environmental Management* **70**, 275-282.
- Department of Groundwater Resources (2001). *Groundwater Guide Manual Book, Phetchaburi Province*. Department of Groundwater Resources.

- Department of Groundwater Resources (2011).
- Department of Groundwater Resources (2014). Hydrological Units, edited by Department of Groundwater Resources.
- Department of Mineral Resources (2014). *Geology of Thailand*. Department of Mineral Resources: Bureau of Geological Survey
Department of Mineral Resources, Bangkok, Thailand.
- Drabbe, J. & Badon Ghijben, W. (1887). *Nota in verband met de voorgenomen putboring nabij Amsterdam*. The Hague.
- Essink, G. H. P. O. (2001). *Ocean & Coastal Management* **44**, 429–449.
- Fetter, C. W. (2001). *Applied hydrogeology*, 4th ed. Upper Saddle River, N.J.: Prentice Hall.
- Freeze, R. A. & Cherry, J. A. (1979). *Groundwater*,
<http://catalog.hathitrust.org/api/volumes/oclc/4493153.html>.
- Galloway, W. E. & Kaiser, W. R. (1980).
- Ghiglieri, G., Carletti, A. & Pittalis, D. (2012). *Journal of Hydrology* **432–433**, 43-51.
- Giménez-Forcada, E. (2010). *Ground Water* **48**, 212-216.
- Giménez-Forcada, E. (2014). *Journal of Hydrology* **517**, 617-627.
- Giménez-Forcada, E. & Sánchez San Román, F. J. (2015). *Groundwater* **53**, 819-824.
- Gopinath, S. & Srinivasamoorthy, K. (2015). *Aquatic Procedia* **4**, 65-71.
- Herzberg, V. H. B. (1901). *fur Gasbeleuchtung und Wasserversorgung* **44**, 815-834.
- Hubbert, M. K. (1940). *The Journal of geology* **48**.
- J.C. Javanaphet (1969). Geological Map of Thailand, scale 1:1,000,000: Department of Mineral Resources of Thailand.
- Kaya, M. A., Özürlan, G. & Balkaya, Ç. (2015). *Environ Earth Sci* **73**, 1151-1160.
- Kouzana, L., Benassi, R., Ben mammou, A. & Sfar felfoul, M. (2010). *Journal of African Earth Sciences* **58**, 242-254.
- Land Developement Department (2011). Land use Map of Phetchaburi.
- McInnis, D., Silliman, S., Boukari, M., Yalo, N., Orou-Pete, S., Fertenbaugh, C., Fayomi, H. & Sarre, K. (2013). *Journal of Hydrology* **505**, 335-345.

- National Aeronautics and Space Administration (2010). *Water Cycle*,
<http://science.nasa.gov/earth-science/oceanography/ocean-earth-system/ocean-water-cycle/>.
- Phetchaburi Rajabhat University (2011). *Application of geographical information system in managing coastal resources, phetchaburi province*,
<http://it.pbru.ac.th/WebsiteGT/rscland.html>.
- Piper, A. M. (1944). *Eos, Transactions American Geophysical Union* **25**, 914-928.
- Piyasin, S. (1975). *Proceedings of the Conference on the Geology of Thailand*, edited by R.B. Stokes, C. Tantisukrit & K. V. C. (Eds.), pp. 25-36. Chiang Mai: Department of Geological Sciences, Chiang Mai University.
- Promma, k. (2013). *HYDROGEOLOGY*. Chulalongkorn University.
- Ramingwong, T. (2003). *Groundwater*. Chaingmai University: Department of Geology.
- Ravindran, A. A. (2013). *Russian Geology and Geophysics* **54**, 1529-1538.
- Sabet, M. A. (1975). *Department of Geophysical Sciences*, 63.
- Sakulrat, J., Chalermyanont, T., Chetpattananondh, P. & Piromlert, S. (2007). *International Conference on Engineering and Environment*. Phuket, Thailand.
- Santicharaenkamol, S., Chalermyanont, T. & Chub-uppakarn, T. (2010). Groundwater of Songkhla Municipal: Quality and Steady State Model, The 8 th Prince of Songkla University Engineering Conference, pp. 25-29. Faculty of Engineering: Faculty of Engineering.
- Satarugsa, P. (2007). *Exploration geophysics*. Khonkaen University.
- Sinsakul, S. (1992). *Journal of Southeast Asian Earth Sciences* **7**, 23-37.
- Skinner, B. J., Porter, S. C. & B., D. (1999). *The Blue Planet: An Introduction to Earth System Science*. New York: John Wiley & Sons Inc.
- Smoor, P. B. (1967). *Hydrochemical facies study of ground water in the Tucson Basin*. University of Arizona.
- Song, S., Lee, J. & Park, N. (2006). *Environmental Geology* **52**, 1207-1219.
- Stuyfzand, P. J. (1993). *Hydrochemistry and Hydrology of the Coastal Dune Area of the Western Netherlands*. The Netherland: KIWA N.V.

Telford, W. M., Geldart, L. P. & Sheriff, R. E. (1990). *Applied Geophysics*. Cambridge University Press.

Thai Marine Meteorological Center (2006). *Climate of Changwat Phetchaburi*, http://www.marine.tmd.go.th/thai/tus_type/phetchaburi.html.

The Royal Institute (2011). *Geology Vocabulary, Geology Vocabulary*.

Uzma, F. (2014). *Water*, <http://www.slideshare.net/uzmafathima545/water-30450377>.

Van Dam, J. C. & Meulenkamp, J. J. (1967). *Geophysical Prospecting* **15**, 92-115.

Van Nostrand, R. G. & Cook, K. L. (1966). *Interpretation of Resistivity Data*. U.S. Government Printing Office.

Veingchanda, P. (2010). thesis, Suranaree University of Technology, School of Geotechnology. Institute of Science. Suranaree University of Technology.

Werner, A. D., Bakker, M., Post, V. E. A., Vandenbohede, A., Lu, C., Ataie-Ashtiani, B., Simmons, C. T. & Barry, D. A. (2013). *Advances in Water Resources* **51**, 3-26.

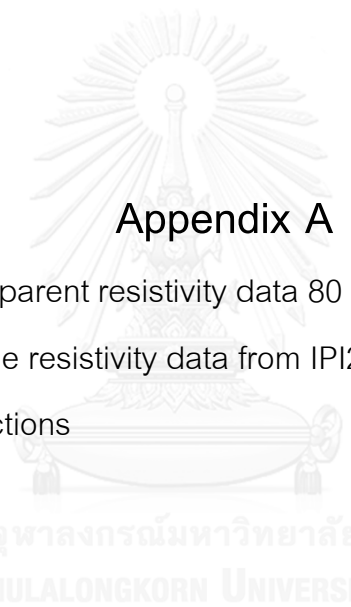
Zghibi, A., Merzougui, A., Zouhri, L. & Tarhouni, J. (2014). *Journal of African Earth Sciences* **89**, 1-15.

Zohdy, A. A., Eaton, G. P. & Mabey, D. R. (1974). *Application of surface geophysics to ground-water investigations*. US Government Printing Office.



APPENDIX

จุฬาลงกรณ์มหาวิทยาลัย
CHULALONGKORN UNIVERSITY



Appendix A

Appendix A1 Apparent resistivity data 80 stations from field

Appendix A2 True resistivity data from IPI2WIN for 4 pseudo cross-sections

จุฬาลงกรณ์มหาวิทยาลัย
CHULALONGKORN UNIVERSITY

Appendix A1: Apparent resistivity data 80 stations from field

Table A1. The position of 80 VES survey points

Station	Zone	East	North	Elevation (m.)	Line bearing	Date of survey	Configuration	Note
St1	47P	603767	1400753	4	S80W	20/2/2557	Schlumberger	IRIS instrument
St2	47P	602793	1401057	5	S80W	20/2/2557	Schlumberger	IRIS instrument
St3	47P	602479	1400986	8	S80W	20/2/2557	Schlumberger	IRIS instrument
St4	47P	602079	1400950	12	EW	20/2/2557	Schlumberger	IRIS instrument
St5	47P	601268	1400782	18	S85W	20/2/2557	Schlumberger	IRIS instrument
St6	47P	600497	1400721	23	EW	20/2/2557	Schlumberger	IRIS instrument
St7	47P	599544	1400719	33	EW	20/2/2557	Schlumberger	IRIS instrument
St8	47P	598738	1400639	39	EW	20/2/2557	Schlumberger	IRIS instrument
St9	47P	598126	1400615	48	EW	20/2/2557	Schlumberger	IRIS instrument
St10	47P	596843	1400539	65	EW	20/2/2557	Schlumberger	IRIS instrument
St11	47P	604121	1406178	6	N80W	20/2/2557	Schlumberger	IRIS instrument
St12	47P	603889	1406219	9	N80W	20/2/2557	Schlumberger	IRIS instrument
St13	47P	603288	1406458	4	NS	20/2/2557	Schlumberger	IRIS instrument
St14	47P	602912	1406264	5	S80W	20/2/2557	Schlumberger	IRIS instrument
St15	47P	602296	1406207	10	S80W	20/2/2557	Schlumberger	IRIS instrument
St16	47P	601937	1406193	12	S80W	21/2/2557	Schlumberger	IRIS instrument
St17	47P	601450	1406192	16	S80W	21/2/2557	Schlumberger	IRIS instrument
St18	47P	600945	1406142	19	EW	21/2/2557	Schlumberger	IRIS instrument
St19	47P	600504	1406156	22	EW	21/2/2557	Schlumberger	IRIS instrument
St20	47P	599166	1406348	22	N80W	21/2/2557	Schlumberger	IRIS instrument
St21	47P	598391	1406659	33	N80W	21/2/2557	Schlumberger	IRIS instrument
St22	47P	597256	1406662	38	EW	21/2/2557	Schlumberger	IRIS instrument
St23	47P	596672	1406523	42	EW	21/2/2557	Schlumberger	IRIS instrument
St24	47P	606184	1414472	5	S68E	21/2/2557	Schlumberger	IRIS instrument
St25	47P	605561	1414369	9	NS	21/2/2557	Schlumberger	IRIS instrument
St26	47P	604822	1415019	7	N60E	21/2/2557	Schlumberger	IRIS instrument
St27	47P	603652	1414939	5	S68E	21/2/2557	Schlumberger	IRIS instrument
St28	47P	603109	1415001	9	EW	21/2/2557	Schlumberger	IRIS instrument
St29	47P	602691	1415378	13	EW	21/2/2557	Schlumberger	IRIS instrument
St30	47P	601888	1415147	17	NS	21/2/2557	Schlumberger	IRIS instrument
St31	47P	601208	1415036	19	NS	21/2/2557	Schlumberger	IRIS instrument
St32	47P	599654	1414996	29	S60W	22/2/2557	Schlumberger	IRIS instrument
St33	47P	598221	1415158	42	NS	22/2/2557	Schlumberger	IRIS instrument
St34	47P	608346	1419819	2	NS	22/2/2557	Schlumberger	IRIS instrument
St35	47P	607251	1419975	7	EW	22/2/2557	Schlumberger	IRIS instrument
St36	47P	606334	1419920	9	EW	22/2/2557	Schlumberger	IRIS instrument
St37	47P	605242	1420376	9	NS	22/2/2557	Schlumberger	IRIS instrument
St38	47P	604505	1420567	10	N80E	22/2/2557	Schlumberger	IRIS instrument
St39	47P	603826	1420444	11	S74E	22/2/2557	Schlumberger	IRIS instrument
St40	47P	603177	1420905	12	EW	22/2/2557	Schlumberger	IRIS instrument
St41	47P	602321	1420800	10	NS	22/2/2557	Schlumberger	IRIS instrument
St42	47P	600706	1420903	7	N54E	22/2/2557	Schlumberger	IRIS instrument
St43	47P	599451	1421337	15	N30W	22/2/2557	Schlumberger	IRIS instrument
St44	47P	598340	1421580	19	S20W	22/2/2557	Schlumberger	IRIS instrument
St45	47P	596442	1421913	33	S15W	22/2/2557	Schlumberger	IRIS instrument

Station	Zone	East	North	Elevation (m.)	Line bearing	Date of survey	Configuration	Note
St46	47P	595256	1422059	41	N80W	22/2/2557	Schlumberger	IRIS instrument
St47	47P	594505	1422676	32	N30E	22/2/2557	Schlumberger	IRIS instrument
St48	47P	600669	1423375	23	EW	23/2/2557	Schlumberger	IRIS instrument
St49	47P	597994	1424975	27	NS	23/2/2557	Schlumberger	IRIS instrument
St50	47P	602466	1423198	17	N60W	23/2/2557	Schlumberger	IRIS instrument
St51	47P	608589	1423537	1	NS	23/2/2557	Schlumberger	IRIS instrument
St52	47P	606279	1418791	17	N30W	23/2/2557	Schlumberger	IRIS instrument
St53	47P	601159	1419843	24	EW	23/2/2557	Schlumberger	IRIS instrument
St54	47P	596063	1420067	22	EW	23/2/2557	Schlumberger	IRIS instrument
St55	47P	601115	1418483	20	EW	23/2/2557	Schlumberger	IRIS instrument
St56	47P	599690	1417760	61	N20W	23/2/2557	Schlumberger	IRIS instrument
St57	47P	597503	1417550	84	S70E	23/2/2557	Schlumberger	IRIS instrument
St58	47P	601582	1416705	20	N20W	23/2/2557	Schlumberger	IRIS instrument
St59	47P	605525	1419741	13	S80E	23/2/2557	Schlumberger	IRIS instrument
St60	47P	604466	1417763	11	N80W	23/2/2557	Schlumberger	IRIS instrument
St61	47P	603646	1416415	10	N15E	23/2/2557	Schlumberger	IRIS instrument
St62	47P	600779	1412726	31	N70E	23/2/2557	Schlumberger	IRIS instrument
St63	47P	600165	1411042	61	S70W	23/2/2557	Schlumberger	IRIS instrument
St64	47P	602748	1411062	16	S24E	23/2/2557	Schlumberger	IRIS instrument
St65	47P	603870	1412499	14	N85E	24/2/2557	Schlumberger	IRIS instrument
St66	47P	596628	1412116	77	EW	25/2/2557	Schlumberger	IRIS instrument
St67	47P	599222	1409028	52	N30W	25/2/2557	Schlumberger	IRIS instrument
St68	47P	600259	1408238	54	S80W	25/2/2557	Schlumberger	IRIS instrument
St69	47P	602642	1408727	11	NS	25/2/2557	Schlumberger	IRIS instrument
St70	47P	598333	1407431	42	EW	25/2/2557	Schlumberger	IRIS instrument
St71	47P	600109	1405387	40	S80W	25/2/2557	Schlumberger	IRIS instrument
St72	47P	600291	1403966	49	NS	25/2/2557	Schlumberger	IRIS instrument
St73	47P	601771	1403903	19	S80E	25/2/2557	Schlumberger	IRIS instrument
St74	47P	599916	1401950	47	EW	25/2/2557	Schlumberger	IRIS instrument
St75	47P	597876	1403227	50	EW	25/2/2557	Schlumberger	IRIS instrument
St76	47P	604078	1403299	5	NS	25/2/2557	Schlumberger	IRIS instrument
St77	47P	601523	1399626	33	S70W	25/2/2557	Schlumberger	IRIS instrument
St78	47P	599949	1398821	52	S80E	25/2/2557	Schlumberger	IRIS instrument
St79	47P	602735	1397518	12	NS	25/2/2557	Schlumberger	IRIS instrument
St80	47P	602750	1398925	40	EW	25/2/2557	Schlumberger	IRIS instrument

Table A2. Apparent resistivity value of 80 VES survey points

Spacing		Apparent resistivity (Ohm. m)																										
AB	MN	Sounding No.																										
(m)	(m)	S1	S2	S3	S4	S5	S6	S7	S8	S9	S10	S11	S12	S13	S14	S15	S16	S17	S18	S19	S20	S21	S22	S23	S24	S25	S26	S27
1	0.5	30.7	91.1	28.3	57.5	68.1	57.8	79.2	527.2	44.1	713.1	11.9	160.5	14.0	29.3	74.9	133.5	98.2	269.2	86.56	208.1	149.5	142.9	293.9	12.0	9.5	15.3	41.7
1.5	0.5	28.0	31.4	32.9	264.5	72.1	44.4	105.4	486.4	434.1	658.5	11.7	93.8	11.7	38.2	74.1	179.2	139.9	373.9	89.50	220.4	214.8	172.1	292.4	12.4	9.8	15.7	24.3
2	0.5	27.5	64.7	35.2	174.4	75.8	45.3	123.5	502.2	453.7	606.2	10.9	64.8	11.4	41.5	69.4	184.6	160.9	410.0	101.76	221.1	277.4	279.2	279.2	12.4	9.6	16.7	17.4
3	0.5	22.8	40.0	35.9	68.7	83.3	38.5	124.2	451.9	407.5	429.7	8.8	32.6	10.9	38.8	44.1	109.3	163.0	394.2	98.66	173.8	362.0	151.4	193.3	9.5	8.5	16.4	13.0
3	2.0	21.9	34.8	29.4	59.7	61.5	32.7	156.1	507.2	390.6	510.6	7.6	29.3	9.3	27.3	40.8	88.4	126.9	286.6	73.96	144.4	240.9	110.8	164.4	7.0	8.4	11.5	10.1
5	2.0	11.0	12.2	30.0	27.0	60.2	27.5	141.4	520.1	144.0	382.4	7.0	19.4	8.6	19.5	17.0	30.0	106.8	121.1	83.32	115.3	302.8	84.1	89.6	6.3	7.0	12.3	9.9
7	2.0	8.2	11.6	26.8	20.9	53.7	24.6	114.6	532.7	95.8	235.6	6.4	16.1	8.3	13.9	11.4	17.1	69.6	61.2	76.91	105.1	273.4	52.7	56.2	5.4	5.4	12.1	8.8
10	2.0	5.1	10.1	24.1	20.9	29.5	22.4	98.3	599.3	105.0	97.2	5.4	4.5	7.4	10.0	8.7	11.7	38.2	51.1	48.09	79.3	178.4	28.1	33.4	4.4	3.4	10.1	7.3
10	5.0	5.5	10.0	22.8	11.6	40.8	21.1	100.1	541.4	113.1	112.7	5.2	4.1	7.2	9.9	8.1	11.2	41.1	48.9	55.42	163.4	26.8	32.1	4.2	3.0	10.3	6.8	
15	5.0	3.6	8.4	15.5	10.3	15.2	10.9	54.2	139.3	48.9	3.2	3.7	5.0	7.6	7.1	8.2	15.0	30.4	38.06	31.4	55.8	15.4	19.1	3.4	2.5	6.7	5.2	
20	5.0	3.1	8.0	13.1	7.5	11.3	12.3	126.9	596.9	161.8	34.8	2.4	2.8	4.2	6.2	6.5	6.8	10.8	11.1	21.38	14.9	26.2	16.4	16.4	2.9	2.1	4.5	4.2
25	5.0	2.8	8.4	12.3	8.2	11.0	11.4	159.4	585.4	180.8	29.0	2.1	2.9	4.2	6.2	7.0	9.4	8.4	12.17	10.1	20.0	18.9	17.0	2.2	1.8	4.0	3.8	
30	5.0	2.5	8.8	12.5	9.0	9.5	11.8	184.8	872.6	189.8	27.5	1.9	2.9	4.4	6.3	6.1	7.3	8.9	8.4	11.74	9.4	16.5	22.2	19.4	2.1	1.8	3.6	3.8
35	5.0	2.3	10.8	13.2	8.6	9.7	11.9	206.8	901.2	188.4	29.3	1.8	2.9	4.6	6.6	5.7	7.6	8.9	8.6	14.40	10.0	15.1	25.6	21.9	2.1	1.8	3.5	3.7
40	5.0	2.2	9.9	14.0	10.1	9.2	12.0	236.3	943.8	181.3	30.2	1.9	3.2	4.7	6.8	5.4	7.9	8.7	8.4	16.53	10.4	15.7	28.9	24.3	2.1	1.9	3.3	3.4
45	5.0	2.1	10.9	15.9	9.5	9.0	12.3	286.4	960.8	178.8	32.6	2.1	3.5	4.9	6.7	5.3	8.0	8.9	8.7	12.96	10.9	16.5	31.6	26.7	2.1	1.9	3.3	3.7
50	5.0	2.1	11.1	16.3	11.2	9.1	12.7	285.2	950.1	186.5	36.1	2.3	3.7	5.1	6.8	5.3	8.1	9.0	9.2	13.79	11.6	17.7	35.7	29.3	2.0	1.8	3.3	3.8
60	5.0	2.3	13.2	17.5	13.6	8.9	15.0	327.4	987.6	187.0	72.1	2.8	4.1	5.5	7.2	6.9	8.9	9.4	10.7	13.20	13.5	21.5	41.6	33.5	2.1	1.9	3.3	3.9
70	5.0	2.4	15.0	20.1	18.6	10.2	17.2	344.4	997.3	184.8	88.6	3.6	4.5	5.9	8.0	7.9	9.4	10.1	10.8	15.83	15.9	25.1	48.3	38.3	2.2	1.9	3.3	4.1
80	5.0	2.8	17.1	23.6	16.9	11.0	20.1	378.8	1023.4	203.3	91.5	4.1	5.4	6.8	8.5	8.2	9.9	10.7	12.2	17.81	17.9	29.5	54.3	43.0	2.4	2.0	3.5	4.3
90	5.0	3.0	15.6	25.5	21.6	11.5	22.6	411.9	1016.7	198.3	95.6	4.9	6.0	8.0	9.1	9.1	11.8	12.7	15.1	16.9	18.1	32.9	60.8	46.6	2.6	2.1	3.6	4.5
100	5.0	3.6	15.0	28.4	18.1	11.9	25.3	477.2	1209.3	188.4	103.2	5.9	6.9	8.4	9.7	9.8	13.4	13.1	17.4	20.2	21.3	35.7	66.9	50.4	3.1	2.2	3.6	4.8
110	20.40	4.0	15.9	31.9	21.9	12.7	26.1	503.4	1345.7	201.6	101.6	6.5	7.8	9.9	10.1	10.5	13.2	13.8	16.5	22.6	25.0	39.4	72.6	55.4	3.4	2.4	3.7	5.1
125	20.40	5.0	15.5	32.5	24.9	15.6	32.0	525.6	1569.6	214.4	110.9	8.6	9.6	10.1	12.7	11.4	13.9	16.4	22.4	26.8	30.2	44.0	80.8	60.6	3.6	2.8	4.8	5.7
135	20.40	5.9	14.2	39.5	27.0	20.1	39.8	590.0	1430.1	234.5	138.6	10.1	10.3	10.4	13.0	12.5	15.1	16.2	25.5	28.5	36.1	50.3	84.8	70.7	3.7	3.0	5.4	6.0
150	20.40	7.3	16.3	47.9	29.2	22.2	47.9	643.9	ND	247.9	147.6	12.0	11.6	11.0	14.7	13.2	15.8	17.3	29.3	31.7	40.0	55.4	92.6	77.2	4.6	3.2	5.7	6.2
160	20.40	8.0	19.4	52.2	32.1	32.8	50.4	689.6	ND	257.6	155.7	13.5	12.4	12.3	17.9	14.1	17.8	19.6	30.4	33.0	44.5	59.3	98.4	84.3	5.6	3.5	5.8	7.7
175	20.40	9.2	25.6	54.7	35.9	28.7	57.5	744.4	ND	287.1	163.4	15.6	13.5	13.1	17.6	15.3	20.1	24.2	31.6	35.2	48.6	62.6	104.3	90.0	7.1	3.8	5.7	8.0
185	20.40	10.4	34.9	56.7	39.7	34.5	63.7	786.3	ND	300.0	180.2	17.4	14.3	14.3	18.6	15.9	22.3	25.5	32.8	37.5	50.4	65.3	111.1	100.4	7.6	4.0	6.0	9.6
200	20.40	12.0	40.1	60.3	41.3	40.3	69.8	841.6	ND	357.9	200.0	20.1	15.6	15.0	20.6	17.0	24.5	30.3	37.0	37.6	51.3	69.9	120.4	109.6	8.0	4.4	6.2	10.3

Table A2. Apparent resistivity value of 60 VES survey points (continue)

Spacing		Apparent resistivity (Ohm. m.)																										
AB	MN	Sounding No.																										
(m)	(m)	S128	S129	S130	S131	S132	S133	S134	S135	S136	S137	S138	S139	S140	S141	S142	S143	S144	S145	S146	S147	S148	S149	S150	S151	S152	S153	S154
1	0.5	33.5	19.3	50.5	119.7	219.1	205.6	411.1	99.2	186.9	5.8	22.2	115.9	2.5	441.6	33.9	297.2	256.3	276.3	79.1	163.2	10.6	69.30	98.1	72.5	121.5	16.8	1620.1
1.5	0.5	37.1	20.1	39.4	114.7	261.1	259.7	395.0	91.1	174.0	3.8	20.2	111.6	3.1	211.7	27.6	407.6	278.9	359.1	84.2	133.2	13.4	68.30	88.4	41.3	126.5	19.5	1290.2
2	0.5	35.0	20.4	39.1	119.6	279.6	309.4	378.7	94.1	140.1	3.0	20.0	91.5	3.2	103.2	28.1	210.1	305.4	374.6	104.9	102.9	15.5	73.00	84.6	35.6	91.9	20.3	1176.7
3	0.5	38.7	17.7	31.6	104.3	274.3	341.1	224.6	69.8	65.5	2.4	17.0	42.9	3.5	26.2	28.1	143.1	334.6	356.4	147.3	79.6	15.5	69.00	51.4	22.4	46.0	25.6	1047.0
3	2.0	25.6	16.9	25.6	79.4	274.6	292.2	109.4	70.7	65.8	2.1	15.9	41.6	2.4	32.0	21.8	124.0	331.9	325.9	153.2	62.8	13.4	56.00	46.5	25.4	38.6	20.7	1093.2
5	2.0	16.8	12.2	20.9	60.8	241.3	262.8	73.8	22.0	26.7	2.1	10.8	6.2	3.0	10.3	22.8	67.1	347.2	309.6	230.5	62.2	11.3	62.00	28.4	7.9	14.5	23.4	1140.8
7	2.0	13.9	10.9	17.3	50.8	220.6	200.7	38.0	17.2	12.8	2.0	9.4	4.6	3.6	9.8	22.3	50.9	331.1	313.8	281.1	48.2	9.6	66.50	19.5	2.4	6.2	22.7	1107.0
10	2.0	28.6	9.1	14.6	35.5	204.7	124.6	22.7	8.7	6.9	2.0	9.1	4.1	4.2	9.8	19.9	35.2	256.4	277.5	296.9	37.9	9.1	69.50	21.9	1.4	2.8	17.7	916.7
10	5.0	10.7	9.2	14.1	38.1	198.7	122.6	17.4	14.4	6.0	1.8	8.1	3.9	3.9	7.9	19.0	36.8	281.6	251.4	263.8	36.7	9.1	51.70	24.8	2.1	2.9	20.2	1031.0
15	5.0	6.9	7.2	10.8	24.1	169.4	54.0	6.0	14.4	3.3	2.0	6.7	4.5	4.0	5.7	14.8	22.9	223.7	177.1	209.2	16.6	7.8	44.50	21.0	1.1	1.8	11.1	821.7
20	5.0	5.0	7.3	8.3	18.1	120.8	31.9	3.2	7.9	2.0	2.0	5.7	4.2	4.1	4.1	11.1	19.5	150.3	92.7	134.1	12.0	7.7	43.30	19.8	1.3	1.6	8.6	406.2
25	5.0	4.4	7.8	7.8	17.3	85.1	28.9	1.9	6.7	1.6	2.0	4.9	4.2	4.1	3.5	8.6	13.7	90.4	69.4	93.5	10.8	8.2	40.80	16.8	1.5	1.6	7.5	282.7
30	5.0	4.4	8.2	8.1	15.7	61.4	32.4	1.6	3.3	1.5	2.0	4.8	3.8	4.2	3.2	7.1	12.9	63.7	34.2	66.0	10.8	8.6	41.10	14.4	1.8	1.6	7.5	220.1
35	5.0	4.6	8.8	8.4	13.0	41.0	35.0	1.6	2.3	1.5	2.0	4.2	3.7	4.2	3.3	6.3	12.6	45.5	27.9	51.1	11.2	8.4	36.40	12.9	1.9	1.6	7.4	227.0
40	5.0	4.7	10.0	8.4	11.6	26.4	36.4	1.7	2.2	1.6	2.0	3.4	3.3	4.1	3.3	6.4	11.8	34.3	23.1	42.0	11.7	8.9	34.40	11.6	1.9	1.7	7.4	192.7
45	5.0	4.7	10.3	8.2	11.8	18.7	38.2	1.7	2.1	1.6	1.9	3.5	3.2	4.1	3.4	6.5	12.0	28.1	22.0	28.9	12.0	9.0	33.60	10.0	2.2	1.7	7.6	158.2
50	5.0	4.9	11.2	8.1	11.4	14.2	38.9	2.0	2.0	1.6	1.9	3.0	3.0	4.0	3.5	6.7	12.0	25.4	19.9	19.8	12.5	8.8	32.00	8.5	2.8	1.8	8.3	122.0
60	5.0	6.4	11.8	8.6	11.3	14.1	42.1	2.6	1.9	1.7	1.9	2.7	2.9	4.0	4.0	7.9	12.3	21.6	20.0	18.1	16.9	8.7	34.2	7.2	2.0	2.0	9.0	101.5
70	5.0	6.9	11.5	8.8	12.1	15.2	42.9	2.7	2.0	1.8	2.0	2.8	2.8	4.0	4.5	8.7	14.0	21.9	21.7	18.9	18.3	9.1	31.4	5.9	2.1	2.3	9.2	62.9
80	5.0	7.1	12.7	9.7	12.7	15.8	53.2	3.4	2.1	2.0	2.1	3.00	2.6	4.1	5.3	10.0	15.3	24.6	22.5	19.8	22.1	9.7	28.5	5.3	2.1	2.3	10.1	56.4
90	5.0	6.2	14.8	10.1	12.5	17.2	59.2	3.6	2.4	2.2	2.1	3.1	2.7	4.2	5.8	11.1	18.5	25.4	22.8	20.0	27.7	9.9	27.8	4.9	2.3	2.5	10.9	87.3
100	5.0	8.2	19.5	10.5	13.4	18.0	59.2	3.7	2.4	2.2	2.2	3.20	2.8	4.3	7.9	12.0	22.2	27.90	26.3	25.7	32.4	9.9	27.1	4.6	2.4	2.8	10.5	108.1
110	20.40	9.2	20.6	11.3	13.9	18.9	67.7	3.9	3.1	2.4	2.5	3.00	2.8	4.6	8.5	13.1	23.5	30.40	28.5	27.5	33.4	9.9	26.2	4.3	2.4	2.7	11.8	92.5
125	20.40	9.7	19.9	12.4	16.6	19.6	70.0	4.0	3.3	2.7	2.7	3.40	3.2	5.1	10.1	14.6	26.4	31.40	34.6	30.8	45.6	10.3	26.5	4.2	2.5	3.1	13.8	118.2
135	20.40	11.6	18.4	13.0	17.5	20.3	77.4	3.8	4.1	3.1	3.0	3.40	3.4	5.5	11.0	15.9	30.3	33.50	40.8	35.4	50.1	10.7	27.0	4.2	2.4	3.3	15.6	123.6
150	20.40	11.7	20.2	14.4	19.9	21.6	82.1	4.1	4.4	3.7	3.3	3.7	4.7	6.5	12.3	16.7	37.2	36.80	46.7	36.9	56.0	11.4	28.0	4.3	2.3	4.0	18.8	139.9
160	20.40	12.6	22.3	15.0	20.5	21.9	89.3	4.4	4.4	4.2	3.4	3.9	5.0	7.1	13.4	17.6	42.1	38.70	55.6	39.1	56.0	11.6	28.40	4.5	2.4	3.9	19.0	145.7
175	20.40	13.0	24.6	16.5	21.4	24.0	94.9	4.5	4.4	4.6	3.7	4.10	5.5	8.4	14.4	19.4	48.3	40.10	60.4	43.9	67.3	12.7	30.00	4.6	2.6	4.2	20.3	159.9
185	20.40	13.8	26.3	17.7	25.1	26.1	100.0	5.3	4.6	5.0	4.0	4.30	5.7	8.6	15.7	20.2	55.4	44.50	77.5	45.1	80.0	13.1	31.00	4.7	2.7	4.6	21.4	160.8
200	20.40	15.3	26.5	19.0	26.9	28.2	104.8	6.0	5.0	5.1	4.2	4.60	6.0	9.3	18.0	20.9	57.3	48.90	82.3	55.2	90.6	13.6	33.00	4.9	2.6	5.0	22.5	175.9

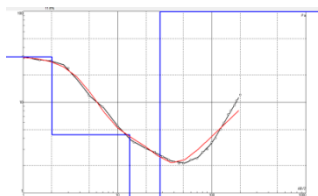
Table A2. Apparent resistivity value of 60 VES survey points (continue)

Spacing		Apparent resistivity (Ohm. m)																										
AB	MIN	Sounding No.																										
(m)	(m)	S165	S166	S167	S168	S169	S160	S161	S162	S163	S164	S165	S166	S167	S168	S169	S170	S171	S172	S173	S174	S175	S176	S177	S178	S179	S180	
1	0.5	301.6	751.6	499.2	242.6	3.3	19.3	1.9	92.0	132.9	108.0	19.8	369.1	48.9	183.2	19.0	221.5	358.1	121.7	126.6	300.6	44.6	104.3	136.4	39.9	43.4	51.8	
1.5	0.5	112.7	417.7	769.8	108.9	2.9	12.4	2.1	91.4	119.1	119.1	18.6	357.1	73.6	246.6	22.6	198.3	297.1	179.6	138.7	301.4	41.7	106.0	135.6	36.2	47.7	69.9	
2	0.5	78.5	483.2	994.9	79.8	3.1	9.9	2.2	78.5	108.5	79.0	16.5	344.1	96.3	289.8	24.6	184.6	359.3	225.3	151.6	253.8	42.7	87.6	130.1	42.4	50.7	44.1	
3	0.5	63.3	471.3	1,147.7	73.1	3.2	4.1	2.5	55.9	34.8	65.5	13.2	308.1	133.7	388.7	25.7	130.1	364.3	255.0	117.2	187.0	34.5	59.1	92.4	37.6	61.2	19.4	
3	2.0	54.1	712.2	917.4	66.3	2.9	4.7	2.4	53.9	30.4	63.0	10.9	286.1	89.4	310.1	23.3	105.6	281.8	204.9	98.7	128.8	30.4	69.4	79.7	29.8	66.7	15.2	
5	2.0	51.1	297.8	880.8	71.1	2.9	2.6	2.7	26.4	38.7	50.0	9.2	272.1	97.7	341.0	20.7	68.8	244.1	174.5	53.5	54.7	36.9	20.2	37.2	27.2	27.2	65.5	7.8
7	2.0	43.6	174.5	606.5	73.9	2.7	2.6	3.1	21.7	29.3	41.2	7.5	230.1	77.5	243.8	18.4	55.0	247.6	116.3	23.7	32.3	41.8	8.5	20.3	22.7	58.2	4.5	
10	2.0	36.0	113.6	291.4	69.9	2.6	2.8	3.5	20.6	37.4	31.3	7.2	146.0	48.5	108.9	11.9	53.3	197.2	63.4	14.9	16.7	63.0	2.3	13.7	17.3	41.8	4.5	
10	5.0	32.3	92.9	307.5	76.1	2.5	2.6	3.3	20.7	35.4	29.8	6.9	129.0	44.2	118.1	11.9	59.1	213.6	71.5	13.9	18.4	65.2	2.5	13.5	15.8	47.1	6.2	
15	5.0	27.9	55.9	84.7	51.7	2.2	3.2	4.6	16.5	50.9	22.6	5.2	50.5	24.5	43.3	10.8	40.2	170.7	34.1	13.2	13.9	89.6	1.6	12.7	11.7	20.8	4.6	
20	5.0	20.4	33.3	44.1	26.9	2.1	2.8	4.8	16.1	46.4	16.4	5.0	29.3	22.0	18.6	9.1	23.9	85.3	23.2	10.6	14.9	103.4	1.5	8.5	10.4	15.1	4.6	
25	5.0	16.2	23.8	34.9	16.6	2.0	2.4	4.7	13.7	26.4	14.0	5.0	25.3	25.3	12.8	8.9	15.3	24.2	21.8	11.5	15.1	123.3	1.6	9.7	10.8	13.1	4.9	
30	5.0	14.0	28.2	32.1	11.7	2.0	2.8	5.0	13.0	18.3	12.4	5.3	28.2	28.9	10.8	9.5	13.6	11.7	23.2	11.9	16.4	135.4	1.6	10.4	11.7	12.6	5.1	
35	5.0	13.4	29.3	35.3	10.5	2.0	2.6	5.1	13.1	14.9	11.5	5.4	32.1	33.0	10.2	9.8	14.1	10.4	25.0	12.0	18.3	134.8	1.5	12.0	13.2	12.9	6.7	
40	5.0	12.8	41.2	33.1	10.4	2.0	2.8	5.2	13.6	14.2	10.8	5.6	36.2	37.0	10.4	10.0	13.4	10.8	27.6	11.9	19.8	131.2	1.6	13.3	14.3	13.3	7.1	
45	5.0	13.4	46.4	38.1	9.2	2.0	2.9	5.3	13.0	14.2	10.6	5.4	38.6	41.0	10.5	9.9	13.6	11.6	31.0	12.4	22.5	142.1	1.6	14.8	16.5	13.9	8.5	
50	5.0	13.5	58.9	37.6	8.9	2.0	2.8	4.9	14.0	14.1	10.1	5.8	40.7	45.5	10.8	10.0	16.2	14.6	34.7	12.7	24.6	188.2	1.8	18.1	16.8	15.4	9.9	
60	5.0	13.9	73.8	40.1	9.0	2.2	3.0	5.0	13.5	15.4	10.4	5.6	38.9	56.4	11.9	9.3	17.2	13.9	42.1	14.0	28.9	190.6	2.3	21.4	21.4	18.0	9.1	
70	5.0	15.0	52.6	49.1	9.7	2.2	3.0	5.0	12.6	18.9	10.5	6.4	44.2	67.6	13.1	9.6	22.6	14.1	49.1	15.5	33.3	190.6	2.3	24.9	24.4	22.0	11.5	
80	5.0	16.5	66.8	50.2	9.5	2.2	3.0	5.2	13.7	20.9	11.2	6.9	53.2	79.5	16.6	10.7	23.8	14.4	56.2	16.6	38.2	184.8	2.7	28.0	28.0	25.2	11.9	
90	5.0	19.8	67.9	57.1	11.6	2.2	3.3	5.6	13.8	20.0	11.1	7.1	61.1	90.4	17.6	11.1	23.8	28.8	64.2	21.3	43.1	157.7	3.0	31.6	31.6	28.5	13.3	
100	5.0	19.1	68.3	68.9	13.1	2.1	3.3	6.1	14.5	21.3	11.6	7.9	69.9	101.5	18.1	11.8	24.3	26.2	72.0	24.9	47.3	188.4	3.2	34.3	34.7	32.3	12.4	
110	20.40	20.5	67.7	61.8	12.3	2.2	3.4	6.4	14.5	24.9	12.0	8.7	70.2	110.3	18.9	12.6	25.8	25.9	81.1	24.2	50.6	199.9	3.8	36.5	36.3	37.9	14.1	
125	20.40	23.6	80.6	65.9	13.8	2.3	3.5	7.1	17.8	28.6	13.5	9.1	78.2	125.9	19.3	13.4	23.6	20.6	93.4	28.2	55.3	225.6	4.4	40.3	38.7	42.6	15.4	
135	20.40	25.7	51.8	67.3	15.6	2.3	3.5	7.5	18.9	30.1	15.2	9.8	84.2	138.4	21.4	14.1	29.2	44.9	99.7	31.1	67.4	241.9	4.8	43.6	42.3	48.9	16.5	
150	20.40	26.9	52.0	90.9	18.4	2.4	3.5	8.2	20.0	40.6	16.0	10.7	98.1	149.6	22.6	15.3	40.5	87.5	109.6	29.5	60.9	267.4	5.0	45.9	44.3	60.1	17.6	
160	20.40	28.4	95.9	101.3	16.7	2.5	3.6	8.3	21.5	33.7	16.6	11.0	106.1	160.4	24.0	16.7	43.3	70.7	115.3	31.6	63.3	265.8	5.8	48.9	48.9	71.3	19.6	
175	20.40	30.4	95.4	122.6	18.5	2.5	3.7	9.3	21.5	35.7	17.4	11.8	111.2	175.6	24.5	17.5	48.2	30.5	126.7	34.5	68.0	274.5	5.6	53.4	51.6	81.3	23.0	
185	20.40	32.7	116.7	120.6	23.4	2.6	3.8	9.9	24.9	37.9	18.5	12.4	138.2	188.4	26.3	18.6	50.3	34.1	130.9	36.5	68.6	300.1	6.0	55.6	54.3	89.6	23.9	
200	20.40	32.1	122.3	132.4	22.4	2.7	3.9	11.1	26.9	41.3	19.7	12.8	140.2	197.1	27.4	19.5	52.3	36.9	141.2	33.2	72.3	305.4	6.2	57.8	57.8	94.5	26.9	

Appendix A2: True resistivity data from IPI2WIN for 4 pseudo cross-sections

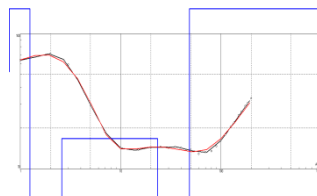
Line A-A'

St 1



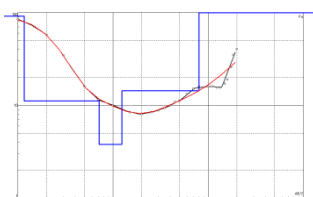
N	p	h	d	Alt
1	31.6	2.03	2.03	-2.026
2	4.36	11.5	13.5	-13.49
3	0.7	14.8	28.3	-28.3
4	1760			

42-29



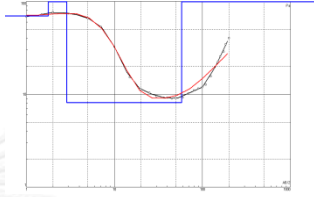
N	p	h	d	Alt
1	52.4	0.6	0.6	-0.6
2	181	0.646	1.25	-1.246
3	4.52	1.34	2.59	-2.588
4	16.7	20.8	23.3	-23.35
5	5.4	25	48.3	-48.32
6	2227			

St 2



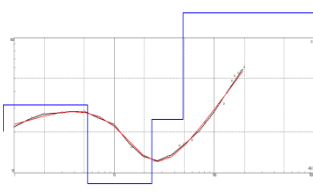
N	p	h	d	Alt
1	58.2	0.254	0.254	-0.2542
2	367	0.511	0.765	-0.765
3	12.2	4.09	4.86	-4.858
4	6.57	52.2	57.1	-57.05
5	1931			

St 5



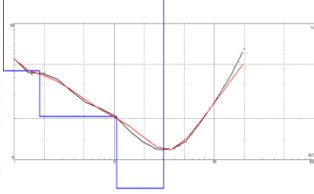
N	p	h	d	Alt
1	70	1.78	1.78	-1.776
2	181	1.1	2.88	-2.875
3	8.14	55.1	57.9	-57.95
4	704			

St 3



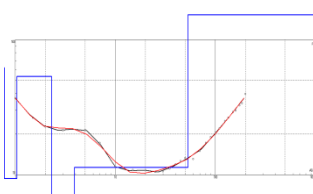
N	p	h	d	Alt
1	20.4	0.6	0.6	-0.6
2	31.8	4.82	5.42	-5.417
3	8.31	18.2	23.6	-23.64
4	24.9	25	48.6	-48.6
5	8846			

St 6



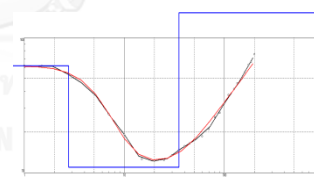
N	p	h	d	Alt
1	7578	0.142	0.142	-0.1416
2	44.9	1.65	1.79	-1.793
3	20.8	8.75	10.5	-10.55
4	6.16	20.5	31.1	-31.06
5	3184			

42-28



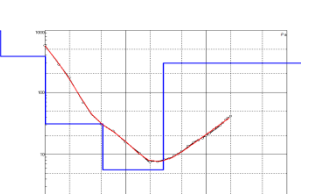
N	p	h	d	Alt
1	61.9	0.502	0.502	-0.5024
2	9.37	0.534	1.04	-1.037
3	53.5	1.27	2.31	-2.31
4	3.1	1.6	3.91	-3.909
5	11.4	49.3	53.2	-53.16
6	630			

F6



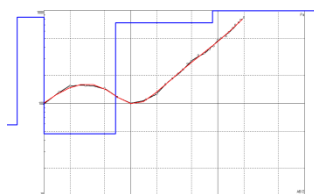
N	p	h	d	Alt
1	61.9	2.77	2.77	-2.768
2	11	32.4	35.1	-35.14
3	15869			

St 4



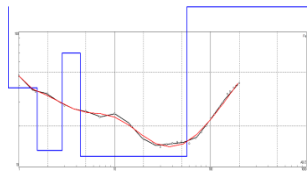
N	p	h	d	Alt
1	2323	0.279	0.279	-0.2789
2	382	0.736	1.02	-1.015
3	31	4.19	5.21	-5.209
4	5.62	24.1	29.3	-29.32
5	298			

St 7



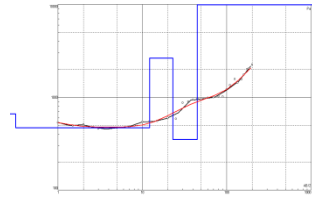
N	p	h	d	Alt
1	58.7	0.492	0.492	-0.492
2	842	0.505	0.997	-0.9969
3	47	5.65	6.65	-6.65
4	734	80.3	86.9	-86.95
5	41670			

F5



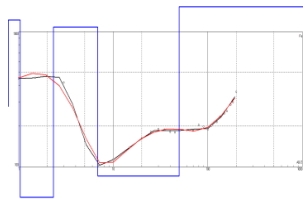
N	p	h	d	Alt
1	4373	0.148	0.148	-0.1484
2	38.5	1.41	1.55	-1.554
3	13.2	1.28	2.83	-2.83
4	69.6	1.55	4.38	-4.378
5	12	52.3	56.7	-56.72
6	1587			

St 8



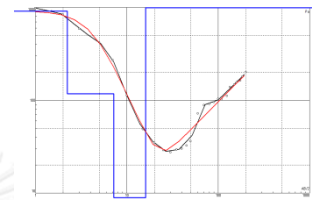
N	p	h	d	Alt
1	661	0.315	0.315	-0.3149
2	468	11.9	12.2	-12.19
3	2646	10.8	23	-22.98
4	350	21.8	44.8	-44.77
5	1.5E+5			

St 9



N	p	h	d	Alt
1	280	0.373	0.373	-0.3734
2	1219	0.665	1.04	-1.038
3	16.4	1.29	2.33	-2.326
4	1084	4.54	6.86	-6.863
5	85.5	42.7	49.6	-49.6
6	12298			

St 10

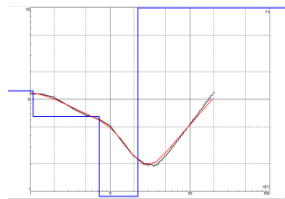


N	p	h	d	Alt
1	911	2.23	2.23	-2.233
2	118	4.97	7.2	-7.199
3	8.94	8.86	16.1	-16.06
4	24416			



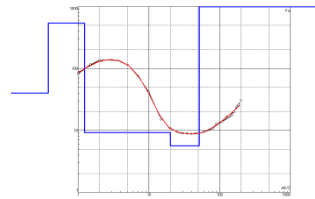
Line B-B'

St 11



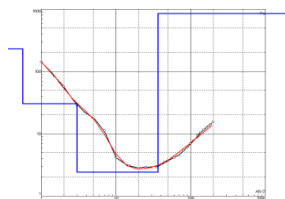
N	p	h	d	Alt
1	12.4	1.08	1.08	-1.085
2	6.51	6.24	7.33	-7.328
3	0.838	14.9	22.3	-22.27
4	1943			

St 17



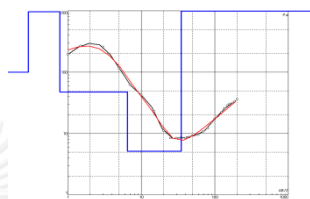
N	p	h	d	Alt
1	39.9	0.378	0.378	-0.3776
2	536	0.853	1.23	-1.23
3	9.22	18.8	20.1	-20.06
4	5.64	31.1	51.2	-51.19
5	2372			

St 12



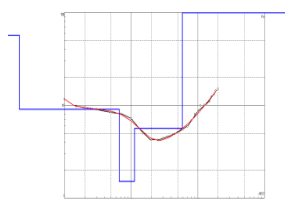
N	p	h	d	Alt
1	230	0.563	0.563	-0.563
2	30.3	2.45	3.01	-3.013
3	2.42	33.5	36.5	-36.47
4	852			

St 18



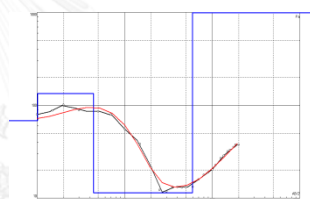
N	p	h	d	Alt
1	99.8	0.29	0.29	-0.2903
2	965	0.491	0.781	-0.781
3	47.3	5.7	6.48	-6.481
4	5.12	28.6	35	-35.04
5	2142			

St 13



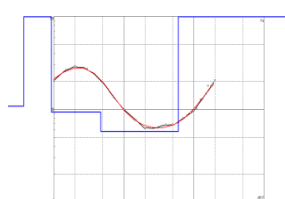
N	p	h	d	Alt
1	56.9	0.209	0.209	-0.2094
2	9.09	6.42	6.63	-6.626
3	1.51	4.55	11.2	-11.17
4	5.64	47.5	58.7	-58.72
5	161			

St 19



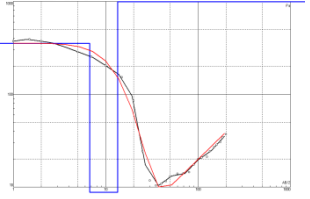
N	p	h	d	Alt
1	68.3	1.02	1.02	-1.017
2	133	3.39	4.41	-4.407
3	11.4	55.1	59.5	-59.47
4	2464			

St 14



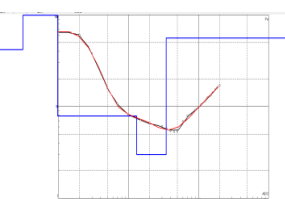
N	p	h	d	Alt
1	10.8	0.37	0.37	-0.3699
2	99.3	0.546	0.916	-0.916
3	9.32	3.74	4.66	-4.655
4	5.78	55.4	60	-60.04
5	1015			

St 71



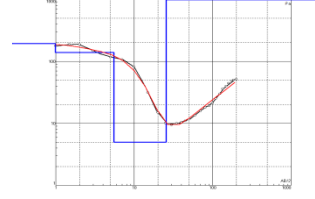
N	p	h	d	Alt
1	354	6.73	6.73	-6.73
2	1.36	6.7	13.4	-13.43
3	1113			

St 15



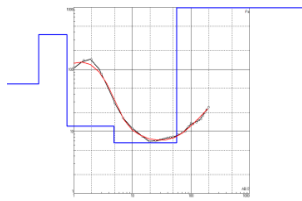
N	p	h	d	Alt
1	41.7	0.31	0.31	-0.3097
2	126	0.663	0.973	-0.9726
3	7.9	12.1	13.1	-13.12
4	2.99	21.4	34.5	-34.5
5	56.1			

St 20



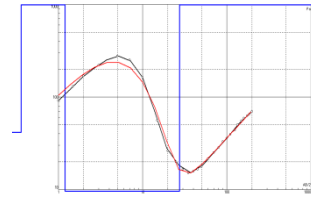
N	p	h	d	Alt
1	194	0.991	0.991	-0.9907
2	139	4.5	5.49	-5.486
3	4.99	20.2	25.7	-25.72
4	2079			

St 16



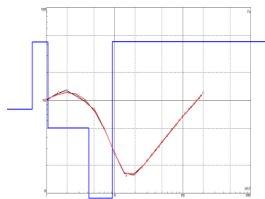
N	p	h	d	Alt
1	58.2	0.254	0.254	-0.2542
2	367	0.511	0.765	-0.765
3	12.2	4.09	4.86	-4.858
4	6.57	52.2	57.1	-57.05
5	1931			

St 21



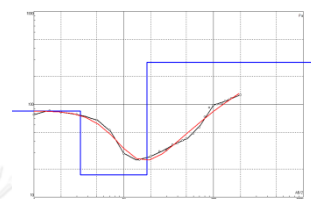
N	p	h	d	Alt
1	41.5	0.359	0.359	-0.3592
2	1488	0.835	1.19	-1.194
3	9.57	26.3	27.5	-27.46
4	3721			

St 22



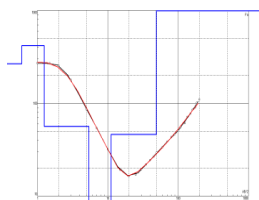
N	p	h	d	Alt
1	80	0.616	0.616	-0.6157
2	424	0.435	1.05	-1.051
3	50.3	3.13	4.18	-4.184
4	4.2	5.11	9.3	-9.297
5	427			

42-126



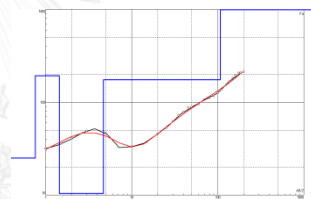
N	p	h	d	Alt
1	84.7	3.3	3.3	-3.297
2	17.4	14.8	18.1	-18.12
3	283			

St 23



N	p	h	d	Alt
1	266	0.6	0.6	-0.6
2	420	0.646	1.25	-1.246
3	56.5	4.13	5.38	-5.375
4	5.75	5.79	11.2	-11.16
5	46.3	38	49.2	-49.16
6	6571			

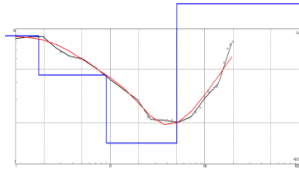
42-125



N	p	h	d	Alt
1	25	0.761	0.761	-0.7611
2	193	0.68	1.44	-1.441
3	10.4	3.24	4.68	-4.68
4	175	102	107	-106.9
5	7490			

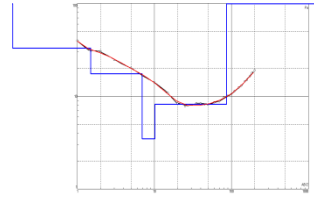
Line C-C'

St 24



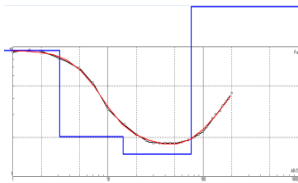
N	p	h	d	Alt
1	8.88	1.76	1.76	-1.755
2	4.55	7.37	9.12	-9.12
3	1.42	41.3	50.4	-50.38
4	760			

St 30



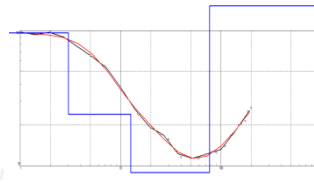
N	p	h	d	Alt
1	4291	0.144	0.144	-0.144
2	32.9	1.34	1.48	-1.484
3	17.5	5.46	6.94	-6.944
4	3.49	3.22	10.2	-10.16
5	8.19	76.1	86.3	-86.26
6	1034			

St 25



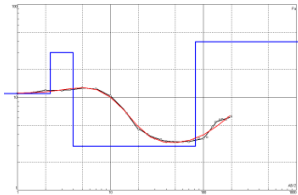
N	p	h	d	Alt
1	9.38	3.11	3.11	-3.113
2	2.02	11.3	14.5	-14.45
3	1.49	60.1	74.6	-74.55
4	757			

St 31



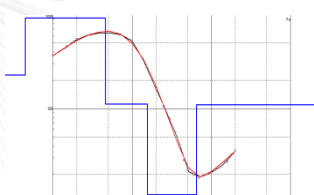
N	p	h	d	Alt
1	96.2	3.02	3.02	-3.016
2	24.1	9.61	12.6	-12.63
3	8.91	64.4	77	-76.98
4	3074			

St 26



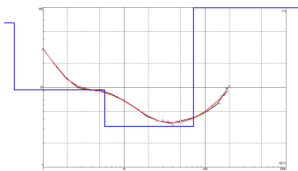
N	p	h	d	Alt
1	11	2.24	2.24	-2.244
2	30.2	1.71	3.95	-3.95
3	2.96	78.1	82	-82.01
4	39.7			

41-205



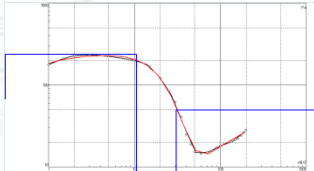
N	p	h	d	Alt
1	228	0.448	0.448	-0.4479
2	917	4.13	4.58	-4.576
3	111	11	15.6	-15.56
4	12.2	49.3	64.8	-64.84
5	110			

St 27



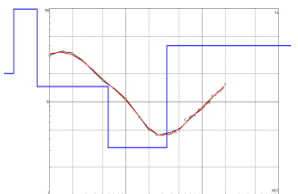
N	p	h	d	Alt
1	63.9	0.44	0.44	-0.4401
2	9.25	5.34	5.78	-5.783
3	3.23	66.5	72.2	-72.23
4	651			

St 32



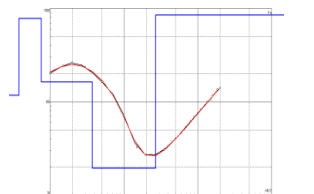
N	p	h	d	Alt
1	67.8	0.127	0.127	-0.1267
2	238	10.4	10.6	-10.57
3	5.03	19.9	30.5	-30.48
4	49.7			

St 28



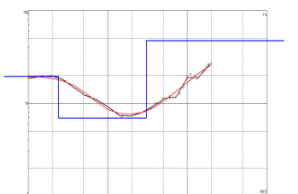
N	p	h	d	Alt
1	20	0.341	0.341	-0.3406
2	98.2	0.347	0.687	-0.6872
3	14.5	5.17	5.86	-5.859
4	3.23	28.7	34.6	-34.58
5	40			

41-191



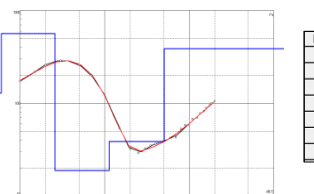
N	p	h	d	Alt
1	118	0.379	0.379	-0.3794
2	783	0.382	0.762	-0.7616
3	164	2.96	3.72	-3.719
4	19.4	23.2	26.9	-26.91
5	851			

St 29



N	p	h	d	Alt
1	19.5	2.39	2.39	-2.391
2	6.9	28.2	30.6	-30.57
3	47.4			

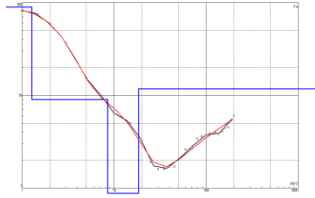
St 33



N	p	h	d	Alt
1	128	0.6	0.6	-0.6
2	565	1.99	2.59	-2.591
3	18.9	8.73	11.3	-11.32
4	38.8	39.4	50.8	-50.76
5	387			

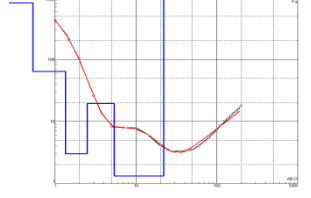
Line D-D'

St 34



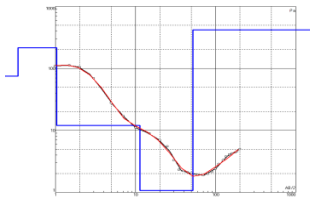
N	p	h	d	Alt
1	88.9	1.27	1.27	-1.273
2	8.95	7.24	8.51	-8.514
3	0.483	9.92	18.4	-18.43
4	11.8			

St 41



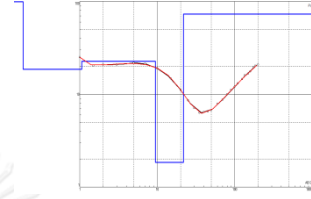
N	p	h	d	Alt
1	811	0.534	0.534	-0.5336
2	63.8	0.816	1.35	-1.35
3	2.99	1.14	2.49	-2.495
4	19.5	2.9	5.4	-5.396
5	1.32	16.6	22	-22
6	1662			

St 35



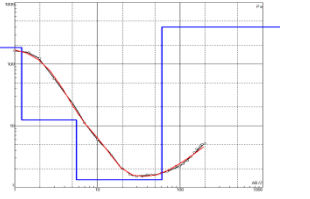
N	p	h	d	Alt
1	75.4	0.342	0.342	-0.3423
2	216	0.698	1.04	-1.041
3	12	10.2	11.3	-11.29
4	1.08	40.9	52.2	-52.24
5	417			

St 42



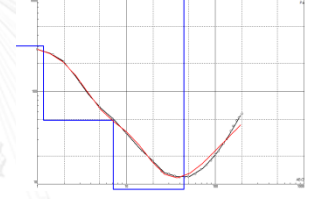
N	p	h	d	Alt
1	386.2	0.1859	0.1859	-0.1859
2	18.56	0.8786	1.065	-1.0645
3	22.74	0.396	9.461	-9.4607
4	1.849	12.28	21.74	-21.739
5	73.01			

St 36



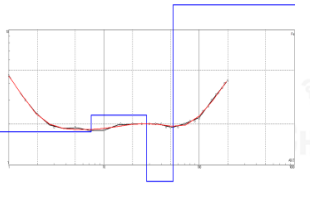
N	p	h	d	Alt
1	185	1.22	1.22	-1.217
2	12.4	4.33	5.55	-5.545
3	1.33	55.1	60.7	-60.66
4	402			

St 43



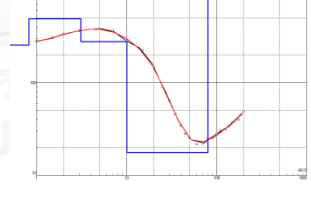
N	p	h	d	Alt
1	308	1.18	1.18	-1.176
2	48.8	5.96	7.13	-7.133
3	8.75	37.2	44.3	-44.31
4	3488			

St 37



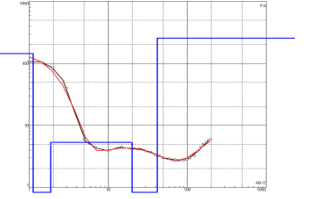
N	p	h	d	Alt
1	7.951	0.4673	0.4673	-0.4673
2	1.758	6.854	7.321	-7.3209
3	2.333	20.66	27.98	-27.98
4	0.7526	25.22	53.2	-53.196
5	383.4			

St 44



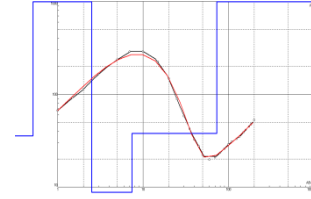
N	p	h	d	Alt
1	255	0.824	0.824	-0.8235
2	482	2.29	3.12	-3.115
3	278	6.95	10.1	-10.06
4	17.6	69.5	79.6	-79.57
5	1408			

St 39



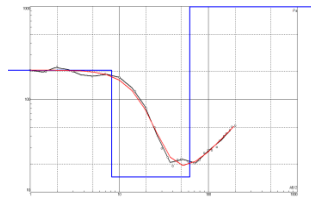
N	p	h	d	Alt
1	144	1.12	1.12	-1.116
2	0.831	0.753	1.87	-1.869
3	5.34	18.3	20.1	-20.12
4	0.725	21.8	41.9	-41.89
5	256			

41-174



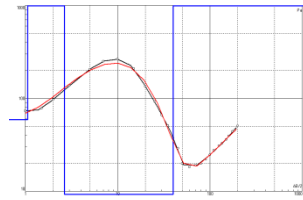
N	p	h	d	Alt
1	35.6	0.515	0.515	-0.5153
2	1363	1.99	2.51	-2.507
3	2.42	4.91	7.41	-7.415
4	37.8	65.5	72.9	-72.92
5	1041			

41-173



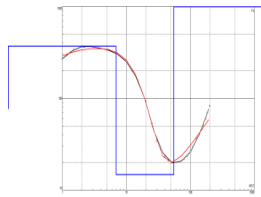
N	p	h	d	Alt
1	295	8.21	8.21	-8.21
2	14.5	53.4	61.6	-61.61
3	2894			

St 46



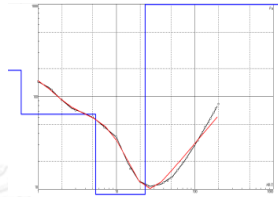
N	p	h	d	Alt
1	59.2	1.06	1.06	-1.062
2	1583	1.59	2.66	-2.655
3	9.26	37.3	39.9	-39.95
4	2108			

St 45



N	p	h	d	Alt
1	77.3	0.0898	0.0898	0.0898
2	371	6.8	6.89	-6.889
3	14.8	48.3	55.1	-55.14
4	9441			

St 47



N	p	h	d	Alt
1	193	0.609	0.609	-0.609
2	64.5	4.8	5.41	-5.406
3	5.75	17.8	23.2	-23.23
4	5822			



Appendix B

Appendix B1 Well data from pre-field

Appendix B2 Well data from collecting groundwater samples field

Appendix B3 Calculate for Ion Balance

Appendix B4 Standard curve AAS

Appendix B5 Standard curve IC

Appendix B1: Well data of pre-field
 Table B1. Well data from pre-field

Sample No.	Well No.	Utm		Well depth	screen	Elevation	Accuracy	Depth of water	Water table	Temperature	pH	TDS	EC	Salt	Aquifer
		East	North												
GW1-1	5408D002	596963	1406900	140	18-30, 89-92	54	2	5	49	30.1	7	1272	1900	949	Gr
GW1-2	5608G006	597237	1407008	140	18-30	54	3	5	49	29.1	6.96	1307	1951	975	Gr
GW1-3	DCD14819	598426	1406695	36	30-33	39	3	6.66	32.34	30.5	6.93	1410	2120	1050	Qcl
GW1-4	5408D026	597988	1406225	90	26-38, 38-88	46	3	8.78	37.22	31	7.2	925	1382	691	Qcl+Gr
GW1-5	MU287	599484	1406364	48	40.5-46.5	38	2	6.3	31.7	33.2	8.04	436	652	325	Qcl
GW1-6	DCD14826	599003	1406071	48	42-45	39	2	6	33	30.1	7.15	1430	2130	1070	Qcl
GW1-7	MU134	599142	1406175	42	36-42	39	2	6.56	32.44	29.7	7.7	1088	1622	811	Qcl
GW1-8	7771	599600	1406238	42	36-42	34	3	3.5	30.5	31.5	10.18	898	1340	670	Qcl
GW1-9	DCD14809	598833	1404187	42	36-39	33	2	7.13	25.87	35.8	6.95	998	1762	682	Gr
GW1-10	5403H042	596519	1401418	90	24-90	59	2	3.47	55.53	30.1	8.05	873	1304	651	Gr
GW1-11	MU135	596964	1401482	31.5	24-30	59	2	3.14	55.86	29.8	7.53	446	667	333	Qcl
GW1-12	MU441	596152	1401182	31.5	24-30	59	2	5.2	53.8	29.6	7.44	1650	2470	1230	Qcl
GW1-13	Q179	595901	1422250	72	36-42, 48-54	38	2	23.32	14.68	31.3	7.18	487	722	362	Qcl+PCms
GW1-14	Q181	595355	1422516	60	42-48, 54-60	39	2	24.5	14.5	30.6	6.73	209	314	156	Qcl+PCms
GW1-15	DCD14781	594787	1422741	42	36-39	33	4	4.5	28.5	30	6.76	487	733	366	Qcl
GW1-16	C428	595032	1422217	60	42-54	45	2	18	27	29.1	6.97	201	302	151	Qcl+PCms
GW1-17	5408D011	595090	1422206	72	42-54, 64-72	49	3	15.2	33.8	31	6.78	218	323	162	Qcl+PCms
GW1-18	PW2405	601463	1419929	23	10.76-16.88	17	5	0.6	16.4	30.5	7.19	1069	1594	798	Qcl
GW1-19	5508C108	601114	1419661	50	36-42	17	3	0.63	16.37	29.8	7.03	759	1131	566	Qcl
GW1-20	MU255	601365	1419082	70.5	60-66	19	2	0.7	18.3	N/A	N/A	N/A	N/A	N/A	Qcl

Table B1. Well data from pre-field (continue)

Sample No.	Well No.	Utm		Well depth m.	screen m.	Elevation m.	Accuracy m.	Depth of water m.	Water table m.: asl.	Temperature °C	pH	TDS mg/l	EC µs/cm	Salt µs/cm	Aquifer
		East	North												
GW1-21	C545	601651	1418580	36	30-36	19	2	1.75	17.25	30.5	7.43	370	537	277	Qcl
GW1-22	MU697	602367	1419199	82.5	24-28	16	2	2	14	29.4	7.64	519	775	387	PC
GW1-23	¶1605	603369	1419634	60	30-40	16	4	8	8	29.5	6.99	2090	3120	1560	PC
GW1-24	PCR16	603532	1421994	60	18-24	18	2	2.6	15.4	33.1	7	3580	5360	2680	Qcl+PC
GW1-25	¶0424-2	608963	1424032	30	12.0-16	16	3	14.64	1.36	29.7	6.49	497	743	371	Qfd
GW1-26	¶1604	609530	1424346	96	72-84	9	2	7.74	1.26	32.2	7.46	1261	1870	943	Qcl
GW1-27	Private	607703	1420084	98	90-96	8	2	7.23	0.77	32.7	7.92	1050	1566	783	Qcl
GW1-28	¶86	607489	1416828	50	30-36	10	2	7.5	2.5	31.8	7.43	1920	2870	1430	Qcl
GW1-29	C334	607507	1416843	126	72-78	6	4	0.98	5.02	N/A	N/A	N/A	N/A	N/A	Qcl
GW1-30	¶88	607095	1416142	70	16-22, 64-68	13	3	10.15	2.85	29.6	7.64	2920	4360	2180	Qcl
GW1-31	MU586	601364	1415807	58	34-38, 54-58	19	3	3.1	15.9	34.1	6.98	834	1246	623	PCms
GW1-32	MU331	601109	1414472	67.5	30-33, 63-66	18	3	3.26	14.74	32.6	8.29	693	1035	518	PCms
GW1-33	DOH1441	600794	1414543	60	34-38, 54-58	25	3	12.4	12.6	37.5	7.88	425	637	318	Qcl+PCms
GW1-34	MU580	600560	1414168	72	44-48, 68-72	28	2	5.01	22.99	39.61	7.13	607	904	452	PCms
GW1-35	DCD14775	600544	1413892	77.1	72-75	29	2	7.5	21.5	39.7	7.18	480	715	358	PCms
GW1-36	MU587	600608	1413625	72	24-28	28	3	7	21	39.7	7.08	569	848	424	PCms
GW1-37	DCD14773	600113	1413395	72	66-69	34	3	16.5	17.5	38.5	7.38	507	755	378	PCms
GW1-38	AFD8794	599404	1415600	60.98	42-48	37	2	9.6	27.4	32.8	8.47	722	1077	537	Qcl+PCms
GW1-39	DCD14766	598969	1415312	65.1	36-40, 68-72	39	2	15	24	32.6	7.77	851	1269	634	PCms+Gr
GW1-40	MU588	599557	1414946	72	36-40, 68-72	33	3	8.5	24.5	29.9	7.34	683	1022	510	PCms
GW1-41	MU584	598315	1412637	58	42-46, 54-58	54	3	15	39	35.7	7.62	623	934	466	PCms+Gr
GW1-42	MU363	599814	1412073	66	60-66	39	2	5.9	33.1	31.2	7.03	624	932	466	Qcl
GW1-43	C402	601069	1419905	36	30-36	16	2	0.45	15.55	N/A	N/A	N/A	N/A	N/A	Gr
GW1-44	5608C028	601656	1397443	66	36-42, 60-66	35	2	12	23	N/A	N/A	N/A	N/A	N/A	Gr

Table B1. Well data from pre-field (continue)

Sample No.	Well No.	Utm		Well depth m.	screen m.	Elevation m.	Accuracy		Depth of water m.	Water table m.: asl.	Temperature °C	pH	TDS mg/l	EC µs/cm	Salt µs/cm	Aquifer
		East	North				m.	m.								
GW1-45	5508C027	600911	1409454	120	78-90	24	2	2	11.2	12.8	N/A	N/A	N/A	N/A	N/A	Gr
GW1-46	5508C026	601229	1409148	102	66-72	18	2	2	5.4	12.6	N/A	N/A	N/A	N/A	N/A	Qcl
GW1-47	5608C007	598448	1412207	74	42-48, 54-60	53	3	3	12	41	N/A	N/A	N/A	N/A	N/A	Gr
GW1-48	DCD14768	599586	1418236	72	66-69	36	3	3	11.3	24.7	N/A	N/A	N/A	N/A	N/A	PCms
GW1-49	DCD14779	599882	1418587	59.1	54-57	19	2	2	13	6	N/A	N/A	N/A	N/A	N/A	PCms
GW1-50	5608C045	597927	1423099	61	12-16, 20-24, 52-56	18	2	2	1.7	16.3	N/A	N/A	N/A	N/A	N/A	Qcl
GW1-51	5403H043-2	597374	1400045	142	24-142	143	2	2	24.87	118.13	N/A	N/A	N/A	N/A	N/A	Qcl+Gr
GW1-52	5408C021	598798	1399044	80	36-80	56	3	3	7.8	48.4	N/A	N/A	N/A	N/A	N/A	Gr
GW1-53	DCD14787	599589	1423189	42	36-39	16	4	4	6	10	N/A	N/A	N/A	N/A	N/A	Qcl
GW1-54	5408D001	597022	1407165	102	36-42	57	2	2	8	49	N/A	N/A	N/A	N/A	N/A	Gr
GW1-55	5408D022	601572	1405197	73	24-30, 66-72	19	2	2	4	15	N/A	N/A	N/A	N/A	N/A	Qcl
GW1-56	C417	598888	1417979	120	102-114	23	2	2	7.38	15.62	N/A	N/A	N/A	N/A	N/A	Gr

Appendix B2 Well data from collecting groundwater samples field

Table B2. Well data from collecting groundwater samples field

Sample No.	Well No.	Utm		Well depth m.	Screen		Elevation m.	Accuracy m.	Depth of water m.	Water table m.: asl.	Temperature °C	pH	TDS mg/l	EC µs/cm	Salt µs/cm	Aquifer
		East	North		m.	m.										
W1	MU287	599485	1406366	48	40.5-46.5	38	2	6	32	32	28.5	6.79	205	306	153	Qcl
W2	5608G006	597237	1407015	140	18-30	54	3	5.5	48.5	48.5	28	6.66	1307	1951	975	Gr
W3	5408D026	597985	1406227	90	26-38, 38-86	46	4	8	38	38	30.4	7.26	773	1155	577	Qcl+Gr
W4	MU747	598259	1406443	42	34-42	38	2	2	36	36	29.8	7.42	607	905	453	Gr
W5	PCR9	599258	1405479	80	72-80	36	2	2.9	33.1	33.1	29.7	7.54	718	1071	536	Gr
W6	C629	599471	1405735	30	24-30	37	3	3.5	33.5	33.5	28.4	7.1	905	1348	675	Qcl
W7	MU134	599148	1406172	42	36-42	39	4	6.75	32.25	32.25	29.3	10.45	739	1105	553	Qcl
W8	Private	599604	1406235	42	36-42	34	4	4	30.35	30.35	31.2	10.18	761	1137	567	Qcl
W9	Private	598945	1406464	78	36-42, 62-78	37	3	3.6	33.4	33.4	30.7	10.3	781	1170	583	Gr
W10	MU753	600328	1406673	51	24-28, 44-48	30	3	3.8	26.2	26.2	29.5	8.03	602	465	232	Qcl
W11	Private	600139	1405665	40	35-40	35	3	6.56	28.44	28.44	26.7	9.59	825	1360	605	Qcl
W12	1642	599828	1405031	50	42-48	35	3	6.1	28.9	28.9	29.1	9.76	781	1166	583	Qcl
W13	DCD14827	598620	1404879	87	78-85	38	2	4	34	34	32.2	7.07	805	1230	597	Gr
W14	5508C019	598717	1404818	156	42-152	39	2	8.1	30.9	30.9	29.2	9.89	757	1130	565	Gr
W15	DCD14809	598833	1404185	42	36-39	33	5	8.13	24.87	24.87	29	7.24	779	1162	581	Gr
W16	Private	596152	1401178	31.5	24-30	66	4	4.6	54.4	54.4	28.6	9.38	1650	2470	1230	Qcl
W17	MU135	596968	1401484	31.5	24-30	59	2	3.2	55.8	55.8	28.7	10.37	397	594	297	Qcl
W18	Private	598874	1398809	N/A	N/A	30	3	N/A	N/A	N/A	26.8	10.12	1720	3024	1325	N/A
W19	Private	599101	1399708	80	60-70	48	2	11.5	36.5	36.5	30.2	10.08	801	1196	598	Gr
W20	Private	598166	1400836	100	60-70	54	3	14.6	39.4	39.4	30.6	10.78	591	883	441	Gr
W21	5408D022	601572	1405197	73	24-30, 66-72	19	2	5.5	13.5	13.5	26.6	10.25	782	1168	584	Qcl

Table B2. Well data from collecting groundwater samples field (continue)

Sample No.	Well No.	Utm		Well depth m.	Screen m.	Elevation m.	Accuracy m.	Depth of water m.	Water table m.: asi.	Temperature °C	pH	TDS mg/l	EC µs/cm	Salt µs/cm	Aquifer
		East	North												
W22	DCD14772	600710	1412395	78	12-16,20-24,52-56	22	3	10.5	11.5	26.8	7.19	556	830	415	Ocl+PCns
W23	5608C045	597927	1423099	61	12-16, 20-24, 52-56	18	4	1.8	16.2	28.6	10.27	375	562	281	Ocl
W24	MU563	598233	1423851	16	12.0-16.0	14	4	1	13	28.5	9.71	900	1347	673	Ocl
W25	MU564	598959	1423362	18	14-18	10	4	1	9	25.6	9.48	843	1130	726	Ocl
W26	5408D011	595088	1422206	72	42-54, 64-72	49	3	31.3	17.7	28.3	11.15	195	292	146	Ocl+PCns
W27	Q167	595555	1423070	90	24-30	25	3	3	22	27.6	8.97	494	739	369	Ocl
W28	¶1607	594472	1422610	30	12.0-18.0	29	3	1.8	27.2	28.2	9.52	391	584	292	Ocl
W29	Private	595678	1421856	60	54-60	45	2	18.2	26.8	28.5	11	267	400	199	PCns
W30	MU283	598870	1418875	66	54-60	32	4	12.55	19.45	28.2	9.49	420	627	313	PCns
W31	PCR10	599314	1418422	100	84-90	26	4	6.7	19.3	27.3	10.07	460	687	343	PCns
W32	DCD14768	599568	1418232	72	66-69	36	4	12	24	27.2	10.29	503	375	752	PCns
W33	MU348	600114	1412498	61.5	54-60	32	2	13.88	18.12	25.1	10.07	507	757	378	PCns
W34	MU363	599816	1412076	66	60-66	39	2	6	33	27.8	10.22	548	1015	409	Ocl
W35	MU571	599873	1411706	44	40-44	36	2	5	31	30.3	10.11	762	1138	568	Ocl
W36	MU332	599070	1411457	31.5	7.5-10.5	43	2	6.45	36.55	29.2	10.08	649	971	485	Ocl
W37	MU359	598836	1410651	37.5	32-37	39	3	1.9	37.1	29.5	8.5	780	1267	765	Ocl
W38	MU557	598822	1410899	64	24-27, 57-60	39	3	1.85	37.15	29.1	7.06	565	848	424	Ocl+Gr
W39	MU458	597809	1411756	61.5	54-60	55	4	19.1	35.9	29.8	7.31	239	357	178	PCns
W40	5606C007	598448	1412207	74	42-48, 54-60	53	5	19.2	39.8	29.9	9.87	426	631	312	Gr
W41	MU361	599110	1412570	55.5	24-27	39	4	13.35	25.65	28.4	10.07	559	834	417	PCns
W42	MU335	599455	1412506	64.5	60-63	37	4	7	30	26.2	10.25	454	677	338	PCns
W43	MU549	598990	1413665	72	64-72	39	3	8.2	30.8	29.9	9.92	621	929	464	Gr
W44	DCD14766	598866	1415313	65.1	36-40, 68-72	39	3	15.2	23.8	30.1	9.45	753	1124	562	Gr
W45	AFD8794	599408	1415589	60.98	65-60	37	3	10.56	26.44	29.3	11.01	531	793	396	Ocl+PCns
W46	MU588	599553	1414947	72	36-40, 68-72	33	3	8.7	24.3	29	9.33	254	379	190	PCns

Table B2. Well data from collecting groundwater samples field (continue)

Sample No.	Well No.	Utm		Well depth m.	Screen m.	Elevation m.	Accuracy m.	Depth of water m.	Water table m., asl	Temperature		pH	TDS mg/l	EC µs/cm	Salt µs/cm	Aquifer
		East	North							°C	°C					
W47	DCD14773	600113	1413395	72	66-69	34	3	17	17	32.2	8.87	649	970	484	PCms	
W48	MU578	600487	1413347	70	30-33,63-66	30	3	9.3	20.7	29.5	7.5	629	939	470	Qcl+PCms	
W49	DOH11441	600791	1414541	60	34-38, 54-58	25	2	12.8	12.2	28.7	8.74	340	514	256	Qcl+PCms	
W50	MU331	601104	1414466	67.5	30-33, 63-66	18	2	3.45	14.5	29.1	8.45	660	986	493	PCms	
W51	MU586	601359	1415802	58	34-38,54-58	19	3	3.98	15.02	28.4	8.64	762	1138	569	PCms	
W52	MU697	602364	1419204	82.5	24-28	16	2	2.2	13.8	28.6	7.29	397	598	299	Pr	
W53	41605	603370	1419640	60	30-40	16	3	8.2	7.8	29.2	7.37	2090	3120	1560	Pr	
W54	PCR16	603532	1421992	88	18-24	18	4	2.51	15.49	29.8	8.3	3580	5360	2680	Qcl+Pr	
W55	486	607487	1416828	50	30-36	10	4	7	3	42	9.65	1920	2860	1430	Qcl	
W56	488	607100	1416141	70	16-22,64-68	13	2	9.7	3.3	29.5	8.92	2920	4360	2180	Qcl	
W57	C545	601649	1418575	36	30-36	19	3	1.96	17.04	27.2	9.37	207	310	155	Qcl	
W58	Private	601426	1416606	ND	ND	18	4	ND	ND	26.6	9.97	784	1169	585	ND	
W59	5708C002	599730	1422937	32	14-18, 26-30	18	3	6	12	N/A	N/A	N/A	N/A	N/A	Qcl	
W60	5608C017	597640	1416787	76	64-76	56	4	24.4	31.6	N/A	N/A	N/A	N/A	N/A	Qcl+Gr	
W61	5608C028	601656	1387443	66	36-42, 60-66	35	2	12.5	22.5	N/A	N/A	N/A	N/A	N/A	Gr	
W62	5708A015	607488	1416843	87	74-80	20	2	9	11	N/A	N/A	N/A	N/A	N/A	Qcl	
W63	5708C004	599119	1413588	140	30-36	35	3	19	16	N/A	N/A	N/A	N/A	N/A	Qcl	
W64	5708C044	604069	1403426	125	78-125	8	2	2	6	N/A	N/A	N/A	N/A	N/A	Gr	
W65	C334	607507	1416843	126	72-78	6	3	0.36	5.64	N/A	N/A	N/A	N/A	N/A	Qcl	
W66	C402	601069	1419905	36	30-36	16	2	1	15	N/A	N/A	N/A	N/A	N/A	Qcl+Gr	
W67	C417	599888	1417979	120	102-114	24	2	10.5	13.5	N/A	N/A	N/A	N/A	N/A	Gr	
W68	C428	595032	1422217	60	42-54	43	3	18.9	24.1	N/A	N/A	N/A	N/A	N/A	Qcl+PCms	
W69	DCD14771	599221	1419090	53.1	48-51	30	2	15.3	14.7	N/A	N/A	N/A	N/A	N/A	Qcl+PCms	
W70	DCD14775	600544	1413892	77.1	72-75	30	3	7.9	22.1	N/A	N/A	N/A	N/A	N/A	PCms	
W71	DCD14779	599882	1418587	59.1	54-57	19	3	13	6	N/A	N/A	N/A	N/A	N/A	Qcl+PCms	

Table B2. Well data from collecting groundwater samples field (continue)

Sample No.	Well No.	Utm		Well depth m.	Screen m.	Elevation m.	Accuracy m.	Depth of water m.	Water table m.: asl.	Temperature °C	pH	TDS mg/l	EC µs/cm	Salt µs/cm	Aquifer
		East	North												
W72	DCD14780	598764	1412403	48	42-45	47	2	10.8	36.2	N/A	N/A	N/A	N/A	N/A	PCms+Gr
W73	DCD14787	599589	1423189	42	36-39	17	3	6	11	N/A	N/A	N/A	N/A	N/A	Qcl



Appendix B3: Calculated for Ion Balance

Table B3. Calculated ion balance for chemical analysis of groundwater samples

Sample No.	Ca ²⁺ (meq/l)	Mg ²⁺ (meq/l)	Na ⁺ (meq/l)	K ⁺ (meq/l)	HCO ₃ ⁻ (meq/l)	CO ₃ ⁻² (meq/l)	SO ₄ ²⁻ (meq/l)	Cl ⁻ (meq/l)	NO ₃ ⁻ (meq/l)	Σ cations	Σ anions	*Error Balance %
W1	1.766	0.461	4.165	0.313	0.840	0.840	0.149	2.313	0.046	6.705	4.188	23.105
W2	5.017	1.556	6.913	0.115	2.240	2.240	0.504	6.058	0.276	13.601	11.318	9.162
W3	4.935	1.457	4.772	0.146	2.160	2.160	0.253	2.513	0.107	11.309	7.193	22.247
W4	2.414	1.095	3.565	0.215	1.320	1.320	0.015	3.632	0.025	7.289	6.312	7.185
W5	2.476	1.432	2.791	0.344	2.120	2.120	0.005	2.240	0.000	7.044	6.485	4.130
W6	2.395	1.498	5.635	0.410	1.185	0.747	0.275	6.184	0.564	9.938	8.955	5.202
W7	2.090	0.741	5.022	0.377	0.600	0.600	0.001	6.465	0.022	8.229	7.688	3.402
W8	2.259	0.988	5.989	0.281	1.944	0.600	0.037	6.068	0.000	9.517	8.649	4.783
W9	2.940	1.062	1.748	0.197	2.174	0.000	0.103	2.390	0.206	5.947	4.873	9.927
W10	0.878	0.716	2.374	0.234	0.800	0.000	0.207	3.377	0.002	4.202	4.386	-2.149
W11	2.339	1.523	5.533	0.446	2.320	0.000	0.200	6.098	0.751	9.841	9.370	2.452
W12	3.461	1.687	5.000	0.341	1.960	0.000	0.120	4.721	0.526	10.490	7.327	17.754
W13	3.521	2.798	4.487	0.168	1.840	0.000	0.340	4.788	0.104	10.974	7.071	21.629
W14	2.940	2.798	4.009	0.121	1.760	1.760	0.050	4.646	0.000	9.869	8.216	9.137
W15	3.429	1.621	3.939	0.174	2.392	0.000	0.001	5.097	0.011	9.163	7.501	9.978
W16	4.297	2.025	10.478	1.100	2.600	0.000	0.917	9.473	2.063	17.899	15.052	8.641
W17	2.262	0.963	1.391	0.532	2.600	0.000	0.267	1.581	0.013	5.148	4.462	7.142

Table B3. Calculated ion balance for chemical analysis of groundwater samples (continue)

Sample No.	Ca ²⁺ (meq/l)	Mg ²⁺ (meq/l)	Na ⁺ (meq/l)	K ⁺ (meq/l)	HCO ₃ ⁻ (meq/l)	CO ₃ ⁻² (meq/l)	SO ₄ ²⁻ (meq/l)	Cl ⁻ (meq/l)	NO ₃ ⁻ (meq/l)	Σ cations	Σ anions	*Error Balance %
W18	8.399	2.288	8.678	0.121	2.000	2.000	1.770	11.292	0.760	19.487	17.822	4.461
W19	3.506	1.498	1.761	0.372	2.995	0.000	0.257	2.051	0.677	7.137	5.979	8.826
W20	4.050	0.996	1.409	0.119	3.107	0.000	0.256	1.955	0.089	6.573	5.406	9.745
W21	2.277	1.514	5.783	0.417	2.000	0.000	0.213	7.099	0.238	9.991	9.550	2.255
W22	2.494	1.136	4.678	0.229	1.680	0.000	0.088	5.768	0.002	8.537	7.539	6.208
W23	3.050	0.790	1.930	0.257	1.154	0.000	0.548	3.808	0.005	6.027	5.516	4.433
W24	3.544	2.683	5.326	0.168	1.120	0.000	1.360	7.873	0.254	11.720	10.608	4.982
W25	4.683	3.885	8.643	0.155	1.120	0.000	1.495	13.459	0.076	17.366	16.150	3.630
W26	0.781	0.329	1.435	0.361	0.360	0.000	0.027	0.975	0.859	2.905	2.220	13.368
W27	2.858	0.716	2.957	0.500	1.390	0.000	0.019	3.656	0.150	7.030	5.215	14.824
W28	2.292	0.807	2.696	0.325	1.551	0.000	0.001	3.538	0.013	6.119	5.103	9.056
W29	0.943	0.280	1.078	0.605	0.960	0.960	0.004	1.420	0.070	2.906	3.413	-8.031
W30	2.264	0.584	1.865	0.418	2.043	0.000	0.129	2.468	0.041	5.132	4.680	4.608
W31	2.252	0.963	3.609	0.231	1.160	0.000	0.179	2.831	0.005	7.255	4.175	26.942
W32	2.224	1.012	1.743	0.471	2.000	0.670	0.001	1.811	0.006	5.451	4.489	9.680
W33	2.808	1.078	3.052	0.257	2.172	0.000	0.076	3.666	0.386	7.195	6.300	6.632
W34	2.564	1.078	5.139	0.221	1.021	0.000	0.179	7.313	0.071	9.002	8.584	2.377
W35	2.274	1.416	5.852	0.400	1.354	0.000	0.208	7.600	0.139	9.942	9.301	3.334
W36	2.960	1.794	3.565	1.465	1.840	0.000	0.504	5.031	0.000	9.785	7.375	14.043
W37	2.930	1.465	5.365	1.491	1.600	0.000	0.609	6.985	0.023	11.251	9.216	9.942
W38	6.262	3.012	9.370	1.102	2.000	0.000	2.741	10.711	0.009	19.746	15.461	12.171
W39	0.773	0.486	1.435	0.386	0.567	0.000	0.048	1.811	0.075	3.080	2.501	10.366

Table B3. Calculated ion balance for chemical analysis of groundwater samples (continue)

Sample No.	Ca ²⁺ (meq/l)	Mg ²⁺ (meq/l)	Na ⁺ (meq/l)	K ⁺ (meq/l)	HCO ₃ ⁻ (meq/l)	CO ₃ ⁻² (meq/l)	SO ₄ ²⁻ (meq/l)	Cl ⁻ (meq/l)	NO ₃ ⁻ (meq/l)	Σ cations	Σ anions	*Error Balance %
W40	2.085	0.938	3.478	0.312	0.520	0.000	0.034	2.834	0.004	6.813	3.392	33.522
W41	2.444	1.119	3.809	0.286	1.720	1.720	0.509	2.741	0.307	7.658	6.997	4.512
W42	2.237	0.914	3.296	0.404	1.240	0.000	0.063	2.442	0.116	6.850	3.861	27.902
W43	3.796	1.556	4.078	0.362	1.720	1.720	0.111	4.346	0.610	9.791	8.507	7.020
W44	2.910	1.350	3.583	0.307	1.760	1.760	0.053	4.801	0.000	8.150	8.373	-1.354
W45	1.805	0.296	2.648	0.313	1.360	1.360	0.227	1.754	0.463	5.063	5.164	-0.991
W46	1.234	0.642	1.409	0.211	0.889	0.533	0.119	0.436	0.003	3.496	1.980	27.687
W47	3.057	1.383	3.896	0.331	2.240	0.000	0.178	3.792	1.056	8.667	7.265	8.798
W48	3.536	1.506	3.704	0.436	1.440	0.000	0.211	1.498	1.206	9.183	4.355	35.666
W49	1.227	0.988	1.830	0.751	1.187	1.200	0.175	1.710	0.033	4.796	4.306	5.378
W50	3.304	1.811	4.017	0.536	1.320	1.320	0.080	5.189	0.025	9.668	7.935	9.848
W51	3.636	1.062	3.665	0.340	2.000	0.467	0.089	4.820	0.186	8.703	7.561	7.023
W52	3.252	0.840	2.791	0.083	1.466	1.333	0.246	2.828	0.076	6.966	5.949	7.876
W53	10.701	2.510	12.539	0.124	1.200	1.200	1.558	25.941	0.653	25.874	30.552	-8.290
W54	1.898	3.111	28.913	0.358	1.680	1.680	3.488	41.949	0.252	34.280	49.049	-17.723
W55	3.666	2.584	12.374	0.239	1.920	1.337	0.504	18.654	0.000	18.863	22.414	-8.603
W56	4.100	3.440	23.522	0.387	2.160	2.160	3.346	26.355	0.000	31.449	34.021	-3.928
W57	3.010	1.029	2.452	0.269	2.080	2.080	0.257	2.596	0.072	6.759	7.085	-2.354
W58	0.746	0.313	0.661	0.183	0.320	0.000	0.002	1.224	0.009	1.902	1.555	10.028
Sea water	41.950	89.171	482.884	10.152	2.347	2.347	58.204	596.960	0.000	624.157	659.857	-2.780

*remark: acceptable % error balance ±10 % (ALS Environmental)

Appendix B4: Standard curve AAS

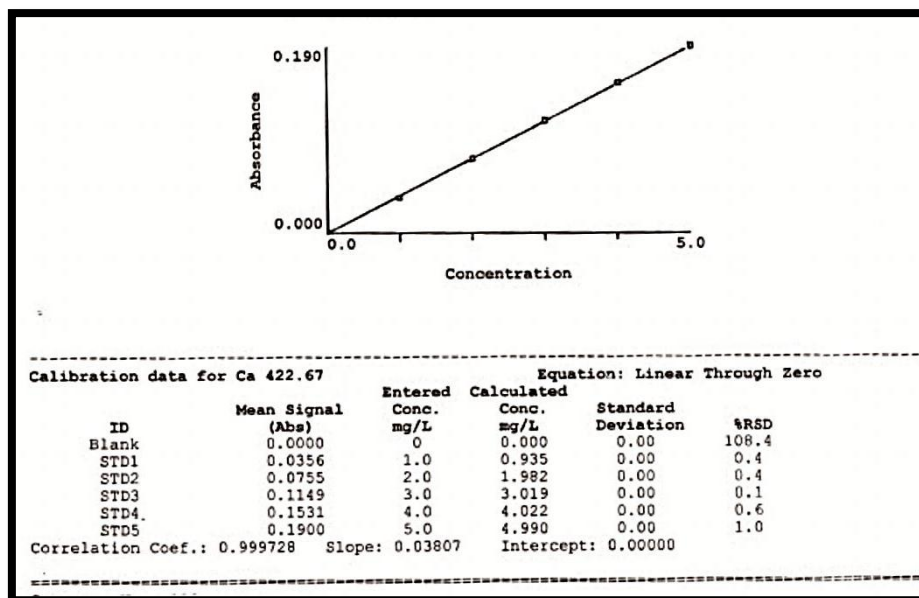


Figure B5.1 AAS standard curve of Ca analysis

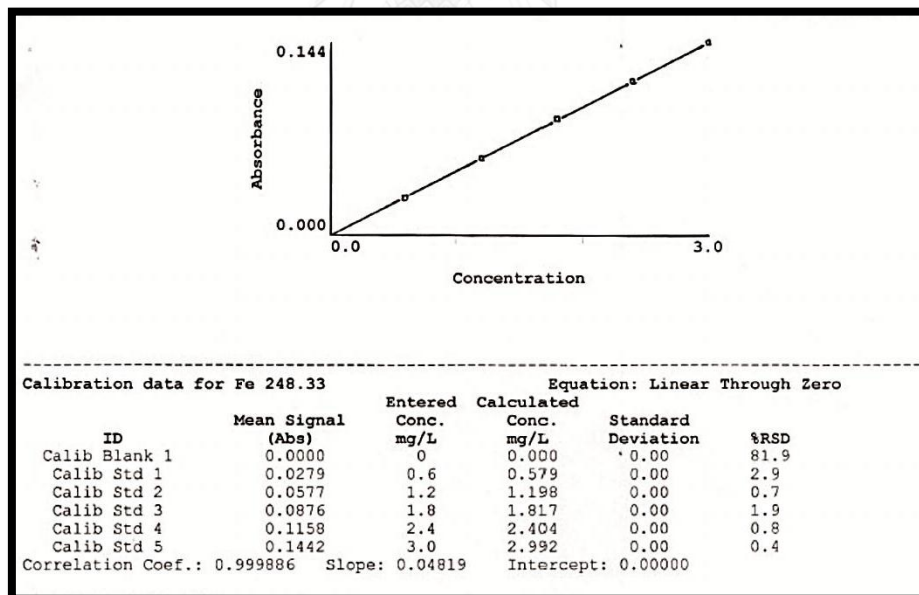


Figure B5.2 AAS standard curve of Fe analysis

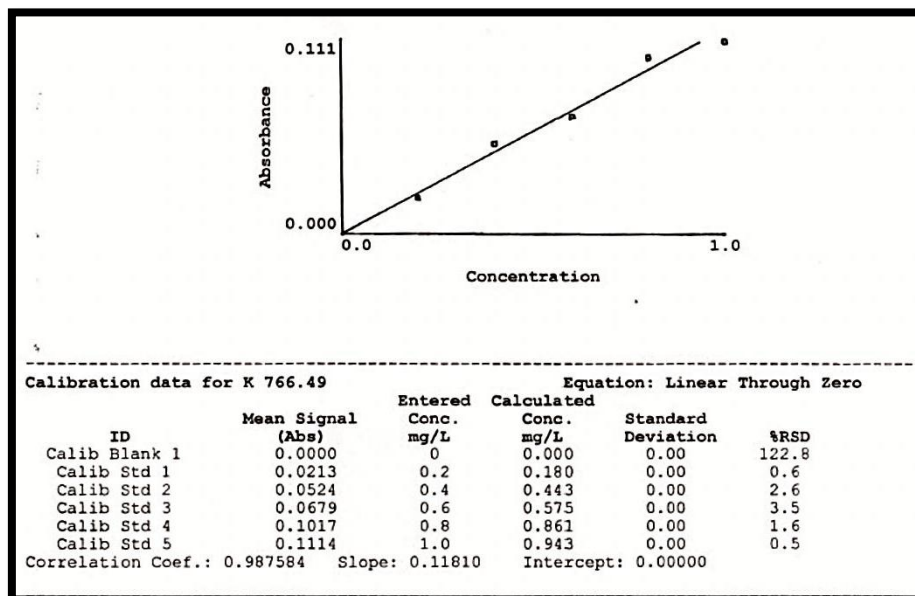


Figure B5.3 AAS standard curve of K analysis

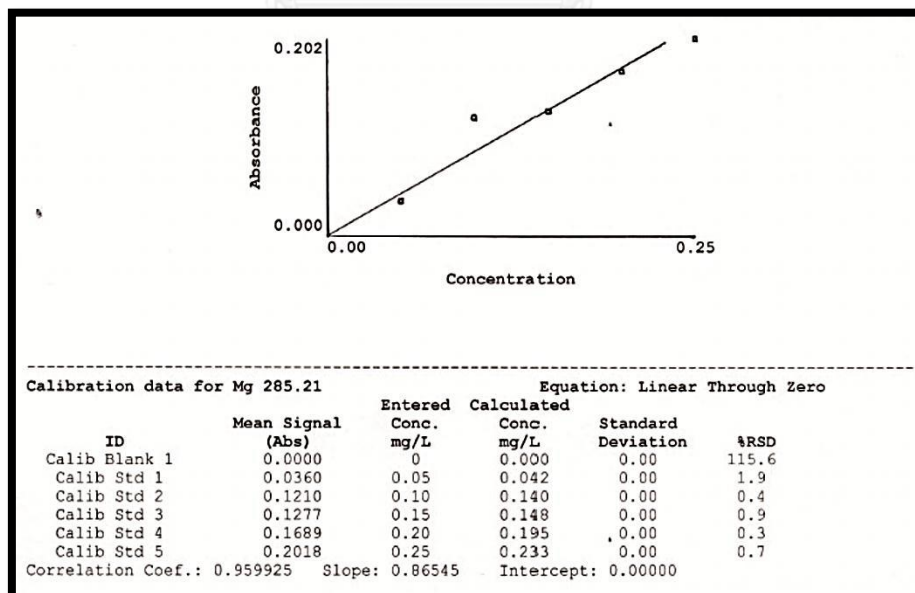


Figure B5.4 AAS standard curve of Mg analysis

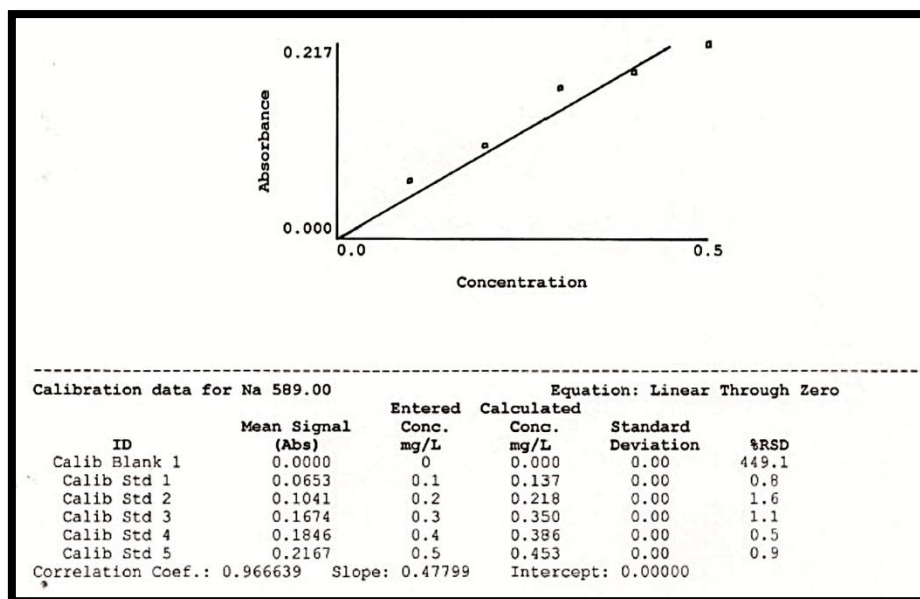
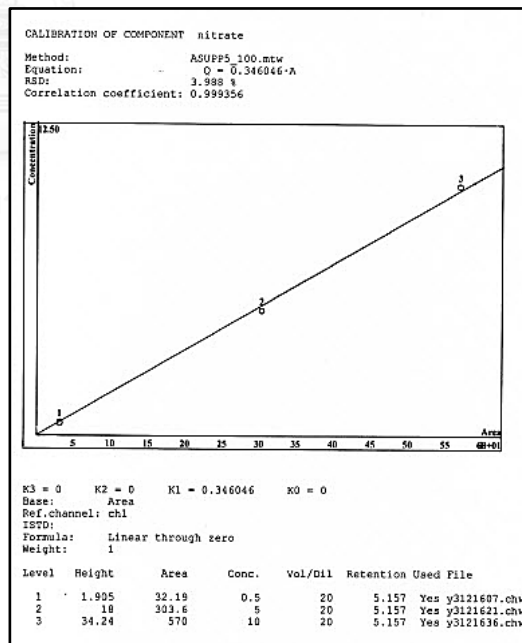
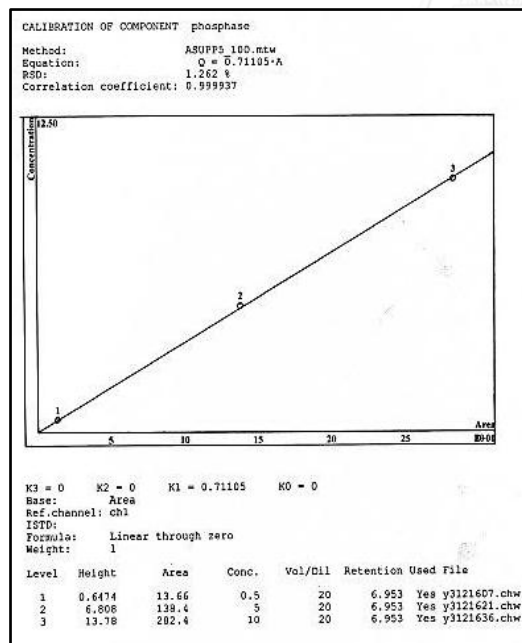
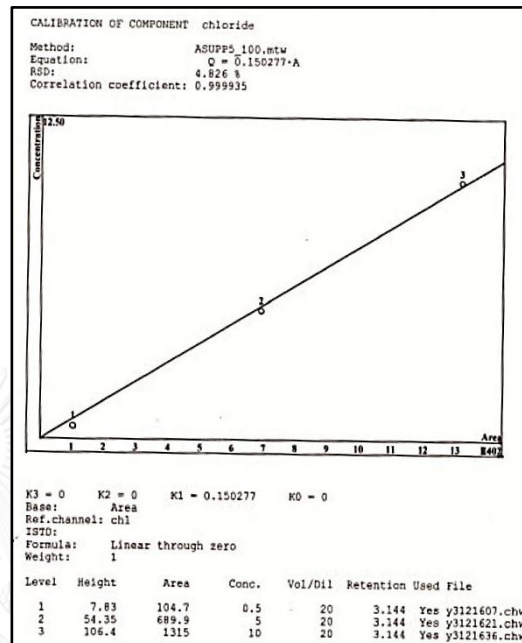
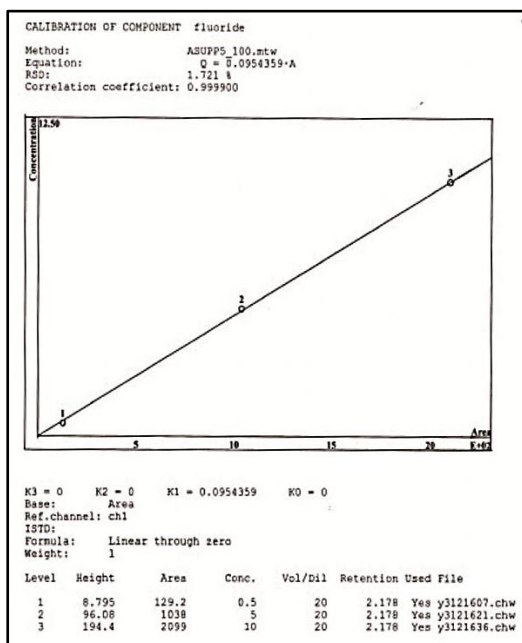
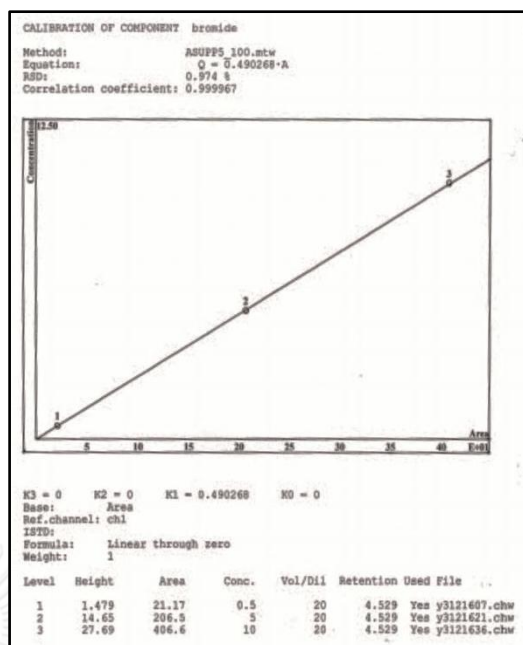
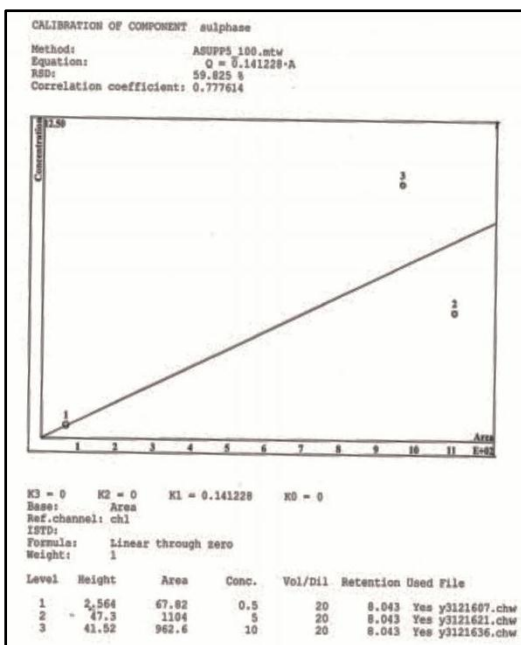


Figure B5.5 AAS standard curve of Na analysis

Appendix B5: Standard curve IC

Standard 1: concentration 0.5 ppm





Report date: 3/23/2557 14:13:11
 Printed by: Metrohm

Ident: std1
 Analysis from: 3/12/2557 16:07:56
 File: y3121607.chw
 Modified:
 Method: ASUPPS 100.mtw
 Run operator: Metrohm
 Analysis number: 269

Last save: 3/12/2557 17:19:26
 Last save: 3/12/2557 17:04:29

SAMPLE:
 Vial number: 1
 Volume: 20.0 µL
 Dilution: 1.00
 Amount: 1.0000

COLUMN: METROSEP A SUPP 5 - 100 (6.1006.510)
 Size: 4.0 x 100 mm
 Number:
 Part.size: 5.0 µm

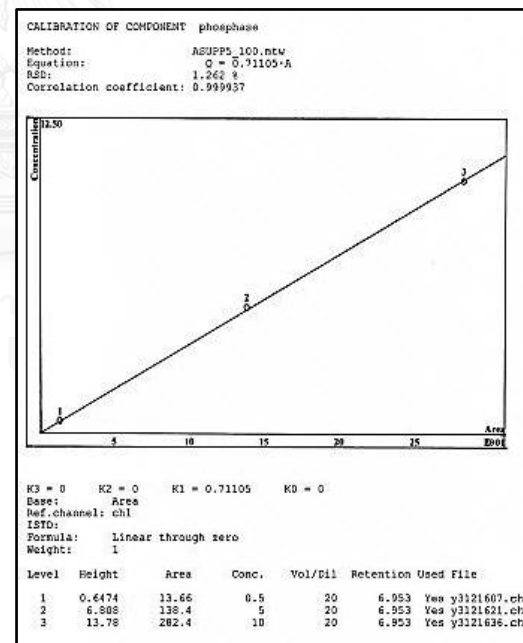
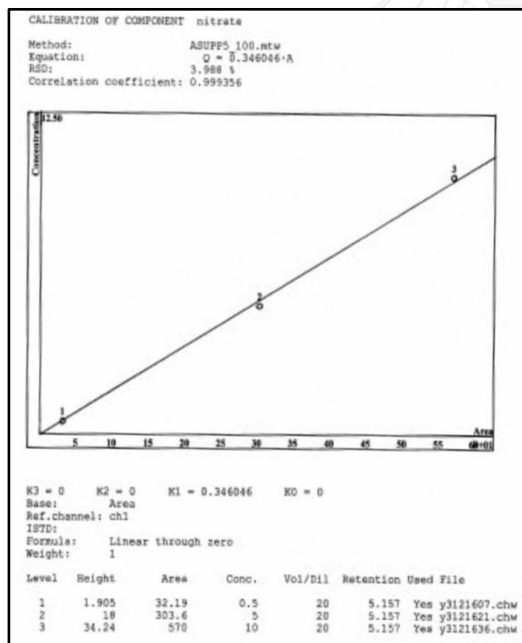
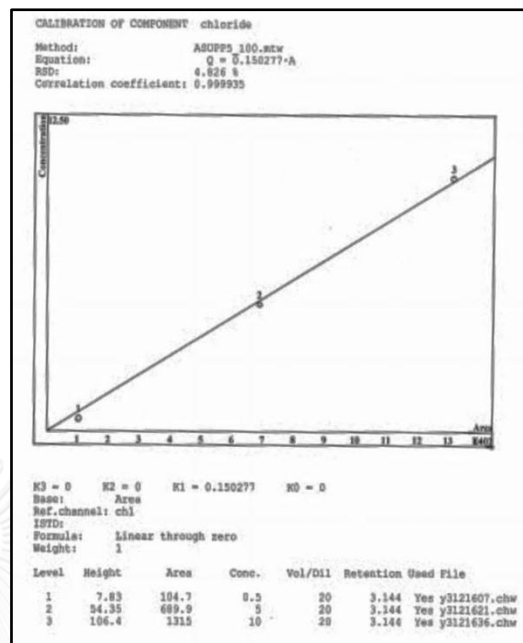
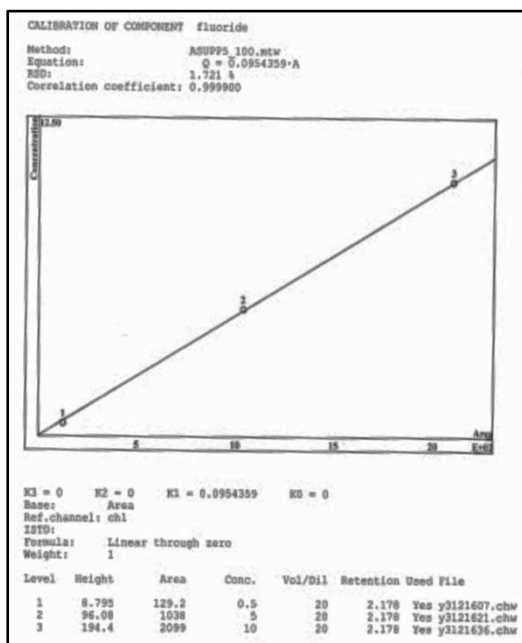
ELUENT: 3.2 mM Na2CO3 / 1.0 mM NaHCO3

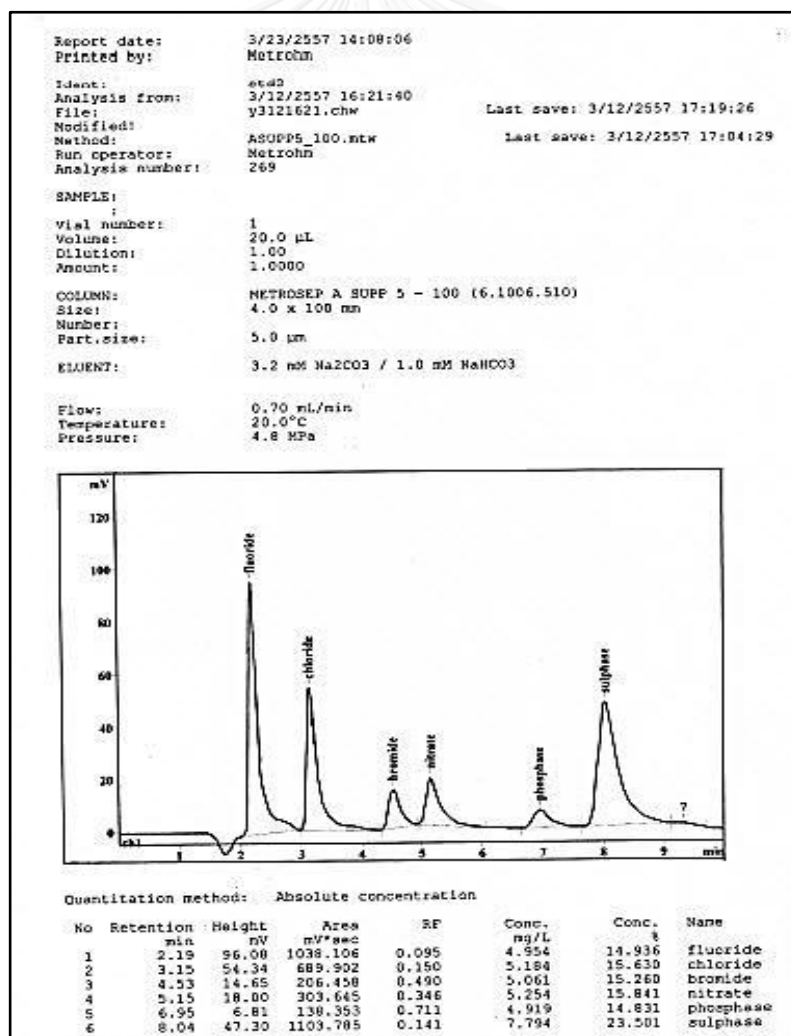
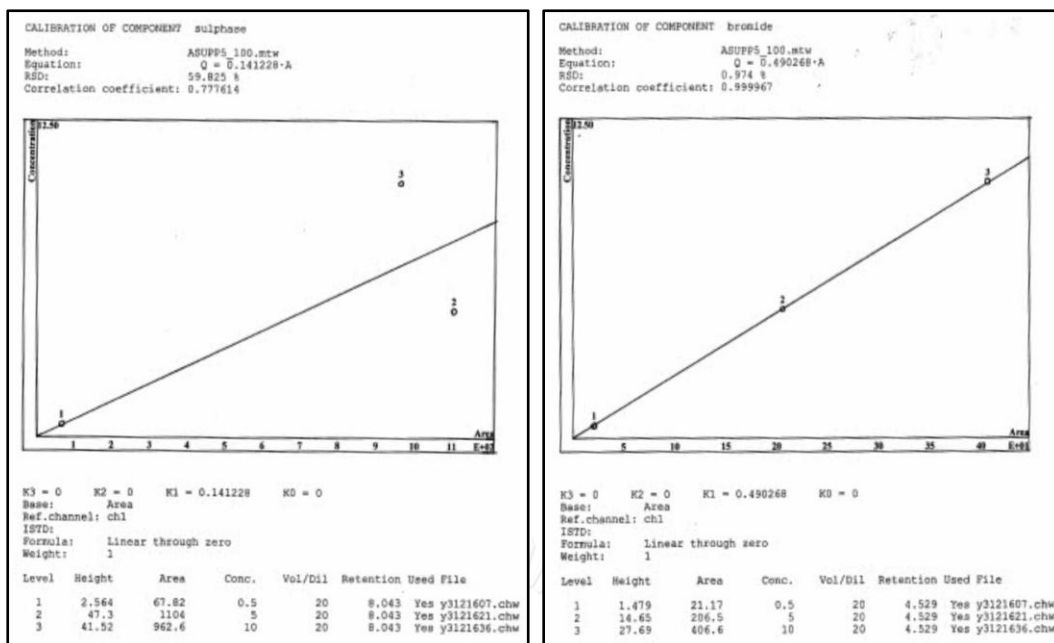
Flow: 0.70 mL/min
 Temperature: 20.0°C
 Pressure: 4.8 MPa

Quantitation method: Absolute concentration

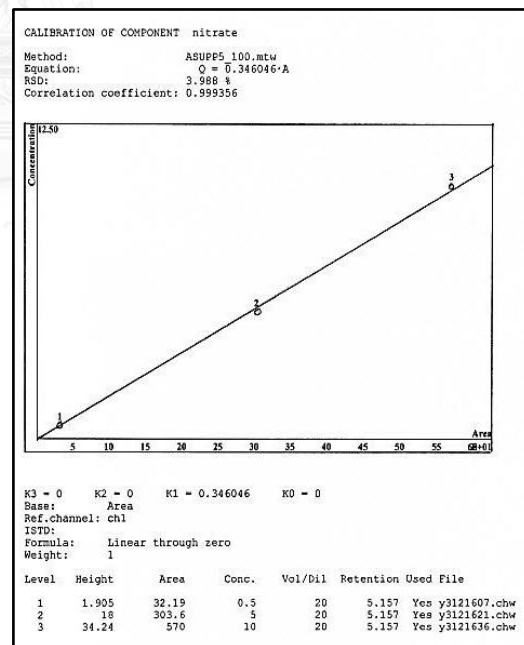
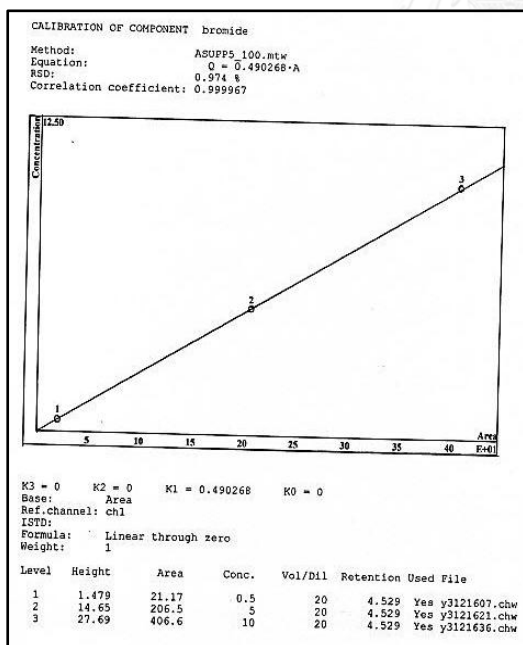
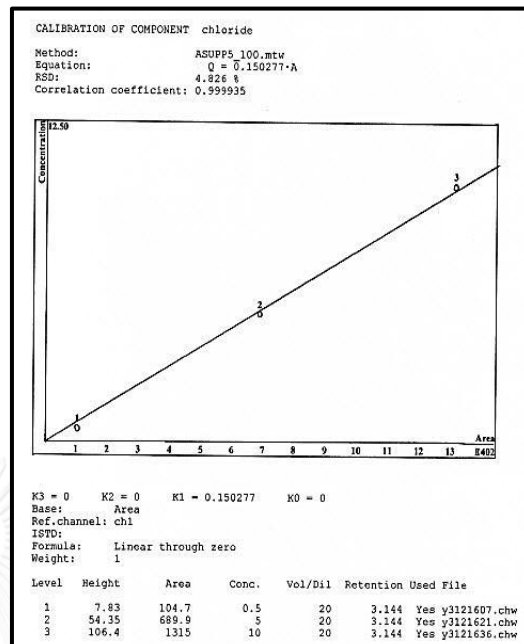
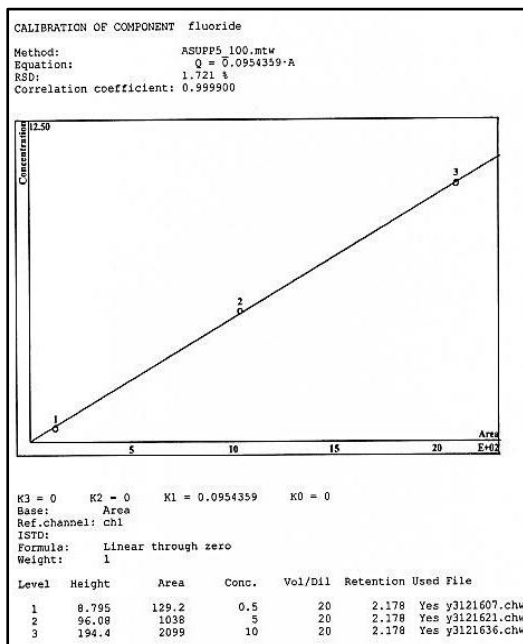
No	Retention min	Height mV	Area mV*sec	RF	Conc. ng/L	Conc. %	Name
1	2.18	8.79	129.218	0.095	0.617	17.908	fluoride
2	3.14	7.83	104.656	0.150	0.786	22.838	chloride
3	4.53	1.48	21.168	0.490	0.519	15.070	bromide
4	5.16	1.90	32.190	0.346	0.557	16.175	nitrate
5	6.95	0.65	13.655	0.711	0.485	14.099	phosphate
6	8.04	2.56	67.824	0.141	0.479	13.909	sulphate

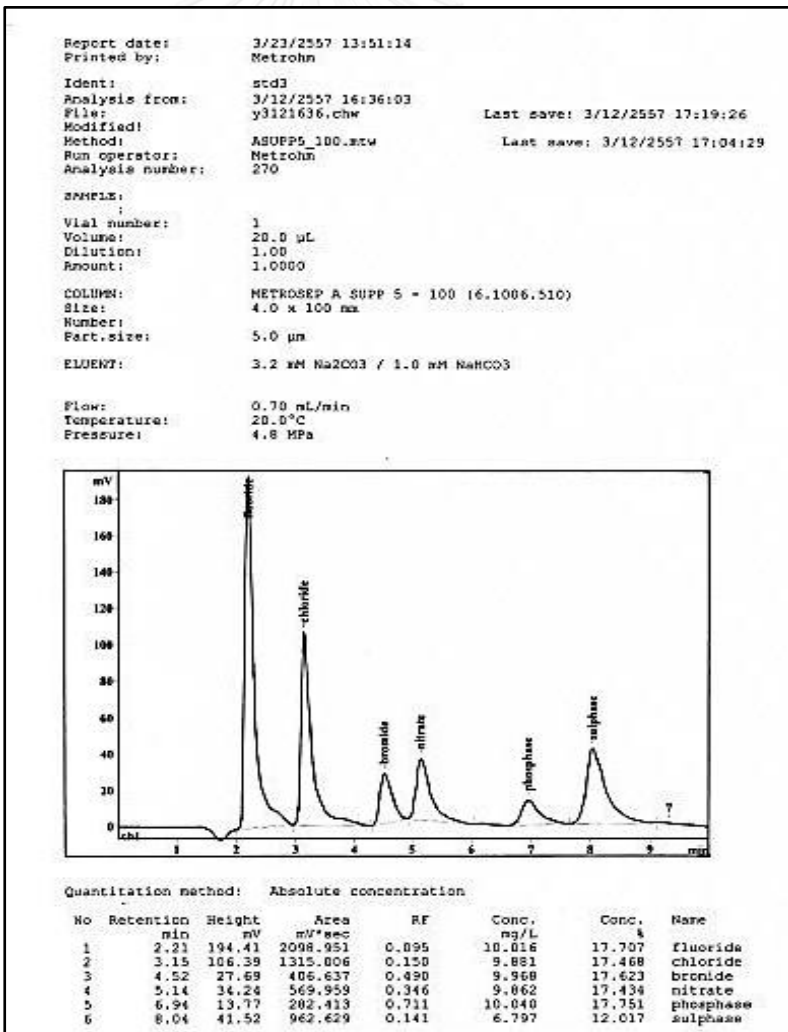
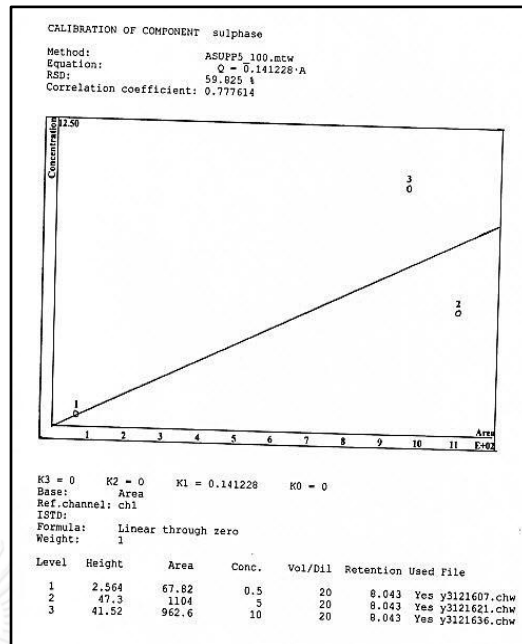
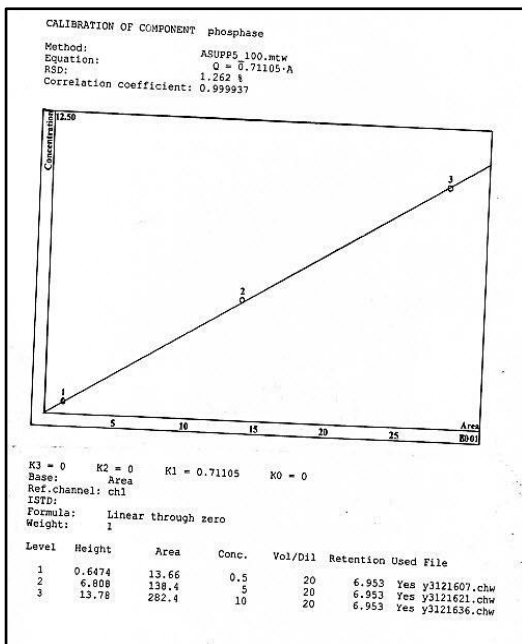
Standard 2; concentration 5 ppm.





Standard 3; concentration 10 ppm.



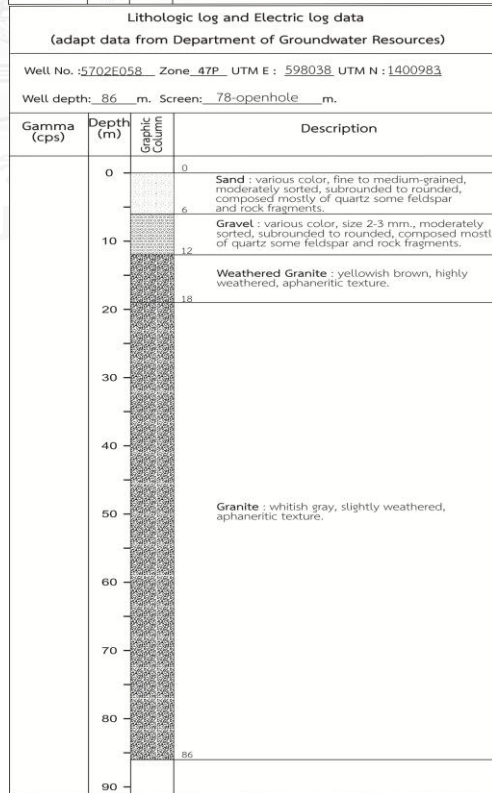
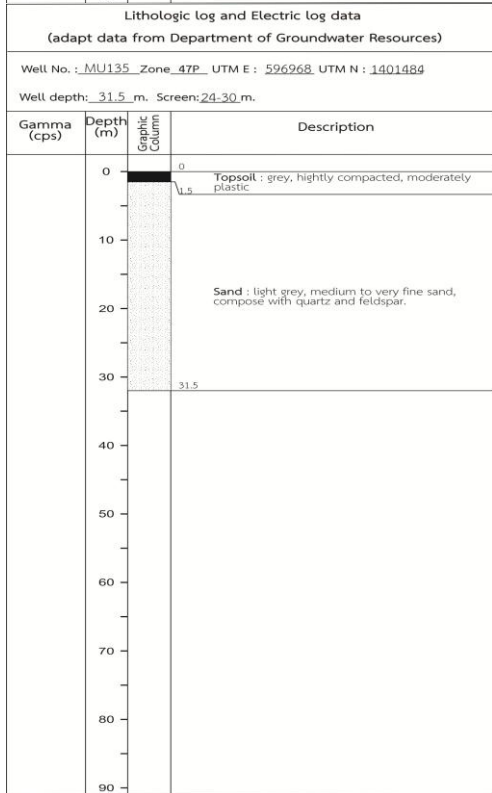
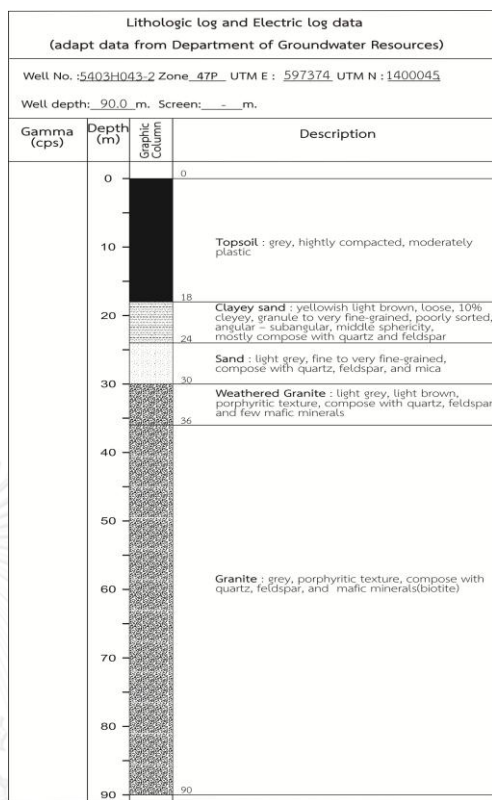
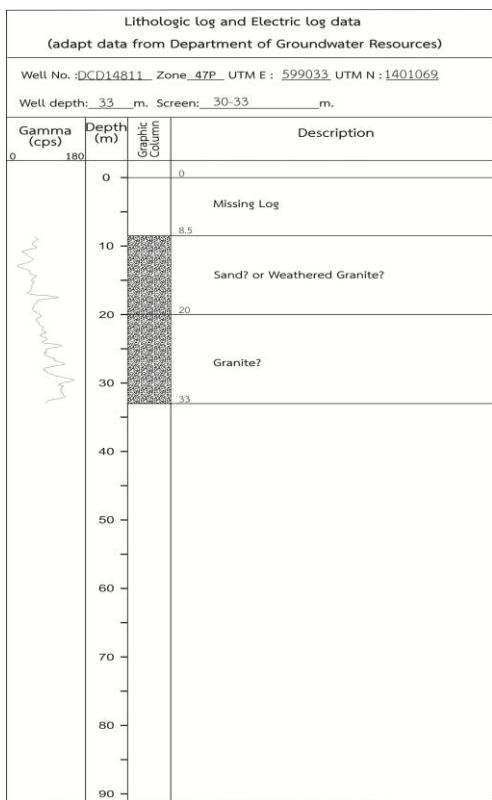


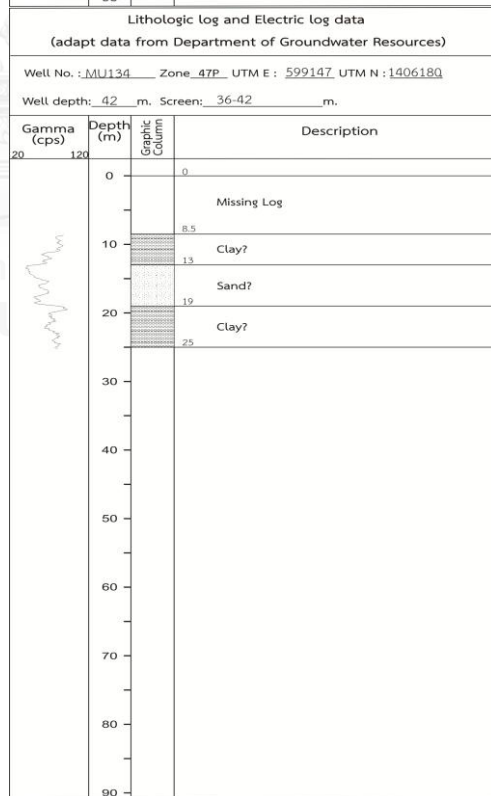
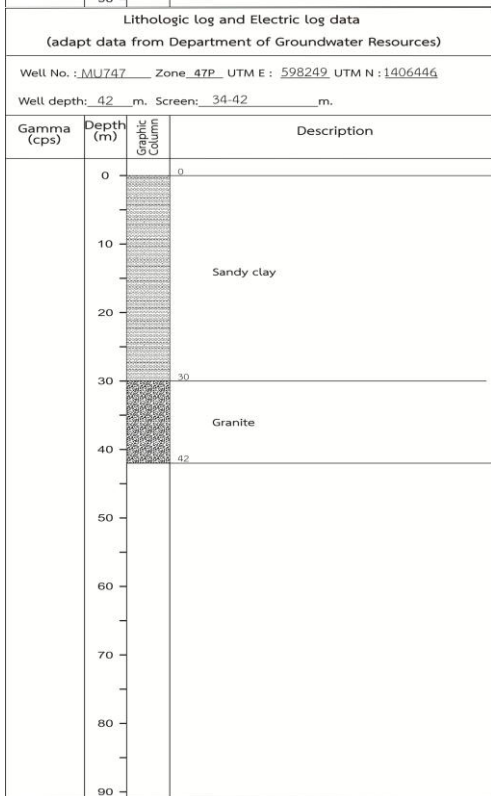
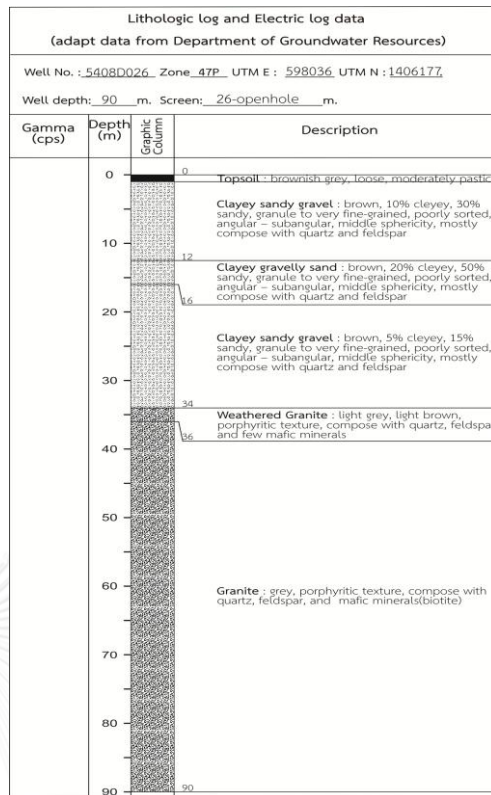
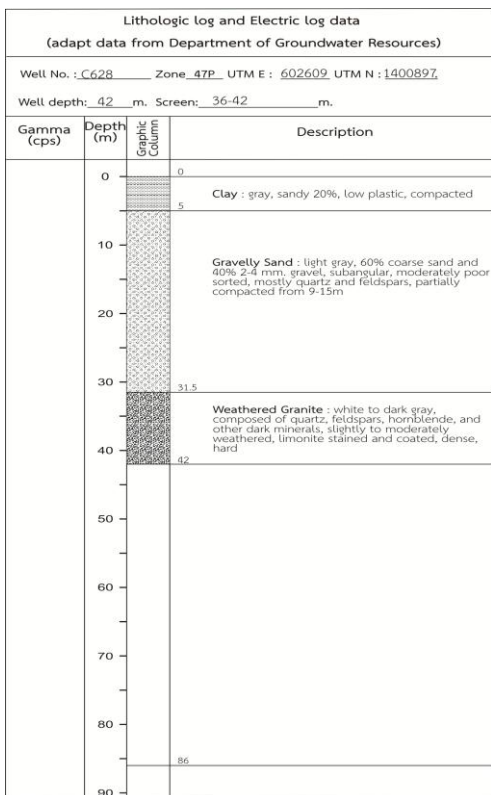
Appendix C

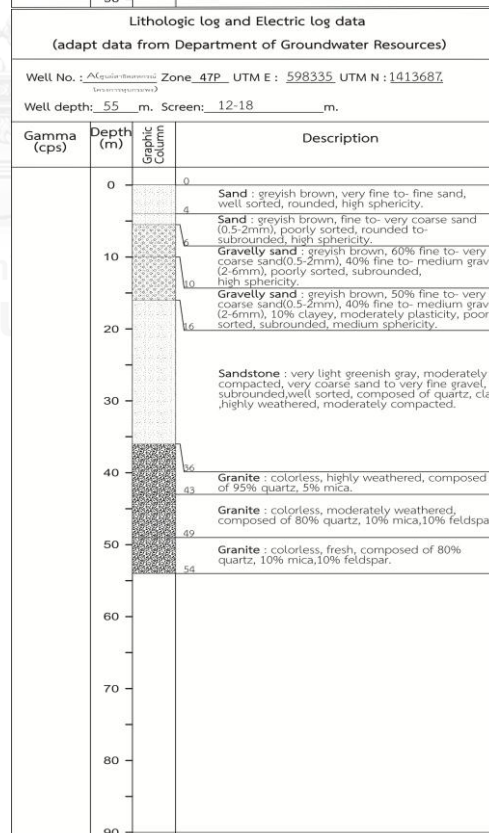
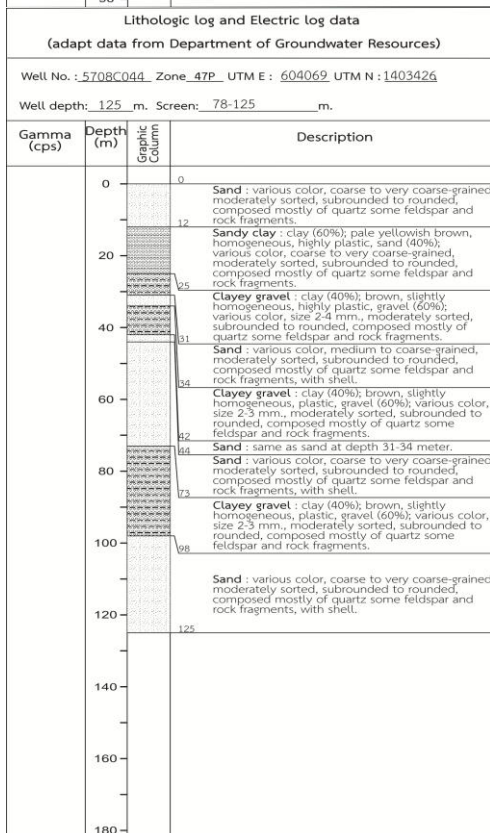
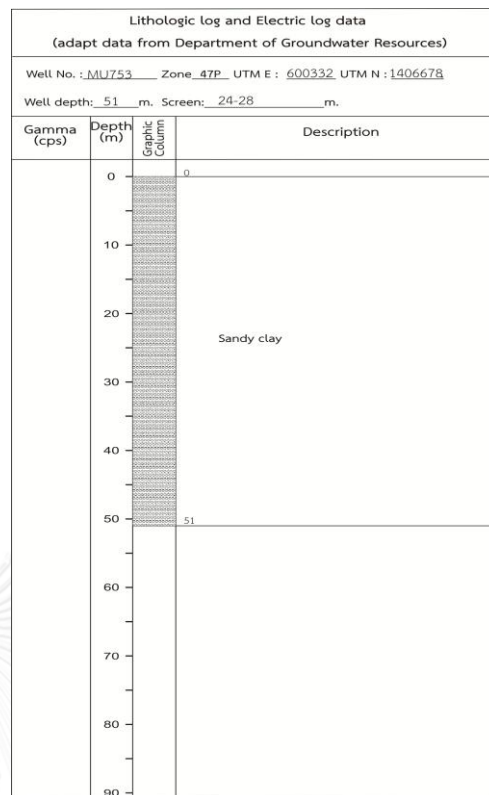
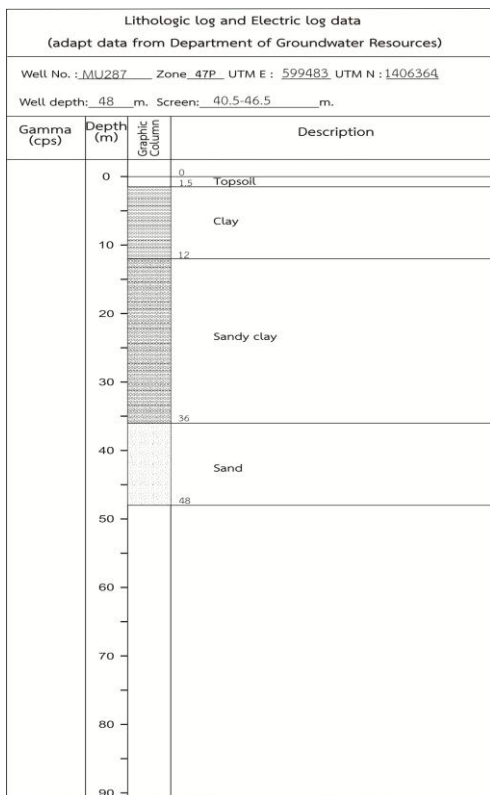
Appendix C1: Lithologic log and electric log data

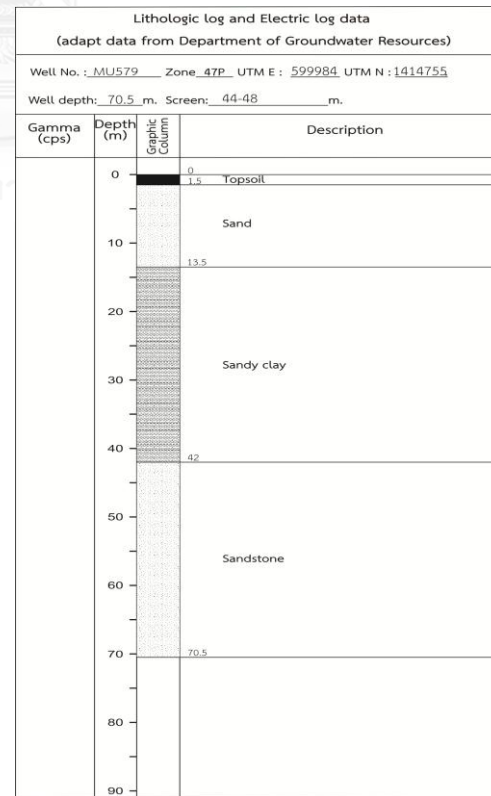
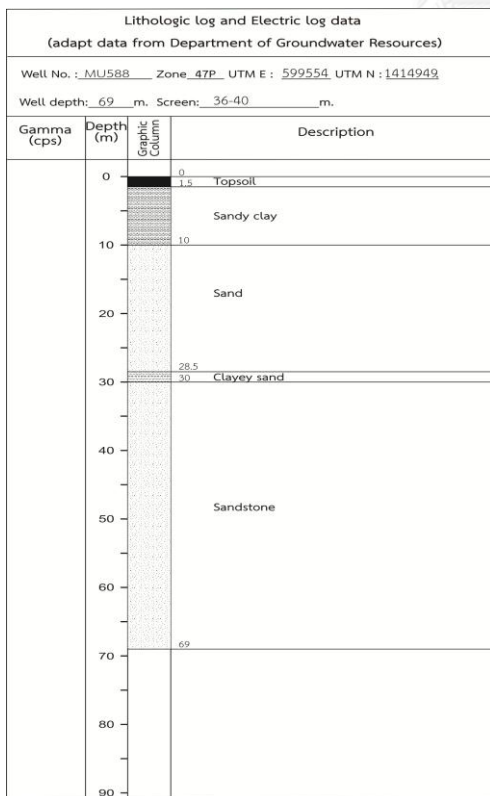
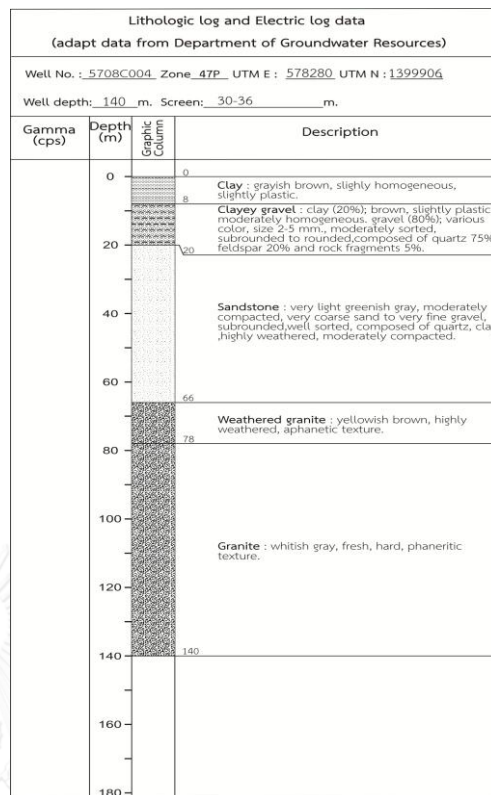
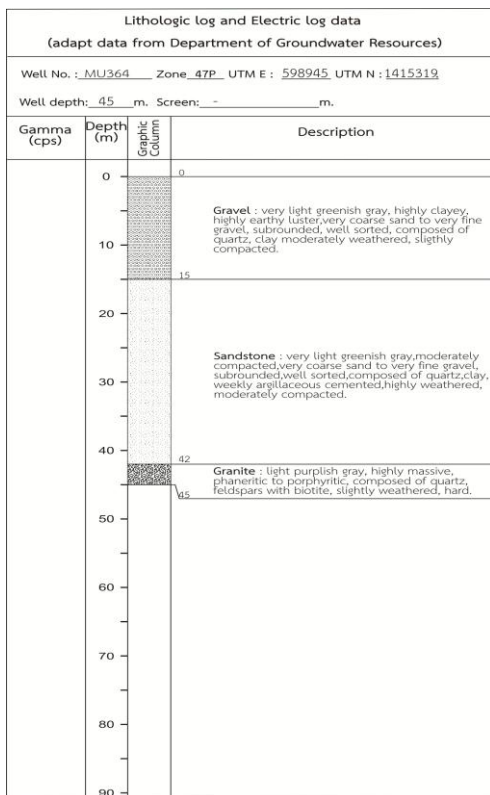


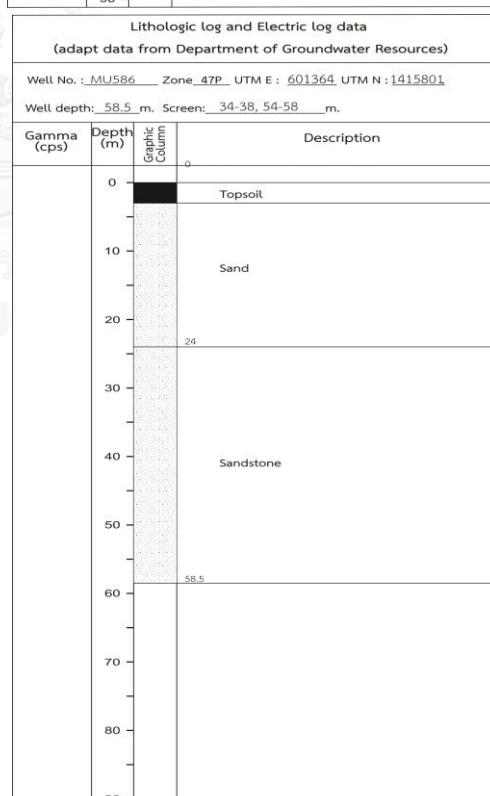
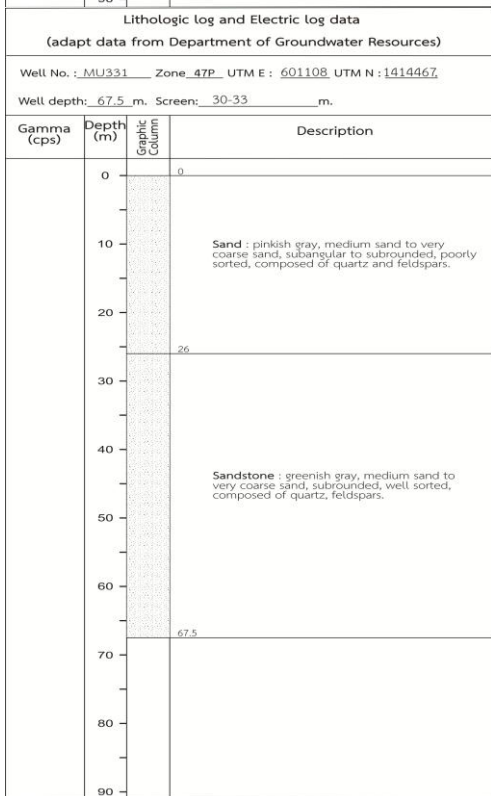
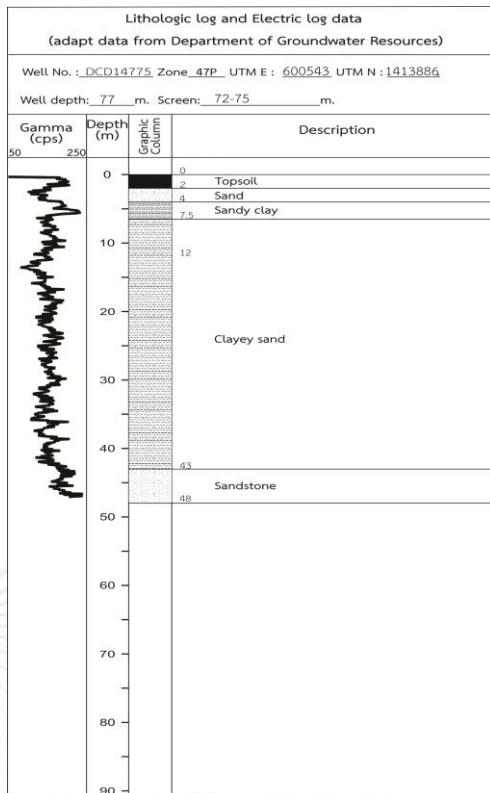
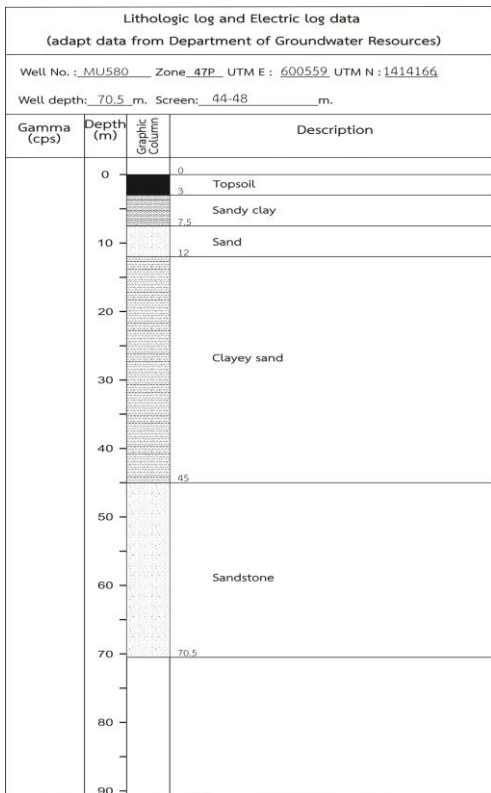
Appendix C1: Lithologic log and electric log data

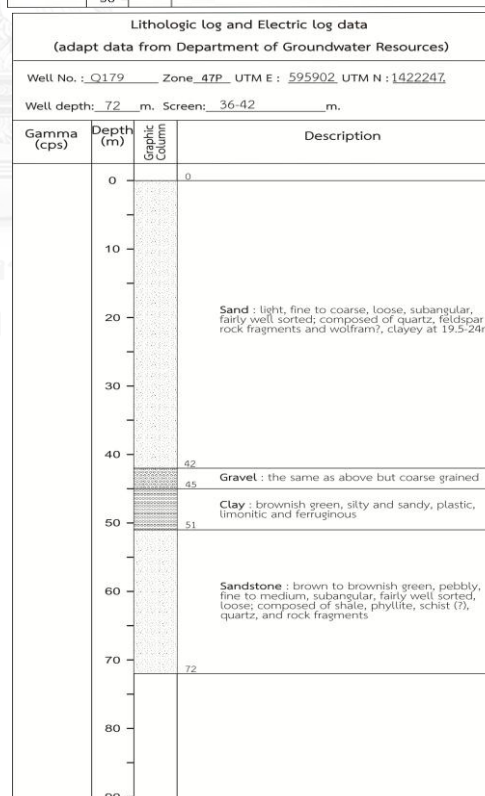
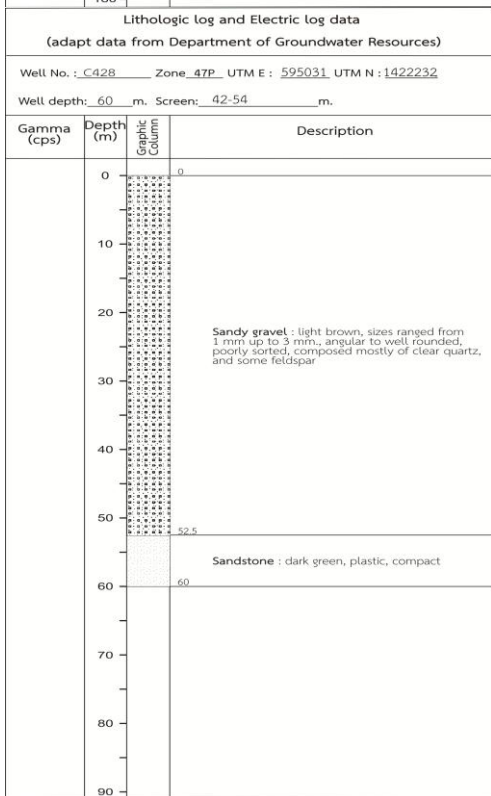
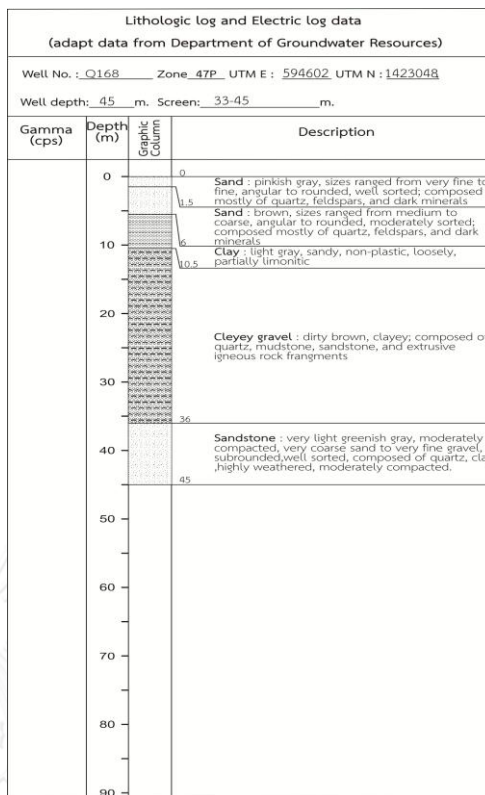
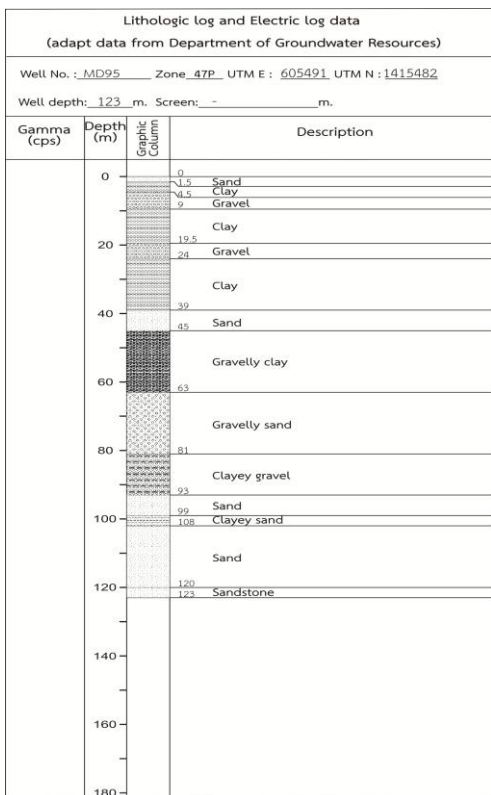


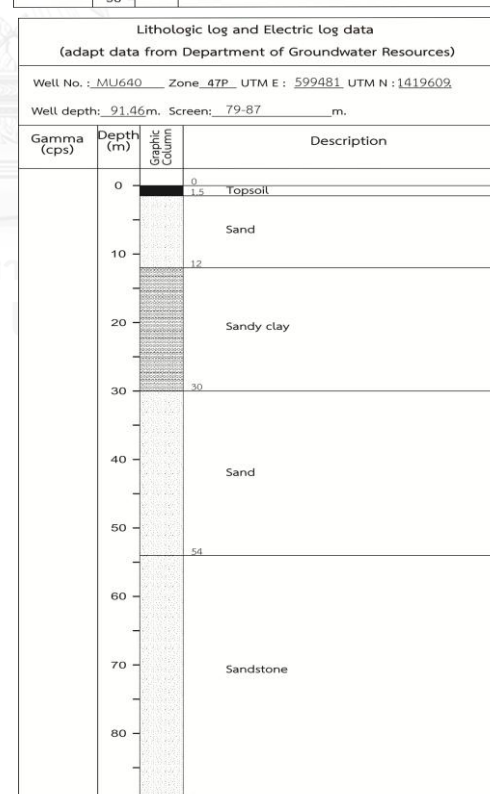
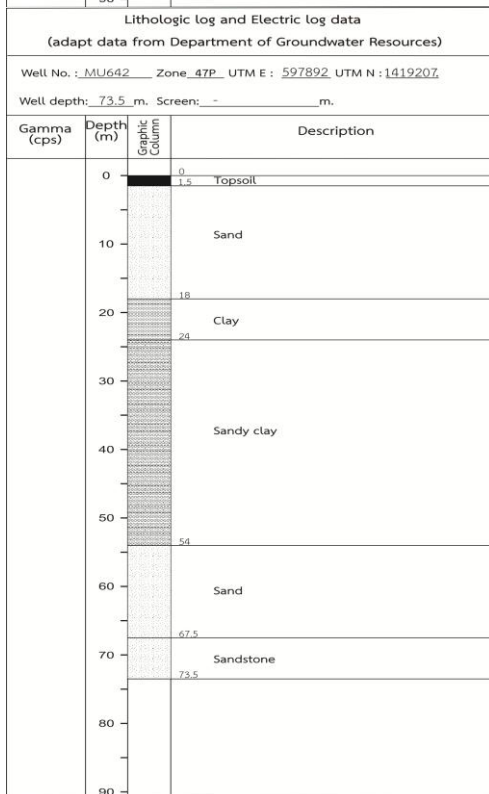
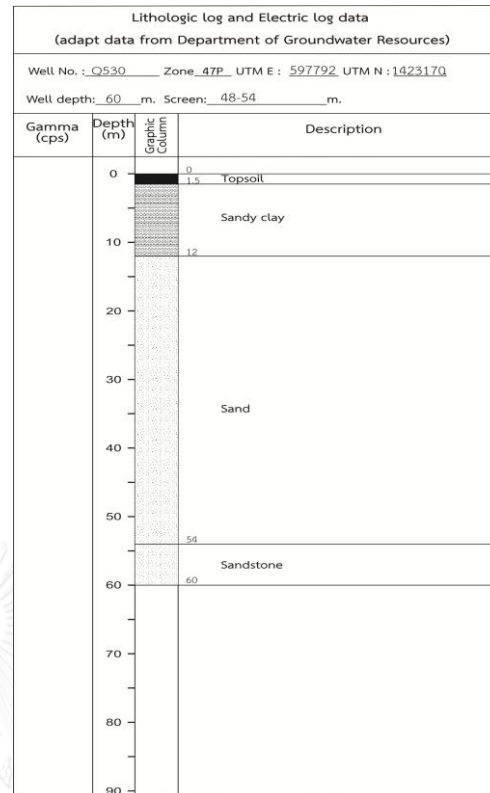
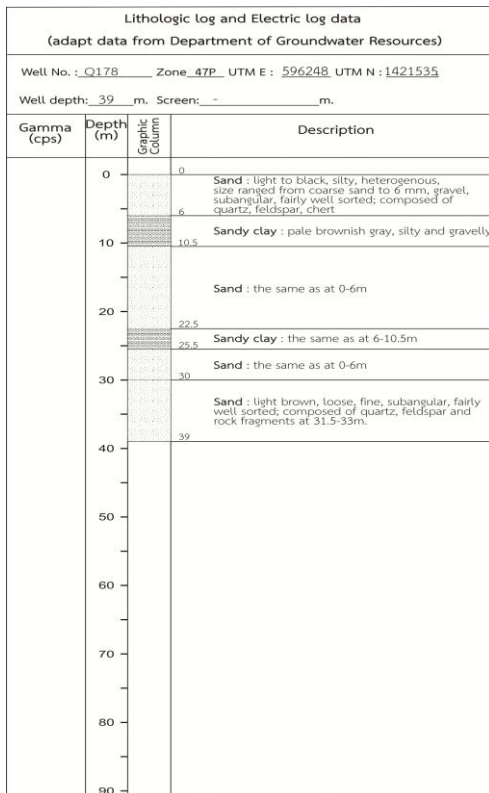


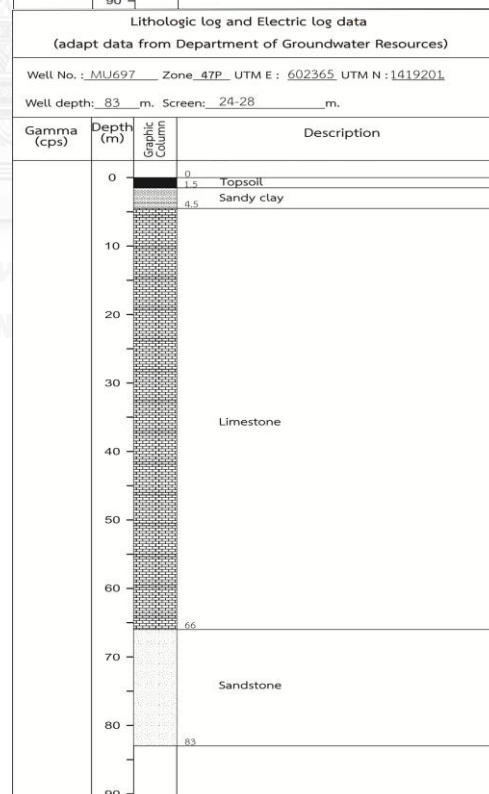
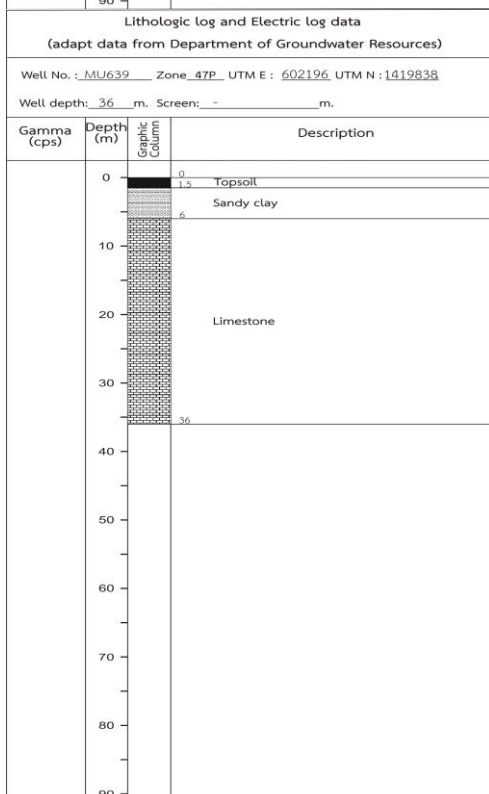
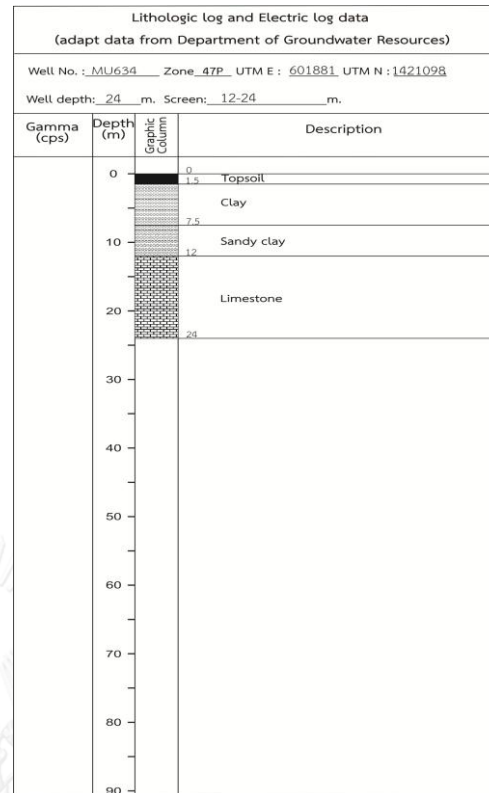
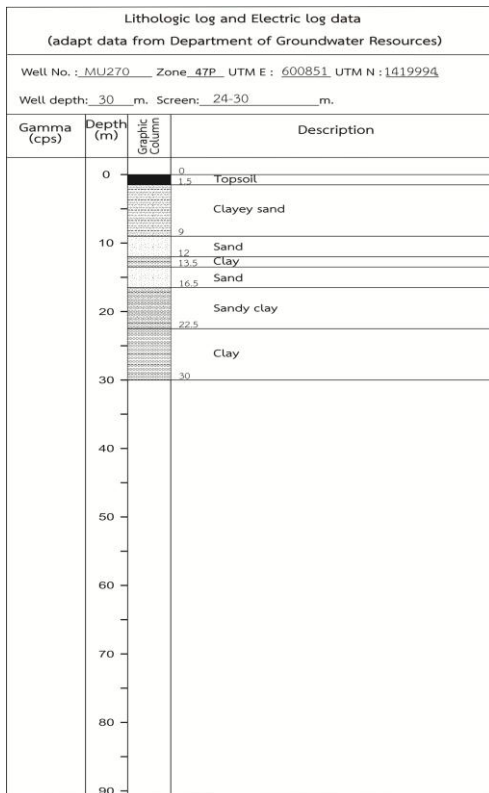


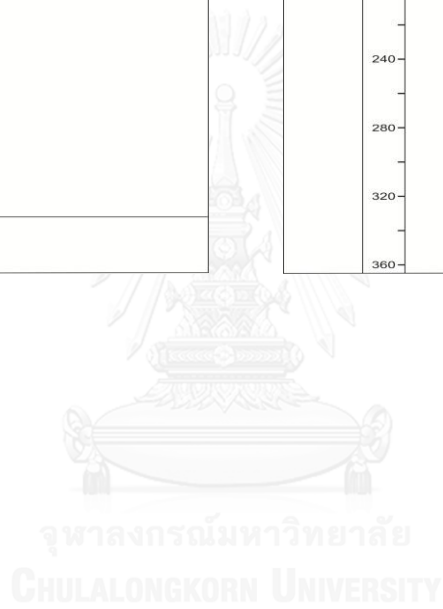
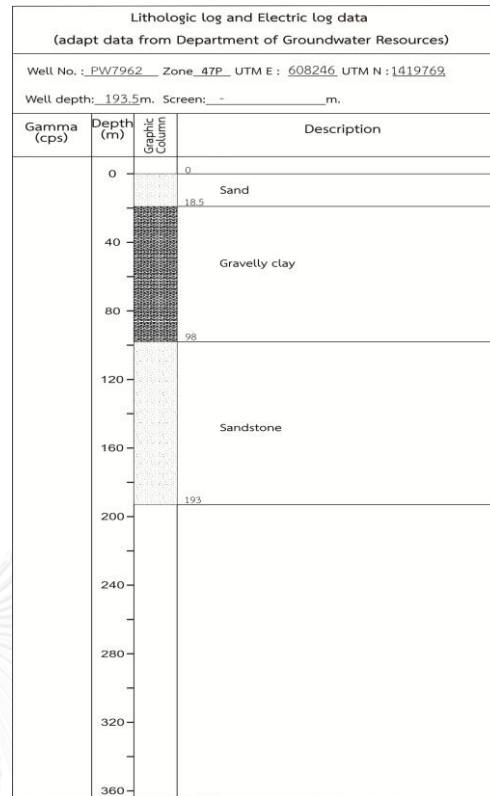
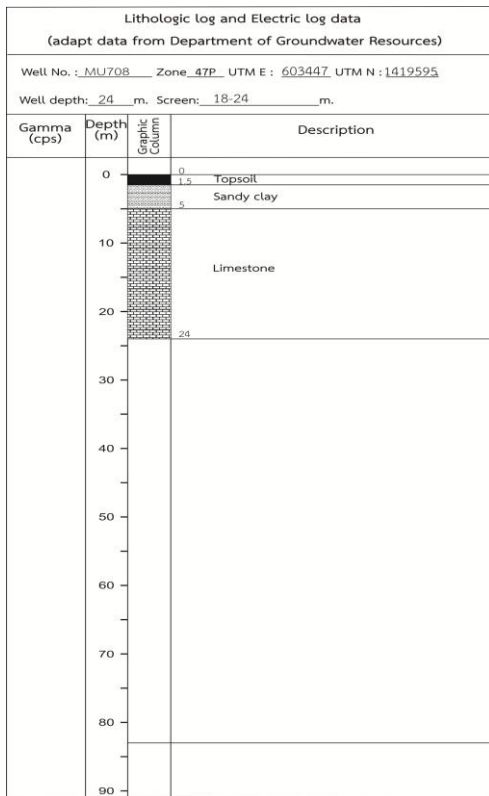












VITA

Miss Jiraporn Sae-Ju was born in Amphoe Hat-Yai, Changwat SongKhla, Thailand on March 25, 1989. She received a Bachelor of Science (Geology) from Chiangmai University in 2010. After then she entered Department of Geology, Faculty of Science, Chulalongkorn University for a Master of Science degree study. She has joined the Department of Groundwater Resources (DGR), Ministry of Natural Resources and Environment, Royal Thai Government in 2013.

